Doctoral theses at NTNU

Jogeir Myklebust

Techno-economic modelling of value chains based on natural gas

- with consideration of CO_2 emissions

Norwegian University of Science and Technology
Department of Industrial Economics and Technology Management
ISBN 978-82-471-2129-0 Electronic
ISBN 978-82-471-2127-6 Printed

NTNU
Innovation and Creativity

Acknowledgements

This thesis is the result of three years of research at NTNU. I am grateful that my contract also included a year of teaching and supervision, which have kept me busy while waiting for manuscripts or motivation to return, and helped preserve my sanity. My progress and motivation has been a roller coaster ride; some days, or even weeks, I have felt totally stagnated, and then some pretty good ideas appear out of nowhere and compensate. However, this thesis would have never been completed, had it not been for all the people who accompanied me these years.

First, I want to thank my supervisor Asgeir Tomasgard. His knowledge and insight in the research opportunities as well as knowledge of what it takes to get the result publishable has been invaluable. I am especially grateful for him giving me the freedom to explore the problems at my own pace and for his patience while waiting for me to learn how to get things right. Thanks also to my colleges at the department, in particular, but not limited, to Henrik Anderson, Kjetil Midthun, Matthias Nowak and Peter Schütz. They always answer my frustrated queries and help me regardless of whether my problems are trivial or interesting.

Jogeir Myklebust

Trondheim, January 2010

Contents

Introduction

This thesis presents and discusses techno-economic models for value chains based on natural gas (NG). The research has been financed by the Research Council of Norway through project 165818 "Optimal design and operation of gas-processing plants". Technologically speaking, processing of natural gas means to separate the "rich gas" from the gas wells into "dry gas", "wet gas" and other products (Mokhatab, Poe, and Speight, 2006). However, in this thesis "processing" is given the wider meaning of preparation for utilization.

The main usage of NG is combustion to exploit the energy. One of the combustion products is CO_2. Human made emissions of CO_2 and other greenhouse gases (GHG) are a likely cause of climate change. Climate change is an issue that gets more and more attention in the media, and it is among the top issues on the political agenda. The atmospheric concentration of GHGs has risen faster than ever in human history, and we are entering uncharted territory. Continuing the current irreversible GHG accumulation is a risky strategy. Drastic emission cuts are unpopular because of the associated costs. Four of our papers concern minimization of costs of reducing carbon emissions from gas usage relative to business as usual.

Three alternatives for emission reduction are considered. For modest abatement levels, the lowest cost option is to increase the efficiency of existing technologies. Intermediate abatement levels are not possible without drastic technology changes such as carbon capture and sequestration (CCS). Carbon can be captured before combustion by reforming the hydrocarbons to hydrogen, or after combustion by absorbing CO_2 from the exhaust. Removal after combustion is feasible for large stationary units such as power plants. For small units such as vehicles it is not practical to store emissions on board, and the carbon must be removed before the vehicles are filled. (Gibbins and Chalmers, 2008)

The thesis consists of two parts. The first part is this introduction, which is structured as follows: The scientific contribution of the papers and my role in research and writing processes are presented in Section 1.1. Section 1.2 explains how the physical and chemical properties of NG shape its role in present and future energy markets. Section 1.3 outlines how technological limitations and interactions can be represented mathematically in energy economic models. Section 1.4 discusses how the prices that are necessary input to some of the techno-economic models can be obtained. The second part consists of the five papers.

1.1 The contribution of the papers

In all five papers, we have generally applied known methods to new problems in new contexts. Understanding the context involves an overview of possible technological or economic interactions, and the application of suitable methods requires knowledge of their possibilities and limitations. The added insight of each included feature is balanced against the corresponding increase of computational cost. All writing and modelling has been performed under supervision and in close cooperation with the mentioned co-authors.

Paper 1 and 2

- Paper 1: *Optimizing investments for hydrogen infrastructure in the transport sector*
- Paper 2: *Short-term optimization of a hydrogen value chain for the transport sector*

Paper 1 and 2 present and discuss a complementing pair of optimization models for respectively investment in and operation of a hydrogen infrastructure for the transport sector. Most of the existing work in this area seems not to include optimization models, and the few contributions that do have scopes that are either wider or narrower. Models with wider scope that include hydrogen are typically multi-sector/multi-fuel energy system optimization models, for example applications of the partial equilibrium model Balmorel (2009) and IEA's MARKAL (MARKet ALlocation)(ETSAP, 2009) that minimizes total system costs. Karlsson and Meibom (2008), Endo (2007),Tseng, Lee, and Friley (2005) and DTI (2007) have simulated some of the effects of the hydrogen introduction in Scandinavia, Japan, the US and the UK, respectively. An example of a hydrogen transport sector model with a narrower focus is the local distribution model of Lin, Ogden, Fan, and Sperling (2005).

A fine resolution in the time dimension is necessary because a coarse resolution would obscure short-term fluctuations around average values. Investment decisions cannot be optimized with a short horizon (with capital costs reformulated as equivalent short-period leases) because of the economies of scale (EOS), and that the needed scales vary from year to year. The size of capacity increments affect average cost, so taking capacity needs several years into the future account could reduce average cost. If the long-term investment schedule and the details of the short-term operations were optimized jointly, then the intractable combination of a long horizon and a fine resolution would be necessary. Hence, we decomposed the framework into models of complementing horizons and resolutions.

The operational model has a fine resolution that makes it able to return information about capacity utilization and short-run cost, but unable to optimize

investment in capacities because of its short horizon. On the other hand, the long-run model can optimize investment decisions but not capacity utilizations. Therefore capacity utilizations are given as input parameters to the investment model from the operational model, and investment decisions are given as input parameters to the operational model from the investment model. Demand, prices, and efficiencies are assumed to change over time. Therefore operation of the infrastructure is formulated with separate static processes for each time step. Each time step in the short-run model is connected by storage levels and transport lags, and each time step in the long-run model is connected by accumulated investments.

Our main research contribution is the identification of technological constraints with important consequences for investment and operational decisions and mathematical formulations of these constraints. Both of the models solve to a reasonable optimality gap with commercial software on a basic PC when applied to our three different cases. The modelling is based on the work of the Master's students Holth and Saue (2005). My contributions are more general and less computationally complex mathematical formulations, performing a literature survey to place the model into its context, as well as writing the papers.

- Co-authors: Christina B. Holth, Liv Elise S. Tøftum and Asgeir Tomasgard
- Paper 1 and 2 are being reviewed for publication.

Paper 3

- Paper 3: *An optimization-simulation model for a simple LNG process*

Paper 3 presents and discusses the development and implementation of a heuristic search to fine-tune the settings of a process for liquefaction of NG to LNG that is modelled in Aspen HYSYS (Aspen Technology, Inc., 2009). The gas liquefaction process, called Prico (Barclay and Denton, 2005), is based on a single circuit with a mixed refrigerant. Our implemented hybrid search, which consist of a global Tabu Search (TS) (Glover, 1986) and local Nelder-Mead Downhill Simplex (NMDS) (Nelder and Mead, 1965), is similar to Chelouah and Siarry (2005) and Hedar and Fukushima (2006) who have implemented the method on analytical test functions.

To our knowledge such hybrid search methods have not yet been applied to real problems. However, Cavin, Fischer, Glover, and Hungerbüler (2004) apply a TS algorithm to a batch plant. Differently from our sequence based plant model, their plant is modelled analytically with a set of differential and algebraic equations.

No off-the-shelf search procedure seems to exist that can be easily combined with HYSYS or other numerical/iterative tools for process modelling. Solvers

that can be applied to equation based (analytical) tools that simulate static processes do exist, but the liquefaction processes are rather complicated and therefore benefit from the more rigorous numerical tools. Numerical tools do not return gradient information.

The development and implementation of a cost minimizing heuristic that operates without gradient information is our main contribution. In-depth understanding of both the technological process details and the technical details of the search procedure have been necessary to chose efficient search parameters, and the credit for this essential part must be shared. At the research stage I have contributed to the development and practical implementation of the search procedure, and modified it with error handling routines. I have also written the associated sections of the papers as well as contributing towards our attempt to make them readable to both our research communities.

- Co-authors: Audun Aspelund[1], Truls Gundersen, Matthias P. Nowak and Asgeir Tomasgard
- Paper 3 is available on-line in *Computers & Chemical Engineering*[2]. The tables of the paper are slightly rearranged for typographical reasons, and the typos we were allowed to correct between the acceptance of the paper and the printing of it are corrected. The content is the same.

Paper 4

- Paper 4: *Optimization-Simulation of a Combined LNG and LCO_2 Transport Chain*

Paper 4 presents and discusses the development and implementation of a heuristic hybrid search to the *liquid energy chain* (LEC)(Aspelund and Gundersen, 2009). As in paper 3, the search procedure is based on a TS and NMDS hybrid search, and the technological model is implemented in HYSYS. The LEC is a combined ship based transport chain for inbound liquefied natural gas (LNG) and outbound liquid CO_2 (LCO2). The combined carrier returns thermal energy in the form of LCO2 from the regasifier to the liquefaction plant in addition to the usual LNG the other direction.

Our results show that it is beneficial to optimize settings such as the pressures, temperatures and flow rates jointly rather than individually for the ship and the terminals. In comparison to the application of our TS-NMDS hybrid search in paper 3, the implementation in paper 4 is modified to handle a larger number of decision variables by keeping the less influential variables constant during the

[1]Corresponding author
[2]doi:10.1016/j.compchemeng.2009.10.018

TS part. My role at the research and writing stages is essentially the same as for paper 3.

- Co-authors: Audun Aspelund[3], Truls Gundersen, Matthias P. Nowak and Asgeir Tomasgard
- Paper 4 is being reviewed for publication.

Paper 5

- *Forecasting gas component prices with multivariate time series models*

Price scenarios are important input for the decision makers in the NG industry (Midthun, 2007). In paper 5, we present and discuss a multivariate statistical model for prediction of monthly prices of gas based on trend, seasonal effects and serial correlations. Our available time series consist of transactions in the north European wet gas market from 1995 to 2006. Rather than the input and product prices that the above models are based on, our dataset consist of prices of wet gas (butanes, propane and naphtha; sometimes called natural gas liquids, NGL).

Also in this case our contribution contains a context evaluation that is seen in combination with the possibilities and limitations of our available method of analysis. We have developed a model and implemented it in the commercial software STAMP™(Koopman, Harvey, Doornik, and Shephard, 2009). STAMP™ is based on estimation with the Kalman filter, which is able to handle time varying parameters because of its on-line operation. To our knowledge this method has not been applied for multivariate estimation of similar price series. However, Serletis and Gogas (1999) analyse a time series of dry gas, wet gas and crude oil prices in the North American market, where the prediction error of a regression model is modelled as deterministic chaos. Lee, List, and Strazicich (2006) analyse 11 non-renewable natural resource real prices from 1870 to 1990 (including dry gas). Serletis (2007) discusses the dynamics of the gas market in a broader setting that also include other energy such as oil and electricity.

Our approach is technically similar to Pindyck (1999) and Westgaard, Faria, and Fleten (2008). Pindyck (1999) analyses the long-run evolution of prices of oil, natural gas and coal, and also use a Kalman filter. Westgaard et al. (2008) analyse possible stochastic trends and seasonal patterns in gas component prices from 1995-2006. Differently from our *multi-variate* model, both these studies use *univariate* unobservable component models. Our extension is to estimate a set of energy prices as a system, exploiting potential information about *one* dependent variable in the preceding disturbances of the *other* dependent variables.

[3]Corresponding author

My main role is to elaborate correlations that are likely to be consequences of the supply and demand side features of the wet gas market, to have a critical look at the estimated models, and a share of the writing process.

- Co-authors: Sjur Westgaard[4] and Asgeir Tomasgard
- This paper is being reviewed for publication.

1.2 The role of natural gas in the energy market

In order to keep the living standard at the level consumers are used to, a large share of total energy demand must be satisfied by fossil fuels such as NG, oil and coal to keep energy prices low. Therefore, we will probably consume fossil fuels for a few more years. About one fifth of the world's primary energy demand is met by NG, and IEA (2008) expects this share to rise over the next twenty years. The different types of primary energy are substitute inputs to the production of fuel and energy intensive products. When gas is used rather than coal, both the direct usage and conversion into the common intermediate product synthesis gas (syn-gas) is done with simpler capital.

On the other hand, transportation of gas requires more complicated and less efficient capital than solid or liquid fuels. Coal is still abundant and has a lower market price per energy unit than oil and gas. However, conversion of coal into products traditionally made from oil or gas is capital intensive and inefficient, and therefore motivated by security of supply rather than cost advantage (Vallentin, 2008; Mokhatab et al., 2006).

Eventually, our use of fossil fuels must end because it is a finite resource. Moreover, it could end earlier if the environmental consequences are given enough weight. Combustion of coal and hydrocarbons cause local pollutants such as NO_x, SO_2 and particles as well as the global CO_2 emissions (Tzimas, Merciera, Cormosa, and Peteves, 2007). Measured per energy unit, combustion of NG is cleaner than other fossil fuels both concerning global emissions and local pollutants. Therefore, it could be used to bridge the gap and reduce emissions from coal before enough energy from renewable sources becomes available. However, like most power plants, gas plants have lifetimes of several decades and their average costs are relatively low once the irreversible investment costs are paid. As a consequence, replacing coal plants with gas plants rather than renewable power production is a quick fix that could slow down the inevitable transition, called a technological "lock-in" of capital stock (Unruh, 2000).

A practical contribution of this thesis is to reduce the cost of cutting CO_2 emissions. Of our considered alternatives, improving efficiency of existing usage has

[4]Main author

the lowest marginal cost, but the potential will rapidly get exhausted. Efficiency improvement is, as a consequence, best suited as a near-term solution. Capturing carbon before or after combustion is higher up the marginal abatement cost curve. For high abatement levels, efficiency improvements will be intra-marginal and contribute towards lower *average* abatement costs (Bayon, Hawn, and Hamilton, 2009). The results of our hydrogen infrastructure model indicate that the CO_2 prices must rise considerably from today's level before CCS becomes an intra-marginal technology. For efficiency, the carbon cap should be at the abatement level where the marginal abatement cost equals the marginal damage from carbon emissions. Hence, the *marginal* cost of cutting emissions will depend on the (politically agreed) marginal damage, but the average cost will still depend on the available abatement technology.

Emissions are not totally eliminated with CCS technology, the last 10-20% are impractical to capture (IPCC, 2005, ch 3). In order to put a model into perspective it is important see beyond its formulated objective and consider whether it is consistent with possible "upper level" objectives. In our case one such upper level objective could be to minimize GHG emissions. Whether or not our local minimization of intermediate abatement costs is consistent with minimization of total emissions depends on the context. In our cases the context could be either a carbon tax or an emissions cap regime. For a situation with a carbon tax, Baker, Clarke, and Shittu (2008) argue that if the cost of "80%-technologies" are reduced, then we risk a substitution away from 100%-technologies.

NG reformed to hydrogen to fuel cars can be used to eliminate their direct emission of CO_2 and local pollutants. However, traditional automotive fuel is separated from crude oil rather than reformed. *Separation* from oil is a less capital intensive and more energy efficient process than *reforming* from gas. So until the oil gets even scarcer relative to gas, hydrogen production will not happen without government support. The government support is motivated by the possibility to capture CO_2 and the reduction in local pollution. In theory, the net impact on the GHG concentration from fossil fuelled cars could be the same, and perhaps at a lower cost, if the price of fossil fuels included carbon offsets that finance emission reductions relative to *business as usual* elsewhere. A practical problem is that the *additionality* of GHG emission reductions must be documented, which is not always possible (Bayon et al., 2009).

Hydrogen is in fierce competition with other environmental initiatives for subsidies, tax breaks and other types of support. Hydrogen from reforming of NG competes with hydrogen produced with electrolysis. For efficient resource allocation, electrolysis should take place only when the alternative value of the electric energy is sufficiently low. Our hydrogen infrastructure model is formulated with this issue in mind.

Electricity and combined heat and power plants consume 70% of the total final consumption of NG (IEA, 2008). Disregarding costs and emissions, gas power plants have the advantage of flexibility in comparison with intermittent sources such as wind and wave, and slower-ramping thermal such as coal and nuclear (Eydeland and Wolyniec, 2003). As a consequence, gas power plants could be a necessary complement in systems dominated by intermittent or inflexible generation that otherwise would have low security of supply.

Not all gas usage is non-renewable or contributes to climate change. A by-product from landfills, called biogas, consists of methane (CH_4) that is chemically identical to the CH_4 in dry gas. Per carbon atom, CH_4 has about 20 times stronger GHG potential than CO_2, so combusting or converting landfill gas rather than venting it reduces the impact on the climate correspondingly. Our hydrogen infrastructure model is relevant for biogas and other feedstocks in place of NG for decentralized production.

Fourier (1824) is credited with the discovery that gases in the atmosphere make the surface temperature of the Earth higher than it would be otherwise. When visible light hits the surface of the earth it is partly reflected, and the remainder is absorbed and emitted as radiant heat. Visible light passes easily through the atmosphere, but infra-red light (radiant heat) has a longer wave length that corresponds to the energy levels of the GHG molecules. The heat that cannot escape accumulates and causes the globe to heat.

The atmospheric concentration of CO_2 vary with a long geological cycle, and individual atmospheric carbon atoms are recycled in a shorter biological cycle with no net impact on the concentration (Cox, Betts, Jones, Spall, and Totterdell, 2000). This biological cycle, where growing plants bind carbon temporarily until they rot, burn or get eaten by animals, should not be confused with the human interference with the geological cycle. The geological cycle has a length of hundreds of millions of years. The atmospheric concentration falls when organic material gets trapped under layers of mud and cannot return. Gradually the organic material turns to coal, oil or gas. When a volcano happens to erupt through a layer of fossil material, then the carbon returns to the atmosphere.

When humans burn fossil fuels we have a similar interference. During the 200 years since the start of the industrial era, the CO_2 concentration has increased from 260-70 to 380 ppm (Wigley, 1983). Even in a geologic time perspective this rate of change is infrequent. Warm sea is able to absorb less CO_2, when the glaciers melt then less sunlight will be reflected, when the permafrost melts then organic material will rot, rain forests can turn to desserts and so on. The climatic system is rather complicated with such self-reinforcing feedback loops and time lags, so the eventual consequence of this sudden change is still unknown. The observed change in the global temperature over the last hundred years that can be attributed to the mentioned accumulation of greenhouse gas is less than one

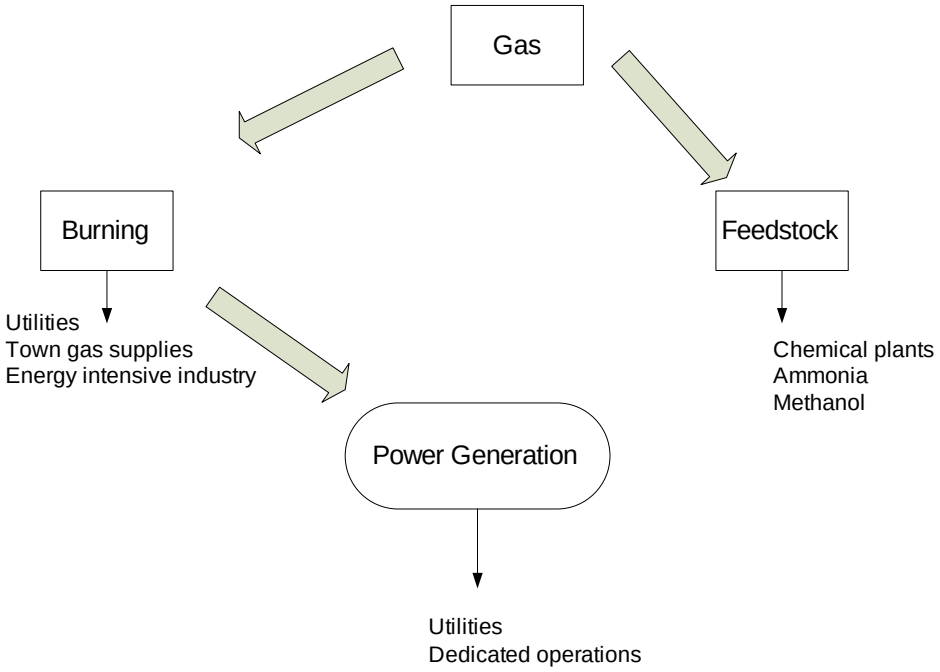

Figure 1.1: Alternative uses of dry gas

degree. One degree does not seem to be much to worry about, but it corresponds to a large amount of energy that can upset meteorological balances and trigger feedback loops. We do not know which scenario will occur, but preparing only for the best case could get expensive if it turns out that we have to adapt to a very different climate (Stern, 2006).

Physical and chemical properties of natural gas

Regardless of the final usage of the NG, the stream of rich gas from the well must be pre-processed to ensure safe operation of the infrastructure. The first stage of this treatment is a phase separation, followed by recovery of anti-freeze, metals such as mercury and acids such as CO_2 and H_2S. After the pre-treatment, the different hydrocarbons are separated into dry and wet gas. Dry gas is the main component, and it consists mainly of methane. Dry gas can be prepared further as illustrated in Fig. 1.1 (Seddon, 2006). Some of chemicals synthesized from methane are used as fuels, and others are inputs to the production of goods where the energy content is not the primary purpose. Examples of non-energy

products are cement, fertilizer, metals, and glass. Examples of synthesized fuels are hydrogen and Fisher-Tropsch (F-T) diesel. Conversion is beneficial for example when the raw gas is of such a quality that it is impractical to process it to pipeline grade, if the reserve is too small to defend investment in a liquefaction plant, or when pipelines would be impractical for geographical and other reasons (Mokhatab et al., 2006, ch 1.8). Conversion of gas to other chemicals, such as the gas to liquid (GTL) products methanol, F-T diesel and ammonia, is usually less energy efficient than to ship and use the NG as it is. However, GTLs have other advantages, they are liquids near ambient temperature and pressure, and they are therefore cheaper to transport (Seddon, 2006, ch 8,12). In order to tell whether conversion is preferable, the costs of alternatives such as conversion to other chemical products on site should be compared to the cost of the best suited of the transport alternatives.

There are several transport alternatives for dry gas. It can be compressed for shipment in pipelines or gas cylinders, or it can be liquefied to LNG. The relative importance of fixed and variable cost components vary across the mentioned alternatives. For large volumes and long distances, the relatively low investment cost per km of LNG shipment can justify the high cost of terminals at each end. For large volumes and relatively shorter distances, the relatively low variable cost of pipeline transport of compressed gas balances its rather high investment cost per km. For small volumes, the variable cost is less important and transport in gas cylinders is preferred because it has the lowest fixed cost.

The different alternatives for NG preparation differ in their energy efficiency. Gas compression is the least inefficient, followed by the phase transition into LNG, and the most inefficient is synthesis into new chemicals. We evaluate the efficiency of the physical or chemical processing of an energy stream with the change in a measure of energy quality called *exergy*. The exergy level corresponds to the theoretical maximum amount of electricity or mechanical work the given energy stream can be converted into.

The physical properties that make it a stable molecule explains why conversion of methane causes relatively large exergy losses. The practically only naturally occurring reaction of methane is with oxygen to the very stable molecules CO_2 and water (Seddon, 2006, ch 7). Therefore the main method for methane conversion involves a partial (oxygen deficit) combustion into a mixture of hydrogen and carbon monoxide, called synthesis gas (syn-gas). Unlike methane, syn-gas has the instability (potential energy) that is necessary for reactions. A conversion from methane to syn-gas is like rolling a ball up a hill, energy must be added to the system. Due to friction the total energy of the system will inevitably loose quality. The extra costs of converting methane rather than selling it as it is, is not only lost energy quality but also the capital cost of more complicated and expensive processing equipment. Syn-gas can also be made by partial combus-

tion of other fuels such as wood or coal, which then substitute for dry gas as an input to energy intensive products. In fact, the first syn-gas production was the conversion of coal in gasworks in the 19th century (Tarr, 2004).

So even if hydrogen is not yet produced commercially to be used as an energy carrier, the production process is a mature technology (Gibbins and Chalmers, 2008). Therefore, cost and efficiency surprises on both the upside and downside are unlikely.

1.3 Mathematical representation of gas in techno-economic models

Technological relationships must be formulated mathematically in order to be integrated in economic models. In models developed by economists alone, technological constraints are usually kept simple and limited to mass and energy balances, and aggregated production or cost functions. This is an opportunity for researchers who are interested technological details. The representations of real world processes in optimization models need not be limited to analytical equations and inequalities. Heuristics exist that can handle numerical formulations, which can give a relatively more realistic representation of for example fluid mechanics and thermodynamics.

Boyle (1660) provide one of the earliest mathematical models of the properties of gas, the inverse proportion between pressure and volume. Carnot (1824) is often described as the "Father of thermodynamics". He made an idealised mathematical model of a system able to transfer heat from a cold reservoir to a hot, called the Carnot cycle, which is an essential mechanism in NG liquefaction. Several experiments have been performed and statistically analysed between Boyle's days and today. Combinations of such empirical equations form the technological constraints of our optimization models. An important cost component of the equipment employed to prepare and transport gas is the mechanical work that must be added. Such addition requires capital and energy. For example, the investment costs of compressors are approximated with mathematical functions of discharge pressure and effect. Similarly, a compressor's effect is approximated with a function of flow rate and how much it increases pressure. Weymouth (1912) formulated mathematically the properties of gas flow in pipelines. In his model, gas flow is a function of the pipeline's end pressures, length and diameter.

Linearised versions of equations for compressor work and pipeline flow are among the constraints of the models described in paper 1 and 2. Other constraints in these two models are linear mass and energy balances, and investment cost functions that non-convex due to economies of scale (EOS). The non-convex functions are linearised with special ordered sets of type 2 (SOS2), (Beale and

Tomlin, 1969). SOS2 is based on binary variables, and the resulting problem is a mixed integer program (MIP). This structure, where the constraint set for the whole model consists of analytical equations that can be solved simultaneously, is a suitable application for mathematical programming (MP). The models in paper 1 and 2 are implemented and solved with Xpress-IVE version 1.18.02. The MIP solver is based on Dantzig (1963)'s simplex method in combination with dual simplex, Newton barrier interior point, branch-and-bound and branch-and-cut algorithms (Dash, 2007). MP based solvers can guarantee convergence to the global optimum *of the model* (Floudas, 1999; Edgar, Himmelblau, and Lasdon, 2001). If too few equations are included in the model, then the model optimum could be very different from the real world optimum. Such models can be made more realistic by adding more (possibly non-linear) equations. If too many equations are added then the model gets intractable and cannot be solved within reasonable time.

The two models of NG liquefaction described in paper 3 and 4 are hard to formulate sufficiently realistic with a tractable equation based model. Therefore, the models consist of individual equation sets for each process unit that are solved sequentially. The cost of making the model more realistic with such numerical formulations is that no gradients will be available, and such model formulations cannot be combined with MP solvers. This provides a role for heuristics, which can be applied to sequentially solved models and other instances that do not return gradient information. Paper 3 describes an application of a meta-heuristic to find the static settings such as refrigerant composition, flows, temperatures and pressures that minimize energy waste during NG liquefaction with a PRICO process (Barclay and Denton, 2005). Paper 4 describe a similar method applied to a value chain that consists of a combined LNG regasifier and CO_2 liquefier, and a combined LNG and LCO_2 carrier.

An illustration of the need for accurate modelling is the temperature difference between the hot feed stream and the cold refrigerant stream of a heat exchanger (Gundersen and Naess, 1988). In this case good solutions could be close to infeasible solutions. A small temperature difference is good for efficiency because less mechanical work needs to be added to the system. If the difference is zero then the heat transfer will be reversible (without losses), but take infinitely long time (or an infinitely large heat exchanger). And if the sign of the temperature difference is reversed then the stream that was supposed to be chilled will be heated. Therefore it can be beneficial to focus on fine-tuning of details such as pressures, temperatures, and flow rates to get as close as possible to the ideal thermodynamic limit.

You cannot know a-priori where the optimization effort will pay-off the most, but existing research results can give an indication. According to Seddon (2006) there are no major opportunities to improve the fundamentals of the LNG pro-

cess. Liquefaction of NG is an energy and cost intensive process, and LNG plants usually keep the same design during their lifetime. Ignoring all structure in the time dimension is convenient because it lets us direct all computational capacity towards the details of the process to get it close to the limit of what is thermodynamically possible.

An opportunity to improve existing economic models

Unlike natural scientists - economists cannot do real world experiments, but must resort to experiments on models. Several types of models exist. The two types considered in this thesis are optimization models for planning and econometric models for statistical analysis. A basic simplification in both econometric and optimization models is to isolate the interesting phenomena. In this case you must identify possible interactions, balance the insight and computational complexity that the features add, and then formulate the worthwhile interactions mathematically. A useful model is rigorous enough to give new insight, and still simple enough to be solvable with the available computer in the available time. The available time for computations usually depends on the type of problem. Long-term decisions such as investments can sometimes wait until the next day or later so more time is available for an accurate solution. Short-term decisions, on the other hand, could in some instances get outdated unless its available within minutes.

The priority of which phenomena to give the most realistic representation cannot always be done a-priori. In addition to ignoring feedbacks (for example pressure/flow or volume/average cost), a model can be simplified by aggregating variables. Typical aggregation is to make the resolution in one or more dimension (*time* in paper 1,2 and 5) coarser. Coarseness increase when numbers that vary within intervals are collapsed into their sums or averages. Such aggregations make variables that are zero on average disappear, for example flow in and out of storages. If storage operation is the phenomena you find interesting then you need fine enough time steps for flows in and out to occur at distinct points. In econometric time series modelling, aggregation of points in time could be necessary to reduce serial correlation.

Apparently most of the existing models used to plan the introduction of hydrogen do not apply optimization methods. Wietschel, Hasenauer, and de Groot (2006) provide a survey of alternative hydrogen pathways discussing costs and CO_2 emissions. They aggregate estimates of the resulting costs and emissions from each pathway. Their survey is similar to our approach in the sense that it does not take into account the indirect impact on prices and emissions elsewhere in the energy system, nor the additional cost of fuel cell vehicles. Different types of fuel cell vehicles are included in the survey of Svensson, Möller-Holst,

Glöckener, and Maurstad (2007), who have studied the theoretical emissions of a selection of well to wheel car fuel value chains. Stiller, Svensson, Möller-Holst, Bünger, Espegren, Holm, and Tomasgard (2008) compare analytically different alternatives to supply hydrogen in Germany that is produced with energy from Norway. Neither Svensson et al. (2007) nor Stiller et al. (2008) attempt to optimize the value chain. On the other hand, several types of LNG value chain optimization models exist. For example Foss and Halvorsen (2009) who have optimized the dynamic properties of an LNG value chain, and Grønhaug and Christiansen (2009) who have optimized the LNG fleet management, liquefaction plants, and regasification terminals.

Computational resources are usually limited, so there is an inevitable trade-off between width of scope and level of detail. Energy system models are typically aggregated in geography and time dimensions and technological details must be highly stylized. Most MARKAL applications do for example assume linear investment cost (no economies of scale, EOS). They are therefore less suitable to aid the investment planning of individuals. This issue provides a role for lower level models such as ours where details rather than width are given priority.

In our planning models, the decision makers are assumed to behave as if they do not influence input factor or product prices. Therefore, all decisions are optimized conditional on prices. The absence of a volume/price feedback reduces mathematical complexity, and if the real decision makers actually do this assumption, it also increases realism. Regardless of whether decision makers believe that they influence prices or not, prices are determined by their interaction with other relevant decision makers. Relative to our "lower level" minimization of the individual decision makers' cost, a market interaction equilibrium model or a total energy system model could be at an "upper level". Typical past responses of market clearing prices to external events can also be analysed statistically.

Market equilibrium prices will only lead to an optimal resource allocation when the owners of all factors have enforceable property rights and are rational and informed so all prices are fair. The right to emit fossil CO_2 is one of the input factors in our planning models. From the point of view of the decision makers, the cost to society due to the accumulation of emissions has previously been external and "free". For an efficient resource allocation, all costs should be internalized with a carbon price equal to the true societal cost. The cost of climate gas emissions would equal the marginal damage to the victims (Kolstad, 2000). Damages are not directly measurable in monetary units, but probably closer to the present carbon price than zero.

We assume that decentralized decision makers treat the carbon price as an exogenous variable that internalizes the marginal damage, and chose a level of abatement and a type of technology where their private marginal costs and benefits balance. Due to the positive externalities from the development of technol-

ogy, introducing a carbon price cannot guarantee an efficient level of spending on abatement technology development. For efficiency, positive externalities should be internalized with subsidies (analogous the internalization of negative externalities with taxes). Therefore a carbon price will not necessarily be the optimal energy market instrument. In order to balance the positive and negative externalities, several types of tradable certificates that replicate combinations of taxes and subsidies have been developed (Bye and Bruvoll, 2008). Our decision support models can be modified to take such incentives into account.

Exchange of data between models of complementing priorities is studied in several papers. McFarland, Reilly, and Herzog (2004) present a methodology that translates bottom up engineering information for two CCS technologies into production functions. These functions are intended for computable general equilibrium (CGE) models of the world economy such as the MIT Emissions Prediction and Policy Analysis (EPPA). Nakata (2004) discusses energy-economic models in general and explains how various modelling levels ranging from top-down macroeconomic to bottom-up engineering models complement each other when run recursively. Pacific Northwest National Laboratory's Global Change Assessment Model (GCAM) (Edmonds, Wise, Pitcher, Richels, Wigley, and MacCracken, 1996) is an integration of the ERB (Edmonds-Reilly-Barns) energy-economic model, the Model for the Assessment of GHG Induced Climate Change (MAGICC), and the Model for Evaluating the Regional and Global Effects of GHG reduction policies (MERGE) model.

Many researchers are specialists and have outstanding knowledge of one discipline, and are aware of all possible interactions and feedbacks within their own field. Other researchers have more overview, and are able to formulate models that include feedbacks or limitations that originate in a combination of disciplines, such as markets and physics. For example, McFarland et al. (2004) are concerned that economists extrapolate technological progress beyond what is thermodynamically possible. Technological knowledge can also be used to aid meaningful decompositions. For example, if there are no interaction between the process details of an LNG liquefier and its size, i.e. it scales up or down linearly, then these two features can be optimized individually. Economic knowledge to identify whether there are or are not interactions with the world outside the modelled system is useful to find suitable model end-points. Markets where the decision makers assume they have no influence over prices (no volume/price feedback) are suitable end-points for value chain models. For example, we have chosen the input factor markets at the upstream end and consumers of fuel at the downstream end as the boundaries of our hydrogen models.

The hydrogen and LNG infrastructure cases have very different properties both financially and physically. Thus they are able to illustrate how the real-world structure affects the mathematical properties of the corresponding model, and

then how the preferred solution method depends on the mathematical properties of the model. For hydrogen distribution cases, we assume prices, volumes, and efficiencies vary over time. Therefore we formulated a model that takes this into account. Because the model's focus is on the timing and type of investments, there are less resources left for rigorous modelling of technological details. On the other hand, the relatively energy intensive LNG process benefits more from details such as thermodynamics rather than a complicated structure in geography or the time dimension. In order to give a more realistic representation of the feedback loops and circular references, we have formulated a model based on individual equation sets for each process unit, which are solved sequentially so no gradient information is available. Meta-heuristics (MH) work without gradient information, and therefore can be applied to numerical models. The disadvantage of MHs is that they cannot prove optimality, only search for better solutions.

1.4 Gas price models

Both the LNG and the hydrogen infrastructure optimization frameworks are designed for a single sector with a single energy carrier, so the decision maker treats all prices as exogenous. Long-run price forecasts are necessary to make good investment decisions. Such forecasts can for example can be provided by optimization models that are able to return the prices that balance supply and demand because they include the entire system of provisions and usages of energy resources. These prices can be direct decision variables or indirect shadow prices. Short-run price forecasts to base operational decisions on can be provided by an econometric model such as the one presented in paper 5.

Regardless of whether decision makers optimize or use "rules of thumb", possible outcomes and their estimated probabilities, called scenarios, are useful. Planning of real and financial asset investments are often conditioned on scenarios for different energy commodities. Further discussions of the role of forecasting in planning and strategy can be found in Makridakis (1996), Makridakis, Wheelwright, and Hyndman (1998), and Gooijer and Hyndman (2006). Discussion of the importance of modelling and forecasting energy prices for real investment analysis can be found in Dixit and Pindyck (1994), Pindyck (1999) and Pindyck (2001).

Econometric regression models are a type of optimization models where the fitment of parameters to a set of observations is optimized rather than physical activities. The influence of the independent variables on the dependent variables is typically additive or transformed to be additive before estimation (Greene, 2000). Then you test statistically the strength of the hypothetical relationship, which is a measure of how well it fits real world data. These tests are only valid if certain assumptions about the statistical properties of the parameters

are met, which could need another layer of tests. The tests typically determine how likely it is that the apparent relationship is not a coincidence. The included independent variables never explain all variation of the dependent variable in a statistical model. Therefore, econometric modelling has several pitfalls. If the independent variables are correlated, it will be difficult to separate their influence. If their mutual correlation is perfect or nearly perfect, it will result in numerical problems. Furthermore, the dependence can vary over time or with circumstances. You cannot tell in advance whether or not the statistical estimates of patterns in historical observations will remain. It is hard to draw a line for how minimal influences should be included, hard to obtain observations of all possible influences, and on whether the independent variables really are independent (no feedbacks from the dependent variables).

The time series literature includes several model types that can be applied to estimate price scenarios. A typical issue in time series modelling is that the underlying stochastic process often turns out to be non-stationary, i.e. its parameters vary over time. If a stochastic process consists of at least one time-varying parameter, then neither the stationary nor the time-varying parameters of that process can be estimated consistently with classical linear regression. Non-stationary processes can sometimes be transformed to be stationary. For example, if the price level is non-stationary, but the price growth is stationary, then the parameters can be fitted to the period-on-period changes in the observations rather than observations directly. Alas, information will be lost when levels are eliminated. In a so-called *state space* model, parameters are estimated on-line with the Kalman filter and need not be stationary. Such models can be applied to test whether each individual parameter is stationary or time-varying (Harvey, 1989; Durbin and Koopman, 2001; Commandeur and Koopman, 2007). Details of the method are available in the STAMP™ software manuals.

Bibliography

Aspelund, A., Gundersen, T., 2009. A liquefied energy chain for transport and utilization of natural gas for power production with CO2 capture and storage - Part 1. Applied Energy 86 (6), 781–792.

Aspen Technology, Inc., December 2009. Aspen HYSYS. `http://www.aspentech.com/hysys/`.

Baker, E., Clarke, L., Shittu, E., 2008. Technical change and the marginal cost of abatement. Energy Economics 30 (6), 2799–2816.

Balmorel, September 2009. the Balmorel project. `http://balmorel.com/`.

Barclay, M., Denton, N., 2005. Selecting offshore LNG processes. LNG Journal 10 (1), 34–36.

Bayon, R., Hawn, A., Hamilton, C., 2009. Voluntary Carbon Markets. Earthscan, London, UK.

Beale, E. M. L., Tomlin, J. A., 1969. Special facilities in a general mathematical programming system for non-convex problems using ordered sets of variables. In: Lawrence, J. (Ed.), Proceedings of the 5th International Conference on Operations Research. Tavistock, London, UK.

Boyle, R., 1660. New experiments physico-mechanical, touching the spring of the air, and its effects. Oxford, UK.

Bye, T., Bruvoll, A., 2008. Multiple instruments to change energy behaviour: The emperor's new clothes? Energy Efficiency 1 (4), 373–386.

Carnot, S., 1824. Réflexions sur la puissance motrice du feu. Chez Bachelier, Paris, France.

Cavin, L., Fischer, U., Glover, F., Hungerbüler, K., 2004. Multi-objective process design in multi-purpose batch plants using a Tabu Search optimization algorithm. Computers & Chemical Engineering 28 (4), 459–478.

Chelouah, R., Siarry, P., 2005. A hybrid method combining continuous tabu search and Nelder-Mead simplex algorithms for the global optimization of multiminima functions. European Journal of Operational Research 161 (3), 636–654.

Commandeur, J., Koopman, S., 2007. An introduction to State Space Time Series Analysis. Oxford University Press, Oxford, UK.

Cox, P. M., Betts, R. A., Jones, C. D., Spall, S. A., Totterdell, I. J., 2000. Acceleration of global warming due to carbon-cycle feedbacks in a coupled climatemodel. Nature 408 (750), 184–187.

Dantzig, G. B., 1963. Linear programming and extensions. Princeton University Press, Princeton, New Jersey.

Dash, 2007. Xpress-Optimizer Reference Manual, Release 18. Dash Optimization Ltd, 560 Sylvan Avenue, Englewood Cliffs, NJ 07632, USA.

Dixit, A. K., Pindyck, R. S., 1994. Investment under uncertainty. Princeton University Press, Princeton, NJ.

DTI, 2007. Meeting the energy challenge, a white paper on energy. Tech. rep., Department of Trade and Industry, United Kingdom.

Durbin, J., Koopman, S., 2001. Time Series Analysis by State Space Methods. Oxford University Press, Oxford, UK.

Edgar, T. F., Himmelblau, D. M., Lasdon, L. S., 2001. Optimization of chemical processes, second edition. McGraw-Hill, New York.

Edmonds, J., Wise, M., Pitcher, H., Richels, R., Wigley, T., MacCracken, C., 1996. An integrated assessment of climate change and the accelerated introduction of advanced energy technologies: An application of MiniCAM 1.0. Mitigation and Adaptation Strategies for Global Change 40 (4), 311–339.

Endo, E., 2007. Market penetration analysis of fuel cell vehicles in Japan by using the energy system model MARKAL. International Journal of Hydrogen Energy 32 (10-11), 1347–1354.

ETSAP, September 2009. Markal. `http://etsap.org/markal/main.html`.

Eydeland, A., Wolyniec, K., 2003. Energy and Power risk management. John Wiley & sons, Hoboken, New Jersey, USA.

Floudas, C. A., 1999. Deterministic global optimization. Kluwer Academic Publishers, Dordrecht.

Foss, B. A., Halvorsen, I. J., 2009. Dynamic optimization of the LNG value chain. In: Alfadala, H., Reklaitis, G. R., El-Halwagi, M. (Eds.), Proceedings of the 1st Annual Gas Processing Symposium. Quatar, pp. 10–18.

Fourier, J., 1824. Remarques générales sur les températures du globe terrestre et des espaces planétaires. Annales de Chimie et de Physique. 27, 136–167.

Gibbins, J., Chalmers, H., 2008. Carbon capture and storage. Energy Policy 36 (12), 4317–4322.

Glover, F., August 1986. Future paths for integer programming and links to artificial intelligence. Computers and Operations Research 13 (5), 533–549.

Gooijer, J., Hyndman, R., 2006. 25 years of time series forecasting. International Journal of Forecasting 22 (3), 443–473.

Greene, W. H., 2000. Econometric Analysis, 4th Edition. Prentice Hall International, Upper Saddle River, N.J.

Grønhaug, R., Christiansen, M., 2009. Supply chain optimization for the liquefied natural gas business. In: Nunen, J. A., Speranza, M. G., Bertazzi, L. (Eds.), Innovations in Distribution Logistics. Vol. 619. Springer, Berlin, DE, pp. 195–218.

Gundersen, T., Naess, L., 1988. The synthesis of cost optimal heat exchanger networks. Computers & Chemical Engineering 12 (6), 503–530.

Harvey, A. C., 1989. Forecasting, structural time series models and the Kalman filter. Cambridge University Press, Cambridge, UK.

Hedar, A. R., Fukushima, M., 2006. Tabu search directed by direct search methods for nonlinear global optimization. European Journal of Operational Research 170 (2), 329–349.

Holth, C. B., Saue, L. E., 2005. Economic optimization of hydrogen infrastructure in the transport sector. Master's thesis, NTNU.

IEA, 2008. World energy outlook. Tech. rep., International Energy Agency, 9 rue de la Fédération 75015 Paris, France.

IPCC, 2005. Carbon dioxide capture and storage. Tech. rep., the Intergovernmental Panel on Climate Change.

Karlsson, K., Meibom, P., 2008. Optimal investment paths for future renewable based energy systems-using the optimisation model Balmorel. International Journal of Hydrogen Energy 33 (7), 1777–1787.

Kolstad, C. D., 2000. Enviromental Economics. Oxford University Press, New York.

Koopman, S., Harvey, A., Doornik, J., Shephard, N., September 2009. Structural Time Series Analyser, Modeller and Predictor. `http://stamp-software.com/`.

Lee, J., List, J., Strazicich, M., 2006. Non-renewable resource prices: Deterministic or stochastic trends? Journal of Environmental Economics and Management 51 (3), 354–370.

Lin, Z., Ogden, J., Fan, Y., Sperling, D., 2005. The hydrogen infrastructure transition model (HIT) and its application in optimizing a 50-year hydrogen infrastructure for urban Beijing. Tech. rep., Institute of Transportation Studies, University of California, Davis, USA.

Makridakis, S., 1996. Forecasting: its role and value for planning and strategy. International Journal of Forecasting 12 (4), 513–537.

Makridakis, S., Wheelwright, S., Hyndman, R., 1998. Forecasting: Methods and Applications. Wiley, New York, USA.

McFarland, J., Reilly, J., Herzog, H., 2004. Representing energy technologies in top-down models using bottom-up information. Energy Economics 26 (4), 685–707.

Midthun, K. T., 2007. Optimization models for liberalized natural gas markets. Ph.D. thesis, Norwegian University of Science and Technology, Trondheim, Norway.

Mokhatab, S., Poe, W. A., Speight, J. G., 2006. Handbook of natural gas transmission and processing. Gulf Professional Publishing, Burlington, MA, USA.

Nakata, T., 2004. Energy-economic models and the environment. Progress in Energy and Combustion Science 30 (4), 417–475.

Nelder, J. A., Mead, R., 1965. A simplex method for function minimization. The Computer Journal 7 (4), 308–313.

Pindyck, R., 1999. The long-run evolution of energy prices. The Energy Journal 20 (2), 1–27.

Pindyck, R., 2001. The dynamics of commodity spot and future markets: A primer. The Energy Journal 22 (3), 1–29.

Seddon, D., 2006. Gas usage & value. PennWell, Tulsa, OK, USA.

Serletis, A., 2007. Quantitative and Empirical Analysis of Energy Markets. World Scientific, Singapore.

Serletis, A., Gogas, P., 1999. The north american natural gas liquids markets are chaotic. The Energy Journal 20 (1), 83–103.

Stern, N., January 2006. The economics of climate change. Technical report, Cabinet Office - HM Treasury, 1 Horseguards Road, London SW1A 2HQ.

Stiller, C., Svensson, A. M., Möller-Holst, S., Bünger, U., Espegren, K. A., Holm, Ø. B., Tomasgard, A., 2008. Options for CO2-lean hydrogen export from Norway to Germany. Energy 33 (11), 1623–1633.

Svensson, A. M., Möller-Holst, S., Glöckener, R., Maurstad, O., 2007. Well-to-wheel study of passenger vehicles in the Norwegian energy system. Energy 32 (4), 437–445.

Tarr, J. A., 2004. Manufactured gas, history of. In: Cleveland, C. J. (Ed.), Encyclopedia of Energy. pp. 733–743.

Tseng, P., Lee, J., Friley, P., 2005. A hydrogen economy: Opportunities and challenges. Energy 30 (14), 2703–2720.

Tzimas, E., Merciera, A., Cormosa, C.-C., Peteves, S. D., 2007. Trade-off in emissions of acid gas pollutants and of carbon dioxide in fossil fuel power plants with carbon capture. Energy Policy 35 (8), 3991–3998.

Unruh, G. C., 2000. Understanding carbon lock-in. Energy Policy 28 (12), 817–830.

Vallentin, D., 2008. Driving forces and barriers in the development and implementation of coal-to-liquids (CtL) technologies in Germany. Energy Policy 36 (6), 2030–2043.

Westgaard, S., Faria, E., Fleten, S.-E., 2008. Price dynamics of natural gas components: Empirical evidence. Journal of Energy Markets 1 (3), 37–68.

Weymouth, T., 1912. Problems in natural gas engineering. Transactions of the American Society of Mechanical Engineers 34 (1349), 185–231.

Wietschel, M., Hasenauer, U., de Groot, A., 2006. Development of European hydrogen infrastructure scenarios-CO2 reduction potential and infrastructure investment. Energy Policy 34 (11), 1284–98.

Wigley, T. M. L., 1983. The pre-industrial carbon dioxide level. Climatic Change 5 (4), 315–320.

Paper I

J. Myklebust, C. B. Holth, L. E. S. Tøftum and A. Tomasgard:

Optimizing investments for hydrogen infrastructure in the transport sector

Submitted to an international journal

Optimizing investments for hydrogen infrastructure in the transport sector

Abstract:
Hydrogen can be produced from any primary energy source, and if it is consumed in fuel cells it does not cause any local emissions. We expect that the demand for hydrogen as an energy carrier in the transport sector will increase because of the political willingness to exploit these properties to reduce pollution and diversify primary energy sources. This paper presents the strategic part of an optimization framework for the development of a hydrogen infrastructure. The choice between electrolysis and steam methane reforming (SMR) at different locations and points in time is used as a test case. SMR can either be centralized, which takes advantage of the process' economies of scale and allows CO_2 capture and sequestration (CCS), or decentralized exploiting existing energy infrastructure. We study one area, which consist of regions of the same population distribution and size as the 16 "Bundesländer" in Germany. We model the regions as a set of nodes with different populations and distances. Both hydrogen demand growth and relative input prices are modelled as deterministic. Our three different cases differ in their combination of these prices. The case results illustrate how different price combinations affect the optimal choice of technology.

2.1 Introduction

Fossil fuels such as oil and natural gas satisfy most of the present transportation sector fuel demand. Hydrogen is one of the energy carriers that energy companies and governments consider a future substitute for fossil fuels. The main motivation to establish a hydrogen infrastructure is to diversify away from fossil fuels, which are depletable and cause large emissions of greenhouse gases (GHG).

In this paper we present an optimization model intended to support the choice of technology, timing and geographic allocation of a hydrogen infrastructure for the transport sector. The model outputs are a cost minimizing investment schedule with a 50 year horizon for hydrogen production, carbon capture and sequestration (CCS), distribution of both H_2 and its by-product CO_2, as well as the yearly operational decisions of these investments. The model inputs are investment costs, feedstock prices, regional populations and demand projections. Though the total inter-regional hydrogen demand is assumed exogenous, the model has the flexibility to allocate demand across the different regions.

To our knowledge, most of the research that concerns the introduction of hydrogen does not apply optimization methods. Wietschel, Hasenauer, and de Groot

(2006) provide a survey of alternative hydrogen pathways discussing costs and CO_2 emissions. They aggregate estimates of the resulting costs and emissions from each pathway. Their survey is similar to our model in the sense that it does not take into account the indirect impact on prices and emissions elsewhere in the energy system, nor the additional cost of fuel cell vehicles. Svensson, Möller-Holst, Glöckener, and Maurstad (2007) have studied the theoretical emissions of a selection of well-to-wheel car fuel value chains. Their study includes several alternative value chains for hydrogen fuel as well as types of hydrogen vehicles. Conventional cars and fuel are included for comparison. They do not attempt to optimize the value chain. Stiller, Svensson, Möller-Holst, Bünger, Espegren, Holm, and Tomasgard (2008) compare analytically different alternatives to supply hydrogen in Germany that is produced with energy from Norway.

Only a few detailed optimization models seem to exist. Ogden (2004) has minimized the total length of a hydrogen pipeline network and the operational costs of various supply chain scales in separate operation steps. However, because these local optimizations are not coordinated, her model cannot take into account economies of scale. Another approach is the dynamic programming model of Lin, Ogden, Fan, and Sperling (2005) for the H_2 infrastructure transition. Their case is a large city, Beijing. In comparison with our model, their model includes more of the details of the local distribution within a region and less of the inter-regional shipment.

Hugo, Rutter, Pistikopulos, Amorelli, and Zoia (2005) present a model of the development of a hydrogen infrastructure that has a dual objective that trades off costs and CO_2 emissions. In our opinion this local trade-off is likely to result in an implicit CO_2 price that is not necessarily consistent with the market price in all other sectors. Like many other models it distinguishes between the various electricity generation technologies' CO_2 emissions, which we believe is irrelevant unless you have a global perspective with respect to both energy sectors and geographical regions. Our optimization framework is designed for a single sector with a single energy carrier. Therefore we model all prices as exogenous in order to avoid such inconsistencies.

Prices need to be output from a multi-sector model spanning several energy carriers and several sectors (e.g. households, industry, transportation). We draw the boundaries of our single-sector model at the secondary/ intermediate energy markets at the upstream end and at consumer fuel demand at the downstream end. Our framework consists of an investment model that is complemented with a short-term operational model (Myklebust, Holth, Saue, and Tomasgard, 2009). The investment model is intended to be run iteratively with global models that include several sectors and fuels to verify prices and exchange quantities. Our investment and operational models' positions relative to other types of models

are illustrated in the graphical classification of Lesourd, Percebois, and Valette (1996) in Fig. 2.1.

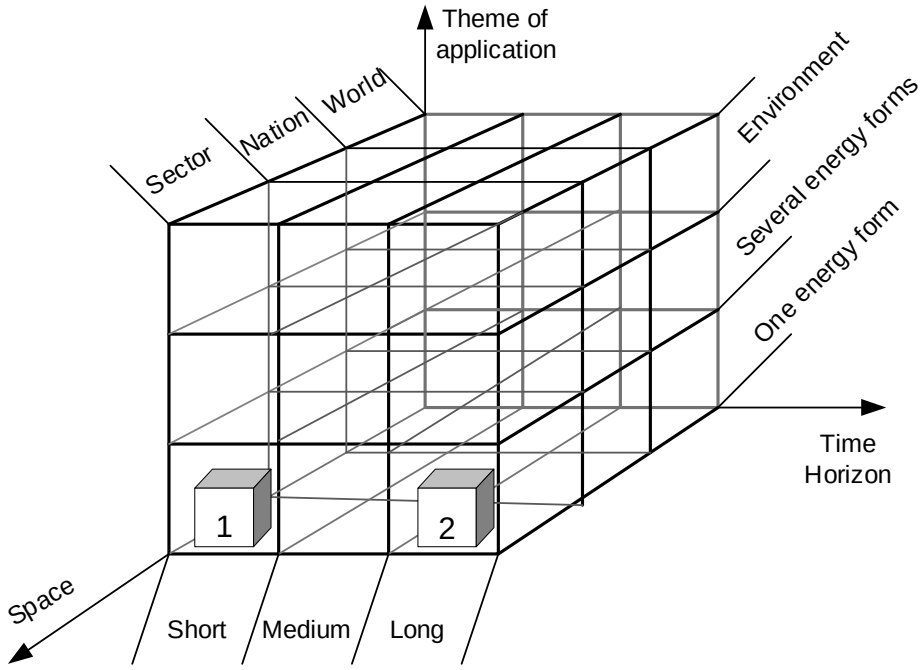

Figure 2.1: The roles of our operational (1) and investment (2) models

Several papers study the exchange of data between energy models that have different foci and hence complement each other. McFarland, Reilly, and Herzog (2004) present a methodology that translates bottom up engineering information for two CCS technologies into the MIT Emissions Prediction and Policy Analysis (EPPA) of the world economy. Nakata (2004) discusses energy-economic models in general and explains how various modelling levels ranging from top-down macroeconomic to bottom-up engineering models complement each other when run recursively. Pacific Northwest National Laboratory's Mini Climate Assessment Model (MiniCAM) (Edmonds, Wise, Pitcher, Richels, Wigley, and MacCracken, 1996) is an integration of the ERB (Edmonds-Reilly-Barns) energy-economic model, the Model for the Assessment of GHG Induced Climate Change (MAGICC), and the Model for Evaluating the Regional and Global Effects of GHG reduction policies (MERGE) model.

The most common multi-sector/multi-fuel infrastructure models that include hydrogen are various applications of Balmoral and IEA's MARKAL (MARKet ALlocation) energy system models. For example Karlsson and Meibom (2008), Endo (2007), Tseng, Lee, and Friley (2005), and DTI (2007) have simulated some of the effects of the hydrogen introduction in Scandinavia, Japan, the US and the UK, respectively. Because the MARKAL family of models include the entire energy market, they capture the interaction of hydrogen production with the rest of the energy system. Hence, they return consistent prices. There is an inevitable trade-off between width of scope and level of detail. MARKAL models typically assume linear investment cost (no economies of scale), which can lead to investments in implausibly small plants. Furthermore, they are more aggregated than our model in terms of geography, time and technological detail, and give too little detail to guide investments. There exist extensions to the MARKAL model that make it possible to include more technological details and hence decrease the aggregation level. However, they do not appear to have been implemented for practical modelling and analysis.

Also more detailed engineering models exist in the current literature. Van den Heever and Grossmann (2003) developed an MINLP optimization model for a hydrogen supply network consisting of five plants, four interconnected pipelines, and 20 customers. Their model has a monthly horizon with 12 hour resolution and it includes compressor load steps in detail. Hendriks (2006) presents a model for a European CO_2 infrastructure. Van Benthem, Kramer, and Ramer (2006) provides an options approach to investment in hydrogen infrastructure that models prices as stochastic processes.

Because our model has a narrower scope than the MARKAL models, it can include more details before it gets intractable. Such details are, for example, the division of the area into geographic regions that makes it possible to model explicitly the physical operation of the individual pipelines through pressures and flow rates. Also the delivery frequencies of trailer operations for different producer and recipient locations can be modelled. Nevertheless, our investment model is still too aggregated in the time dimension to capture short-term demand variations. Hence, it needs to be complemented with an operational model in order to verify that its investment decisions are adequate for the short-term (intra-day) peaks, see Fig. 2.2. For each of the investment model's time periods we minimize the operational cost of a selected 24 hour cycle with hourly resolution. The model of the operational cost minimization is presented separately in the paper Myklebust et al. (2009). If the capacity constraints in the operational model are violated, the concerned capacity requirement is calibrated before a subsequent run of the strategic model.

The modelling framework developed in this paper is general and easily adapted to suit other regions and production technologies. The presented test cases are

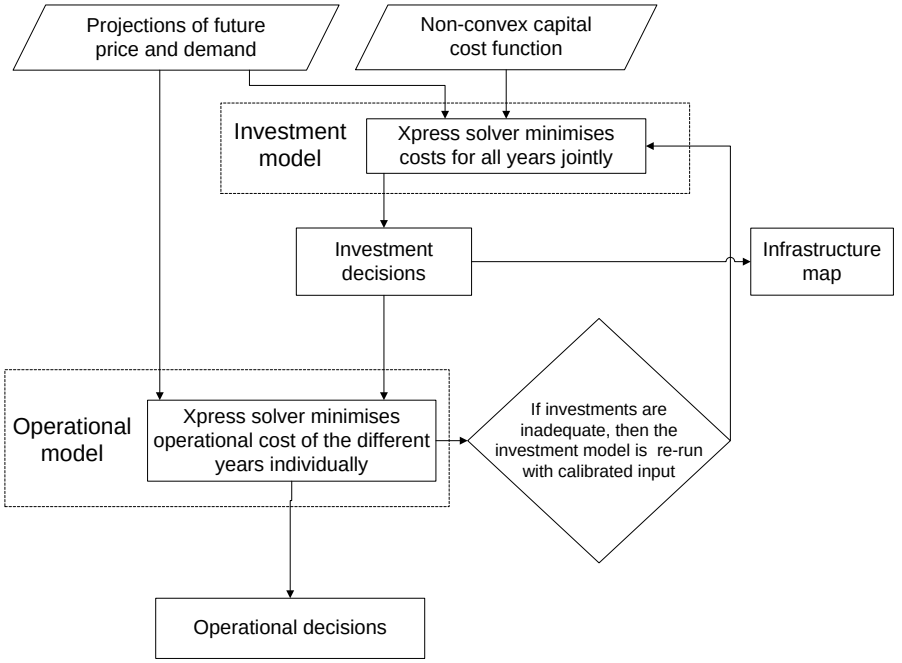

Figure 2.2: The interaction of the strategic and operational models

designed to illustrate the use of the model only. In these cases hydrogen can be produced using any combination of decentralized electrolysis or steam methane reforming (SMR) without CCS, or centralized large-scale SMR with 70% CCS. The designed geographic area is inspired by Germany. However, distances and demand projections are realistic to the order of magnitude only, and consequently not a sufficent basis for actual investment decisions.

In Section 2.2 we describe our model and its assumptions qualitatively. The mathematical formulation is given in Section 2.3. We present the base case, geographical and technological details in Section 2.4. The model is applied to this base case and two alternatives, and the results are discussed in Section 2.5. Section 2.6 concludes the paper.

2.2 Modelled value chain for hydrogen production and distribution

We model a hydrogen value chain based on both SMR and decentralized electrolysis. SMR can be centralized or decentralized. The main driver of the decisions is a requirement to supply enough hydrogen to meet exogenous demand from the transportation sector. This quantity depends on the transportation market size and hydrogen's share of that market. We include two basic methods for the distribution of hydrogen from centralized production, bulk and continuous. We assume all prices are exogenous, which requires perfect markets for all input factors. The geographic area is divided into regions with no internal structure. Prices do not vary across the regions for ease of exposition. Adding a geographic dimension to the price data would not affect computational complexity. Only a few of the regions are candidate locations for the large-scale hydrogen production facilities, while all regions are considered for hydrogen sales.

Hydrogen fuelled vehicles will not be popular before the hydrogen infrastructure exists. This means that the demand for hydrogen fuel in a region can only be stimulated if a hydrogen infrastructure is built there. Because our model is restricted to one sector and one fuel type it requires an exogenous demand projection. However, it does not require demand for individual regions, only the aggregated *inter-regional* demand. Allocation over time is exogenous for the hydrogen sales for all regions combined, but the allocation across different regions is endogenous. The purpose of this distinction is to let the allocation of supply depend on the geographic variations in average infrastructure costs, which depend on the regions' population densities and their distances to large-scale production sites. Consequently, hydrogen supply can be lower in some regions provided that it is sufficiently high in the others.

The physical units included in our optimization model are reformers, electrolysers, compressors, pipelines, storages, trailers and tow trucks. We model a hydrogen infrastructure that can consist of any combination of the following four alternative value chains:

1. Methane is steam reformed to hydrogen at a large-scale plant, and then the gaseous product is transported in bulk to the regional filling stations. This alternative will be modelled with CCS, so instead of paying to emit all produced CO_2, 70% of it will be deposited or sold for enhanced oil recovery (EOR). The consequences of CCS are reduced efficiency and higher capital and operational costs.

2. Methane is steam reformed to hydrogen at a large-scale plant. Now the hydrogen is not transported bulk, but in a set of connected inter-regional pipelines that are supplemented with intra-regional distribution branches.

Relative to bulk transportation, pipelines have higher capital cost and lower operating cost, and are therefore preferred for larger quantities and shorter distances.

3. Differently from the two alternatives above, methane is steam reformed in local small-scale plants without CCS. This requires that the existing infrastructure has enough spare capacity to supply necessary inputs. The local production cannot supply any hydrogen to filling stations in any other region. All produced CO_2 is emitted which requires carbon emission permits.

4. H_2 is produced with decentralized electrolysis of water. This detour via electric energy is relevant if it becomes sufficiently cheap during off-peak hours relative to alternative feedstocks.

The above value chains are illustrated in Fig. 2.3. They are separated by the horizontal lines. Each alternative can utilize any of the equipment above or below these dashed lines but not the solid lines. Both pipeline and bulk distribution must be combined with large-scale reforming. All alternatives require local storage compressors, but of individual types because their suction pressures differ.

We assume that prices and demands over the planning horizon are known already at time 0. Furthermore, we assume that there are no synergies in terms of willingness to share costs for CO_2 infrastructure, for example, if fossil fuelled power plants are located close to the reforming plants. Such interaction is skipped to reduce the computational complexity of the economies of scale (EOS) modelling.

A scale factor is required to ensure investments have sufficient capacities for short-term peaks. One of the intentions of our operational model is to calibrate this factor. For example, in the case study we assume that electricity is potentially cheap enough for electrolysis to be preferred over the other production alternatives during off-peak hours only. Assuming the off-peak hours amounts to one third of the day, then the production peak would be around three times higher than its average value. Hence the scale factor for electrolysers and the compressors required to store their production would equal around 3.

At each point in time there are two exogenous CO_2 prices– one for CO_2 emissions and another for CO_2 disposal (the latter can be positive or negative). The emission price can for example be a tax, an implicit price from a global energy model, or the price of tradable permits. The modelled infrastructure for CO_2 disposal consists of alternative capacities for a single main pipe and individual pipeline branches to all large-scale reformers. The model can easily be extended with alternative CO_2 sinks. We assume that sufficient spare capacity to ship CO_2 for disposal away from the main pipe's end point at the boundary of the modelled area already exists.

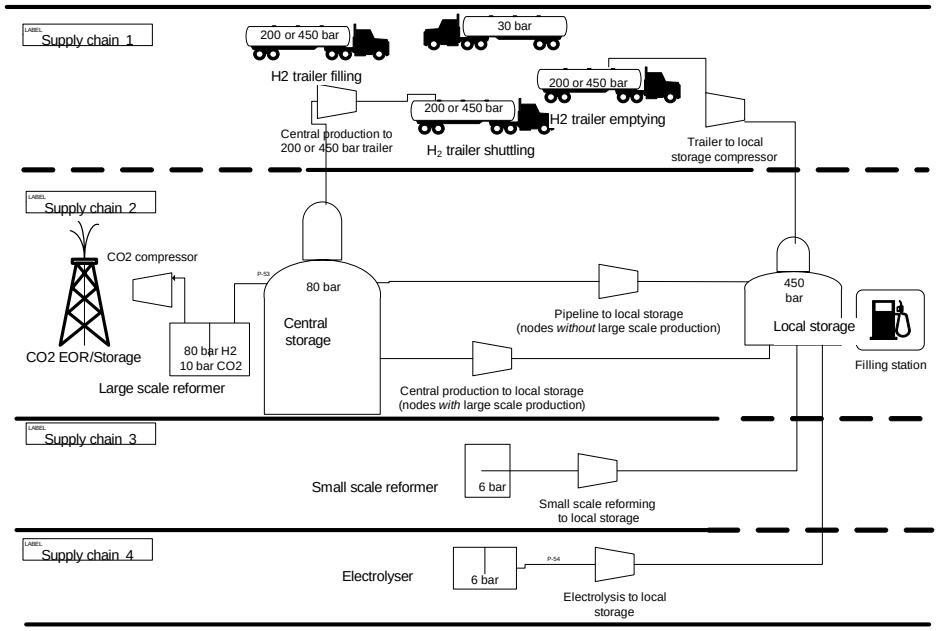

Figure 2.3: Alternative supply chains

All investment decisions need not be explicitly modelled. An example is the dispenser capacity. The total number and cost are constant for a given level of the exogenous inter-regional demand. This amount is added in the post processing. Other costs are assumed to be required in a fixed proportion to production capacity. Examples are decentralized storages and CO_2 compressors. Their costs are added to the large-scale production investment costs.

2.3 The mathematical programming model

Here we give the decision variables and constraints of our long-term infrastructure development model:

Decision variables

$b_{eps} \in \{0,1\}$	Whether it is invested a CO_2 pipeline branch of capacity e from the large-scale reformer at p.
$d_{apqt} \in \mathbb{Z}$	Departure rate [1000/year] of trailer type a from p to q.
$fx_{ept} \in \mathbb{R}$	H_2 flow [PJ/year] from reformer, electrolyser, or compressor of type e at p.
$fy_{apqt} \in \mathbb{R}$	H_2 flow [PJ/year] through a pipe of type a from p to q.
$im_{es} \in \mathbb{R}$	Investment [m€] of main CO_2 pipeline of capacity e.
$ix_{eps} \in \mathbb{R}$	Investment [m€] of equipment of type e at p.
$iy_{apqs} \in \mathbb{R}$	Investment [m€] of transport of type a from p to q.
$m_{es} \in \{0,1\}$	Whether it is invested a main CO_2 pipeline of type e.
$p_{pt} \in \mathbb{R}$	Pressure [bar] in the pipeline junction at p.
$s_{pt} \in \mathbb{R}$	H_2 sales [PJ/year] at p.
$w_{apqt} \in \{0,1\}$	Whether trailers of type a supply node q from p in year t.
$x_{eps} \in \mathbb{R}$	Capacity [PJ/year] of invested compressor, reformer, or electrolyser type e, at p.
$y_{apqs} \in \{0,1\}$	Whether it is invested a pipeline of type a from p to q.
$z_{apqs} \in \mathbb{Z}$	Number of trailers of type (capacity) a invested for operation from p to q.
$\mu_{epsj} \in SOS2$	SOS2 interpolation weight for the investment cost breakpoint j for equipment of type e at p.

Note: For all relevant decision variables, s indicates year of investment and t indicates period of operation.

Table 2.1: Decision variables

Endogenous cost aggregates

$cm_{et} \in \mathbb{R}$	Capital cost [m€/year] for a main CO_2 pipeline of capacity e.
$cx_{ept} \in \mathbb{R}$	Capital cost [m€/year] for equipment of type e operating at p.
$cy_{apqt} \in \mathbb{R}$	Capital cost [m€/year] for pipeline or trailer of type a operating from p to q.
$ou_{et} \in \mathbb{R}$	Operational cost [m€/year] for the main CO_2 pipeline of capacity e.
$ox_{ept} \in \mathbb{R}$	Operational cost [m€/year] for equipment of type e at p.
$oy_{apqt} \in \mathbb{R}$	Operational cost [m€/year] for trailer of type e operating from p to q.

Note: All cost aggregates are annualised, and t indicates period of operation

Table 2.2: Cost aggregates

Sets

$\mathcal{A}$	Shipment alternatives.
$\mathcal{A}^T \subset \mathcal{A}$	H_2 bulk capacity. Test case: {T20, T45}, early (200 bar) or mature (450 bar) trailer tank technology.
$\mathcal{A}^H \subset \mathcal{A}$	H_2 pipeline diameters. Test case: {8", 12", 16"}.
$\mathcal{E}$	Equipment for compression, production, and CO_2 transportation.
$\mathcal{E}^C \subset \mathcal{E}$	CO_2 pipeline types. Test case: {CP_1, CP_2} (small or large).
$\mathcal{E}^E \subset \mathcal{E}$	Electrolysis technology. Test case: {EL_1 , EL_2}(early or mature).
$\mathcal{E}^P \subset \mathcal{E}$	Equipment for production. Test case: {CR, DR (centralized or decentralized reforming), EL_1, EL_2}.
$\mathcal{E}^K \subset \mathcal{E}$	Compressor types.
$\mathcal{E}^{CK} \subset \mathcal{E}^K$	Compressors with *suction* from centralized reformers (CR) or pipeline junctions (PJ). Test case: {PDS (PJ to DS), CDS (CR to DS), T20, T45 (CR to 200 or 450 bar trailers).}
$\mathcal{E}^{DK} \subset \mathcal{E}^K$	Compressors with *discharge* to decentralized storages (DS). Test case: {PDS, CDS, TDS (trailer to DS), EDS (EL1 or EL2 to DS), DDS (DR to DS)}.
$\mathcal{E}^S \subset \mathcal{E}$	Storage types. Test case: {CS, DS}, (centralized or decentralized).
$\mathcal{F}$	Input factors. Test case: {NG, EL_p (on-peak EL), EL_o (off-peak EL), CO_2-e (emission), and CO_2-d (disposal)}.
$\mathcal{I}_p$, $\mathcal{O}_p$	Pipeline junctions with inflow from p and outflow to p respectively.
$\mathcal{N}$	Geographical locations (regions). Test case: $\{1, 2, \ldots, 80\}$.
$\mathcal{N}^L \subset \mathcal{N}$	Locations for centralized reformers. Test case: {14, 41, 49, 65}.
$\mathcal{N}^C \subset \mathcal{N}^L$	Locations for CO_2 pipeline branches. Test case: $\mathcal{N}^L \backslash 41$.
$\mathcal{S}$	SOS2 cost/capacity breakpoints. Test case: {0,...,5}.
$\mathcal{T}$	Investment periods. Test case: $\{5, 10, \ldots, 50\}$.
$\mathcal{W}$	Break points for the Weymouth linearization of pipeline flow.

Table 2.3: Index sets

Constants

A_t	Factor that aggregates and discounts to year 0 all costs that occur during a T year period that ends in year t.
α_t	Minimum inter-regional hydrogen market share.
β_t	Maximum intra-regional hydrogen market share.
B	Tow truck rental cost [m€/km].
C_e	Capacity [million tCO_2/year] of pipeline type e.
D_{pq}	Round trip distance [km] from the central reformer at p to the recipient at q.
Δ_{ept}	Factor that scales the average demands for capacity of type e at p up to the short-term peak (inverted capacity utilisation).
F_t	Total transportation fuel demand [PJ/year].
G_{pq}	Maximum departure rate [1000 trips/year] per trailer shipping from a reformer at p to a recipient at q.
Γ_e	Capital recovery factor [$year^{-1}$] for equipment of type e (converts the initial payment to annual fixed costs).
I_a	Investment cost [m€] per trailer or pipeline of type a.
(J_{ej}, X_{ej})	SOS2 linearisation (investment cost, capacity) [m€, PJ/year] breakpoint j of equipment type e.
(K^I_{wpqa}, K^O_{wpqa})	Breakpoint w [GJ/bar] in the linearised Weymouth flow restriction for a pipeline of type a from p to q.
Λ_{pq}	Percentage hydrogen leakage in a pipeline from p to q.
P_{it}	Price [m€/TWh, PJ, or m tCO_2] of input factor i.
O_e	Variable costs as a percentage of initial payment.
Π_p	Share of total population in region p.
Φ_e	Capacity utilization percentage for equipment of type e.
Q_a	Capacity for a pipeline [PJ/year] or trailer [PJ/1000 trips] of type a.
R	Real discount factor.
S_t	Factor that scales the demand at the end of period t down to its intra-period average for the variable cost equation.
T	Duration [years] between investment periods.
U^P, L^P	Upper and lower pressure bounds [bar] for pipelines.
U_{ie}	Required input factors [TWh, PJ, million tCO_2] of type i per PJ of H_2 flowing from equipment of type e.
Y_e	Lifetime [years] of equipment of type e.
Z_{pq}	Upper bound on the number of trailers operating from the central reformer at p to the recipient at q.

Note: For all relevant parameters, t indicates year of investment or period of operation.

Table 2.4: Input parameters

Objective

In order to keep the model tractable, we chose to restrict the strategic model's investment decisions to a subset of years within the optimization horizon, the first year of each investment period. Subsequent periods start T years apart, so a period that ended in year t started $T-1$ years earlier. The capacity must be sufficient for the period's demand peak that is assumed to occur in its end year. However, variable costs are scaled down from this peak to the value that corresponds to the period's average demand. Annual capital costs are contingent on the investment decisions.

For production, compression, or CO_2 branch pipelines of type e in region p in period t the annual capital and operational cost are denoted cx_{ept} and ox_{ept} respectively. Similarly capital and operational cost of a the main CO_2 pipeline of capacity alternative a are denoted cm_{at} and om_{at}. In addition to the equipment type index a and time index t, the hydrogen transportation variables have two distinct location indices, one for the supplier's location at p and another for its recipient's location at q. The annual capital and operation costs of hydrogen transportation are cy_{apqt} and oy_{apqt} respectively.

The objective is to minimize the net present value of the sum of the capital and operational costs while supplying the required amount of hydrogen:

$$\text{cost} = \sum_{t\in\mathcal{T}} A_t \Bigg(\sum_{e\in\mathcal{E}} \sum_{p\in\mathcal{N}} (cx_{ept} + ox_{ept}) + \sum_{a\in\mathcal{E}^C} (cm_{at} + om_{at}) + \sum_{a\in\mathcal{A}} \sum_{(p,q)\in\mathcal{N}^2} (cy_{apqt} + oy_{apqt}) \Bigg). \tag{2.1}$$

Here A_t is a factor that aggregates costs for all the years within an investment period ending in year t, and discounts at the annual interest rate R to year 0:

$$A_t = \frac{1}{(1+R)^{t-T+1}} + ... + \frac{1}{(1+R)^t}, \quad t \in \mathcal{T}. \tag{2.2}$$

In the implemented case the objective also includes a penalty cost on the node pressures' deviation from the pipeline grid's inlet pressure to get meaningful pressure values. This penalty cost must be kept low relative to the actual costs to avoid excluding pipeline investments for the wrong reason, or investing in pipelines with excessively large diameter.

The exogenous demand

For all periods t there is a demand-satisfaction constraint. It requires that the hydrogen sales s_{pt} summarized over all regions p must be at least the required

inter-regional market share α_t multiplied by the overall fuel demand F_t in the transport sector:

$$\sum_{p \in \mathcal{N}} s_{pt} \geq \alpha_t F_t, \quad t \in \mathcal{T}, \tag{2.3}$$

The model neither takes into account the consumers' cost of switching to hydrogen fuelled vehicles, nor the hydrogen car owners' utility of driving to other regions. So in order to avoid an unrealistically fast demand growth in any individual region at the cost of the other regions, the intra-regional market share cannot exceed β_t in any year t:

$$s_{pt} \leq \beta_t F_t \Pi_p, \quad t \in \mathcal{T}, \quad p \in \mathcal{N}, \tag{2.4}$$

where the demand for transport fuel in region p is its percentage Π_p of the total population multiplied by the total fuel demand F_t in year t.

Mass balances

Regions that are neither considered for centralized reforming, nor are part of the pipeline network, do not export hydrogen. Thus the mass balances for their decentralized storage are sufficient. However, regions that either are part of the pipeline network, or are candidates for centralized production, must have the additional mass balance (2.5) that links them to the other regions. For any such interconnected region p, its sources in any period t are the flow fx_{ept} from its own large-scale reforming and the incoming pipeline flow fy_{aqpt} from the subset of regions q that it receives directly from. Its sinks are the outgoing pipeline flow fy_{apqt} to the subset of regions q it supplies directly to, the amount shipped away in all types of trailers a, the amount filled in local storages from the pipeline network, and the flow directly from the central storage to the local storage in the same region. The amount shipped away in all types of trailers, the amount filled in local storages from the pipeline network, and the flow directly from the large-scale storage to the small-scale storage equal the flow of the corresponding compressor type. Consequently, the flow to all these destinations can be measured as the flow fx_{apt} of each individual compressor type a with inlet at the centralized reformer and discharge to the relevant sink. To get a tidier equation, all compressors with *inlet* at centralized reformers or pipeline junctions are grouped in the index set $\mathcal{A}^{CK}$.

$$fx_{ept} + \sum_{q \in \mathcal{O}_p} fy_{qpt}(1 - \Lambda_{pq}) = \sum_{q \in \mathcal{I}_p} fy_{pqt} + \sum_{a \in \mathcal{A}^{CK}} fx_{apt}.$$
$$e = \mathrm{CR}, \quad p \in \mathcal{N}, \quad t \in \mathcal{T}, \tag{2.5}$$

Here CR is centralized reforming, and the factor $(1 - \Lambda_{pq})$ accounts for leakage from the pipeline from p to q.

All the sales are modelled as if they go via the local storage. This storage has a relatively high pressure so hydrogen from all sources such as pipelines, trailers, local production, or potential large-scale production, must be compressed. Hence the sales at p in period t equal the flow rates fx_{ept} of all compressors e with *discharge* to the decentralized storage. For ease of exposition these compressors are grouped into the set $\mathcal{E}^{DK}$.

$$s_{pt} = \sum_{e \in \mathcal{E}^{DK}} fx_{ept}, \quad p \in \mathcal{N}, \quad t \in \mathcal{T}. \tag{2.6}$$

Equipment and capacities

All installed capacity has a finite lifetime. In order to model this, the upper bound on any flow is the sum of capacities that are invested in sufficiently recently.

Production and compression

The annual flow fx_{ept} in production or compression equipment e, in year t at p cannot exceed the sum of all capacity x_{eps} installed strictly less than Y_e years earlier:

$$\Delta_{ept} fx_{ept} \leq \sum_{s=t-Y_e+1}^{t} \Phi_e x_{eps}, \quad s \geq 0,$$
$$e \in \mathcal{E}, \quad p \in \mathcal{N}, \quad t \in \mathcal{T}. \tag{2.7}$$

Here x_{eps} is the capacity of equipment type e at p invested in period s. Y_e and Φ_e are the equipment lifetime and maximum utilization percentage respectively. The exogenous factor Δ_{ept} corresponds to inverted average capacity utilisation, and it scales the average capacity requirement to the level that corresponds to the short-term peak.

The outlet pressure of the reformers and electrolysers are less than the local storage pressure so compression is required. Consequently, the flow rate of the compressor with discharge to the local storage and suction from either reforming or electrolysis equals the relevant production rate:

$$fx_{apt} = fx_{ept}, \quad a \in \mathcal{E}^P, \quad e = e(a), \quad p \in \mathcal{N}, \quad t \in \mathcal{T}, \tag{2.8}$$

where a is type of production at p in year t. A compressor of type $e(a)$ compresses production of type a for the local storage.

Continuous supply of hydrogen in pipelines

Hydrogen flows in pipelines from higher pressure junctions to lower pressure junctions. This feature is approximated by a linearized version of the Weymouth

equation (Tomasgard, Rømo, Fodstad, and Midthun, 2007). The linearisation is done around pairs of inlet and outlet pressures. The Weymouth break points K^I_{wapq}, K^O_{wapq} are functions of selected pressures pairs w, the pipeline diameter a, the distance between the junctions p and q, and a factor required to get the a flow rate unit consistent with the rest of the model. The only constraint that binds is the one which corresponds to the breakpoint based on the selected pressure pair closest to the actual pair. Thus the flow fy_{pqt} from p to q in year t is limited to:

$$fy_{pqt} \leq \sum_{a \in \mathcal{A}^H} K^I_{wapq}\, p_{pt} - K^O_{wapq}\, p_{qt}, \\ w \in \mathcal{W}, \quad p \in \mathcal{N}, \quad q \in \mathcal{I}_p, \quad t \in \mathcal{T}, \tag{2.9}$$

where the pressures at the adjacent junctions at p and q are p_{pt} and p_{qt} respectively. Pipeline flow is possible only if there is a pipeline with remaining lifetime. In order to avoid non-linearity we formulate this provision as a separate constraint:

$$fy_{pqt} \leq \sum_{s=t-Y_a+1}^{t} \sum_{a \in \mathcal{A}^H} Q_a y_{apqs}, \quad y_{apqs} \in \{0,1\}, \quad s \geq 0, \\ a \in \mathcal{A}^H, \quad p \in \mathcal{N}, \quad q \in \mathcal{I}_p, \quad t \in \mathcal{T}, \tag{2.10}$$

where the binary variable y_{apqs} indicates whether a pipeline of type a from p to q is invested in period s. Y_a is lifetime. Q_a is slightly larger than any realistic pressure dependent pipeline capacity.

All the large-scale reformers have the same fixed outlet pressure U^P, which functions as a boundary condition for the pipeline network.

$$p_{pt} = U^P, \quad p \in \mathcal{N}^L, \quad t \in \mathcal{T} \tag{2.11}$$

An upper bound on pressure would typically be redundant because the upstream end pressure is fixed and the pressure cannot get higher at the downstream pipeline junctions without costs. To avoid non-linearity, the cost of operating the compressors are modelled as if their suction pressures were fixed. This simplification hides the cost of pipeline pressure falls, so the objective function must include a penalty on pressure falls to compensate. This penalty would induce an unbounded solution unless there is an upper bound, U^P, on the pipeline junction pressure p_{pt}:

$$p_{pt} \leq U^P, \quad p \in \mathcal{N}, \quad t \in \mathcal{T}, \tag{2.12}$$

where p is location of the pipeline junction and t the period. However, a lower bound L^P on pressure is necessary to avoid implausibly investment in thin or

long pipelines:

$$p_{pt} \geq L^P, \quad p \in \mathcal{N}, \quad t \in \mathcal{T}. \tag{2.13}$$

Bulk supply of hydrogen using trailers

The constant G_{pq} (measured in 1000 trips/year) is the maximum annual delivery rate of a single truck. An annual delivery rate per truck less than 365 is equivalent to round trip times exceeding 24 hours. Such long trips are excluded in order to reduce search space and simplify our operational model (Myklebust et al., 2009). This maximum delivery rate is inversely proportional to the round trip time, which is a function of the distance from p to q and the truck's speed. The annual trailer delivery rate is modelled with continuous variables, but the number of tow trucks is discrete. The number of tow trucks z_{apqt} rented in period t to operate from p to q must be adequate for at least the delivery rate d_{apqt} (1000 trips/year):

$$\begin{aligned} d_{apqt} \leq G_{pq} z_{apqt}, \quad z_{apqt} \in \mathbb{Z}, \quad s \geq 0, \quad 1000 G_{pq} \geq 365 \\ a \in \mathcal{A}^T, \quad (p,q) \in \mathcal{N}^L \times \mathcal{N}, \quad t \in \mathcal{T}. \end{aligned} \tag{2.14}$$

The tow truck picks up the trailer left at the previous delivery, rather than waiting for its own to be emptied. Thus the number of trailers purchased is the number of rented tow trucks plus one. This requires a big-M type constraint.

$$\begin{aligned} z_{apqt} \leq Z_{pq} w_{apqt}, \quad z_{apqt} \in \mathbb{Z}, \quad w_{apqt} \in \{0,1\}, \quad 1000 G_{pq} \geq 365 \\ a \in \mathcal{A}^T, \quad (p,q) \in \mathcal{N}^L \times \mathcal{N}, \quad t \in \mathcal{T}, \end{aligned} \tag{2.15}$$

where Z_{pq} is the largest relevant number of trailers for the considered route. This restriction also sets an upper bound on the number of rented trucks z_{apqt} and hence reducing search space. The binary variable, w_{apqt} takes the value 1 only if a recipient at q is supplied by trailers of type a from large-scale reformer at p in year t. Hence the total number of purchased trailers is $z_{apqt} + w_{apqt}$. The compressors required to fill low and high pressure trailers from the central reforming are of different types. Both the trailer type and its corresponding filling compressor are denoted by the same index a. The flow fx_{apt} through the compressor at p must be sufficient to fill the unit amount Q_a multiplied by the departure rate d_{apqt}:

$$\begin{aligned} fx_{apt} = \sum_{q \in \mathcal{N}} Q_a d_{apqt}, \quad d_{apqt} \in \mathbb{Z}, \\ a \in \mathcal{A}^T, \quad p \in \mathcal{N}^L, \quad t \in \mathcal{T}. \end{aligned} \tag{2.16}$$

In this steady-state model annual departure from p and arrival rates at q are the same and denoted by d_{apqt}. The discharge fx_{eqt} to a decentralized storage

from compressors with suction from trailers equals the sum of arrivals from all centralized reformers multiplied by the quantity Q_a per arrival:

$$fx_{eqt} = \sum_{a\in\mathcal{A}^T}\sum_{p\in\mathcal{N}^L} Q_a l_{apqt}, \quad d_{apqt}\in\mathbb{Z}, \quad 1000G_{pq}\geq 365,$$
$$e=\text{TDS}, \quad q\in\mathcal{N}, \quad t\in\mathcal{T}, \tag{2.17}$$

where TDS indicates trailer to decentralized storage compressor.

CO_2 infrastructure

The CO_2 infrastructure is modelled as a "backbone" pipeline system. The nodes with reforming produce an amount of CO_2 proportional with the factor U_{ca} to the hydrogen production. The main pipe needs to have sufficient capacity to handle the CO_2 flow from all the central reformer locations p except the one in the region at the boundary of the area. Similarly to other capacity constraints, the current capacity is determined by the investments with remaining lifetime.

$$\sum_{p\in\mathcal{N}^C} U_{ca} fx_{apt} \leq \sum_{s=t+1-Y_e}^{t}\sum_{e\in\mathcal{E}^C} C_e m_{es}, \quad m_{es}\in\{0,1\}, \quad s\geq 0,$$
$$a=\text{CR}, \quad c=\text{CO}_2\text{-d}, \quad t\in\mathcal{T}, \tag{2.18}$$

where C_e is the capacity of a CO_2 pipeline of type e, CR is centralized reforming, CO_2-d indicates compressed CO_2 for disposal or EOR, and m_{es} indicates whether a main CO_2 pipeline of type e is invested in period s. Y_e is the pipeline's lifetime and $\mathcal{N}^C$ the subset of large-scale reformers that must be connected to the CO_2 infrastructure.

The length of a CO_2 pipeline branch depends on which central reformer it is connected to. Hence the cost of the individual branches cannot be included in the general reformer cost, which is independent of location, but needs to be modelled explicitly.

$$U_{ca} fx_{apt} \leq \sum_{s=t-Y_e+1}^{t}\sum_{e\in\mathcal{E}^C} C_e b_{eps}, \quad b_{eps}\in\{0,1\}, \quad s\geq 0,$$
$$c=\text{CO}_2\text{-d}, \quad a=\text{CR}, \quad p\in\mathcal{N}^C, \quad t\in\mathcal{T}. \tag{2.19}$$

b_{eps} indicates whether a branch pipe of type e is invested in at p.

Variable costs

There are two types of variable costs in our model; maintenance costs and consumed input factors. There are no operational costs related to the pipeline flow

apart from operation of storage compressors, which are modelled separately. The variable cost oy_{apqt} of a pipeline from p to q during period t consists of its maintenance cost only, which is proportional to the initial investment iy_{apqs} with the factor O_a. Available capacity is represented through all investments with remaining lifetime:

$$oy_{apqt} = O_a \sum_{s=t-Y_e+1}^{t} iy_{apqs}, \quad a \in \mathcal{A}^H, \quad (p,q) \in \mathcal{N}^2, \quad t \in \mathcal{T}, \quad s \geq 0, \tag{2.20}$$

where a is the pipeline type, p and q are its end points, t is the period that the cost is attributed to, and s is when it was built.

The maintenance cost of the towed vehicle and its composite tanks is included in the cost of the filling stations. In addition to the indirect cost of operating the compressors, the variable cost of operating the trailers includes their rental cost. This is the product of the p to q round trip distance in kilometres, D_{pq}, the rental B per thousand kilometres, and the annual departure rate in thousand trips d_{apqt}:

$$oy_{apqt} = D_{pq} B \;\; d_{apqt}, \quad a \in \mathcal{A}^T, \quad (p,q) \in \mathcal{N}^L \times \mathcal{N}, \quad t \in \mathcal{T}. \tag{2.21}$$

The variable cost ox_{ept} of production or compression type e at p in period t consists of two components. Maintenance, proportional to the initial investment ix_{eps} in year s (of equipment with remaining lifetime) with the factor O_e, and input consumption proportional to its hydrogen flow rate fx_{ept} with the unit demand U_{ie} of input factor i and its price P_{it}. Because the hydrogen demand grows during the period, and consequently its proportional inputs too, the parameter S_t is required to scale the period-end peak fx_{ept} down to the intra-period average, which is more relevant for the period's aggregated costs.

$$\begin{aligned} ox_{ept} = &\sum_{i \in \mathcal{F}} P_{it} U_{ie} S_t f x_{ept} + O_e \sum_{s=t-Y_e+1}^{t} ix_{eps}, \\ &e \in \mathcal{E}, \quad p \in \mathcal{N}, \quad t \in \mathcal{T}. \end{aligned} \tag{2.22}$$

Decentralized SMR requires emission permits for all produced CO_2 as an input along electricity and natural gas. Centralized reforming require permits for the part of produced CO_2 that is emitted. Because the offset market is supposed to equalize all individual polluters' marginal abatement costs, we assume offsets can be bought and sold in any relevant quantities at the same price. This will simplify the mathematical model as the permits' opportunity cost will not depend on whether the polluters' initial allowances happened to be too high or too low. The CO_2 disposal cost coefficient can be positive or negative depending on whether the recipient requires payment or is willing to pay.

Investment dependent fixed costs

If an investment is made, the investment cost will be accounted for as annual fixed costs for all years during its lifetime. In order to model this, we scale the cost of investments with remaining lifetime with the capital recovery factor Γ_e (Park and Sharp-Bette, 1990). This factor is a function of the equipment's lifetime, Y_e and the discount rate, R.

Economies of scale in production and compression

We use special ordered sets of type 2 (SOS2) (Williams, 1999) to linearise the non-convex investment cost of equipment that are subject to economies of scale. The variable ix_{eps} is the initial investment cost for reformers, compressors and other equipment at p in period s. The SOS2 breakpoints are indexed over $j \in \mathcal{S}$ and are denoted J_{ej} for investment cost and X_{ej} for capacity. The variables μ_{epsj} are interpolation weights for the breakpoints.

$$\begin{aligned} ix_{eps} &= \sum_{j \in \mathcal{S}} J_{ej} \mu_{epsj}, \\ x_{eps} &= \sum_{j \in \mathcal{S}} X_{ej} \mu_{epsj}, \\ 1 &= \sum_{j \in \mathcal{S}} \mu_{epsj}, \quad \{\mu_{epsj}\} \in \text{SOS2}, \\ e \in \mathcal{E}^P \cup \mathcal{E}^K, \;\; p \in \mathcal{N}, \;\; s \in \mathcal{T}, \end{aligned} \tag{2.23}$$

Here x_{eps} is the capacity and ix_{eps} is the initial payment for equipment of type e at p in period s. There is zero cost of zero capacity so $(J_{e0}, X_{e0}) = (0, 0)$.

Storage costs are modelled with a fixed part of EUR 10m and a volume dependent part of EUR 2000 per tonne. Consequently, they are subject to economies of scale and are non-convex. In our model we assume that a capacity to store 1/365 of the annual production capacity is required. Moreover, the necessary CO_2 compressor capacity depends only on the reformer capacity. Because these costs can be added to the individual large-scale reformers' SOS2 points they do not increase model complexity.

Discrete pipeline and trailer investment decisions

For all trailer routes, the initial investment payment in the first year of period s is given as iy_{apqs}. It is the product of the cost I_a per trailer of type a, and the number of trailers, $z_{apqs} + w_{apqs}$, which are purchased in period s to supply the

recipient at q with hydrogen from the reformer at p:

$$iy_{apqs} = I_a(z_{apqs} + w_{apqs}), \quad z_{apqt} \in \mathbb{Z}, \quad w_{apqt} \in \{0,1\},$$
$$a \in \mathcal{A}^T, \quad (p,q) \in \mathcal{N}^L \times \mathcal{N}, \quad s \in \mathcal{T}. \tag{2.24}$$

Here z_{apqt} is the number of rented tow trucks, and w_{apqs} is a binary variable that is 1 if $z_{apqt} \geq 1$. We model the investment cost of H_2 pipelines similarly:

$$iy_{apqs} = I_a y_{apqs}, \quad y_{apqt} \in \{0,1\}, \quad a \in \mathcal{A}^H, \quad (p,q) \in \mathcal{N}^2, \quad s \in \mathcal{T}. \tag{2.25}$$

Investment cost of CO_2 pipeline branches are:

$$ix_{eps} = I_e b_{eps}, \quad b_{eps} \in \{0,1\}, \quad e \in \mathcal{E}^C, \quad p \in \mathcal{N}^C, \quad s \in \mathcal{T}, \tag{2.26}$$

where b_{eps} indicates whether a CO_2 pipeline branch of capacity e was invested in period s to connect reformer at p to the main CO_2 pipeline.

Similarly for the main CO_2 pipeline:

$$im_{es} = I_e m_{es}, \quad m_{es} \in \{0,1\}, \quad e \in \mathcal{E}^{\mathcal{C}}, \quad s \in \mathcal{T}. \tag{2.27}$$

Where m_{es} is 1 if a main CO_2 pipeline of capacity e is invested in year s.

We model fixed cost as the annuity equivalent capital cost of the sum over all previous investments with remaining lifetime.

$$cy_{apqt} = \sum_{s=t-Y_a+1}^{t} \Gamma_a iy_{apqs}, \quad s \geq 0, \quad a \in \mathcal{A}, \quad (p,q) \in \mathcal{N}^2, \quad t \in \mathcal{T}. \tag{2.28}$$

Here cy_{apqt} is the investment dependent fixed cost in year t of hydrogen pipelines and trailers that are invested in year s to supply recipients at q with hydrogen produced at p.

The annual fixed cost cx_{ept} in year t of CO_2 pipelines, hydrogen production and compression of type a that are invested in year s is:

$$cx_{ept} = \sum_{s=t-Y_e+1}^{t} ix_{eps}\Gamma_e, \quad e \in \mathcal{E}^{\mathcal{C}}, \quad p \in \mathcal{N}, \quad t \in \mathcal{T}. \tag{2.29}$$

The annual cost of the main CO_2 pipeline is the sum over the annuity equivalent costs of all earlier investments with remaining lifetime:

$$cm_{et} = \sum_{s=t-Y_e+1}^{t} im_{es}\Gamma_e, \quad e \in \mathcal{E}^{\mathcal{C}}, \quad t \in \mathcal{T}. \tag{2.30}$$

2.4 Technological and geographical data

The geographical area that we assume in our test cases has the same population distribution as Germany. We have split its constituent 16 Bundesländer into a total of 80 regions, and we model them as nodes with no internal structure. Lacking real data, the distances for the distribution cost parameters such as the pipeline lengths, and the trailers' travel times and fuel costs, are based on a rectangular grid. However, the nodes' transport energy demand are inferred from their actual share of the total population. We use a 10% interest rate to discount all costs. It is higher than the risk free rate to allow liquidity and risk premiums. Costs that do not depend on decision variables and are added in post processing. Such costs in our case are average capital and operational cost of dispensers is calculated to be around 25 cent/GJ at our chosen discount rate.

Technological data

The total costs include purchase of inputs, operational and maintenance costs in addition to the capital costs. We model the economies of scale in investment with two custom sets of coarse and fine SOS2 linearisation breakpoints for large and small-scale components respectively. For local production and compression, the capacity/cost breakpoints are at 0, 0.05, 0.25, 1, and 5 Petajoule(PJ)/year of H_2. For centralized production and compression, the breakpoints are at 0, 2.5, 10, 30, 200 PJ/year of H_2.

Economies of scale in production and compression

There are four potential investment decisions for hydrogen production; local reforming, centralized reforming, electrolysis with early or mature technology. Large-scale SMR with 70% CCS will be the only alternative considered for centralized large-scale production. The decision to open a large-scale reformer will always require CO_2 compressors of matching capacity, so the same decision variable will take all of these into account. Early and mature electrolysis technologies have the same investment cost but different efficiency. The mature technology is available after 2020 only. We model the economies of scale (EOS) in hydrogen production with the following empirical equation:

$$I(P) = (1 + C)I_0\Big(\frac{P}{P_0}\Big)^{\alpha}, \tag{2.31}$$

where P is capacity in Nm^3/h and I is the consequent investment cost in EUR 1000 . The parameters have the following values:

		Electrolysis	Local reforming	Central reforming	
C	Installation factor	39%	39%	N/A	
I_0	Reference investment cost	2 560	2 378	84 000	[€1000]
P_0	Reference capacity	1000	1000	76 000	[Nm^3/h]
α	Capacity scaling exponent	0.57	0.49	0.7	

All produced hydrogen and CO_2 must be compressed. There are seven different combinations of suction and discharge pressures, which we model as distinct types of compressors. The 450 bar local storages must be filled with compressors of various suction pressures depending on whether their inlet is a pipeline junction, directly from centralized production, from trailers, or from different types of local production. The compressors' main input factor is electricity. The compression of hydrogen from electrolysis happens during off-peak hours and uses the cheaper electricity. However, compression of hydrogen from decentralized reforming happens throughout the day and has to use the more expensive on-peak electricity. Even though they have the same combination of suction and discharge pressures we use two separate decision variables for these compressors. A third compressor type is necessary when hydrogen is received directly from central reformers, a fourth for pipeline deliveries, a fifth for trailers, a sixth and seventh are also necessary to fill the two types of trailers, and the eight for the transport of CO_2. For the CO_2 compressors, everything except the flow rate is assumed constant, and hence the required effect and energy per unit of flow are constant. Investment cost is a non-convex function of effect for all types. All these decisions are modelled with continuous variables and are subject to economies of scale. Hydrogen delivered by pipelines has a pressure that varies according to distance, pipeline diameter and flow rate. To avoid non-linear costs, we assume a pipeline outlet pressure of 50 bar for the pipeline to local storage compressors. This pressure can be recalibrated after an initial run of the model. The effect of a compressor P is a measure of its ability to do mechanical work on the gas. We model the effect as varying linearly with the volumetric flow rate. The coefficient is a thermodynamic function of efficiency, the compressibility of the gas, and ratio of pressures, which we assume are all constant.

$$\frac{P}{Q} = \frac{Z}{n_c}\frac{p_N T_i}{T_N}\frac{N\gamma}{\gamma - 1}\left[\left(\frac{p_{out}}{p_{in}}\right)^{\frac{\gamma-1}{N\gamma}} - 1\right], \tag{2.32}$$

where P is compressor effect in kW and Q is flow rate in Nm^3/s. The parameters

have the following values:

p_N	Normal pressure	101.325	[kPa]
T_N	Normal temperature	293.15	[K]
T_i	Initial gas temperature	298	[K]
p_{in}	Suction pressure	6, 10, 30, 50, or 80	[bar]
p_{out}	Discharge pressure	200 or 450	[bar]
N	Number of compressor stages	1	
n_c	Compressor efficiency	50% (CO_2 and small H_2), 70% (large H_2)	
Z	Compressibility	1.08 (H_2), 0.96 (CO_2)	
γ	Ratio of specific heats	1.41 (H_2), 1.29 (CO_2)	

Source: Ogden (2004)

We assume the compressor's electricity consumption is proportional to its effect. For each compressor type we assume its effect varies with its scale, and everything else such as discharge pressure and efficiency are constant. We have used the following non-convex empirical equation to calculated the cost-capacity breakpoints for compressors:

$$I(P) = (1 + C)I(P_0)\Big(\frac{P}{P_0}\Big)^{\alpha}\Big(\frac{p^{out}}{p_0^{out}}\Big)^{\beta}, \tag{2.33}$$

where P is capacity in kW and I is the consequent investment cost in 1000 €. The parameters have the following values:

	Gas to be compressed	CO_2	H_2	
C	Installation factor	N/A	85%	
I_0	Reference unit investment cost	1518	283	[1000€]
P_0	Reference unit capacity	9130	1000	[kW]
p_0^{out}	Reference discharge pressure	200	100	[bar]
p_0^{out}	Considered discharge pressure	200	200 or 450	[bar]
α	Capacity scaling factor	0.7	0.382	
β	Discharge pressure scaling factor	N/A	0.378	

Investments for the distribution of H_2 and CO_2

The two ways of distributing hydrogen have quite different cost structures. Pipelines have high investment costs relative to operating costs, and for trailer distribution

it is the other way around. We consider a single location and two alternative capacities for the main CO_2 pipeline, but this can easily be expanded for other applications. The pipeline network's downstream end is a region that corresponds to the German city Emden, a hub for North Sea gas pipelines.

Hydrogen pipeline costs

Equation (2.34) from Ogden (2004) is used for preparing the dataset with capital cost per unit length of H_2 transmission pipelines in the US. Like the other cost functions, it is estimated using a statistical relationship between actual pipeline investments, I in 2001-USD per unit of length, and a measure of capacity that in this case is its diameter, D in inches:

$$I(D) = 0.3354D^2 + 11.25D + 2.31. \tag{2.34}$$

This cost function accounts for materials, labour, right of way, and overhead. We assume the same parameters in our case as we have not come across more relevant data. However, we adjusted the price for the 2001 to 2008 inflation and the USD/EUR exchange rate. In order to keep the number of integer variables low, a hydrogen pipeline can have one of a discrete set of alternative diameters: In our case 8", 12", or 16".

The hydrogen is distributed to the local filling stations within the regions in smaller intra-regional distribution pipelines at lower pressure and velocities than the inter-regional transmission pipelines. These local pipelines are not modelled directly, but accounted for by adding an amount to each length of inter regional pipeline. We assume a capital cost of distribution pipes at EUR 0.74m/km. Moreover, we assume six 70 km branch pipelines are built in each 100×100 km area with this infrastructure. This adds EUR 67m to each 100 km of inter-regional pipeline. These numbers are a conversion of data from Ogden (2004) to 2008-EUR using the official exchange rate and inflation. Technological and cost data for such pipelines are summarized in Table 2.7 of the appendix.

Trailer distribution

Hydrogen transported in bulk is compressed further from 80 bar at the pressurized reformer to either 200 or 450 bar, for early and late trailer tank technologies, respectively. The pressure in the trailers' composite tubes falls as the hydrogen is pumped out. We assume it will be economical to end the unloading when it has fallen to 30 bar. Thus the local compressors then need to be able to handle suction pressures down to 30 bar during the discharge. It will be necessary to invest in compression capacity for the transition from 530 kg (64 GJ net of the 30 bar left on return) at 200 bar to 1200 kg (132 GJ) at 450 bar in the trailer composite tubes available from 2020.

CO_2 pipeline costs

The largest CO_2 pipeline capacity is just sufficient for the CO_2 from the largest reformer at the end of the model's horizon, and the smaller capacity about half that. This will likely overstate the minimum costs since the optimal capacity may be different from these two capacities. Technological data for the CO_2 pipelines are listed in Table 2.7 of the appendix. The CO_2 pipeline branches that connect the different large-scale reformers to the main pipe may be of different lengths, so their individual costs will depend on which of them they are connected to as well as on their capacity. The capital cost of selected capacities for compression at the reformer and re-compression are calculated using eq. (2.33). The costs of the CO_2 pipelines are estimated using an empirical Equation (Ogden, 2004):

$$I(Q, L) = I(Q_0, L_0)\Big(\frac{Q}{Q_0}\Big)^{\alpha}\Big(\frac{L}{L_0}\Big)^{\beta}, \tag{2.35}$$

where Q is flow in tCO_2/day, L is pipeline length in km, and I is unit cost in USD/m. The parameters have the following values:

Q_0	Reference flow	16 000	[tCO_2/day]
L_0	Reference pipeline length	100	[km]
I_0	Unit cost reference pipeline	700	[$/m]
α	Flow scaling factor	0.48	
β	Length scaling factor	0.24	

Demand projection

Mantzos, Capros, and Kouvaritakis (2003) expect transport demand to grow at an annual rate of 1.5% until 2010, then at 1.0% until 2020, and at 0.5% until 2030. We use this growth profile but assume that demand will continue to grow at 0.5% after 2030 as well. The annual German energy consumption for road transport in 2006 was 2230 PJ (Eurostat). We extrapolate this volume at the 1.5% rate to 2300 for our base year 2008. Hydrogen will satisfy a limited share of this demand.

The EU has set a goal of a 5% market share for hydrogen by 2020. Much of the industry considers this estimate very optimistic, and in our test case we use 2% as the minimum average market share for 2020 and increase it gradually towards 10% in 2050. These market shares are represented in the model through parameters α_t of minimum inter-regional market shares. In order to mimic the demand from car fleets in the first periods of the horizon, we allow the maximal intra-regional market share β_t to be relatively high compared to α_t initially. We assume that β_t gradually decreases towards α_t to ensure better accessibility of hydrogen towards the end of the horizon.

Input factor price projections

In the base case prices are projected from their average 2008 level. At the time of writing, natural gas three days ahead spot prices and intra-day spot electricity prices are available from the European Energy Exchange AG (2009), and emission offset prices can be found at the European Climate Exchange (2009). The average electricity price between 22:00 and 06:00 was EUR 43/MWh, and we use this as the off-peak price. The price between 06:00 and 22:00 was EUR 76/MWh and we use this as the on-peak price. The average spot NG price was EUR 7/GJ. Emissions are settled by retiring offsets at the end of each year, but offsets are traded all times. The average price of an EUA contract in 2008 was EUR 23/tCO_2e.

We have used actual 2008 prices for the base case. In order to show how the model can be used for analysis, we have chosen two further combinations of reasonable price paths illustrating conditions for choosing other technologies. These three test case are summarized in Table 2.8 and plotted in Fig. 2.4.

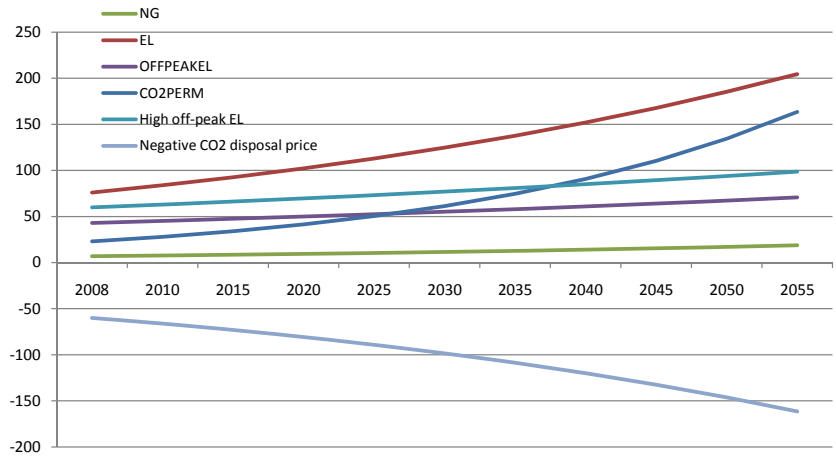

Figure 2.4: Exogenous price paths of the input factors

In the two other cases relative prices are manipulated to analyse when decentralized reforming would be included in the technology mix. In one case the initial period off-peak electricity price is increased to EUR 60/MWh in the base year and growing at an annual rate of 2% and reaching EUR 99/MWh by the end period. In the other alternative case the disposal cost of CO_2 is *minus* EUR 60/tCO_2 in the base year, and declines further at an annual rate of 3% to minus EUR 161/tCO_2.

The most important input to steam methane reforming is NG, which consists mainly of methane. We assume the NG price grows at an annual real risk free discount rate of 2% from its initial level of EUR 7/GJ and reaches EUR 18/GJ at the end of the model horizon. See for example Garnier and Wilhelmsen (2005) for a motivation for the choice of rate, and Hotelling (1931) for a motivation for why we use it as the price growth of non-renewable resources. Moreover, we consider a survey of price prediction models outside the scope of our study. We assume that the NG plants will be used as the marginal generator during on-peak hours in the future, so the on-peak rate grows at the same 2% rate as NG and increases from EUR 76/MWh initially to EUR 204/MWh at the end of the horizon. However, off-peak electricity is less likely to be generated from non-renewable sources so we assume a lower growth rate of 1% from EUR 43/MWh initially to EUR 70/MWh in the final period. The CO_2 permit is not a non-renewable resource in the traditional sense, but a politically determined quantity. We have assumed 4% as the annual growth rate of carbon offset price to ensure it is at least as high as the purchasing power growth, and assume it grows at this rate from EUR 23/tCO_2 initially to EUR 163/tCO_2 in the final period. In the base case the CO_2 disposal cost is zero. These price and volume growth parameters are somewhat arbitrary and chosen deliberately for illustration purposes.

In addition to NG, methane can also be supplied from other primary energy such as biomass or coal, in this case they must be close enough substitutes after gasification. When the methane comes from fossil sources such as NG or coal it requires CCS or CO_2 emission offsets, when it comes from renewable sources it does not. This issue requires a minor modification of the model. In this implementation of the model the input prices and hydrogen quantities vary across time periods only.

2.5 Test case results and discussion

The base case result is that there will be only decentralized reforming the first three periods, and only electrolysis thereafter. Maps that illustrate the investment schedule are plotted in Fig. 2.8. In these maps, a grey cloud illustrates local reforming, a brown cylinder illustrates centralized reforming, and a yellow lightning illustrates local electrolysis. Because we have assumed that the off-peak electricity price will grow at a lower rate than the natural gas price, electrolysis will eventually become the most cost efficient production technology. In our case it happens in year 2028, if the difference in price growth rates were smaller the transition would happen later and vice versa. For the base case, breakdown of costs and production methods are illustrated in Fig. 2.5. The thicker the line the higher the capacity.

Centralized production will improve its cost effectiveness over decentralized production for large volumes, high CO_2 emission price, or negative CO_2 disposal price. However, a high CO_2 price will not make centralised production more competitive in comparison to electrolysis, which dominates in the base case in the final years when the volume is high. Consequently, a higher CO_2 price would lead to an earlier transition from decentralised reforming to electrolysis rather than the introduction of centralised production. Hence, in our alternative scenarios we have increased the electricity price and reduced the CO_2 disposal costs respectively.

In the scenario where we assume a negative CO_2 disposal cost, hydrogen is supplied by decentralized production until 2018. If the demand growth rate had been lower then centralized production would have been introduced later and vice versa. Maps that illustrate the investment schedule are plotted in Fig. 2.10. The dashed blue lines illustrate trailer distribution, and solid blue lines illustrate hydrogen pipelines. A breakdown of costs and production methods from this case is given in Fig. 2.7.

The cost advantage of electrolysis obviously depends on the electricity price. In the case where we assume a higher initial price level of electricity, it will take more years before its price relative to other feedstocks is low enough to make it competitive. In this scenario decentralized reforming is preferred the initial periods of the horizon when natural gas still is cheap relative to off-peak electricity, but volumes are still too low for centralized reforming. In the middle of the horizon, volumes are large enough for centralized production, but electricity is still too expensive to compete. Because of the assumed lower growth rate of off-peak electricity, it eventually becomes the preferred technology at the end of the horizon under all scenarios. A breakdown of costs and production methods from the high electricity price scenario in Fig. 2.6. Maps that illustrate the investment schedule under the same scenario are plotted in Fig. 2.9.

The average capital cost is about 50 cent/GJ in the periods when hydrogen is mainly produced with small-scale SMR. The average variable cost is about €25/GJ in the first year, and then grows at about the same rate as the prices of the main feedstocks. Average capital costs stay fairly constant in the base case. Sekanina and Pucher (2006) expect the consumption of hydrogen in a fuel cell vehicle to be 1.5kg/100km (0.2GJ/100km), so the cost *before* taxes will be €5-6/100 km initially. For comparison, a modern diesel vehicle with a consumption of 5 litre/100 km would have about the same cost if fuel prices were around €1.00-1.20/litre. This is the range of typical *after* tax prices of diesel in Europe. Furthermore, the consumers must combine the fuel with cars to satisfy their transportation demand. Hydrogen fuelled cars still cost considerably more than conventional cars. Nevertheless, hydrogen might not be the lowest cost alternative to reduce CO_2 emissions, but for emission cuts of a particular extent it would

become the marginal technology. Marginal technologies are more interesting than the intra marginal because they determine the marginal costs and hence price of emission cuts. Furthermore, cars that are not powered by fuel cells or batteries emit more than climate gasses, for example NOx and CO. The right to emit these gasses are not traded in a market, and consequently involve a cost to society that is hard to determine (Kolstad, 2000). If these unobservable costs are given enough consideration, then hydrogen could be a more cost efficient alternative.

Energy input cost amounts to about 90-95% of total annual cost, the remaining 5-10% are capital costs. Energy consumption is proportional to the production rate, a continuous variable, and capital costs depend on discrete investment decision. Consequently, a 2-4% bound for the integer solution is reached quickly, after 2-3 seconds. Technical details are summarized in Table 2.5 of the appendix. Solutions that rely on centralized production requires more integer variables, such as number of pipelines and trailers, than solutions dominated by local production. The base case solves relatively quickly because the input price combinations motivate decentralized production. Both input prices and quantities grow exponentially. However, costs decline exponentially due to discounting, so the objective function will not be dominated by any particular time period. All cases were run with Xpress Optmizer Version 18.00.04. for 6 hours on a laptop with a T7700 2.40GHz processor and 4GB RAM.

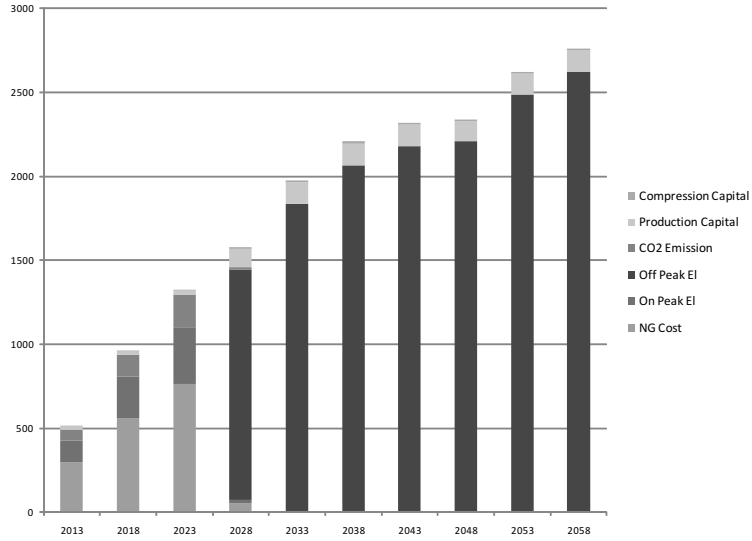

(a) Energy required to create the hydrogen comes to about half the total cost, a third is energy for compression, and between a sixth and a tenth is CO_2 emission permits. Capital costs amount to a mere five per cent

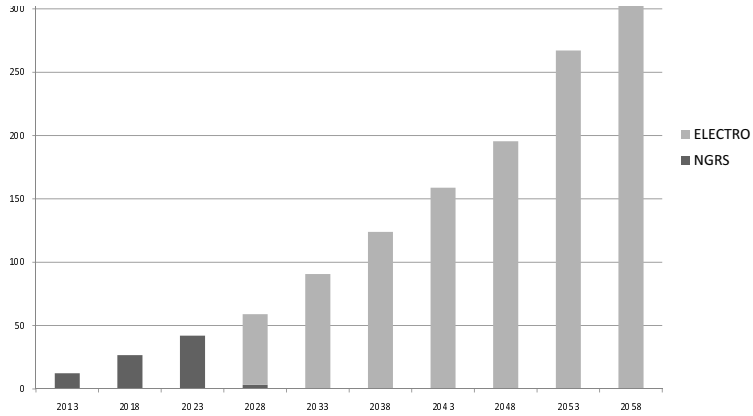

(b) Local reforming is the dominating technology in the early years, but eventually electrolysis replaces it

Figure 2.5: Breakdown of cost and production technology for the base case price scenario.

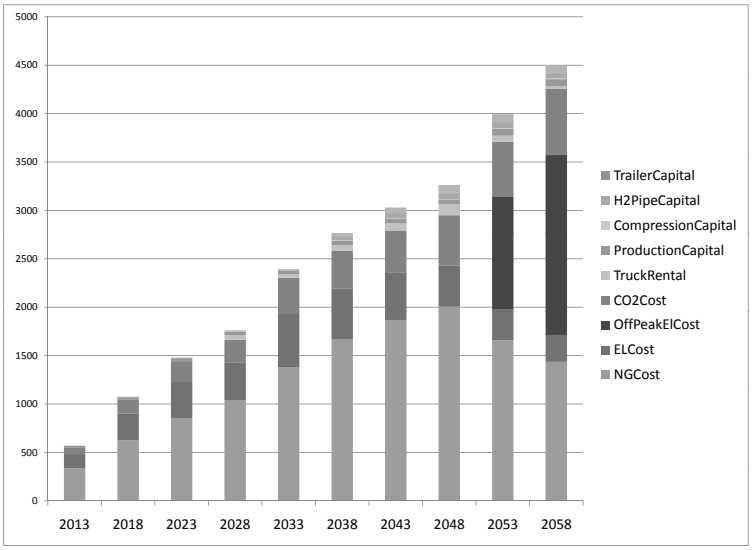

(a) Variable cost dominates even for the most capital intensive alternatives.

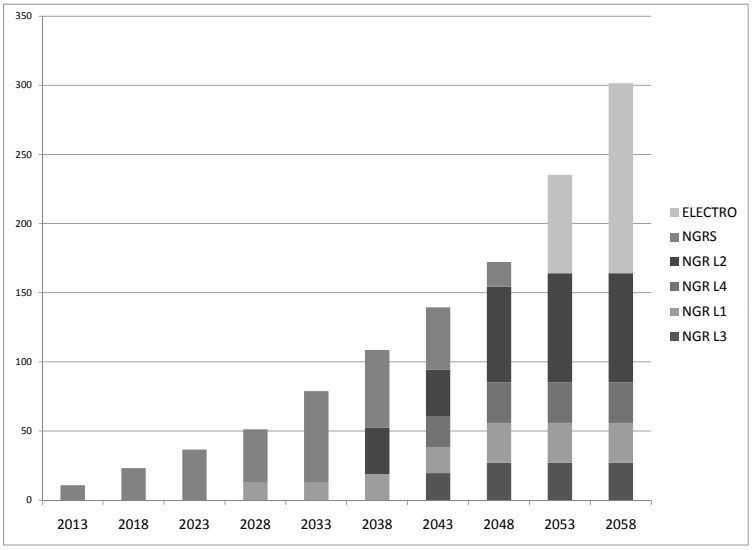

(b) Decentralized production with electrolysis dominates the final periods.

Figure 2.6: Breakdown of cost and production technology for the high off-peak electricity price scenario

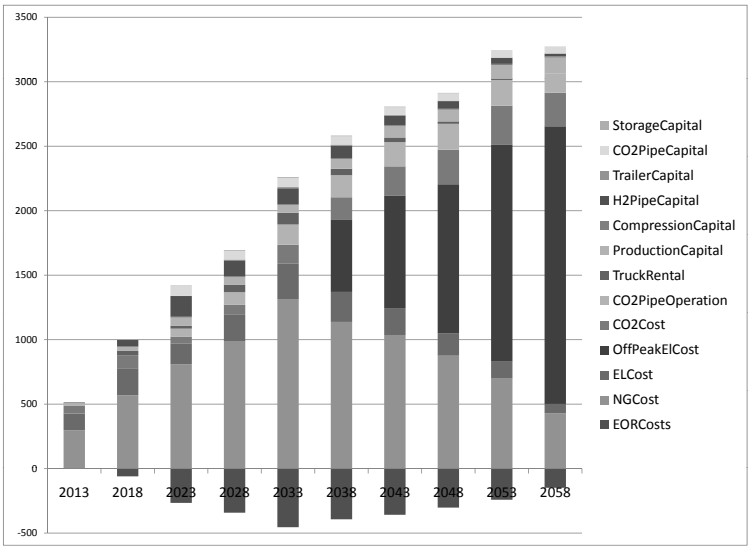

(a) The negative CO_2 disposal costs are illustrated with downward pointing columns. Average cost will obviously fall when an input factor gets a negative price.

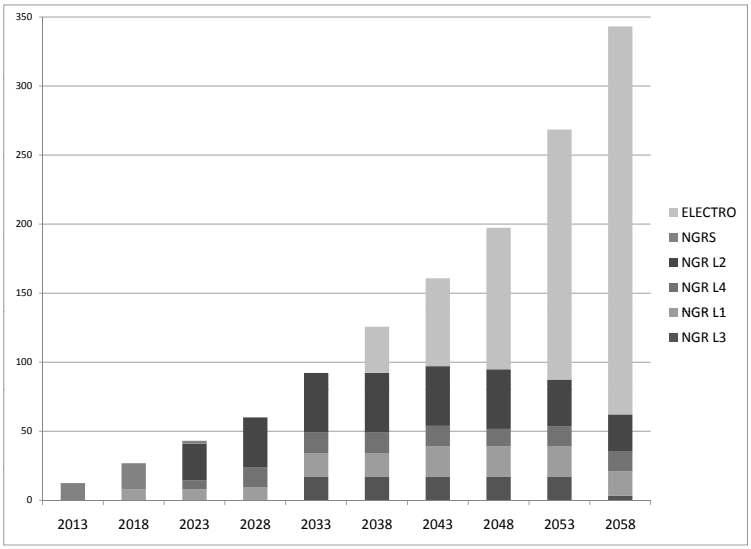

(b) A negative CO_2 disposal price gives centralized reforming a cost advantage relative to decentralized reforming.

Figure 2.7: Breakdown of cost and production technology for the negative CO_2 deposition price scenario

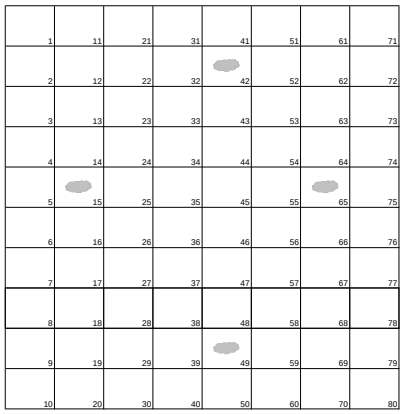

(a) Local reforming only from the start

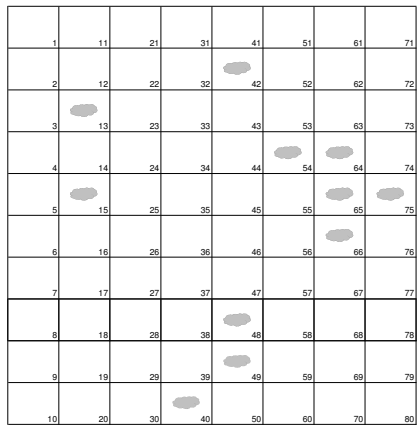

(b) In 2023 there is local reforming at more locations.

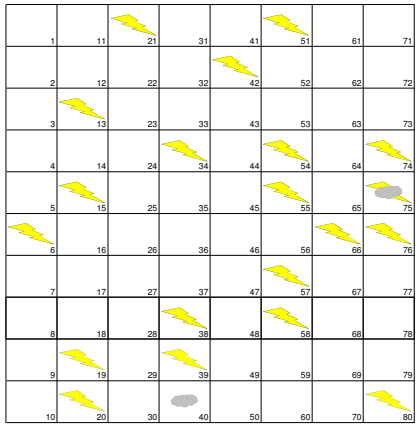

(c) From 2028 electrolysis is the preferred choice.

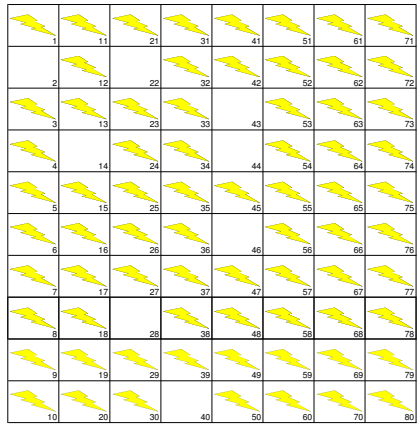

(d) In 2058 there is electrolysis in nearly all regions.

Figure 2.8: Combination of different technologies at different points in time for the base case.

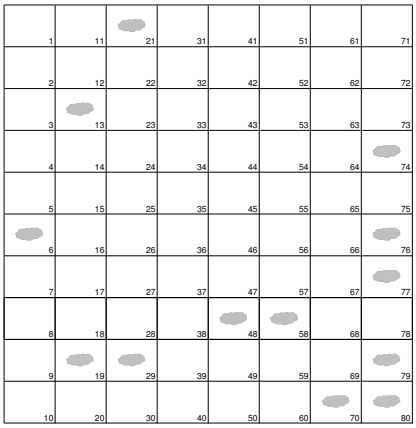

(a) Local reforming only until 2023

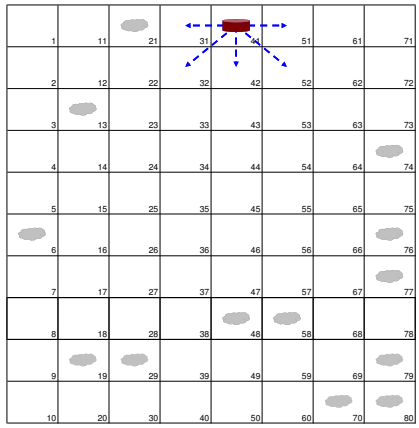

(b) In 2028 the first large-scale reformer is added. Hydrogen is transported with trailers to five adjacent regions.

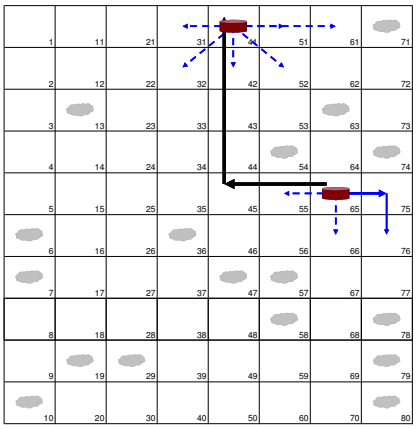

(c) In 2038 two more large-scale reformers with CO_2 pipelines are added, as well as trailers and pipelines for H_2 distribution.

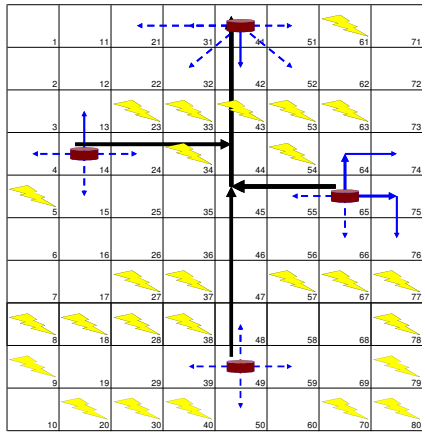

(d) In 2053 the decentralized production with electrolysis starts to dominate.

Figure 2.9: Combination of different technologies at different points in time for the high off-peak electricity price scenario

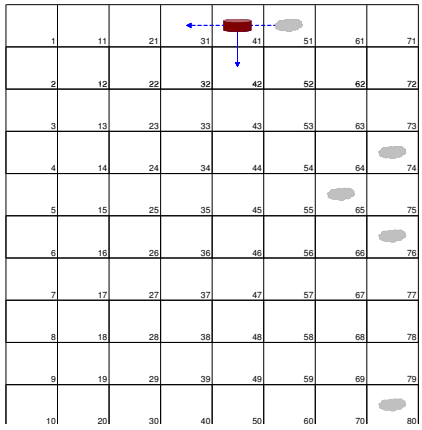

(a) The first centralized reformer appears in 2018 in the region where additional CO_2 infrastructure is unnecessary

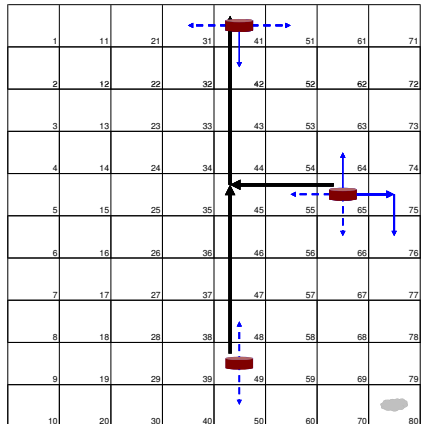

(b) In 2028 two more centralized reformers are added. Hydrogen is transported with trailers and pipelines to other regions.

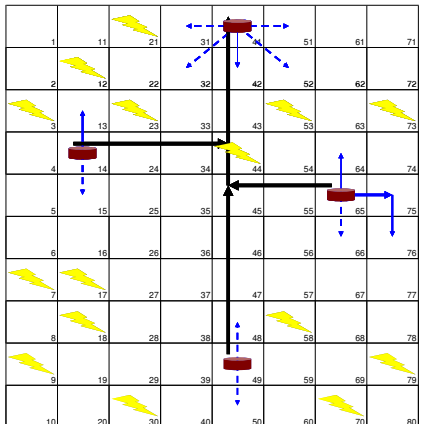

(c) In 2038 decentralized electrolysis is added at 15 locations.

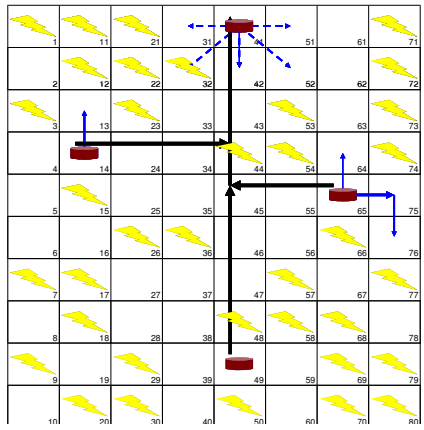

(d) In 2048 hydrogen is available at 52 of the 80 locations.

Figure 2.10: Combination of different technologies at different points in time for the negative CO_2 deposit cost scenario

2.6 Conclusion

We have developed a hydrogen production and distribution cost minimization framework with timing, location, and choice of technology that are driven by volume and prices. It consists of an investment and an operational model, which we present in two separate papers. This paper focuses on the investment model. It selects the most economical production or transportation type for given relative prices and geographic characteristics. Economies of scale in production are traded off against distribution costs. The model is general and can handle several types of supply technologies. In order to illustrate how the model results respond to different volumes and combinations of prices, we assume that the different feedstock prices grow at individual rates. As well as varying relative to each other, the feedstock prices vary relative to capital costs, which we assume are constant over time. Furthermore, the hydrogen demand is also assumed to grow constantly to illustrate how investment decisions responds to changes in volume. The alternative supply technologies have different requirements of the various feedstocks as well as different returns to scale. Consequently, the model output is able to illustrate how technologies enter and exit in response to changes in volumes and relative prices.

We have tested the model on three cases. In the given cases the alternative production technologies are electrolysis and local or centralized reforming. Centralized reforming requires distribution, which can be of two types; trailers or pipelines. In the base case prices are projected from their actual values in 2008. In the two alternative cases the off-peak electricity price is projected from a higher level and negative CO_2 deposition costs respectively. The result of the most realistic test case is that there will only be decentralized reforming the first 15 years, and in the following periods decentralized electrolysis only. In the high electricity price case one centralized reformer will be introduced after 20 years, and its production is distributed with trailers initially. In later periods more centralized reformers are added and the volumes get large enough to make pipeline distribution preferable to some of the destinations. In the case with negative CO_2 disposal costs the first centralized reformer is introduced after ten years, and hydrogen is distributed with a combination of pipelines and trailers depending on volumes and distances. The mentioned cases are only intended for illustration purposes. The case results indicates that our model is a capable tool for gaining insight into the various trade-offs that must be evaluated in an infrastructure planning process.

The development of a contingency plan or another type of model that is able to take uncertainty into account is left for future work.

Acknowledgements

We thank (former) Norsk Hydro, the NorWays project and Christoph Stiller at Ludwig-Bölkow-Systemtechnik GmbH who have helped us with some technological details, Matthias Nowak for help with technical issues, and Adrian Werner for helpful comments. All errors remain our own.

Bibliography

DTI, 2007. Meeting the energy challenge, a white paper on energy. Tech. rep., Department of Trade and Industry, United Kingdom.

Edmonds, J., Wise, M., Pitcher, H., Richels, R., Wigley, T., MacCracken, C., 1996. An integrated assessment of climate change and the accelerated introduction of advanced energy technologies: An application of MiniCAM 1.0. Mitigation and Adaptation Strategies for Global Change 40 (4), 311–339.

Endo, E., 2007. Market penetration analysis of fuel cell vehicles in Japan by using the energy system model MARKAL. International Journal of Hydrogen Energy 32 (10-11), 1347–1354.

European Climate Exchange, September 2009. EUA daily futures contracts. `http://www.ecx.eu`.

European Energy Exchange AG, September 2009. Power, intraday spot. `http://www.eex.com`.

Garnier, J., Wilhelmsen, B.-R., 2005. The natural real interest rate and the output gap in the euro area. The European Central Bank working paper series (14), 27.

Hendriks, C., 2006. CO2 pipeline schemes and cost curves for the European sector. In: GHGT-8 8th International Conference on Greenhouse Gas Control Technologies. Trondheim, Norway.

Hotelling, H., 1931. The economics of exhaustible resources. Journal of Political Economy 39, 137–175.

Hugo, A., Rutter, P., Pistikopulos, S., Amorelli, A., Zoia, G., 2005. Hydrogen infrastructure strategic planning using multi-objective optimization. International Journal of Hydrogen Energy 30 (15), 1523–1534.

Karlsson, K., Meibom, P., 2008. Optimal investment paths for future renewable based energy systems-using the optimisation model Balmorel. International Journal of Hydrogen Energy 33 (7), 1777–1787.

Kolstad, C. D., 2000. Enviromental Economics. Oxford University Press, New York.

Lekva, H., Aam, S., Hagen, E., Gjølberg, O., Riis, T., Kismul, A., 2004. Hydrogen som fremtidens energibærer. Tech. Rep. NOU 2004: 11, Olje- og energidepartementet, Hydrogenutvalget, Oslo, Norway.

Lesourd, J., Percebois, J., Valette, F., 1996. Models for energy policy. Routledge, London, UK.

Lin, Z., Ogden, J., Fan, Y., Sperling, D., 2005. The hydrogen infrastructure transition model (HIT) and its application in optimizing a 50-year hydrogen infrastructure for urban Beijing. Tech. rep., Institute of Transportation Studies, University of California, Davis, USA.

Mantzos, L., Capros, P., Kouvaritakis, N., 2003. European energy and transport trend to 2030. Tech. rep., National Technical University of Athens (NTUA), Greece.

McFarland, J., Reilly, J., Herzog, H., 2004. Representing energy technologies in top-down models using bottom-up information. Energy Economics 26 (4), 685–707.

Myklebust, J., Holth, C.B., M., Saue, L., Tomasgard, A., 2009. Short-term optimization of a hydrogen value chain for the transport sector, working Paper, NTNU.

Nakata, T., 2004. Energy-economic models and the environment. Progress in Energy and Combustion Science 30 (4), 417–475.

Ogden, J. M., 2004. Conceptual design of optimized fossil energy systems with capture and sequestration of carbon dioxide. Tech. rep., Princeton Environmental Institute, Princeton, USA.

Park, C. S., Sharp-Bette, G. P., 1990. Advanced Engineering Economics. John Wiley & Sons, New York, USA.

Sekanina, A., Pucher, E., 2006. H2-automotive: New vehicle technologies and propulsion systems. Technical report F2006SC01, Vienna University of Technology, Austria.

Stiller, C., Svensson, A. M., Möller-Holst, S., Bünger, U., Espegren, K. A., Holm, Ø. B., Tomasgard, A., 2008. Options for CO2-lean hydrogen export from Norway to Germany. Energy 33 (11), 1623–1633.

Svensson, A. M., Möller-Holst, S., Glöckener, R., Maurstad, O., 2007. Well-to-wheel study of passenger vehicles in the Norwegian energy system. Energy 32 (4), 437–445.

Tomasgard, A., Rømo, F., Fodstad, M., Midthun, K. T., 2007. Geometric modelling, numerical simulation and optimization. Springer Verlag, New York, USA, Ch. Optimization Models for the Natural Gas Value Chain.

Tseng, P., Lee, J., Friley, P., 2005. A hydrogen economy: Opportunities and challenges. Energy 30 (14), 2703–2720.

Van Benthem, A., Kramer, G., Ramer, R., 2006. An options approach to investment in a hydrogen infrastructure. Energy Policy 34 (17), 2949–2963.

Van den Heever, S. A., Grossmann, I. E., 2003. A strategy for the integration of production planning and reactive scheduling in the optimization of a hydrogen supply network. Computers and Chemical Engineering 27 (12), 1813–1839.

Wietschel, M., Hasenauer, U., de Groot, A., 2006. Development of European hydrogen infrastructure scenarios-CO2 reduction potential and infrastructure investment. Energy Policy 34 (11), 1284–98.

Williams, H. P., 1999. Model Building in Mathematical Programming, 4th Edition. John Wiley & Sons, New York, USA.

Appendix: Computations

	Actual 2008 prices	High off-peak EL price	Neg. CO_2 disposal price
Optimality gap	0.91%	1.93%	2.66%
Integer solutions #	6	16	151
Objective value [m€]	19053	22894	18398

Table 2.5: Technical details

Appendix: Basis for the Datasets

	Local electrolysis	Local reforming	Central reforming
Lifetime [years]	25	25	25
Utilization [% of time]	95	95	98
Maintenance [% of inv.]	2	3	3
Efficiency [%]	71	69	67
CO_2 emission $[\frac{tCO_2}{GJ\ H_2}]$	N/A[5]	0.0822	0.0254
CO_2 capture $[\frac{tCO_2}{GJ\ H_2}]$	-	0	0.0594
H_2 pressure [bar]	6	6	80

Sources: Ogden (2004) and Lekva, Aam, Hagen, Gjølberg, Riis, and Kismul (2004)

Table 2.6: H_2 production

[5]Potential indirect emissions from electrolysis are not accounted for.

	H_2 8"	H_2 12"	H_2 16"	CO_2 small	CO_2 large
Lifetime [years]	35	35	35	35	35
Recompression $[\frac{MWh}{tCO_2}]$	N/A	N/A	N/A	0.010	0.010
Pipeline vol. [m^3/100km]	3200	7300	13000	N/A	N/A
Maximum flow	940 [GJ/h]	2800 [GJ/h]	6000 [GJ/h]	513 [tCO_2/h]	1540 [tCO_2/h]
Unit inv. [M€/100km]	218	225	233	60	101
Maintenance [% of inv.]	0.5	0.5	0.5	0.5	0.5

Source: Ogden (2004)

Table 2.7: Technological and Economical data for pipelines

	Actual 2008 prices	High off-peak EL price	Neg. CO_2 disposal price	Annual growth rate
CO_2 offset price [€/t]	23	23	23	+4%
On-peak [€/MWh]	76	76	76	+2%
Off-peak [€/MWh]	43	60	43	+1%
NG price [€/GJ]	7	7	7	+2%
CO_2 disposal [€/t]	0	0	-60	-3%

Source: Average 2008 prices from the European Energy Exchange AG (2009) and the European Climate Exchange (2009). Other numbers are subjectively chosen.

Table 2.8: Input prices for the test cases.

Suction from	Central reforming			Local prod.	Pipeline	Trailer
Discharge to	200 bar trailer	450 bar trailer	CO_2 pipeline	Local storages		
Lifetime	25	25	25	25	25	25
Mainten. [%] of inv.	2.5	2.5	2.5	2.5	2.5	2.5
El. cons. $[\frac{MWh}{GJ}]$, $[\frac{MWh}{tCO_2}]$	0.005	0.010	0.135	0.048	0.024	0.018	0.010
Efficiency [%]	70	70	50	70	70	70	70
p_{out}/p_{in}	200/80	450/80	200/10	450/80	450/6	450/50	450/30

Source: (Former) Norsk Hydro

Table 2.9: Technological and economic data for compressors.

Paper II

J. Myklebust, C. B. Holth, L. E. S. Tøftum and A. Tomasgard:

Short-term optimization of a hydrogen value chain for the transport sector

Submitted to an international journal

Short-term optimization of a hydrogen value chain for the transport sector

Abstract:
Introduction of the energy carrier hydrogen is one of the alternatives to reduce our dependence on scarce and polluting fossil fuels. A large selection of hydrogen-supply technologies exists, and we have developed an optimization framework to find the lowest cost combination of these. If the investment scheduling and the details of the short-term operations were optimized jointly then the model would get intractable, so it is decomposed into two models of different horizons and resolutions. The short-run model verifies the feasibility of the investment decisions. Additionally, it provides a more accurate estimate of the variable costs of operating the chosen infrastructure. The investment model has a time horizon of 50 years and a resolution of 5 years. The operational model has an hourly resolution and a time horizon of 24 hours.
This paper presents the operational part of this optimization framework. It adapts the short-term scheduling of electrolysis to the hour-dependent electricity price, the hour-by-hour operation of storages, trailer departures, and pipeline pressures. The available capacities are decisions provided by the investment model. Its investments will cover average demand that is scaled with a capacity utilisation factor to take short-term peaks into account. The operational model is designed to quantify how much the short-term variations influence average capacity utilisation.
We have chosen these horizons and resolutions to illustrate the models. The operational model is general and can be adapted to any other seasonal pattern within the investment model's resolution.

3.1 Introduction

Hydrogen is one of the energy carriers that governments and energy companies consider a substitute for fossil fuels in the transport sector. One of the advantages of hydrogen is that there is a wide selection of supply technologies. This wide selection makes it hard to see directly what is the best combination of alternatives, and an optimization model could be an useful aid. Our optimization framework consist of the short-term optimization model that we present in this paper and the investment model presented in Myklebust, Holth, Saue, and Tomasgard (2009). The investment decisions require a long horizon, and the short-term operations require a fine resolution. A combination of fine resolution and a long horizon in one model would be computationally intractable. Hence, we decompose the optimization framework into a complementing pair of opti-

mization models. The investment model has a 50 year horizon that is aggregated into ten five-year periods. The adequacy of the investments to handle short-term peaks is verified through individual runs of the operational model for each of the investment model's periods. The time perspective of each run of the operational model is represented with a 24 hour window in Fig. 3.1.

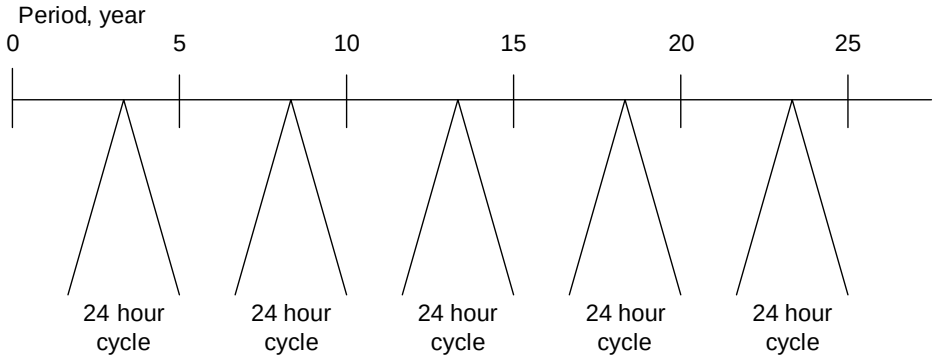

Figure 3.1: Time resolution of investment and operational models

The contribution of our modelling framework is to complement global energy system models such as applications of Balmoral or IEA's MARKAL (MARKet ALlocation). Our model's input data are price and demand projections that can be provided by economic models, and constants that are approximations from engineering models. Several papers study the exchange of data between models that have different foci and hence complement each other. See the investment model paper (Myklebust et al., 2009) for a more detailed discussion of model interactions. Examples of such applications are Karlsson and Meibom (2008), Endo (2007), Tseng, Lee, and Friley (2005), and DTI (2007) who simulated introduction of hydrogen in the energy markets of Scandinavia, Japan, the US and the UK respectively. Our pair of models are meant to be used iteratively with the global models to verify that their costs and time horizons are adequate, to verify the competitiveness and effectiveness of different energy sources used to produce hydrogen in a system perspective, to indicate an investment strategy with capacities, locations, technology choices, and similar decisions.

McFarland, Reilly, and Herzog (2004) present a methodology that translates bottom-up engineering information for two power generation technologies with carbon capture and sequestration (CCS) into the MIT Emissions Prediction and Policy Analysis (EPPA), a top-down model of the world economy. McFarland et al. (2004) focus on the limits that the basic laws of thermodynamics put on

efficiency improvements, technology penetration rates and capital stock vintaging. Unlike our approach they have not formulated an optimization model; they provide parameter estimates and analytical production functions to be used in computable general equilibrium (CGE) models. See Nakata (2004) for an elaborated discussion of how bottom-up energy models (such as our optimization model) and top-down macroeconomic models complement each other.

The reminder of this paper is organised as follows. In Section 3.2 we describe the operational model of the hydrogen value chain and its assumptions qualitatively. We present a mathematical formulation in Section 3.3. The technological and geographical assumptions are discussed in Section 3.4. The results of the base case and two alternative cases follow in Section 3.5. Section 3.6 concludes the paper.

3.2 Operation of the hydrogen value chain

The main objective of the operational model is to investigate whether the investments are adequate for the short-term demand peaks. If not, then the operational model output can be used to quantify the extent that the capacity utilisation limits of the long-term investment model should be calibrated. Once the adequacy of the investments is verified, then the short-term model can be used to evaluate the variable cost estimates of the investment model. A further advantage of developing these models in parallel is that we gain some insight into the consequences of alternative ways of formulating the required aggregations. All our implemented cases have a short-term horizon of 24 hours. This horizon is recurring in the sense that hour 24 precedes hour 1. Other recurring horizons, such as a week, would require minor modifications. The short-term objective is to minimize the variable costs. The supply technologies and their capacities are fixed at values optimized by the investment model. These fixed values differ across points in both time and geography. Figure 3.2 illustrates an example of an infrastructure that combines several technologies. All production and distribution facilities are already invested in so their costs are sunk and can be ignored. Provided the investment model returned the necessary capacities, hydrogen can be supplied using the production technologies steam methane reforming (SMR) and electrolysis, and can be transported utilising any combination of the transportation methods bulk and continuous. We assume a deterministic setting where all relative factor prices and demanded quantities over the planning horizon are exogenous and known, and we disregard bounds on feedstock supply.

The operational model takes the investments decided with the investment model as given and optimizes the operation of them. The investments will be any combination of the following four alternative value chains:

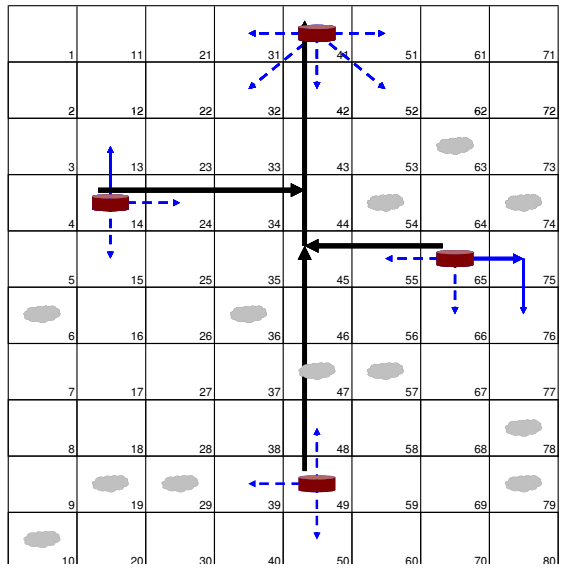

Figure 3.2: An example of infrastructure that combines several supply technologies is the investment model decision for year 2043 in the high electricity price case. Black arrows are CO_2 pipelines, solid blue arrows are H_2 pipelines, dotted blue arrows are trailer routes, grey clouds are decentralized reforming, and brown boxes are centralized reforming.

1. Methane is steam reformed to hydrogen at a large scale plant, and then the gaseous product is transported in bulk to the regional filling stations. This alternative will be modelled with CCS, so instead of paying to emit all produced CO_2, 70% of it will be deposited or sold for enhanced oil recovery (EOR). The costs of CCS are reduced efficiency and higher capital and operational costs.

2. Methane is steam reformed to hydrogen at a large scale plant. Rather than bulk transport it is transported in a set of connected inter-regional pipelines that are supplemented with intra-regional distribution branches. Relative to bulk transportation, pipelines have higher capital cost and lower operating cost, and are, consequently, preferred for larger quantities and shorter distances.

3. Methane is steam reformed in local small scale plants without CCS. This requires that the existing infrastructure has enough spare capacity to supply necessary inputs. The local production cannot supply any hydrogen

to filling stations in any other region. All produced CO_2 is emitted and requires carbon offsets.

4. H_2 is produced with decentralized electrolysis of water. This detour via electric energy is relevant if it becomes sufficiently cheap during off-peak hours relative to alternative feedstocks.

The above value chains are illustrated in Fig. 3.3. They are separated by the horizontal lines. Each alternative can utilize any of the equipment above or below these dashed lines but not the solid lines. Both pipeline and bulk distribution must be combined with large scale reforming. All alternatives require local storage compressors with the same outlet pressure, but because their inlet pressures vary they are modelled as distinct process units.

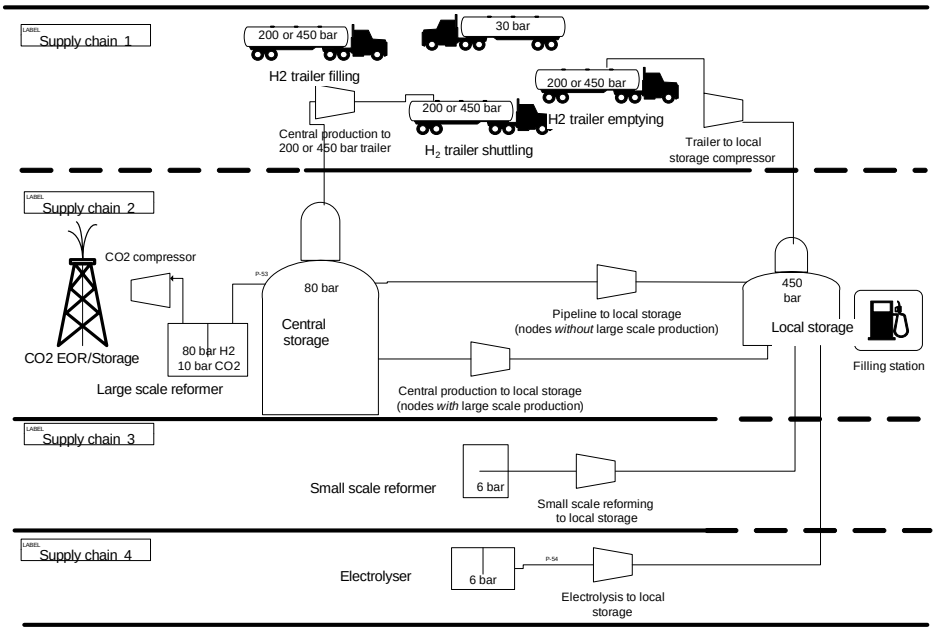

Figure 3.3: Alternative supply chain combinations

We assume there is a natural gas market and an electricity market in all regions and that all the hydrogen producers are price takers. Electricity cannot be stored, so wind, wave, thermal, or other types of generation that cannot be ramped down are priced lower during the night when demand is low. The plot of electricity prices in Fig. 3.4 illustrates such intra-day variation. The most important reason to choose an hourly resolution is to capture the scheduling of electrolysis and

the flow in and out of storages. For individual hours it is sufficient that the storage levels stay within given bounds. Net flow in and out of the storages can vary within the short-term planning horizon, but must balance over the horizon. The pipeline network can also be used as a short-term storage, called linepack. This requires separate variables for flow in and out for the same inter-regional pipeline at the same point in time. Furthermore, trailers can either adapt their arrival rates to short-term demand variations or adapt their departure rates to the varying hydrogen availability at the reformers. In the investment model only the *average* trailer departure rates of each period is modelled, which could require fewer trailers than the short-term peak departure rates.

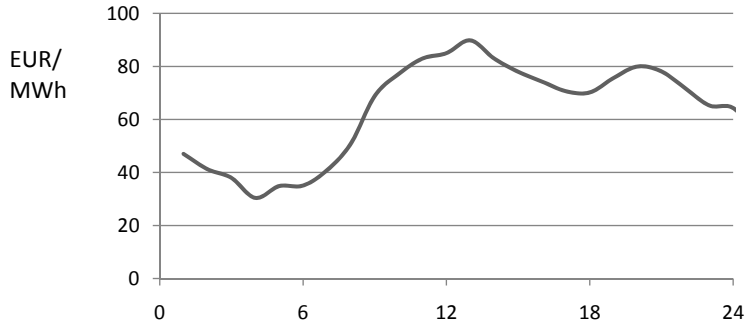

Figure 3.4: German average hour by hour electricity prices in 2008. Source: European Energy Exchange AG (2009).

In order to ensure feasibility of the operational model and to obtain information about potential bottlenecks, we allow some of the capacities that are set by the investment model to be exceeded. These violations are penalized in the objective function. The penalties are not realistic, rather they are intended to guide the solution process. However, if no non-violating feasible solution can be found, then high penalties help to quantify the minimum violation.

Short-term demand peaks are invisible in the investment model, only intra-period average values are included in its capacity constraints. Hence, flow variables with average values that are lower than the peaks need to be scaled up in order to ensure adequate investments. For example, if the production rate is kept constantly equal to the average demand, then the excess production during the hours when demand is less than average must be added to a storage, and vice versa. Alternatively, you could invest in high enough production capacity to satisfy short-term demand peaks directly without the use of storages. A combination of the two would also be possible. Because of economies of scale (EOS) the investment costs of these two alternatives to handle short-term demand fluctua-

tions cannot be translated into the equivalent short-term leasing costs, and the short-term model cannot be used to do the trade-off. The investment model is able to take EOS into account, but it is still unable to trade-off storage and production flexiblity costs. Information about short-term peaks is communicated from the operational model to the investment model with capacity utilisation bounds. The average utilisation (net outflow) a storage is zero, so there are no role for storages in the long-term model, therefore there are no constraint where utilisation bounds from the short-term model can be taken into account. In order to deal with this issue, we assume that the production capacity constraint *cannot* be violated, but the compression, shipment and storage capacities *can* be violated. We made this assumption because it is good for efficiency to keep the production rate steady. Hence, demand fluctuations are dampened thorough smoothing by linepack and other storages, instead of ramping the production rate up and down. This assumption is a choice of the model operator.

3.3 Mathematical Formulation

The constants, variables and sets are summarized below:

Constants

The capacities that are decision variables in the optimization framework's investment part are parameters in the operational part. Hence, there are two types of input data: Technological parameters, price and quantity projections that are exogenous to our framework, and capacities that are output of the investment model. Capacities and demand vary across the long-term time periods.

A_e	Indicator of whether a main CO_2 pipe of type e exists.
D_p	Hydrogen demand [GJ/h] in region p.
J_{ep}	Indicator of whether a CO_2 branch pipe of type e is available from a large scale reformer at p to the main pipeline.
W_{epq}	Indicator of whether trailers of type e supply region q from centralized production at p.
X_{ep}	Capacity [GJ/h] of equipment type e at p.
Y_{epq}	Indicator of whether a H_2 pipeline of diameter e from p to q exists.
Z_{epq}	Number of H_2 trailers of type e available from p to q.

Table 3.1: Investment decisions and hydrogen demand allocation

B	Trailer rental cost [€/km].
C_e	Capacity [tCO_2/h] of CO_2 pipeline of type e.
E_e	Penalty [€/GJ or GJ/h] for violation of capacity type e.
G_{apq}	Factor [GJ/bar] that converts from average pressure to linepack level in a pipeline from p to q of diameter a.
H_{pq}	Duration [hours] of a p to q return trip including filling.
K^I_{wpqa}, K^O_{wpqa}	Weymouth break point [GJ/bar] number w in the linearized flow from p to q in a pipeline of diameter a.
L_{pq}	Length [km] of a p to q return trip.
P_{ih}	Price [€/GJ], [€/MWh], or [€/tCO_2] of input factor i in hour h.
Π_p	Share of the area's combined population in region p.
$S_{max,e}, S_{min,e}$	Maximum and minimum levels of storage type e as percentages of sales or production capacity.
U^P, L^P	Upper and lower pressure bounds [bar] for the pipeline network.
V_h	Fuel demand hour h as percentages of average hourly demand.
Λ_{pq}	Percentage leaked from the p to q H_2 pipeline.

Table 3.2: Exogenous input data

Decision variables

$a_{eqh} \in \mathbb{Z}$	Arrival rate of trailers of type e to region q.
$d_{epqh} \in \mathbb{Z}$	Departure rate of trailers type e from p towards q.
$e_{qh} \in \mathbb{R}$	H_2 level [GJ] in the trailers in region q.
$fi_{pqh} \in \mathbb{R}$	H_2 flow [GJ/h] in at p for the pipeline to q.
$fo_{pqh} \in \mathbb{R}$	H_2 flow [GJ/h] out at q of the pipeline from p.
$fx_{eph} \in \mathbb{R}$	H_2 flow [GJ/h] from equipment e in region p.
$n_{epqh} \in \mathbb{Z}$	Trailers of type e commuting between p and q.
$p^{jnt}_{ph} \in \mathbb{R}$	Pressure [bar] in the pipeline junction at p.
$\overline{p_{pqh}} \in \mathbb{R}$	Average pressure [bar] in the pipeline from p to q.
$lp_{pqh} \in \mathbb{R}$	H_2 linepack level [GJ] in the pipeline from p to q.
$so_{eph} \in \mathbb{R}$	H_2 flow [GJ/h] out of storage type e at p.
$si_{eph} \in \mathbb{R}$	H_2 flow [GJ/h] into storage type e at p.
$sl_{eph} \in \mathbb{R}$	H_2 level [GJ] in storage type e at p.
$vx_{ep}, vy_{epq} \in \mathbb{R}$	Violation [GJ/h] of capacity e in region p or arc pq.

Table 3.3: For all decision variables, h indicates hour.

Sets

$\mathcal{A}$	Shipment alternatives.
$\mathcal{A}^T \subset \mathcal{A}$	Bulk shipment. Test case: {T20, T45} (200 or 450 bar trailers).
$\mathcal{A}^H \subset \mathcal{A}$	H_2 pipeline diameters. Test case: {8", 12", 16"}.
$\mathcal{E}$	Compressor, production, and storage types.
$\mathcal{E}^S \subset \mathcal{E}$	Storage types. Test case: {CS, DS} (centralized or decentralized).
$\mathcal{E}^P \subset \mathcal{E}$	Production types. Test case: {EP (electrolysers), DR (decentralized reformers), CR (centralized reformers)}.
$\mathcal{E}^{PD} \subset \mathcal{E}^P$	Decentralized production. Test case: {EP, DR}.
$\mathcal{E}^{KC} \subset \mathcal{E}^{\mathcal{K}}$	Compressor types with *suction* from centralized storages or pipeline junctions. Test case: {PJ (pipeline junction) to DS (decentralized storage), CS (centralized storage) to DS, CS to T20, CS to T45.}
$\mathcal{E}^{KD} \subset \mathcal{E}^{\mathcal{K}}$	Compressor types with *discharge* to decentralized storages. Test case: {PJ to DS, T20 or T45 to DS, DR to DS, EP to DS, CR to DS}.
$\mathcal{E}^C$	CO_2 pipelines. Test case: {CO_2-P1, CO_2-P2} (small or large).
$\mathcal{F}$	Input factors. Test case: {NG (natural gas), EL (electricity), CO_2-d (disposal), CO_2-o (CO_2 offsets)}.
$\mathcal{I}_p$, $\mathcal{O}_p$	Pipeline junctions with inflow from p and outflow to p respectively.
$\mathcal{N}$	All the geographical regions. Test case: $\{1, 2, \ldots, 80\}$.
$\mathcal{N}^L \subset \mathcal{N}$	Locations of decentralized reformers. Test case: {14, 41, 49, 65}.
$\mathcal{N}^C \subset \mathcal{N}^L$	Possible CO_2 pipeline inlet locations. Test case: $\mathcal{N}^L \backslash \{41\}$.
$\mathcal{W}$	Weymouth linearization breakpoints. Test case: $\{1, 2, \ldots, 15\}$.

Table 3.4: Sets of indices

Constraints

Variable cost minimization objective

The input factors to hydrogen production and compression are natural gas, electricity, carbon emission offsets and carbon disposal. If the application requires it the factor price P_{ih} or any other constant can be defined with geographic (p), time (h), or other dimensions. For locations with large scale reforming the disposed CO_2 can have either a positive or negative cost coefficient. It is positive if the CO_2 recipients require payment, but negative if they are willing to pay.

$$\begin{aligned} cost = & \sum_{e\in\mathcal{E}} \sum_{p\in\mathcal{N}} \sum_{h=1}^{24} \sum_{i\in\mathcal{I}} P_{ih} U_{ie} fx_{eph} \\ & + \sum_{a\in\mathcal{A}} \sum_{(p,q)\in\mathcal{N}^2} \sum_{h=1}^{24} L_{pq} B \;\; n_{apqh}. \end{aligned} \tag{3.1}$$

Here the first factor is the cost of H_2 production and compression, which is the product of the factor price P_{ih}, unit requirement U_{ie}, and the H_2 flow fx_{ep}, summarized over all hours h, input factors i, equipment types e and locations p. The second factor is the cost of delivering centralized production at p with trailers to region q. This is the product of the total length of the p to q round trip, L_{pq}, the tow truck rental cost per km, B, and the number n_{apqh} of trailers in operation, summarized over all types a, locations (p, q) and hours h. In the implemented case the objective also includes penalty costs of the pipeline junction's pressure deviation from the pipeline grid's inlet pressure to avoid arbitrary low pressures, as well as penalty costs of violating capacities. We model no direct variable costs of operating pipelines, only the indirect compression work.

Storage balances

The hour by hour sales' (deterministic) variation is modelled with the factors V_h that scale short-term average demand D_p of the given region p in hour h. All the hydrogen goes via the decentralized storages (DS) regardless of whether it is produced centrally or locally. Thus each small scale storage's outflow, so_{eph}, is required to cover local demand during the relevant hour:

$$so_{eph} \geq V_h D_p, \quad e = \text{DS}, \quad p \in \mathcal{N}, \quad h = 1, 2, .., 24. \tag{3.2}$$

All decentralized storage inflow requires compression. Consequently, the total inflow si_{mph} will be the combined flow fx_{eph} of all compressor types with *discharge* to a decentralised storage (DS), $\mathcal{E}^{KD}$.

$$si_{mph} = \sum_{e\in\mathcal{E}^{KD}} fx_{eph} \;\; m = \text{DS}, \quad p \in \mathcal{N}, \quad h = 1, 2, \ldots, 24, \tag{3.3}$$

where p is the location of the decentralized storage. A selection of compressors are used to fill a storage, one specific type for each alternative source. Which sources that are available depend on the given investments, and the alternative sources are pipeline junctions, arriving trailers, decentralized production or large-scale storages for centralised production.

In this recurring 24 hour horizon, hour 24 precedes hour 1 to avoid an end of horizon (EOH) effect. Consequently hour 1 must be modelled specifically. In order to satisfy mass balance the net inflow must equal the net increase of storage level from the preceding hour $(h-1)$ to the current hour h:

$$\begin{aligned} si_{eph} - so_{eph} &= sl_{eph} - sl_{ep(h-1)}, \\ si_{ep1} - so_{ep1} &= sl_{ep1} - sl_{ep24}, \\ e \in \mathcal{E}^S, \quad p \in \mathcal{N}, \quad h &= 2, 3, \ldots, 24, \end{aligned} \tag{3.4}$$

where si_{eph} and so_{eph} are flow in and out, sl_{eph} is storage level, e indicates decentralized or centralized type of storage. Flow in and out must balance when summarized over the horizon:

$$\sum_{h=1}^{24} si_{eph} - \sum_{h=1}^{24} so_{eph} = 0, \quad e \in \mathcal{E}^S, \quad p \in \mathcal{N} \tag{3.5}$$

Bounds on injection and withdrawal rates are not modelled. However, all storage levels sl_{mph} must stay within specified bounds during all individual hours. At any hour h, the level in any centralized storage (CS) must stay within the percentages S_m^{min} and S_m^{max} of the capacity X_{ep} of the centralized reformer at p:

$$\begin{aligned} S_m^{min} X_{ep} \leq sl_{mph} &\leq S_m^{max} X_{ep} + vx_{mp}, \\ m = \text{CS}, \quad e = \text{CR}, \quad p \in \mathcal{N}^L, \quad h &\in \{1, 2, \ldots, 24\}, \end{aligned} \tag{3.6}$$

where vx_{mp} is potential storage capacity violation and CR is centralized reforming. For all decentralized storages (DS) the level must be within the percentages S_m^{min} and S_m^{max} of the given hydrogen demand, D_p.

$$\begin{aligned} S_m^{min} D_p \leq sl_{mph} &\leq S_m^{max} D_p + vx_{mp}, \\ m = \text{DS}, \quad p \in \mathcal{N}, \quad h &\in \{1, 2, \ldots, 24\}, \end{aligned} \tag{3.7}$$

Because the sales vary from hour to hour and the production rate should be kept as steady as possible, all the large scale production goes via the large scale storages. The flow into the centralized storages during hour h equals the centralized production fx_{eph}.

$$si_{mph} = fx_{eph}, \quad m = \text{CS}, \quad e = \text{CR}, \quad p \in \mathcal{N}^L, \quad h \in \{1, 2, \ldots, 24\}, \tag{3.8}$$

where CS indicates central storage, CR indicates central reforming and p is the location of the central reformer and storage.

Regions that neither are locations for centralized reforming nor are part of the pipeline network do not interact with other regions, so the mass balances for their decentralized storage (3.3) is sufficient. However, the remaining regions must have the additional mass balance (3.9) that links them to all other regions. The sources in such a region p are the flow so_{mph} out of its central storage and the incoming pipeline flow fo_{qph} summarized over all pipeline junctions $\mathcal{O}_p$ with outlet to p. Its sinks are the outgoing pipeline flow fi_{pqh} summarized over all pipeline junctions $\mathcal{I}_p$ with inlet from p, the trailer deliveries summarized over all types of trailers a, the amount filled to its decentralized storage from the pipeline network, and the flow to its decentralized storage directly from its centralized storage. The amount shipped away in trailers equals the suction rate of the trailer filling compressors. The amount filled to local storages from the pipeline network equals the suction rate of the relevant compressor. Similarly, the flow directly from the large scale storage to the small scale storage in the same region equals the suction of the dedicated compressor. For the sake of clarity all compressors with *suction* from centralized storages or pipeline junctions are grouped in the index set $\mathcal{A}^{KC}$. Consequently, the flow to all these destinations can be measured as the suction fx_{aph} of each sink's dedicated compressor.

$$so_{mph} + \sum_{q \in \mathcal{O}_p} fo_{qph} = \sum_{q \in \mathcal{I}_p} fi_{pqh} + \sum_{a \in \mathcal{A}^{KC}} fx_{aph},$$
$$m = \text{CS}, \quad p \in \mathcal{N}, \quad h = 1, 2, .., 24. \tag{3.9}$$

Pipeline provision of transport and short-term storage

Hydrogen flows from pipeline junctions with high pressure to directly connected junctions with lower pressure. Constraint (3.10) relates the flow in a pipeline to the pressures at its end points. This restriction is a linearised version of the Weymouth equation (Tomasgard, Rømo, Fodstad, and Midthun, 2007), which in its original form is non-linear but convex. The linearisation is done around pairs of in- and output pressures. The breakpoints K^I_{wapq}, K^O_{wapq} depend on pressures, pipeline diameter a, distance from p to q, and a factor required to get the appropriate flow unit. This relation is for stationary flow in pipelines where short-term pressure variation is not used to provide storage, called linepack. We approximate it here by assuming that the average of flow fi_{apqh} in at p and fo_{apqh} out at q, is restricted by the junction pressures p^{jnt}_{ph} and p^{jnt}_{qh}.

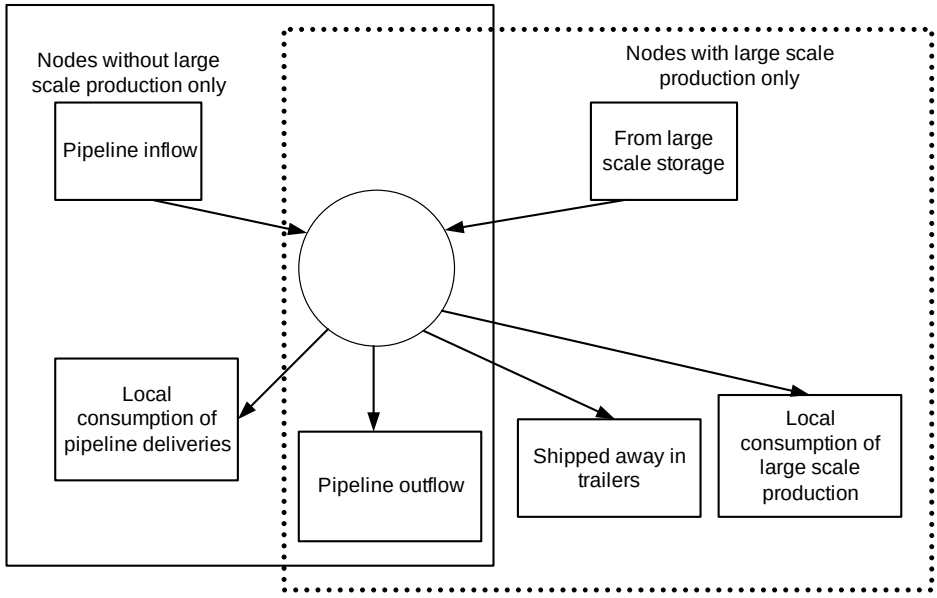

Figure 3.5: Mass balance for regions with large scale production and regions in the pipeline network

$$\frac{1}{2} fi_{apqh} + \frac{1}{2} fo_{apqh} \leq Y_{apq} \left(K^I_{wapq}\, p^{jnt}_{ph} - K^O_{wapq}\, p^{jnt}_{qh} \right),$$
$$w \in \mathcal{W}, \quad a \in \mathcal{A}^H, \quad p \in \mathcal{N}, \quad q \in \mathcal{D}_p, \quad h = 1, 2, .., 24. \tag{3.10}$$

Each Weymouth break point corresponds to a pair of pressures, which sets an upper bound on the flow rate. The only binding constraint is the one that corresponds to the breakpoint w based on the pressure pair closest to the actual pair. If a pipeline of type a exists from p to q in the relevant period then $Y_{apq} = 1$ otherwise $Y_{apq} = 0$ and no flow is feasible.

All large scale reformers have the fixed outlet pressure U^P, which determines the pressure p^{jnt}_{ph} in the pipeline junction where they are located p:

$$p^{jnt}_{ph} = U^P, \quad p \in \mathcal{N}^L, \quad h = 1, 2, .., 24. \tag{3.11}$$

To avoid non-linearity, the costs of operating the compressors are modelled as if their suction pressures are constant. Consequently, the real cost of the pressure fall in the pipelines is ignored, and the chosen pipeline outlet pressures could take any arbitrary value low enough to satisfy Constraint (3.10). To avoid arbitrarily low pressures, pressure falls are penalized. This penalty would induce an unbounded solution unless there is an upper bound on the pressure p^{jnt}_{ph}:

$$p^{jnt}_{ph} \leq U^P, \quad p \in \mathcal{N}, \quad h = 1, 2, .., 24, \tag{3.12}$$

For all regions p and hours h a lower bound L^P on pressure is required for physical reasons:

$$p^{jnt}_{ph} \geq L^P, \quad p \in \mathcal{N}, \quad h = 1, 2, .., 24, \tag{3.13}$$

The flow in and out can differ for individual hours so the pipelines can be used as storages, called linepack. When the inlet flow exceeds the outlet flow, average pressure increases, and vice versa. Linepack lp_{pqh} measured in energy units is approximately proportional to the average pressure $\overline{p_{pqh}}$ in the pipeline from p to q in hour h:

$$lp_{pqh} = G_{apq} \overline{p_{pqh}}, \quad p \in \mathcal{N}, \quad q \in \mathcal{I}_p, \quad h = 1, 2, .., 24, \tag{3.14}$$

where G_{apq} is a factor that depends on the inside volume of the pipeline, which is given by pipeline diameter a and its length from p to q. It also depends on the temperature and the physical properties of hydrogen, but we assume these factors are constant.

Similarly to the other storages, pipelines have to satisfy a mass balance where the net inflow during hour h equals the net increase of linepack level lp_{pqh} from

the preceding hour $h-1$ to the given hour h. In order to avoid end of horizon (EOH) effect and at the same time keep $h-1$ within range when $h=1$, hour 24 precedes hour 1:

$$\begin{aligned} fi_{pqh} - fo_{pqh} &= lp_{pqh} - lp_{pq(h-1)}, \\ fi_{pq1} - fo_{pq1} &= lp_{pq1} - lp_{pq24}, \\ & p \in \mathcal{N}, \quad q \in \mathcal{I}_p, \quad h = 2, 3, .., 24, \end{aligned} \tag{3.15}$$

where fi_{pqh} and fo_{pqh} are rates of flow in at p to all junctions $\mathcal{I}_p$ with inlet from p. Flow summarized over the planning horizon must balance:

$$\sum_{h=1}^{24} fi_{pqh}(1-\Lambda_{pq}) = \sum_{h=1}^{24} fo_{pqh}, \quad p \in \mathcal{N}, \quad q \in \mathcal{I}_p, \tag{3.16}$$

where fi_{pqh} is flow in at p, fo_{pqh} is flow out in a region q that receives directly from p during hour h. Λ_{pq} is the percentage leakage on the way from p to q. The mass balances of all junctions in the pipeline network are taken care of in the combined pipeline and large scale reforming mass balance, Constraint (3.9).

The pressure profile of a pipeline is non-linear, but for simplicity we assume that the average pressure $\overline{p_{pqh}}$ is an equally weighted interpolation of its end pressures p_{ph}^{jnt}:

$$\overline{p_{pqh}} = \frac{1}{2} p_{ph}^{jnt} + \frac{1}{2} p_{qh}^{jnt}, \quad p \in \mathcal{N}, \quad q \in \mathcal{I}_p, \quad h = 1, 2, \ldots, 24. \tag{3.17}$$

Production and compression capacities

The trailer storage mass balances, Constraint (3.26), includes the compression rate fx_{mph} of hydrogen from the trailers to the local storage. The combined centralized storage and pipeline network mass balance, Constraint (3.9), includes both the flow of the compressor with suction from pipelines and discharge to the local storages, and the compression of large scale production for the region's local storage. Flows of decentralized production, Constraint (3.18), and the compressor with suction from central storage and discharge to trailers, Constraint (3.19), are not given by other mass balances.

Both local electrolysis and local reforming have outlet pressures that are less than the local storage pressure, so this production must be compressed. Consequently, flow from each production type will equal its corresponding compressor suction rate:

$$fx_{mph} = fx_{eph}, \quad m \in \mathcal{A}^{PD}, \quad e = e(m), \quad p \in \mathcal{N}, \quad h = 1, 2, \ldots, 24, \tag{3.18}$$

$\mathcal{A}^{PD}$ is the set of decentralized production, $e(m)$ is the dedicated compressor for type m production.

Trailers must be filled at the central large scale storages with compressors of suitable types. The flow fx_{aph} of a compressor with suction from a central storage and discharge to trailers of type a equals the departures d_{apqh} summarized over all destinations q in hour h, multiplied by their capacity Q_a:

$$fx_{aph} = Q_a \sum_{q \in \mathcal{N}} d_{apqh}, \quad a \in \mathcal{A}_T, \quad p \in \mathcal{N}^L, \quad h = 1, 2, \ldots, 24. \tag{3.19}$$

The flow fx_{eph} of a compressor or production equipment of type e in a given region p cannot exceed its capacity X_{ep} and the potential capacity violation vx_{ep} in the relevant period adjusted for its percentage maximum utilization Φ_e;

$$fx_{eph} \leq X_{ep}\Phi_e + vx_{ep}, \quad e \in \mathcal{E}^K \cup \mathcal{E}^P, \quad p \in \mathcal{N}, \quad h = 1, 2, \ldots, 24. \tag{3.20}$$

In order to avoid an implicit trade off between using storages or varying the production level to accommodate short-term demand fluctuations the production capacity cannot be violated.

$$vx_{ep} = 0, \quad e \in \mathcal{E}^P, \quad p \in \mathcal{N}, \tag{3.21}$$

where e is the type of production and p its location.

Bulk transport and short-term storage of hydrogen

Similarly to the pipelines, also the trailers can be used for short-term storage. Only the intra-period *average* trailer arrival rates are included the investment model. Thus there is no incentive to invest in capacity for the short-term demand peaks unless an upper bound on capacity utilisation is communicated from the operational to the investment model. Because of its finer time resolution, the operational model allows arrival rates to vary with the short-term fluctuations, and can therefore quantify a capacity utilisation bound for the investment model. A tow truck that commutes between the large scale reformer at p and the demand centre in region q has completed its round trip and is available for another trip H_{pq} hours after departure. Consequently, in hour h all trailers that departed in hour $h - \lceil H_{pq} \rceil$ and earlier are back and available for another trip. However, trailers that departed in hour $h - \lceil H_{pq} \rceil + 1$ and later are still away and must be included in the number, n_{apqh}, of occupied trailers. This number, n_{apqh}, is all departures, d_{apqi}, summarized over the preceding hours back to the earliest trailer that has not returned yet. We assume that round trips that would last more than 24 hours are not realistic, this also simplifies the mathematical formulation and reduces the number of discrete variables. These preceding hours could be earlier the same day or later the day before. These two situations must be modelled

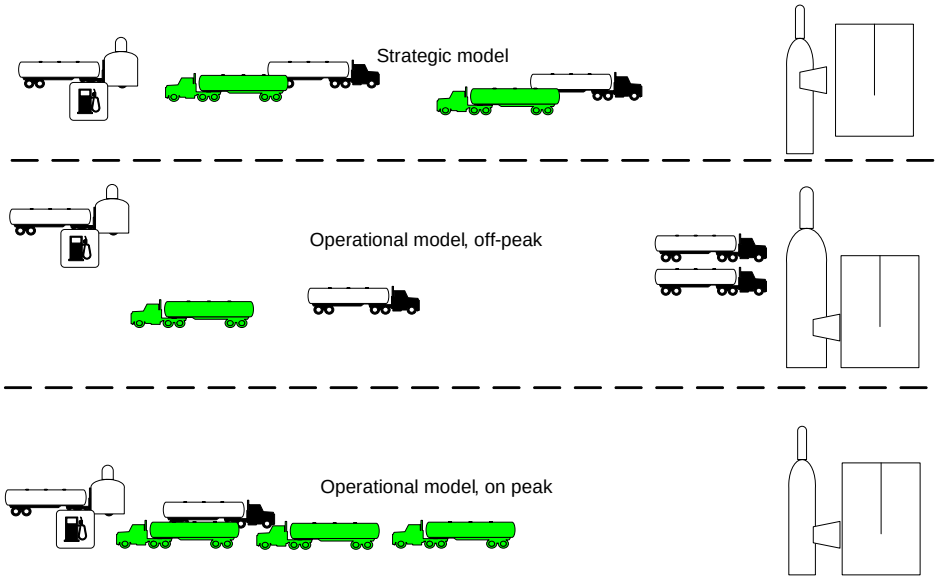

Figure 3.6: Long-term versus short-term trailer scheduling

with individual equations. Constraint (3.22) is for trailers leaving and returning the same day:

$$n_{apqh} = \sum_{i=h-H_{pq}+1}^{h} d_{apqi}, \quad H_{pq} \leq 24,$$
$$a \in \mathcal{A}_T, \quad (p,q) \in \mathcal{N}^L \times \mathcal{N}, \quad h \in \{\lceil H_{pq} \rceil, \lceil H_{pq} \rceil + 1, \ldots, 24\}. \tag{3.22}$$

Here a indicates trailer type, p where they are filled, q the region they supply, h the hour they leave p. Constraint (3.23) models trailers that left the day before. The hour indices of the departures the day before are incremented by 24 to stay in range:

$$n_{apqh} = \sum_{i=h-H_{pq}+25}^{24} d_{apqi} + \sum_{i=1}^{h} d_{apqi}, \quad H_{pq} \leq 24,$$
$$a \in \mathcal{A}_T, \quad (p,q) \in \mathcal{N}^L \times \mathcal{N}, \quad h \in \{1, 2, \ldots, \lceil H_{pq} \rceil - 1\}, \tag{3.23}$$

The number of trailers n_{apqh} is discrete, but need not be modelled explicitly as such because it is a sum of discrete departure rates, d_{apqi}.

One trailer is parked at all trailer supplied regions because the tow truck leaves a full trailer and picks up the empty trailer after the preceding delivery. Hence, one more trailer than tow trucks is necessary for each arc. Whether or not a region is supplied with a trailer is indicated with the binary constant W_{aph}. The number of trailers type a operating between p and q in hour h, n_{apqh}, plus the parked trailer W_{aph} cannot exceed the number of available trailers Z_{apq}, plus the potential capacity violation vy_{apq}.

$$n_{apqh} + W_{aph} \leq Z_{apq} + vy_{apq}, \quad a \in \mathcal{A}_T, \quad (p,q) \in \mathcal{N}^L \times \mathcal{N}, \quad h = 1, \ldots, 24, \tag{3.24}$$

The level of hydrogen stored in the additional trailer e_{aph} cannot exceed its capacity, Q_a:

$$e_{aph} \leq Q_a W_{aph}, \quad a \in \mathcal{A}_T, \quad p \in \mathcal{N}, \quad h = 1, 2, \ldots, 24, \tag{3.25}$$

The flow fx_{mph} compressed from the trailer for the local storage in region p equals the product of the trailers' arrival rate a_{aph} and their unit capacity adjusted for the change in tank level $e_{aph} - e_{ap(h-1)}$ the relevant hour:

$$\begin{aligned} fx_{mph} &\leq \sum_{a \in \mathcal{A}_T} a_{aph} Q_a - (e_{aph} - e_{ap(h-1)}), \\ fx_{mp1} &\leq \sum_{a \in \mathcal{A}_T} a_{ap1} Q_a - (e_{ap1} - e_{ap24}), \\ m &= TS, \quad p \in \mathcal{N}, \quad h = 2, 3, \ldots, 24, \end{aligned} \tag{3.26}$$

where TS indicates a trailer to local storage compressor. It is not practical to return with totally empty tanks, but to have a residue called cushion gas. The level in the trailer e_{aph} does not include the cushion gas. Hence, there is no lower bound on e_{aph} apart from the usual non-negativity constraint.

The rate a_{eqh} of arrivals of trailers type e in hour h at q is the sum of departures d_{epqh} from all large scale production locations p with time lags $\lceil H_{pq}/2 \rceil$ corresponding to the first half of the p to q round trip.

$$\begin{aligned} a_{eqh} &= \sum_{p \in \mathcal{N}^L} d_{epq(h - \lceil H_{pq}/2 \rceil)}, \quad 1 \leq h - \lceil H_{pq}/2 \rceil, \leq 24 \\ a_{eqh} &= \sum_{p \in \mathcal{N}^L} d_{epq(h - \lceil H_{pq}/2 \rceil + 24)}, \quad h - \lceil H_{pq}/2 \rceil \leq 0, \\ a &\in \mathcal{A}_T, \quad p \in \mathcal{N}, \quad h = 1, 2, \ldots, 24, \end{aligned} \tag{3.27}$$

Since the arrival rate a_{aqh} is a sum of integer departure rates d_{apqh} it need not to be explicitly modelled as such.

Pipeline transport of CO_2

The main pipeline must have sufficient capacity to transport the combined flow of compressed CO_2 away from all operating large scale reformers except the one at the end of the main pipeline. As mentioned for the calculation of variable costs in Constraint (3.1), the volume of compressed CO_2 produced at the large scale reformer e at p is the quantity CO_2 captured per unit of H_2, U_{ce} multiplied by the H_2 production, fx_{eph} at p in hour h.

$$\sum_{q \in \mathcal{N}^C} U_{ce} fx_{eqh} \leq \sum_{a \in \mathcal{A}_C} C_a A_a, \qquad (3.28)$$
$$c = \text{CO}_2\text{-d}, \quad e = \text{CR}, \quad h = 1, 2, \ldots, 24,$$

where the CO_2 flow, CO_2-d, is summarized over the locations $\mathcal{N}^C$ of large scale reformers that must have CO_2 infrastructure for disposal or EOR. CR is centralised reforming. A_e is an indicator of whether a main pipeline of type a exits. C_a the capacity of such a pipeline.

For the branch pipelines it is sufficient that they have sufficient capacity for the flow of CO_2 from the reformer at the relevant location p to the main CO_2 pipeline:

$$U_{ce} fx_{eph} \leq \sum_{a \in \mathcal{A}_C} C_a J_{ap}, \qquad (3.29)$$
$$c = \text{CO}_2\text{-d}, \quad e = \text{CR}, \quad h = 1, 2, \ldots, 24, \quad p \in \mathcal{N}^C,$$

where J_{ap} indicates whether there exists a CO_2 branch pipeline of type a from the reformer at p to the main CO_2 pipeline in the relevant period.

3.4 Datasets for the modelled cases

We have tested both the long- and short-term models on the same three cases. These cases differ in the input factor prices. In the base case prices are projected from their average 2008 level. In order to illustrate the conditions when various supply alternatives enter and exit we model two alternative cases where we have changed the electricity and CO_2 disposal prices respectively. In the first alternative case, the electricity price is higher, and in the second alternative we assume the oil companies are willing to pay more for compressed CO_2. We assume unlimited input factor supply in all cases. Obviously, relative prices will affect the optimal combination of hydrogen infrastructure. Consequently, in addition to the prices also the available infrastructure varies between short-term cases.

All the flows and production rates in the investment model have yearly resolution, and in the operational they have hourly resolution. In order to keep the coefficients within close orders of magnitude all flow rates are now measured by the hour, GJ/h, and electric energy is measured in MWh.

Distances, population distribution, fuel demand and base case prices are inspired by Germany. The prices are measured in €/GJ and €/MWh. The technological and financial data are summarized in the Appendix.

Demand projection

The demand development for hydrogen as a transport fuel is common to all three cases. However, the investment model will allocate demand geographically depending on the characteristics of the different cases. In the investment model we define demand as the product of the hydrogen market share and the overall transport fuel demand. The EU has set a goal of 5% market share for hydrogen by 2020. The industry considers this estimate as very optimistic, and we use 2% in 2020 increasing gradually towards 10% in 2050. We use this value as the period dependent hydrogen market share. Furthermore, we assume the fuel demand varies across regions in proportion with their population. The German total annual energy for road transport in 2006 was about 2230 PJ (Eurostat), which we extrapolate at the annual rate of 1.5% to 2300 PJ for our base year 2008. For the growth rates for transport demand we use rates from Mantzos, Capros, and Kouvaritakis (2003), which expect transport demand to grow at a rate of 1.5% until 2010, then 1.0 per cent until 2020, and 0.5% until 2030.

Factor price projections

Sophisticated prediction models for all relevant factor prices do not seem to have been developed yet. The price growth parameters are somewhat arbitrary and are intended to illustrate how the supply technologies vary as the prices change relative to each other. In a deterministic world the real prices of natural gas and other finite resources can be modelled by Hotelling's efficiency rule (Hotelling, 1931). We use 2% as the long-term neutral risk free interest rate (Garnier and Wilhelmsen, 2005), and project the on-peak electricity and natural gas prices to grow at that rate. We assume off-peak electricity generation will become more dominated by renewable sources such that this price will grow at a lower rate of 1%. For sake of simplicity, we model the CO_2 emission price with an annual growth rate of 4% because its availability is politically determined and we assume it must be at least as high as the economic growth in order to have an impact. Furthermore, for illustrative purposes it is advantagous that the prices grow at different rates, which lets us see how different price combinations affect

the choice of technology. The two alternative cases differ from the base case with either higher electricity price, or higher value of CO_2 for EOR.

Technological and geographical parameters

The model can handle any geographic structure, in addition to the technological parameters, only distances, price projections, and a demand projection are required. The regions are modelled as nodes without any internal structure, and all distances are measured between the nodes' centre points. The studied area has a dimension of 800×1000 km, which is divided into 8×10 uniformly spaced regions. The geographic parameters such as distances and population distribution are identical for all cases.

For each operational model case we assume the corresponding infrastructure chosen after the investment model has been run with the same exogenous data. The combination of inputs required to produce a given output with the same equipment is identical for all cases. The availability of equipment given by the investment model is a consequence of the assumed combination input factor prices and varies correspondingly.

We model input factor consumption as proportional to the total distance for transport by trailers, and proportional to flow for production and compression. The parameter that would model a compressor's effect as proportional to its flow is a non-linear function of other (often) endogenous variables such as suction and discharge pressures. In order to avoid non-linear compressor costs, we disregard endogenous suction and discharge pressures. On the other hand, we believe it is safer to assume that variable production costs are linear within the relevant operation range.

As illustrated in Fig. 3.3, hydrogen transported in bulk is compressed further from 80 bar at the pressurised reformer to either 200 or 450 bar depending on the trailer type. The pressure in the trailers' composite tubes increases and decreases proportionally to the amount filled or emptied. We assume the unloading ends at 30 bar. If we assume that the compressor suction pressure stays constantly at 30 bar when supplying the decentralised storage, rather than declines gradually from 200 or 450 bar towards 30, then we overestimate the compressor's energy consumption. Similarly, when trailers are filled at the centralised reformer, we assume the discharge pressure is constant at 200 or 450 bar, rather than increasing gradually from the suction pressure of 80 bar towards the relevant maximum.

In addition to the compressors energy consumption, the variable costs of trailer delivery also depend on the frequency of delivery and the length of each round trip. The trucks towing the hydrogen trailers are leased at a linear rate per kilometre that includes driver and fuel. How frequent each trailer is capable of delivering depends on the time it takes to drive from the relevant central reformer

to the local filling station and the time required at the end points. We assume that 4 hours of preparation are required in addition to the commute. Because the departure rate is modelled with integer variables, this non-linearity does not add any complexity. Return trips that would require more than 24 hours including filling and emptying are ignored. This reduces the number of integer variables, and would probably not be feasible in the real world anyway. Apart from the indirect cost of compressing the H_2 or CO_2, no variable costs of the pipeline infrastructure are modelled.

3.5 Case results and discussion

The short-term model is run separately for each of the investment model's ten five-year periods for all three cases. After an initial run required to calibrate the coefficients that scale the capacity demands, none of the capacity constraints are violated provided the penalty costs are sufficiently high. To which extent the short-term peaks are higher than the average capacity utilization is an operational model output. Hence, it is straightforward to derive the appropriate scaling factors on the flow variables that bound the capacity utilisations in the capacity constraints of the investment model.

The result when the investment model is applied to the base case is that there will only be decentralised reforming the first 15 years, and in the following periods decentralised electrolysis only. Figure 3.7 shows the allocation of electrolysis production to hours with low electricity price, and storage requirements for hours with hight demand. As could be expected, the production is allocated to the hours of the day when the prices are lowest, and to the minimum number of hours. Similarly, Fig. 3.8 illustrates the scheduling of local reforming, which happens evenly through the day because the price of the main input, natural gas, does not vary within the day.

In the case with negative CO_2 disposal costs, the first centralised reformer is introduced after ten years, and hydrogen is distributed with a combination of pipelines and trailers depending on volumes and distances. In the high electricity price case, one centralised reformer will be introduced after 20 years, and its production is distributed with trailers initially. In later periods, more centralised reformers are added and the volumes get large enough to make pipeline distribution preferable to some of the destinations. The other figures provide examples of short-run operations of the two alternative cases where there is centralised hydrogen production with distribution for decentralised consumption. Figure 3.9 illustrates the allocation of large scale production to its three alternative uses, consumption in the region where it is produced, or delivery in pipelines or trailers for consumption at other regions. Figures 3.11 and 3.10 illustrate the variation of

pipeline pressures during the day and how it relates to pipeline flow. Figures 3.12 and 3.13 illustrate examples of the hourly operation of trailers.

The cost of using linepack as a storage substitute is the increased energy consumption in compressors, and more detailed compressor modelling is needed to accommodate this feature. See for example (Nørstebø, Bakken, and Dahl, 2007) for compressor modelling details. Detailed modelling of storages and storage substitutes is left for future research. Similarly to electricity prices, natural gas prices can also follow a seasonal pattern, but with longer periodicity. This price variation could make it optimal to operate them as spread options. This could be implemented in a version of our operational model with a horizon that corresponds to the NG price periodicity.

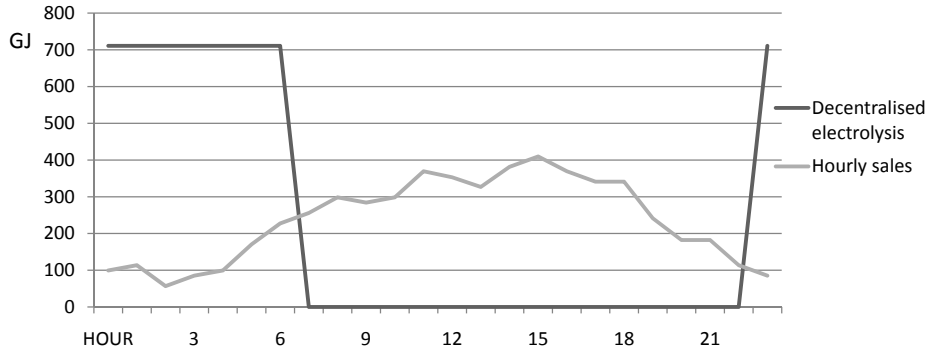

Figure 3.7: The local storage is filled with hydrogen from electrolysis during the hours when electricity is relatively cheap. Sales vary through the day. Example plot is for region 1, year 2058, base case.

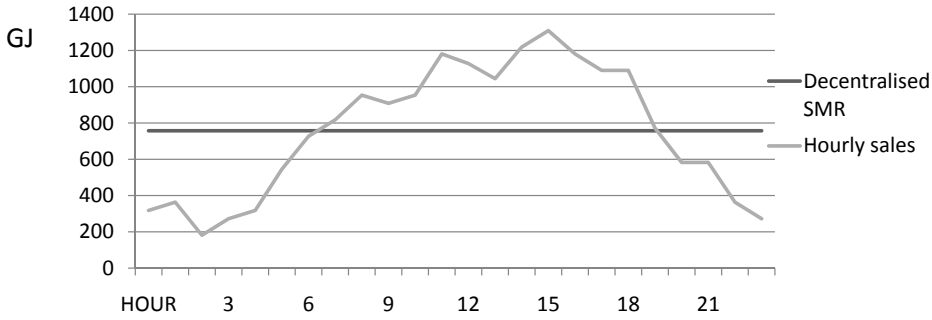

Figure 3.8: The storages makes it possible to keep a steady production rate even if sales vary through the day. Example is from the base case, region 13 year 2013.

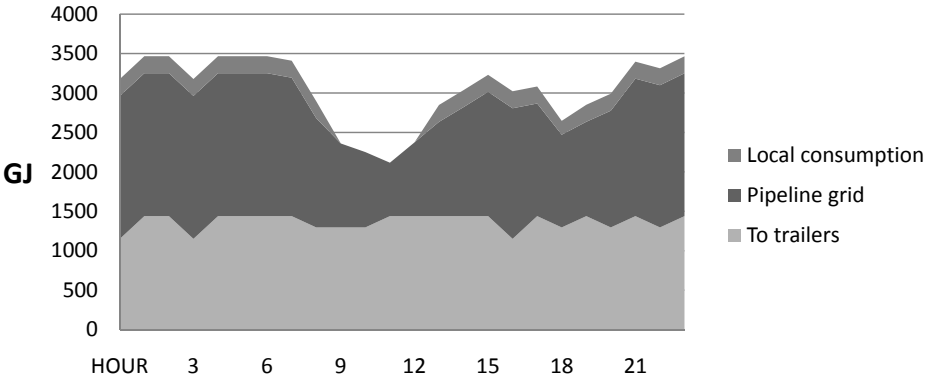

Figure 3.9: Allocation of large scale production to local consumption, pipeline distribution, and trailer distribution. Example from region 14 in year 2048, high off-peak electricity price case.

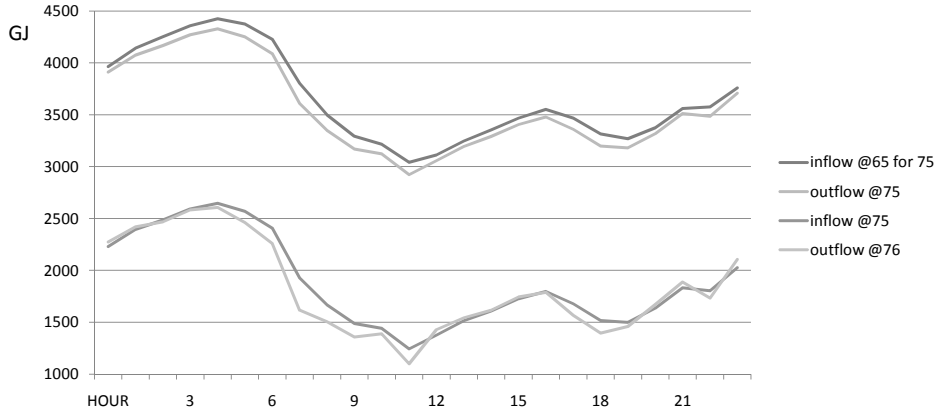

Figure 3.10: Location 65 has a centralised reformer. It supplies region 75 with a direct pipeline, and region 76 indirectly via region 75. Inflow can be different from outflow, and can vary across different hours of the day. Data used for this plot are from the high off-peak electricity price case, year 2058.

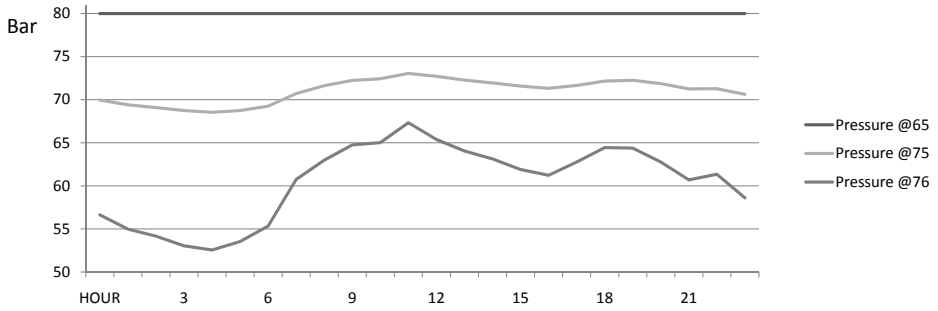

Figure 3.11: The pipeline pressure becomes lower at regions 75 and 76 which are respectively 100 and 200 km away from the reformer at location 65. During the hours of the day when the flow rate is highest (see Fig. 3.10), the pressure drop is highest. Data used for this plot are from the high off-peak electricity price case, in year 2058.

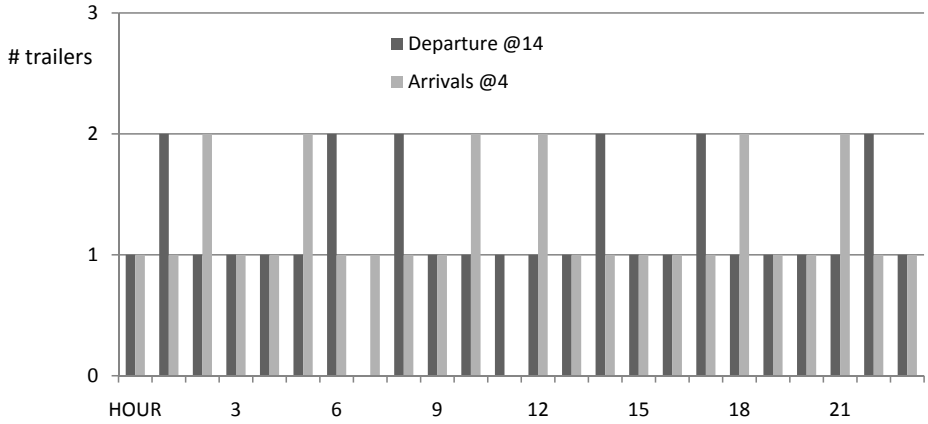

Figure 3.12: The trailers arrive after a time delay corresponding to the distance driven. Example is the supply from region 14 to region 4, that is a 4 hour drive, in year 2048, high off-peak electricity price case.

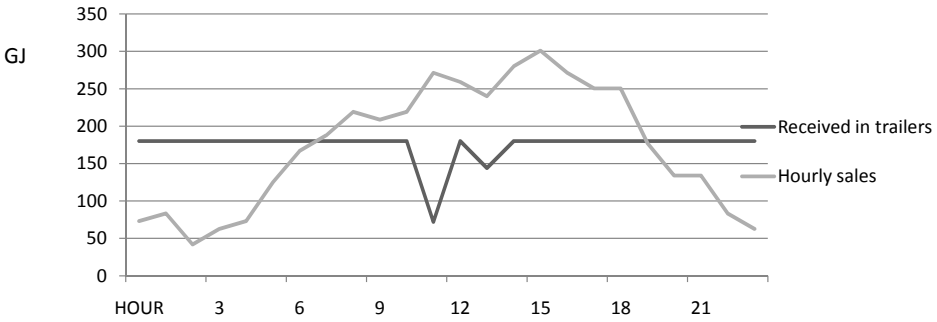

Figure 3.13: The storages make it possible for the trailers to have arrival rates that do not correspond directly to the short-term demand variation. Example is the supply from large scale reformer at 14 to region 4 in year 2048 in the high electricity price case.

3.6 Conclusion

We have developed a hydrogen production and distribution cost minimization framework that is driven by volume and prices. The short-term model consists of a combination of mass balances, pressure dependent pipeline flow equations. The long-term model also includes linearised cost functions of the individual transport and production units. A long horizon is required to capture the economic properties of investments with high upfront costs and long lives in service, and a fine resolution is required to ensure investments are adequate for the short-term peaks. Such combination of fine resolution and a long horizon in one model would be computationally intractable. Hence, we decompose the optimization framework into a complementing pair of optimization models, which we present in two separate papers. This paper focuses on the operational model, which takes the investment model's decisions as parameters along factor prices. It is intended to support the investment model with information about how much the short-term fluctuations affect average capacity utilisation, and more detailed estimates of operational costs.

The combination of technologies is set by separate runs of the investment model with the following three cases: In the base case prices are projected from their actual values in 2008. In the two alternative cases the off-peak electricity price is projected from a higher level and negative CO_2 deposition costs respectively. When the investment model is applied to the base case it recommends only decentralised hydrogen production. For each individual long-term period, the short-term model returns the optimal operation of storages and scheduling of electrolysis. As expected, electrolysis takes place during the hours of low electricity price, and the part of it that is not consumed those hours is stored in order to satisfy demand during the hours when electricity is more expensive. For the cases where hydrogen is produced centrally the model results show the allocation of production to the various supply alternatives for individual hours of the day. The chosen storage capacity seems to have eliminated the requirement of linepack. The trade-off between investment in flexible production, larger pipeline diameters and compressor capacities or conventional storages is left for future research.

Acknowledgements

We thank (former) Norsk Hydro, the NorWays project and Christoph Stiller at Ludwig-Bölkow-Systemtechnik GmbH who have helped us with some technological details, Matthias Nowak for help with technical issues, and Adrian Werner for helpful comments. All errors remain our own.

Bibliography

DTI, 2007. Meeting the energy challenge, a white paper on energy. Tech. rep., Department of Trade and Industry, United Kingdom.

Endo, E., 2007. Market penetration analysis of fuel cell vehicles in Japan by using the energy system model MARKAL. International Journal of Hydrogen Energy 32 (10-11), 1347–1354.

European Climate Exchange, September 2009. EUA daily futures contracts. `http://www.ecx.eu`.

European Energy Exchange AG, September 2009. Power, intraday spot. `http://www.eex.com`.

Garnier, J., Wilhelmsen, B.-R., 2005. The natural real interest rate and the output gap in the euro area. The European Central Bank working paper series (14), 27.

Hotelling, H., 1931. The economics of exhaustible resources. Journal of Political Economy 39, 137–175.

Karlsson, K., Meibom, P., 2008. Optimal investment paths for future renewable based energy systems-using the optimisation model Balmorel. International Journal of Hydrogen Energy 33 (7), 1777–1787.

Lekva, H., Aam, S., Hagen, E., Gjølberg, O., Riis, T., Kismul, A., 2004. Hydrogen som fremtidens energibærer. Tech. Rep. NOU 2004: 11, Olje- og energidepartementet, Hydrogenutvalget, Oslo, Norway.

Mantzos, L., Capros, P., Kouvaritakis, N., 2003. European energy and transport trend to 2030. Tech. rep., National Technical University of Athens (NTUA), Greece.

McFarland, J., Reilly, J., Herzog, H., 2004. Representing energy technologies in top-down models using bottom-up information. Energy Economics 26 (4), 685–707.

Myklebust, J., Holth, C.B., M., Saue, L., Tomasgard, A., 2009. Optimizing investments for hydrogen infrastructure in the transport sector, working Paper, NTNU.

Nakata, T., 2004. Energy-economic models and the environment. Progress in Energy and Combustion Science 30 (4), 417–475.

Nørstebø, V. S., Bakken, L. E., Dahl, H. J., 2007. Optimum operation of export compressors. In: Proceedings of GT2007: ASME Turbo Expo 2007: Power for Land, Sea and Air. ASME, Montreal, Canada.

Ogden, J. M., 2004. Conceptual design of optimized fossil energy systems with capture and sequestration of carbon dioxide. Tech. rep., Princeton Environmental Institute, Princeton, USA.

Tomasgard, A., Rømo, F., Fodstad, M., Midthun, K. T., 2007. Geometric modelling, numerical simulation and optimization. Springer Verlag, New York, USA, Ch. Optimization Models for the Natural Gas Value Chain.

Tseng, P., Lee, J., Friley, P., 2005. A hydrogen economy: Opportunities and challenges. Energy 30 (14), 2703–2720.

Appendix: Basis for the Datasets

	Local electrolysis	Local reforming	Central reforming
Lifetime [years]	25	25	25
Utilization [% of time]	95	95	98
Maintenance [% of inv.]	2	3	3
Efficiency [%]	71	69	67
CO_2 emission $[\frac{tCO_2}{GJ\ H_2}]$	N/A[6]	0.0822	0.0254
CO_2 capture $[\frac{tCO_2}{GJ\ H_2}]$	-	0	0.0594
H_2 pressure [bar]	6	6	80

Sources: Ogden (2004) and Lekva, Aam, Hagen, Gjølberg, Riis, and Kismul (2004)

Table 3.5: H_2 production

	H_2 8"	H_2 12"	H_2 16"	CO_2 small	CO_2 large
Lifetime [years]	35	35	35	35	35
Recompression $[\frac{MWh}{tCO_2}]$	N/A	N/A	N/A	0.010	0.010
Pipeline vol. [m^3/100km]	3200	7300	13000	N/A	N/A
Maximum flow	940 [GJ/h]	2800 [GJ/h]	6000 [GJ/h]	513 [tCO_2/h]	1540 [tCO_2/h]
Unit inv. [M€/100km]	218	225	233	60	101
Maintenance [% of inv.]	0.5	0.5	0.5	0.5	0.5

Source: Ogden (2004)

Table 3.6: Technological and Economical data for pipelines

[6]Potential indirect emissions from electrolysis are not accounted for.

	Actual 2008 prices	High off-peak EL price	Neg. CO_2 disposal price	Annual growth rate
CO_2 offset price [€/t]	23	23	23	+4%
On-peak [€/MWh]	76	76	76	+2%
Off-peak [€/MWh]	43	60	43	+1%
NG price [€/GJ]	7	7	7	+2%
CO_2 disposal [€/t]	0	0	-60	-3%

Source: Average 2008 prices from the European Energy Exchange AG (2009) and the European Climate Exchange (2009). Other numbers are subjectively chosen.

Table 3.7: Input prices for the test cases.

Suction from	Central reforming				Local prod.	Pipeline	Trailer
Discharge to	200 bar trailer	450 bar trailer	CO_2 pipeline	Local storages			
Lifetime	25	25	25	25	25	25	25
Mainten. [%] of inv.	2.5	2.5	2.5	2.5	2.5	2.5	2.5
El. cons. $[\frac{\text{MWh}}{\text{GJ}}]$, $[\frac{\text{MWh}}{\text{tCO}_2}]$	0.005	0.010	0.135	0.048	0.024	0.018	0.010
Efficiency [%]	70	70	50	70	70	70	70
p_{out}/p_{in}	200/80	450/80	200/10	450/80	450/6	450/50	450/30

Source: (Former) Norsk Hydro

Table 3.8: Technological and economic data for compressors.

Paper III

A. Aspelund, T. Gundersen, J. Myklebust, M.P. Nowak and A. Tomasgard:

An optimization-simulation model for a simple LNG process

Computers and Chemical Engineering
doi:10.1016/j.compchemeng.2009.10.018

An optimization-simulation model for a simple LNG process

Abstract:
A gradient free optimization-simulation method for processes modelled with the simulator Aspen HYSYS is developed. The tool is based on a Tabu Search (TS) and the Nelder-Mead Downhill Simplex (NMDS) method. The local optima that result from the TS are fine-tuned with NMDS to reduce the required number of simulations. The tool has been applied to find the total refrigerant flow rate and composition, as well as the refrigerant suction and condenser pressures that minimize the energy requirements of a Prico process. The main strength of this method is that it has a high probability of obtaining a better solution with significantly fewer simulation runs than other metaheuristic methods. Also, by changing the TS step size it is possible to influence the initial search pattern, thereby taking advantage of already gained process knowledge to decrease the optimization time. The method is general and can be applied to other processes modelled in Aspen HYSYS.

4.1 Introduction

Energy and petrochemical process plants consist of unit operations such as separators, valves, expanders, compressors and heat exchangers. Each of these unit operations contributes its own set of more or less realistic thermodynamic equations as well as mass and heat balances. Such equation systems normally have a few degrees of freedom. The units are linked to each other by the material and energy streams, which have their own sets of process variables, such as flow rate, pressure and temperature. The challenging task is to minimize the investment and operating costs of the plant with respect to these process variables. In general, adjustments in the operation of one of the units will have consequences for other units, and these relationships are often nonlinear.

Mathematical programming (MP) and other deterministic optimization methods are widely used in process design as these methods have the ability to find the best possible solution for the mathematical model that describes the process (Edgar, Himmelblau, and Lasdon, 2001). A common example of using MP in process design is the synthesis of heat exchanger networks (HEN). Also, some attempts have been made to connect the HEN with the background process. However, only smaller problems have been solved this way. Two thorough reviews of heat exchanger network synthesis (HENS) were published by Gundersen and Naess (1988) and by Jezowski (1994a), Jezowski (1994b). Furman and Sahini-

dis (2002) have contributed with a critical review and annotated bibliography of 461 papers on HENS. Due to physical laws and economic relations, the mathematical model commonly results in a non-convex nonlinear programming (NLP) problem. Furthermore, with discrete decisions, a mixed integer nonlinear programming (MINLP) problem has to be solved. These types of problems can be hard, or even practically impossible to solve using deterministic global optimization algorithms without further simplification of the model. The main advantage of using equation based programs and global solvers, is that it can guarantee that the global optimum of the *model* is found (Floudas, 1999). However, if the equation based model cannot be solved unless it is made too unrealistic, then the proven optimum may not be the best possible solution in the *real world*.

In order to model the process more rigorously and with less effort, general purpose process simulators are often used. Such process simulators can be divided in two main groups, sequential and equation based simulators. Common to all process simulators is a library consisting of three main parts; thermodynamic relations (equations), fluid properties and pre-defined unit operations (process equipment). The processes are then designed using the unit operations, which are connected by material and energy streams. Since the set of equations are too complicated to be solved analytically, they must be solved recursively to determine settings that are consistent for the entire plant.

In an equation based process simulator the equations for all unit operations as well as the thermodynamic relations are solved simultaneously. It is therefore possible to use equation based process simulators together with deterministic optimization. Equation based models can be made more rigorous by adding more equations. However, for large non-convex NLP problems, no algorithms exist that solve such problems in polynomial time, thus they rapidly get intractable.

Sequential based simulators are very common in the industry as well as in academia and are widely used due to their simplicity and robustness. Another advantage with sequential based process simulators is that their graphical user interface (GUI) can make implementation of the petrochemical process models relatively less time consuming than in equation based tools. In contradiction to equation based simulators, each unit operation is modelled and solved on its own given the input data in the form of material and energy streams. The units are then solved in sequence. To speed up the convergence, numerical methods such as Wegstein are often used. For complicated flow sheets there may be several recycles and the calculation order is normally set to give the lowest possible number of recycles or tear streams (Gundersen and Hertzberg, 1983). The disadvantage with the sequential approach is that the gradient information that deterministic optimization methods require is less accurate and harder to obtain. Since the solutions will change slightly from one run to another due to the sequential behaviour and the tolerances, it may be difficult to develop procedures

for obtaining these gradients. A sequential based process model can be looked upon as a "black-box" and is therefore not suitable for use in global deterministic optimization algorithms.

A process that benefits from rigorous modelling in process simulators is liquefaction of natural gas (LNG). It is an energy and cost intensive process, and due to small temperature differences in the heat exchangers, inaccurate modelling is likely to result in real world infeasibility. The main contribution of this paper is a method that does not require gradients for the heuristic optimization of sequence based simulation models.

In contrast to deterministic methods, Stochastic Optimization (SO) incorporate probabilistic (random) elements either in the objective function, the constraints, or alternatively in the algorithm itself e.g. through random parameter values, random choices or in both. A distinction can be made between Stochastic Programming, where the model is to be optimized with regard to uncertainties in the value of some variables, e.g. the volume and sales price of a product, and Stochastic Algorithms where random elements are used in the search, the latter is also known as Meta Heuristic (MH) methods. In process design the most common MH are Genetic or evolutionary algorithms (GA), Tabu Search (TS), Simulated Annealing (SA) and multi-start Local Searches (MSLS) where a local optimization algorithm is started from several feasible points (Glover, 1986; Holland, 1975; Kirkpatrick, Gelatt, and Vecchi, 1983; Marti, 2003). The main strength with MH methods is that they can be used to optimize a black-box model and are thereby well suited to be implemented together with sequential based process simulators to take advantage of the rigorous thermodynamic packages and unit operations that are already developed. The weakness is that MH methods, in contrast to deterministic methods, cannot guarantee that the best possible solution is found. However, the MH solution might still be better than the exact solution from the globally optimized but simplified deterministic model.

Apart from the modifications required for the error handling in the aggregation of the objective value, the presented method is quite similar to those applied to analytical test functions presented by Chelouah and Siarry (2005) and Hedar and Fukushima (2006). Their models consist of combinations of a global Tabu Search (TS) and a local Nelder-Mead Downhill Simplex (NMDS).

Exler, Antelo, Egea, Alonso, and Banga (2008) have applied a TS based algorithm to an integrated process and control design model. They argue that mathematical programming using global optimization methods (GO) only handle problems that are small, differentiable and continuous. A system of differential and algebraic equations forms their model's restrictions. Their case is similar to the one described in this paper and assumes nothing about the topology of the objective and the model is treated as a black box. Cavin, Fischer, Glover, and Hungerbüler (2004) apply a TS optimization algorithm to a batch plant.

Batch process simulation software is used as a black-box model for the process evaluations. They discuss Genetic Algorithm (GA) versus TS and conclude that there are several factors that make GA unsuitable for such applications. The crossover operations do not always generate valid solutions, and penalty and ad hoc repair operations have a risk of spending most of the computational effort in the handling of errors.

Section 4.2 contains a detailed description of the optimization-simulation framework, including the aggregated objective value, the global TS, the local NMDS, the combined search and the integration between a Process Simulator and the search procedure. The industrial process that the method is applied to, Prico, a simple LNG process, is presented in Section 4.3. The results and plans for further work are presented in Section 4.4. A discussion of the model and the results are found in Section 4.5. Conclusions are found in Section 4.6.

4.2 Optimization-simulation framework

From the point of view of the search algorithm, the objective function of the problem addressed in this paper is a black box. It contains a sequence based simulation model and an error handling algorithm. Since the model is known to have multiple minima and cannot easily and accurately provide any gradient information, it requires global search methods such as Simulated Annealing (SA), Tabu Search (TS) or Genetic Algorithms (GA). Among these, TS is expected to be the best suited for this problem because it gives the best control over how much the solution can change from one step of the search to the next so that less effort is spent on error handling. The reason for combining the global TS with the NMDS local search or descent method, is that the local search usually converges faster to the best solution in the promising area that the TS has detected than the TS would on its own.

The optimization engine consists of a combined TS and NMDS which is connected to the process simulator Aspen HYSYS®(version 2004.2) through Microsoft Excel using Visual Basic for Applications (VBA). The initial expectation, which turned out to be true, is that a large part of the computation time is spent running simulations relative to running the search algorithm; therefore Visual Basic (VBA) is an adequate surrounding layer. It provides the necessary means to get access to the COM functionality of HYSYS, which was crucial for the development. Microsoft Excel is also used as a Graphical User Interface and includes the input data, the TS and NMS settings and numerical as well as graphical results.

The objective value aggregation procedure in the VBA routine consists of the HYSYS simulation and the error handling. At the beginning of each cycle, all relevant values are given to HYSYS, which is then started and runs until it either

converges or warns that it is unable to. Then some of the calculated process values are retrieved, the feasibility status is checked, and the objective value aggregation procedure condenses this information into a single objective value. Seeing it in an abstract way, this procedure replaces the traditional objective function.

The aggregated objective value

The objective value aggregation consists of two parts; the simulation model and an algorithm that condenses the simulation output or the warning message into a single number. This number is a measure of the quality of the evaluated solution. If it is able to find the true objective value of the model then that will be the returned number, otherwise it will handle the error by returning a "very high number" that indicates that the solution is infeasible or that it is inconclusive whether it is feasible. The "very high number" is the same for all types of errors. In both the local and global searches the next solution will always be the best *admissible* of the candidate solutions. Infeasible solutions will never be a candidate, and the rank of such irrelevant solutions relative to each other is of no consequence for the search direction. Hence, the search is able to handle such error indication from the objective value aggregation provided there are not too many of them among the same set of neighbours. These black box characteristics are relevant for the choice of search method. It cannot easily provide any gradients, it has numerous local optima, and if the changes in the submitted solution from one step to the next are too large, the objective value aggregation will not converge. Hence, it is not desirable to include a penalty that makes the farthest points more appealing. All the decision variables in the meta heuristic (MH) searches have finite domains (box constraints), which makes it possible to discretize them. Mass flows, absolute pressures and absolute temperatures can neither be negative nor infinitely high. Equality constraints cannot be formulated as lower or upper bounds and will be relaxed, i.e. their deviation from one or both sides of their target will be given a penalty in the objective value. This addition to the objective value happens inside the objective value aggregation, see Fig. 4.1.

The global Tabu search

Tabu Search (TS) was originally intended to solve discrete problems (Jezowski, 1994b). Its name is due to its utilization of a list of recently visited solutions that cannot be revisited for given number of iterations, called the *Tabu-List* (TL). The intention with this memory is to let the search escape local optima. Consequently, a new *current* solution is not necessarily better than the previous.

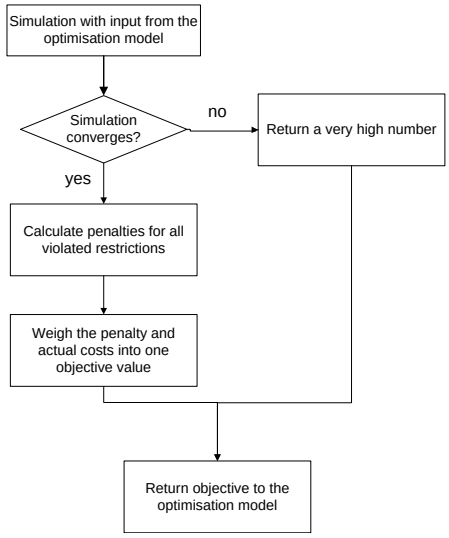

Figure 4.1: The objective value aggregation

The recursion of the TS can be summarized as follows (Gendreau, 2002): The *current* solution, the *best known* solution, the set of *tabu* solutions, and objective value of the best known must be initialised. The solutions have the same dimension as the number of decisions to be optimized. Choose (construct) an initial feasible solution. Set the current and the best known solution equal to the chosen initial feasible solution. Set the best known objective value equal to the value of this initial solution. The tabu list is initially empty. While the termination criterion is not satisfied, rank the *neighbours* of the current solution by objective values, and select the best admissible of them as the new current solution. If the current solution is better than the best known, then update the best known. Record the current solution in the tabu list, and delete the oldest entry if necessary. Proceed from the current solution. When the termination criterion is satisfied, report the best known solution and its corresponding objective value.

Because the TS can only be applied to discrete decisions the continuous variables must be discretized. The variables of the implementation described in this paper are discretized by division of their domains into a finite numbers of steps. At each of the iterations, the candidate decision is to take one of the decision variables a step up or down, while all the other variables stay at the current value. The set of such candidate decisions are called the neighbours of the current solution. Because step sizes are set in advance and the value of one variable at the time changes one step either up or down, the maximum number of neighbour-

solutions is twice the number of decision variables minus the number of variables at their limits. If the current value of one of the decision variables is at either end of its domain, then the only feasible decisions are to stay unchanged or to take a step towards the interior of the domain. In addition to the list of recently visited solutions, separate memory store updates of the corresponding best known solutions and objectives.

Because of the sensitivity of the simulation model to large changes, neighbours that require more than one variable change in the same step will not be tried. The objective value aggregation will evaluate all admissible neighbour solutions of the current solution. A solution is admissible if it is not on the TL and all its decision variables are within their domains. The global search module updates the TL on a first-in-first-out manner. After the last neighbour solution is evaluated the search module will rank them by their objective values, and the best admissible neighbour becomes the new current solution. The number of entries in the TL is a compromise between the chances of revisiting previously identified solutions, and the time it takes to check the candidate solution against this list. In this application the number of iterations is not high enough for the TL to require much memory. Furthermore, the lost opportunity to revisit previous tabu solutions from other directions did not turn out to be important. The discretization will inevitably require rounding of the variables. When the candidate solutions are checked against the TL it is only checked whether they are similar enough, i.e. whether the individual decision variables differ with less than a given percentage. This is to avoid considering two effectively identical solutions as different due to rounding when a potential new current solution is checked against the TL. The *diversification* procedure that is usually implemented in TS would in this case require a selection of solutions that are both diverse and known to be feasible. In order to avoid the labour intensive effort of creating such a selection, the diversification in this implementation happens by increasing the step sizes if the objective ceases to improve. This is formulated with the criterion that if no update of the best known solution has taken place for given number of iterations, then all global step sizes are increased by the same predetermined factor. Once a solution that replaces the best known solution is found, then the step size returns to its initial length.

Nelder Mead Downhill Simplex as local search

The NMDS method is suitable for continuous variables and does not require gradient information (Nelder and Mead, 1965). It is also able to handle the "very high number" responses from the objective value aggregation because it will move away from them in the search space, provided there are not too many of them in the simplex. The NMDS is initiated from a simplex that consists

of $n + 1$ vertices (solutions) that do not lie in a hyperplane, where n is the problem dimension. Each of these n extra vertices are generated by choosing randomly whether to increase or decrease a different variable for each vertex by a predetermined small step from its value in the TS iteration where the NMDS was initiated. This is a downhill method in the sense that the worst (highest objective value) vertex is rejected and replaced with a new vertex that is always better. Then the updated collection of vertices is sorted by their objective values and the procedure is repeated. Finally, the locally optimal solution is the *best* vertex when at least one of the stopping criteria is met. The stopping criteria are an upper bound on the number of iterations and a lower bound on the difference between decision variables for subsequent iterations.

The local search is illustrated in Fig. 4.2 to 4.6 . The procedure requires that the vertices are sorted by their objective values to identify which one is *best* (B), *good* (G, second best), and *worst* (W). The solutions between G and W are less important. It also requires the calculation of a linear combination of the decision variables of B and G called the *midpoint* (M), and the *reflection* (R) of W through M. For each dimension, the differences between the corresponding entries of vertices M and W are calculated. The reflection of the old W, denoted R, is the difference between each individual entry of the vertices M and W weighted with a proportion α and projected in the opposite direction. Unlike the TS, more than one decision can change before the subsequent iteration in the NMDS. This happens whenever the new W is a linear combination of two old solutions with at least two decision variables that are different. There are four alternatives for the replacement of the vertex with the worst objective value with a better one. The chosen one depends on how the objective value changes in various search directions.

If the objective value of R, $f(R)$, is better (lower) than $f(W)$, then the next step is either to *reflect* or to *extend*. Whether we reflect or extend depends on whether or not $f(R)$ is better than $f(B)$. If $f(R)$ is better than the best (lowest), then the M to R direction is likely to be improving and the extension point (E) is calculated. If $f(R)$ is somewhere between $f(G)$ and $f(B)$ it indicates that a better solution is unlike to be found far away in the M to R direction so E is not calculated. The point E is a linear combination of M and R using the weight γ with a value that places E in the same direction away from M as R but a bit further. The solution that turns out to have the best objective value of R and E replaces the old W.

If $f(R)$ is worse (higher) than $f(G)$, then looking further in the M to R direction is not interesting, so the next step will be shorter than to R. However, if $f(R)$ is better than $f(W)$, then R replaces W. The *contraction* point is an interpolation with weight β of the midpoint M and the worst point W. Regardless of that outcome the contraction point C and its objective value $f(C)$ are calculated

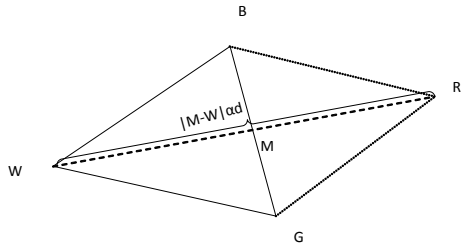

Figure 4.2: The reflection point R is the reflection of W with extrapolation weight α through the midpoint M of the second best point G, and the best point B

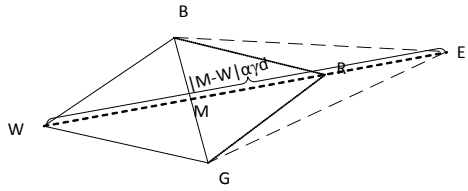

Figure 4.3: The extension point E is extrapolated in the same direction as R but further with the extrapolation weight γ

to check whether the local optimum could be somewhere between. The point C is in the M to R direction but not as far as R. If $f(C)$ is better than $f(W)$, then C replaces W. If not, then the simplex is *shrunk*. The shrink point S is an interpolation with weight δ of the bad point C and the worst point W. The shrinkage requires the vertices W and G to be replaced simultaneously; M replaces G, and S replaces W.

The above geometric moves require the predetermined weights α, β, γ, and δ for calculation of the mentioned linear combinations. In this implementation the interpolation weights are equal, $\beta = \delta = \frac{1}{2}$, and the reflection and extension weights are equal, $\alpha = \gamma = 2$.

The combined search

The interaction of the global and the local search is presented in Fig. 4.7. When the new current solution is identified, it is compared to all its neighbours. If its objective value is more than a predetermined percentage better than all its neighbours it is defined as promising and candidate for a local search. The region of such candidate local optimum is explored with the NMDS method. The NMDS

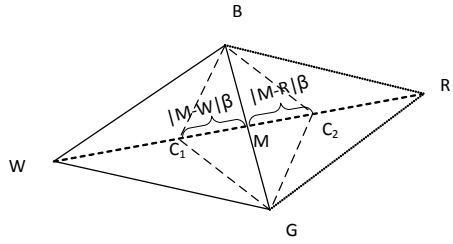

Figure 4.4: There are two alternative contraction points, between W and M or M and B with the interpolation weight β

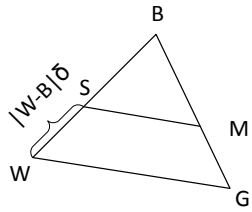

Figure 4.5: Shrinking triangle towards B with the interpolation weight δ

method is very time consuming, so in order to avoid initiating it at too many of the TS iterations, there is a criterion that no local search will be performed if the current objective is more than a given percentage worse than best known objective. This threshold is set slacker when the global search is performed with coarse steps. This is to reduce the chance of stepping over good solutions (points between step end-points). The next global search step after a local search can either start from where the local search stopped, or from the best of the neighbours before the local search. The advantage of the first approach is that it saves searches when moving towards new local optima when all the local searches in a sequence pull in direction of the same solution. The advantage of the latter is that it is faster when moving away from a recently visited local optimum, where the local searches would pull the starting point of the next iteration towards the solution that the global search tries to escape from.

Plots of decision variables such as pressures, flow rates, and temperatures based on lists of visited solutions give a visual impression of how the search evolves from iteration to iteration. These plots provide valuable information for the calibration of parameters such as step sizes and stopping criteria, but they are not required for the search procedure. Since a heuristic (by definition) cannot

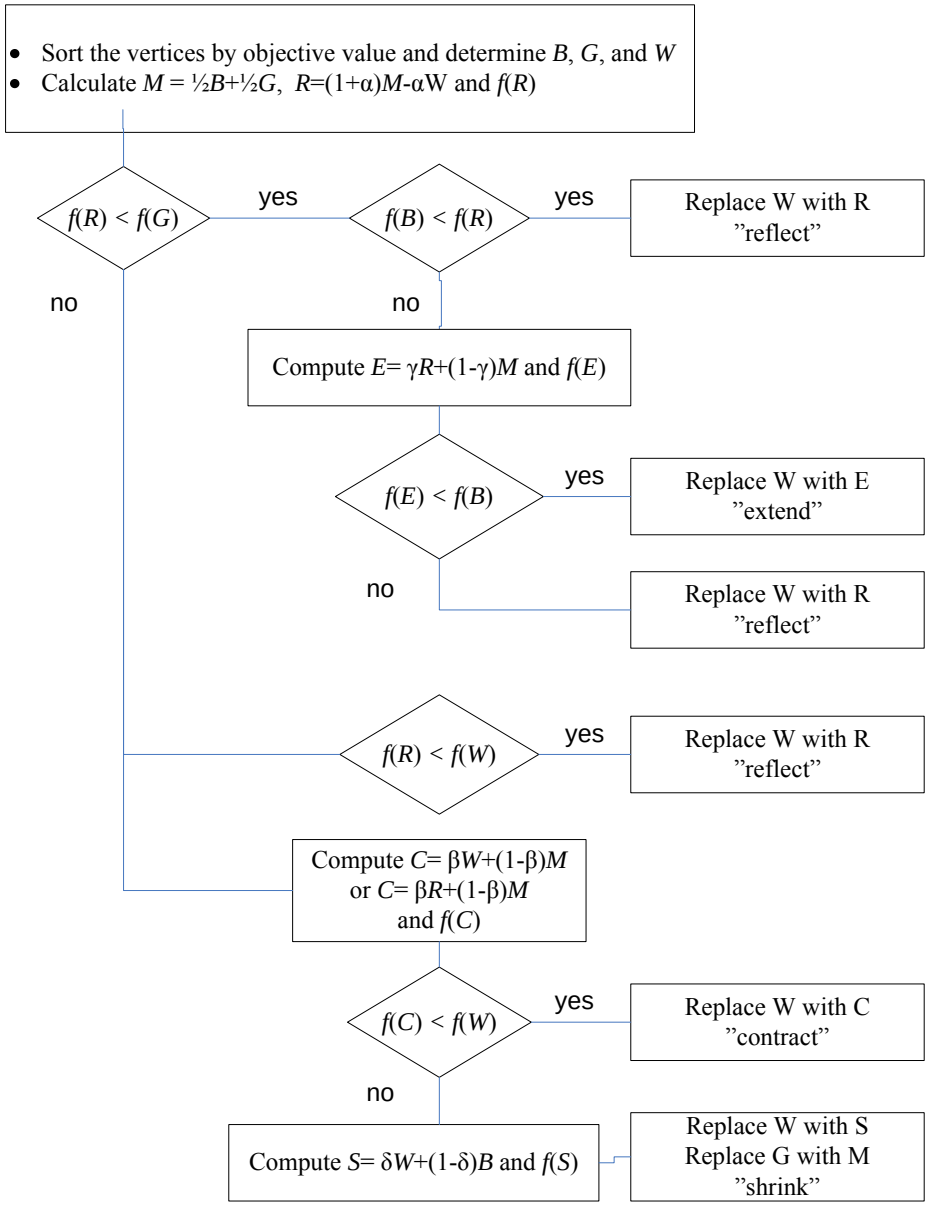

Figure 4.6: Nelder-Mead Downhill Simplex local search

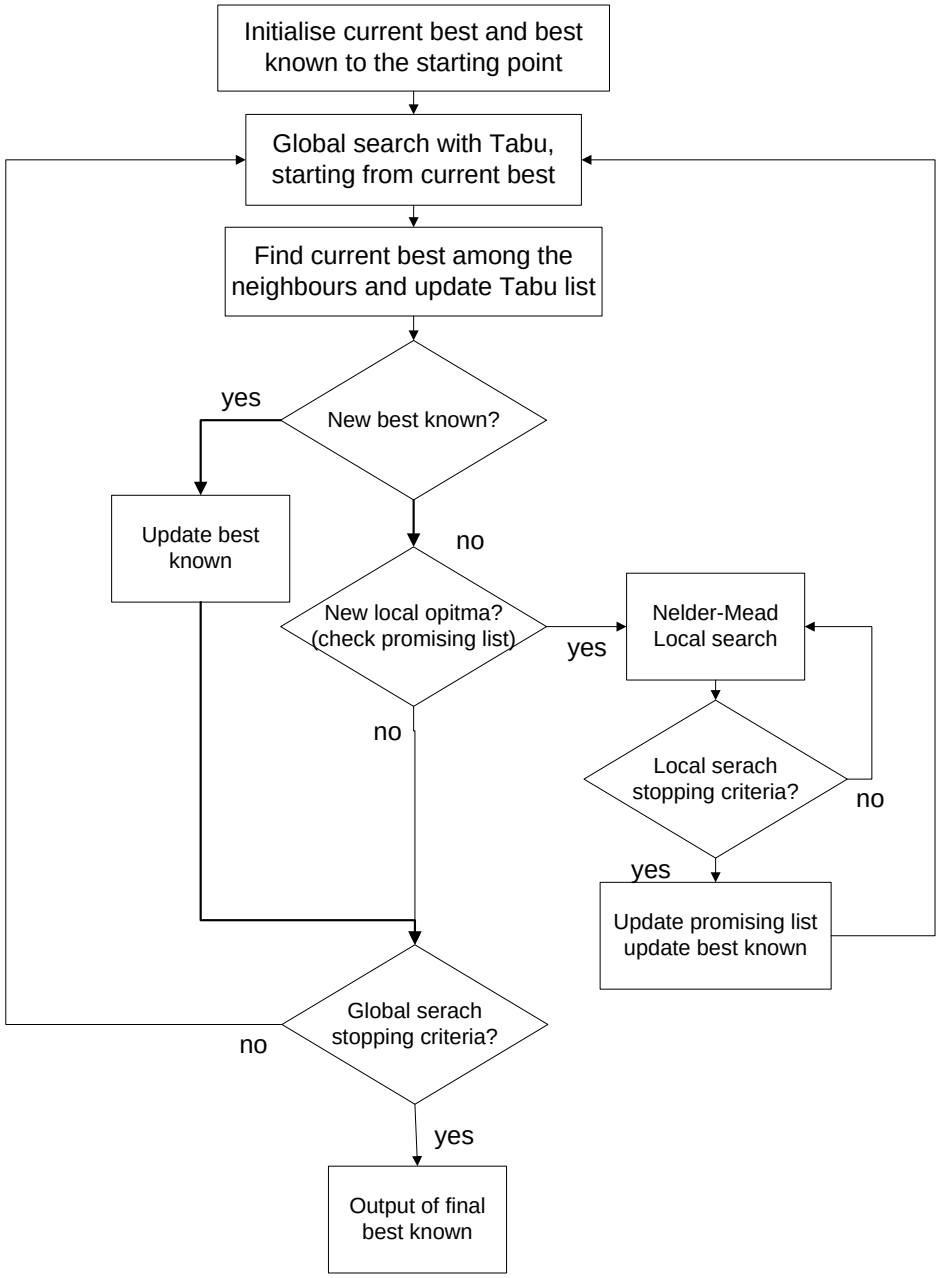

Figure 4.7: The search module

tell whether the optimal solution has been reached or not, the algorithm needs a stopping criterion, and there are many alternatives. The local search has found an optimum when the difference between two adjacent solutions of the search is negligible. A second stopping criterion limits the number of iterations. The global search has several stopping criteria. It either stops after a given length of time, if no improvement in the best known solution has taken place for a given number of global iterations, or after a maximum number of simulations.

Integration between Aspen HYSYS and the search procedure

Aspen HYSYS is an interactive simulation tool for designing and calculating steady state and dynamic processes. It also exposes a COM-interface that allows other programs to set and retrieve process values. Since HYSYS was designed as an interactive tool, some problems arose when integrating HYSYS into the framework. Information about the simulation state appears on the screen but is not readily available to other programs; therefore so called back doors have been used to retrieve information about feasibility of the solution. In the cases where HYSYS displays warning messages, the candidate solution is declared infeasible, and the search continues from the best of the other neighbours.

In the beginning of the VBA routine, the variables are written individually to the Aspen HYSYS file using the COM-interface. The HYSYS simulation is then started by the VBA code and runs until it either converges or warns that it is unable to. Some of the calculated process values needed in the objective aggregation model are retrieved from the Aspen HYSYS file, the feasibility status is checked, and a procedure within the objective value aggregation condenses this information into the objective value.

4.3 Prico process case studies

The Prico process was selected for optimization for two reasons. First, it is a simple LNG process with 7 independent variables, which is too large for the optimization routine that is included in HYSYS, but small enough to be optimized with the optimization-simulation tool. Second, as explained later in this section, it is possible to verify the results by investigating the resulting hot and cold Composite Curves (CCs). In a cost and energy effective LNG process there will be relatively small differences between the hot composite curve (natural gas feed) and cold composite curve (refrigerants) in the heat exchangers, as large temperature differences lead to irreversibilities that reduce the exergy efficiency.

Since natural gas is a multi-component mixture, liquefaction will occur at a sliding temperature interval. Two main approaches are used to design energy

effective LNG processes, cascade processes and multi-component refrigerant cycles. In mixed refrigerant processes, such as the Prico process, the cold composite curve is matched to the hot composite curve using a single refrigeration cycle with a mixed working fluid that will evaporate at a sliding temperature interval; hence only one compressor is needed. An alternative to the Prico process is the Phillips Cascade, which consists of three pure working fluids, propane, ethylene and methane, each cycle with up to three pressure stages. In this way the cold composite curve from the refrigerants can be nicely matched with the natural gas hot composite curve, however, several compressors and heat exchanger passes are needed. In most commercial large scale LNG plants as the Mixed Cascade Refrigeration (MCR) process by APCI and Mixed Fluid Cascade (MFC) by Statoil-Linde, the LNG process is a combination of the cascade and mixed refrigerant process. Barclay and Denton (2005) have provided an overview and description of LNG processes. An overview of the basics of cryogenic processes, including LNG, was presented in a text book by Flynn (2005).

The two most important unit operations in an LNG process are the compressors and the heat exchangers. In general, increasing the size of the heat exchangers will decrease the power requirements in the compressors and thereby increase the efficiency. Equation (4.1) gives the relationship between the heat transferred from the hot stream to the cold stream Q, the overall heat transfer coefficient U, the size of the heat exchanger A, and the driving forces, represented by the logarithmic mean temperature difference (LMTD) between the hot and the cold streams. Equation (4.2) shows the definition of the LMTD for counter current flow.

$$Q = U \cdot A \cdot \Delta T_{LM} \tag{4.1}$$

$$LMTD = \Delta T_{LM} = \frac{(T_{H,in} - T_{C,out}) - (T_{H,out} - T_{C,in})}{\ln\left(\frac{T_{H,in} - T_{C,out}}{T_{H,out} - T_{C,in}}\right)} \tag{4.2}$$

For the same heat (Q) and overall heat transfer coefficient (U), there is an inversely proportional relationship between the size of the heat exchanger (A) and the driving force (ΔT_{LM}). Large driving forces will lead to irreversibilities in the heat exchanger, which again will increase the need for energy transferred to the process through the compressor and thereby both the investment cost and the operational cost for the compressor will increase. On the other hand, if the heat exchanger (HX) is large (small driving forces) then the HX investment cost will increase while the compressor investment and energy costs will be reduced. Hence, there is always a trade-off between the size of the HX and the size of the compressor. Since LNG processes are very energy intensive, the minimum inter-

nal temperature approach (MITA) is usually small. A temperature difference of 2°C is often used in the early design phase.

Even if the trade-off between compressor power and driving forces in the HX is fixed (e.g. by specifying a MITA of 2°C), there are still several variables that can be optimized. Whether the LNG process is good or not can often be seen from the shape of the hot and cold CCs. In general, the area between the CCs should be as small as possible, the pinch point should be in the cold-end of the HX (MITA) and gradually open up at higher temperatures.

There is always degeneration of exergy (irreversibilities) associated with a heat transfer process operating across finite temperature differences. For an infinitesimal amount of heat δQ extracted from a hot stream at temperature T_H, and an ambient temperature of T_0, the inherent change in exergy is given by Eq. (4.3). On a similar basis the exergy supplied to the cold stream at temperature T_C is given by Eq. (4.4). The total irreversibility due to heat transfer between two streams can be expressed as Eq. (4.5) and Eq. (4.6), where η_c is the Carnot factor. It should be noted that the normal sign convention in thermodynamics is not applied, thus the infinitesimal amount of heat δQ is regarded as a *positive* entity. From the equations it can be concluded that exergy losses due to temperature driving forces in the heat exchanger depend on the total duty of heat to be transferred and the temperature difference, and that they are largest at a low temperature.

$$\delta E_H = -\left(1 - \frac{T_0}{T_H}\right)\delta Q \tag{4.3}$$

$$\delta E_C = \left(1 - \frac{T_0}{T_C}\right)\delta Q \tag{4.4}$$

$$\begin{aligned} I &= -\int_0^Q (dE_H + dE_C) = \int_0^Q \left(\left(1 - \frac{T_0}{T_H}\right) - \left(1 - \frac{T_0}{T_C}\right)\right)\delta Q \\ &= \int_0^Q (\eta_{c,H} - \eta_{c,C})\delta Q \end{aligned} \tag{4.5}$$

$$\eta_c = 1 - \frac{T_0}{T} \tag{4.6}$$

Since compressor work to provide refrigeration is proportional to exergy losses, and exergy losses increase with lower temperatures for the same heat transfer temperature difference, the optimal design of an LNG process exhibit CCs that are close to parallel but closest at low temperature (MITA) and gradually opening with increasing temperature. This result can be derived from Eq. (4.2) and Eq. (4.5). Also, as can be seen from Eq. (4.5), to reduce the irreversibilities, the transferred heat (Q) should be as low as possible. Finally, in the Prico process,

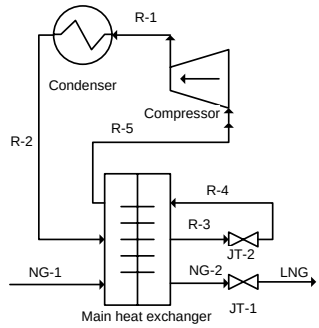

Figure 4.8: The simplified Prico process

the refrigerant leaving the hot end of the HX must be in the gaseous phase, as small amounts of liquids will cause operational problems for the compressors.

Another way to explain the most favourable shape of the Composite Curves is as follows. Refrigeration requires energy, furthermore, the colder the temperature the more energy is required. If the refrigerant is much colder than the natural gas to be cooled, this will merely result in energy losses and higher energy requirements than necessary. Hence, the cold composite curve should be as parallel and close to the hot curve as possible, especially in the cold end where refrigeration is most expensive. Also, the total refrigeration duty should be as small as possible as this means that less of the working fluid (refrigerant) needs to be compressed.

The Prico process as shown in Fig. 4.8, is a simple LNG process using a multi-component mixture as the working fluid. It consists of a main heat exchanger, a compressor, a condenser and two Joule-Thomson (JT) valves. Two compressor stages with intermediate cooling will increase the efficiency, however, the variables will remain the same, and hence, one stage is used in the calculations for simplicity.

In the current example, the natural gas (NG-1) enters the main heat exchanger at a pressure of 60 bar and 20°C where it is cooled, liquefied and subcooled (NG-2) before it is expanded to transport pressure (LNG). The cooling duty is provided by a simple refrigeration cycle using a multi-component working fluid consisting of nitrogen, methane, ethane, propane and butane. At high pressure (R-1) the working fluid is cooled and partly liquefied in a condenser by cooling water or ambient air. The working fluid (R-2) is then subcooled in the main heat exchanger (R-3) before it is expanded to low pressure through a JT-valve (R-4). The expansion leads to a small decrease in temperature and some gas will be formed. This cold fluid at low temperature and low pressure is vaporized to provide cooling and liquefaction of both the refrigerant and the natural gas in a

Process variable	Value	
NG feed flow	100	kg/s
NG feed composition	See Table 4.2	mole %
NG feed inlet pressure	60	bar
LNG pressure	1.05	bar
LNG vapour fraction	0.0	%
Refrigerant HX hot stream outlet temperature	dependent variable	°C
Refrigerant flow	1 variable	kg/s
Refrigerant composition	5 variables (-1 dependent)	mole %
Refrigerant suction pressure	1 variable	bar
Refrigerant condenser pressure	1 variable	bar

Table 4.1: Exogenous, dependent and decision variables in the Prico process

close to counter-current heat exchanger. At the outlet of the heat exchanger, the refrigerant will be in the gaseous phase (R-5) and it is then compressed to high pressure (R-1) before the heat is removed to the surroundings in the condenser (R-2). In the optimization, the outlet temperatures from the main heat exchanger of the hot streams (R-3) and (NG-2) are kept equal.

Optimization variables

In order to get a good match between the hot and cold CCs and thereby reduce the irreversibilities, several parameters can be varied. The most important variables for the Prico process are the flow rate and composition of the refrigerant, the compressor suction pressure (low pressure) and the condenser pressure (high pressure). Table 4.1 shows the selected parameters (fixed) and variables for the optimization of the Prico process.

The Prico process has been optimized in three ways; first keeping the area (UA value) constant and assigning a logarithmic penalty to any deviation from this, then by letting the UA value vary and assigning a cost to the UA in the objective function, and finally by introducing a logarithmic penalty if the minimum internal temperature approach (MITA) is below a specified value. The first approach can be used if a specific heat exchanger is selected, or the plant is already built. The second approach can be used to find the optimum size of the heat exchanger during process design. The last approach is sometimes used in early stage simulations for simplicity.

For cryogenic processes, the MITA is normally set to 1-2°C to avoid large irreversibilities and achieve better exergy efficiencies. However, if the MITA

Name	Type	Nitrogen	Methane	Ethane	Propane	Butane
NG1	Lean gas	0.37	95.89	2.96	0.72	0.06
NG2	Rich gas	0.00	88.80	5.60	3.70	1.90

Table 4.2: LNG compositions

Process variable	Property		
Cooling water	Temperature	15	°C
Condenser	Temperature difference	5	°C
Compressor	Adiabatic efficiency	80	%
Condenser	Pressure drop	1	bar
LNG HX hot refrigerant	Pressure drop	1	bar
LNG HX cold refrigerant	Pressure drop	1	bar
LNG HX feed	Pressure drop	5	bar

Table 4.3: Design Basis

becomes negative by changing some of the process variables (pressure, flow rate or composition), heat will be transported from the cold stream to the hot stream, which is thermodynamically possible but opposite of the intention, hence the HX will be regarded as infeasible and the simulation will return a "a very high number" to the objective function. Therefore a very small MITA of 0.1°C is used to show that the optimization-simulation model is capable of finding a solution that is very close to the acceptable boundaries in the HYSYS simulation.

Two different natural gas compositions have been used; a lean gas and a rich gas. The LNG compositions are shown in Table 4.2. The rich gas is outside the normal LNG specifications and the heavy hydrocarbons (HHC) needs to be removed.

Case	LNG Composition	Heat exchanger specification
1	NG1	Fixed MITA
2	NG1	Fixed UA
3	NG1	Cost UA
4	NG2	Fixed MITA
5	NG2	Fixed UA
6	NG2	Cost UA

Table 4.4: Optimization-simulation cases

Process variable		
Suction pressure	3.5	bar
Condenser pressure	40	bar
HX outlet Temp.	-163.7	°C
Compressor power	145.5	MW
UA	73.0	MW/K
LMTD	5.30	°C
MITA	1.67	°C

Table 4.5: Initial process conditions

A maximum calculation time of 4 hours are used for all cases except case 2 which were allowed to run for 12 hours. It should be noted that the optimization is performed for targeting purposes only; hence the individual temperature/enthalpy curves are not examined.

Initial solution

The optimization-simulation model cannot start from an infeasible point, as the TS then will work "blindfolded" and the random walk will only locate a feasible solution by pure luck. Hence, a feasible starting point is selected for all the runs. Data for the initial process is shown in Table 4.5, the initial variables with upper and lower bounds in Table 4.6, and the resulting composite curves (CCs) are presented in Fig. 4.9. As can be seen, there are two pinch points, one in the cold end (-163°C) and one at - 60°C. From the previous discussion it is clear that the pinch point should be in the cold end and that the CCs should gradually open with increasing temperature, hence the initial solution is most likely not optimal.

Optimization-simulation tool settings

The settings for the global search and the local search in the optimization-simulation model are presented in Table 4.7 and Table 4.8.

4.4 Results

The individual results for case 1, 2 and 3 are found in Table 4.9, whereas the main results from the six optimization cases are shown in Table 4.10. The Composite Curves for case 1 to 3 are shown in Fig. 4.10, Fig. 4.13 and Fig. 4.15. The current and best known solutions for case 1 to 3 are presented in Fig. 4.11, Fig.

Variable	Initial Mole %	Initial mass flow	Lower bound	Upper bound	
Nitrogen	15.2	75.00	19.44	130.56	kg/s
Methane	34.4	97.22	41.67	152.78	kg/s
Ethane	23.7	125.00	69.44	180.56	kg/s
Propane	9.0	69.44	13.89	125.00	kg/s
Butane	17.7	180.56	125.00	236.11	kg/s
Total flow		547.2	269.44	825.00	kg/s
Suction pressure		350	3.0	5.0	bar
Condenser pressure		4000	30.0	60.0	bar

Table 4.6: Initial decision variable values with upper and lower bounds

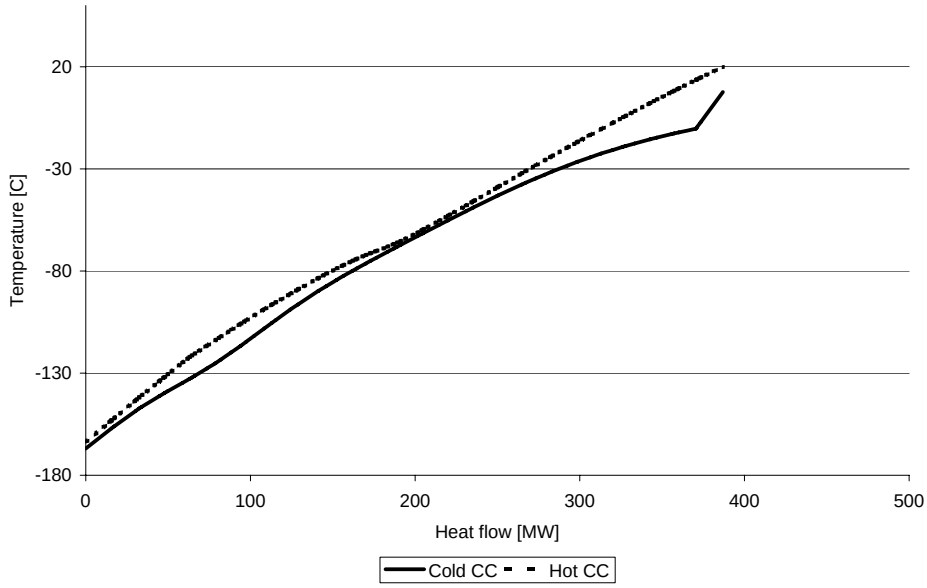

Figure 4.9: Composite curves for the initial solution

Global search parameter		
Expiration from TL	2000	iterations
TS *stopping* criteria; maximum	2000	iterations,
or maximum	4	hours,
or no progress for minimum	1000	iterations
Fine TS step size/global domain width	1/30	
Coarse step switch criterion; no update of best known for minimum	100	iterations
Coarse step size /fine step size	3	
"Promising" criteria, *current* objective better than best neighbour by	0.05	% (fine steps)
	0.5	% (coarse steps)
Promising list store max	50	solutions

Table 4.7: Global Tabu Search settings

Local search parameter		
NMDS *stopping* criteria, maximum	250	iterations,
or average change in decision variables between successive iterations falls below	0.10	% of initial step size
Lower bound on *current*/*best known* objective for *starting* NMDS from a new promising solution	102.0	% (fine steps),
	108.0	% (coarse steps)
NMDS initial step size/local domain width	1/20	
Reflection extrapolation weight	1	
Contraction interpolation weight	0.5	
Extension extrapolation weight	2	
Shrink interpolation weight	0.5	

Table 4.8: Local Nelder-Mead Descent search settings

Case		1	2	3	
HX outlet	Temp.	-163.7	-163.7	-163.7	°C
Compressor	Power	110.5	144.4	171.2	MW
UA		376.9	48.6	32.6	MW/K
LMTD		0.85	6.80	10.39	°C
MITA		0.10	2.93	4.33	°C
Refrigerant	suction pressure	3.54	3.23	3.0	bar
	condenser pressure	31.26	52.37	59.91	bar
	flow	508.6	466.9	481.7	kg/s
	composition				Mole%
	Nitrogen	10.5	15.5	17.7	
	Methane	26.9	28.8	29.1	
	Ethane	37.6	34.5	33.6	
	Propane	2.3	2.2	1.9	
	Butane	22.7	19	17.7	

Table 4.9: Results case 1-3

4.14 and Fig. 4.16 respectively. In addition, the first 350 best known solutions for case 1 are presented in Fig. 4.12.

Case 1: Fixed minimum internal temperature approach

As can be seen from Table 4.9, the MITA is 0.1°C, so there is no penalty for the deviation from the specified value. The small MITA leads to a very small LMTD of 0.85°C, which gives low energy requirements in the compressors, 110.5 MW.

By investigating the composite curves in Fig. 4.10 it can be concluded that the solution is indeed very good. The hot and cold composite curves are very close up to -50°C, where the CCs open. This is the case in all Prico processes. Note that the refrigerant is slightly overheated, so that liquid does not enter the compressor.

Figure 4.11 of case 1 shows the current solution and the best known solution on the left hand axis, an indicator of whether a local search is performed or not on the right hand axis, and the global iteration number on the horizontal axis. In the first iterations of the global search, the solution is constantly improving and not passing any local optima, hence the condition for initiating a local search is not met. After 13 global search iterations, the next solution is only 0.05% better than the best of its neighbours, which satisfies the condition for initiating a local search. The first local optimum is found after 25 iterations, thereafter the objective value gets worse for a few iterations until it comes across a new valley

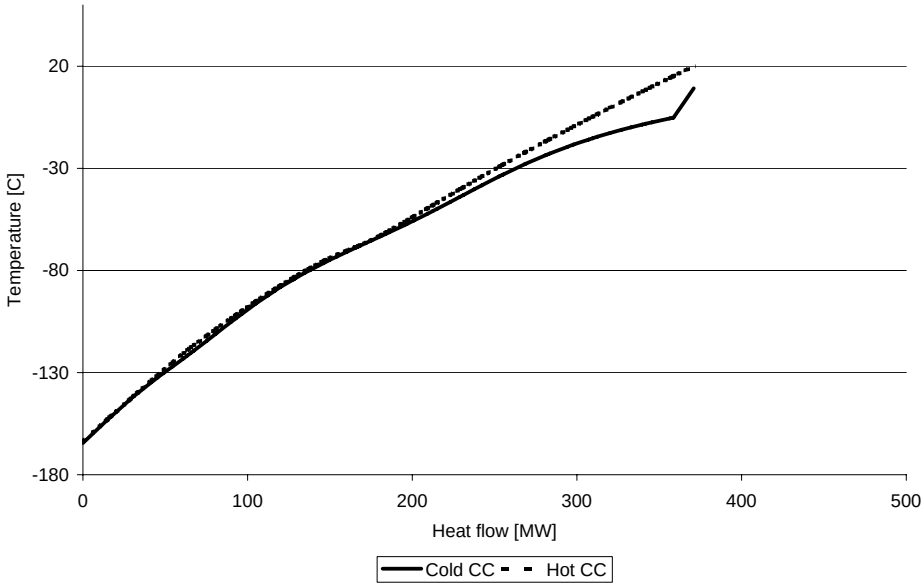

Figure 4.10: Composite curves for case 1

and improves again. This happens several times until the final update of the best known solution in iteration 443. A new valley is found after 800 iterations; however, this local optimum is not as good as the existing best known. As can be seen from the figure, local searches are only performed in areas where good results are obtained.

Figure 4.12 shows a plot of the best known solutions for 350 iterations. By investigating the figure, it can be seen that the optimization-simulation model has covered a large space. In the beginning, the total flow rate (sum of the individual component flow rates) decreases and better solutions are found. Then the condenser pressure decreases and the suction pressure increases at the expense of a higher flow rate. The composition also changes and the optimal solution contain more ethane and butane and less methane and propane.

Case 2: Fixed heat exchanger area

In case 2, the UA value is fixed using a penalty if the UA value is higher or lower than the given value. As shown in Table 4.9, the specified UA of 48.6 MW/K is obtained. This gives reasonably high MITA and LMTD values at the expense of increased power requirements of 144.4 MW. It is also worth noticing that

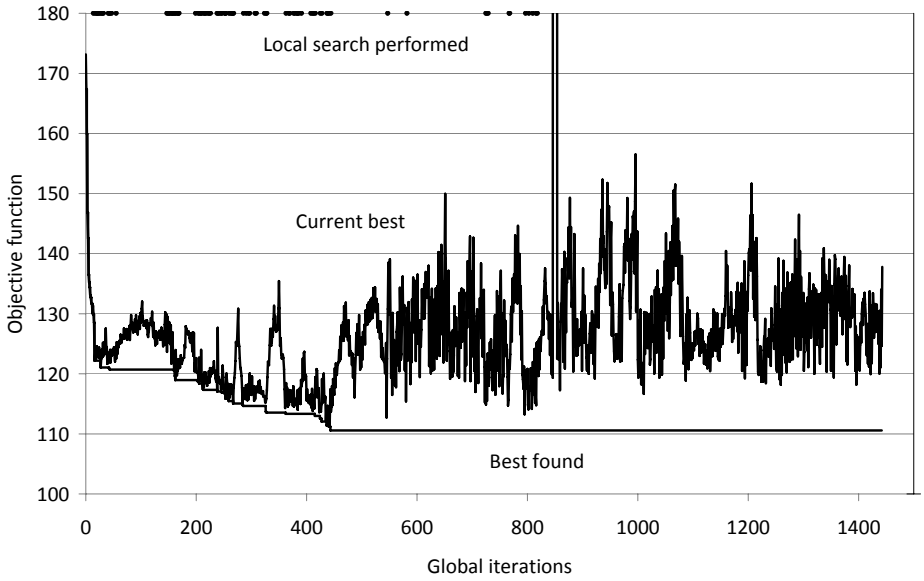

Figure 4.11: *Current* and *best known* solutions for case 1

the refrigerant flow rate and composition as well as the suction and condenser pressures have changed significantly from case 1.

As can be seen from the composite curves in Fig. 4.13 the driving forces are small at low temperatures and gradually increase at higher temperatures. From Fig. 4.14 it can be seen that several local searches are performed, and that the objective values are very similar. This may indicate that the local NMDS performs very well. The tolerances should be reduced so that local searches are done at fewer of the global iterations in order to allow more time for global iterations. This will increase the probability of discovering unvisited valleys with even better solutions.

Case 3: Cost for heat exchanger area

In case 3, a cost for the UA value is assigned and included in the objective function. This is an easier optimization as penalties are avoided. As expected the required power will increase when the heat exchanger area (UA) is decreased compared to case 2. A smaller heat exchanger, of course, means that larger temperature driving forces are required. This will increase the thermodynamic

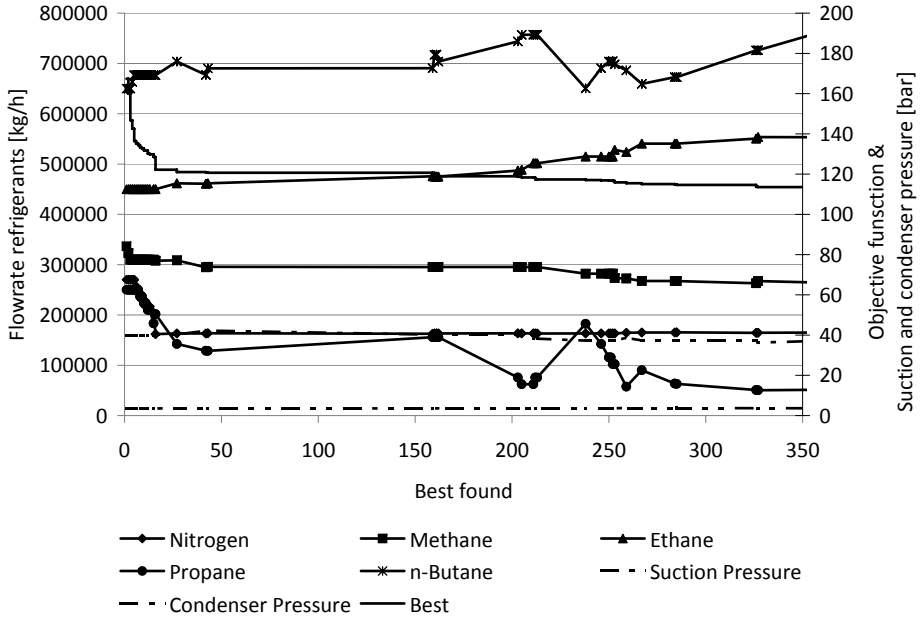

Figure 4.12: The 350 *best known* solutions for case 1

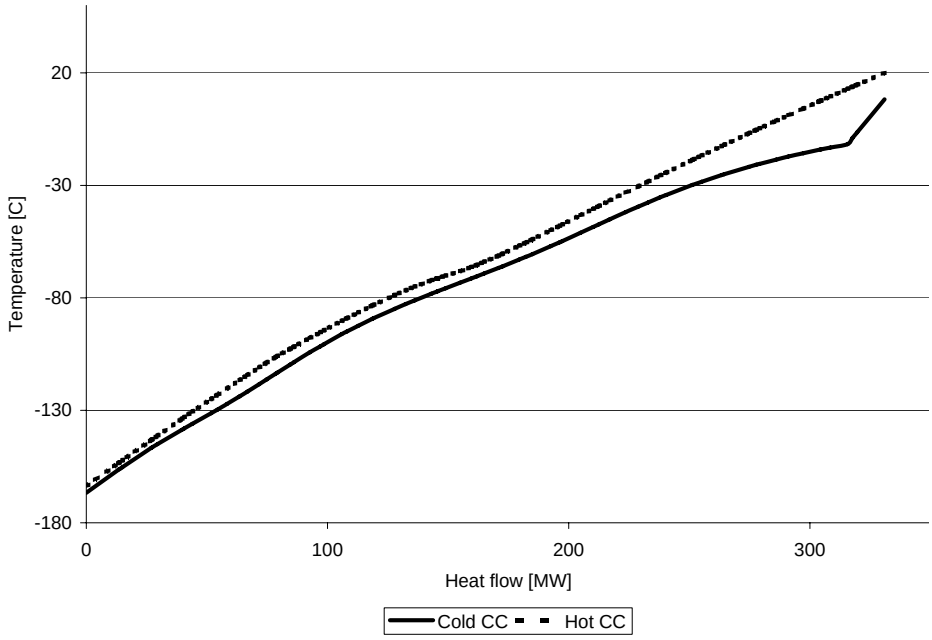

Figure 4.13: Composite curves for case 2

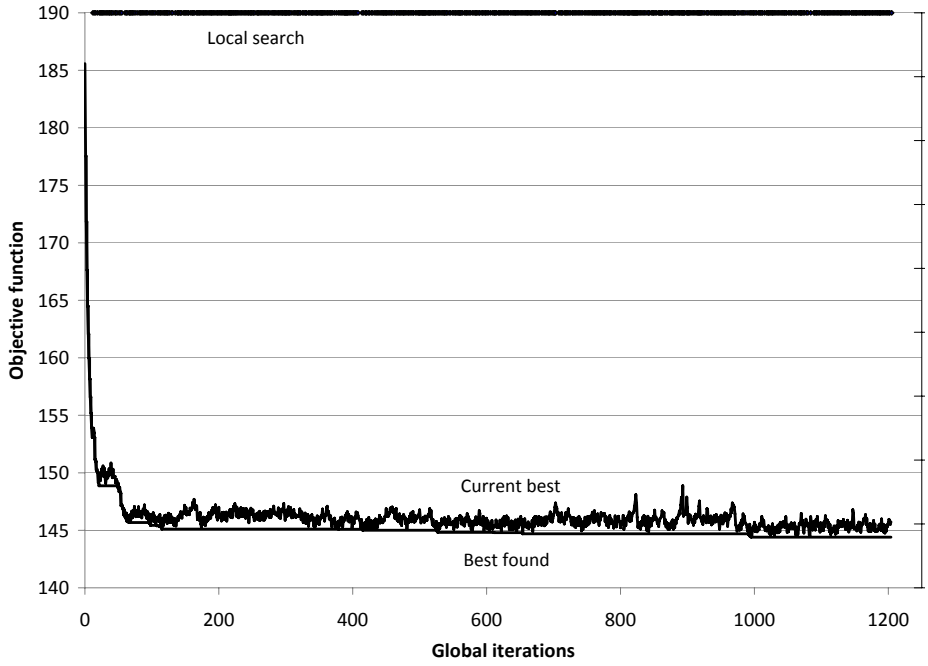

Figure 4.14: *Current* and *best known* solutions for case 2

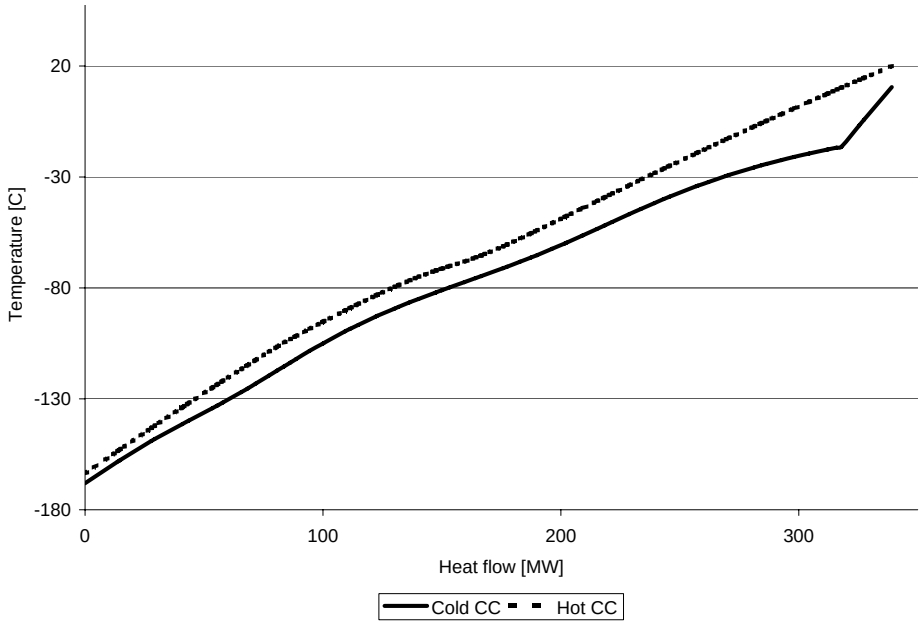

Figure 4.15: Composite curves for case 3

losses (irreversibilities) and increase the need for power to the compressor. Figure 4.15 shows the hot and cold CCs and the main results are given in Table 4.9.

In cases 4-6, a richer composition of the NG feed is used. The same initial values are used, and the CCs have the same shape as for the first three cases. The current and best known solutions also have a similar shape as for cases 1-3. The main results for the six cases are given in Table 4.10. Notice that the MITA is 0.1°C for case 4 and that the total UA is 48.6 MW/K for case 5, implying that there are no penalties for the specified values.

4.5 Discussion

Since the optimization-simulation method is of a heuristic class, it cannot guarantee that a global optimum is found. The best known solution's distance from the true optimum will depend on the starting point, the feasible region, the number of steps across the domain for each variable, the number of iterations performed, the number of iterations required to initiate coarser steps, the criteria for initiat-

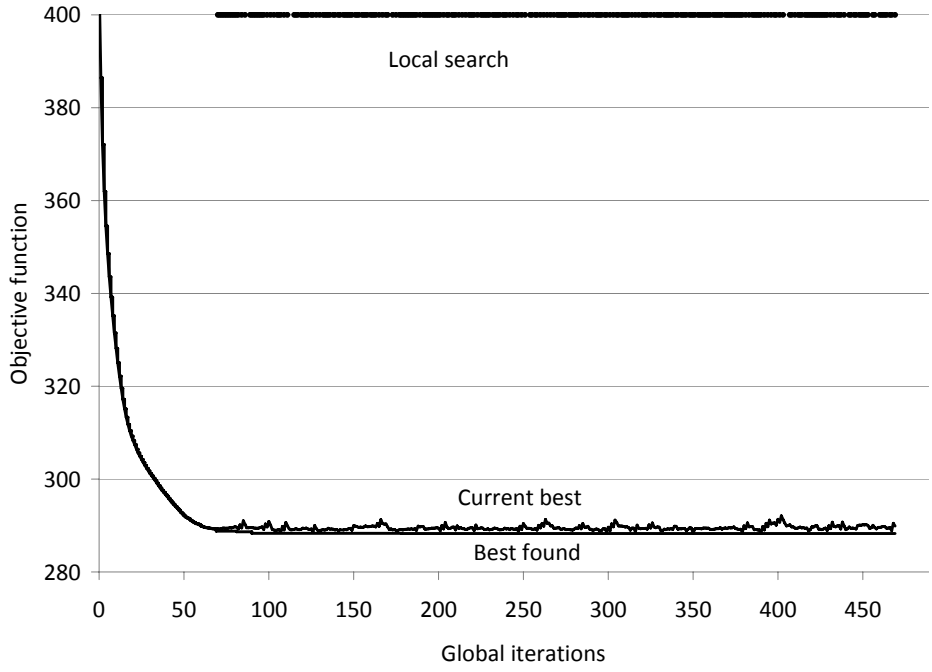

Figure 4.16: *Current* and *best known* solutions for case 3

Test case	HX restr.	NG type	Global iter.	Local searches	Obj. val.	Work [MW]	UA [MW/K]	LMTD [°C]	MITA [°C]
1	Fixed MITA	NG1	1443	91	110.5	110.5	376.9	0.98	0.1
2	Fixed UA	NG1	1205	675	144.5	144.5	48.6	6.80	2.93
3	Cost UA	NG1	470	289	288.7	171.2	32.6	10.39	4.33
4	Fixed MITA	NG2	1949	90	91.4	91.4	538.3	0.65	0.1
5	Fixed UA	NG2	505	265	122.7	122.7	48.6	6.16	2.57
6	Cost UA	NG2	214	130	104.1	153.3	28.9	10.66	4.76

Table 4.10: Main results Case 1 to Case 6

ing a local search as well as the coarseness of the initial simplex and number of iterations in the local search.

The general purpose process simulators, such as Aspen HYSYS, are strongly nonlinear due to complex thermodynamic relations as well as physical-chemical properties. Therefore the objective function may be characterized by a series of narrow valleys and/or steep walls. The main challenge with the presented search is therefore that there may be too coarse steps in the TS, which may cause the search to step over the valley with the true optimum. On the other hand, too fine steps will lead to a very long computational time, and risk excluding the true optimum if it is so far from the initial solution that it cannot be reached within the time constraint. It is therefore important apply a reasonable coarseness of steps and tighten the upper and lower bounds as much as possible to reduce the search space. To overcome these challenges and keep the steps fine inn promising areas and simultaneously speed up the search in regions where the objective is far worse than the best known objective, the TS step size is made coarser by a predetermined factor when the current objective is worse than the best known objective by a given percentage. Furthermore, the NMDS searches are not performed in these regions. Coarser steps will increase the covered space at the cost of potentially missing promising valleys. Many processes will have a relatively flat area around the true optimum, meaning that there are several solutions that are close to optimal. This is especially true when both investment costs and operational costs are included in the objective function. Finally, if the objective function is convex or contains a set of relatively few convex systems, it could be beneficial to replace the NMDS with another search such as sequential quadratic programming (SQP). For most processes this is, however, not the case and this procedure is not implemented.

In case 1, the upper and lower bounds for the refrigerant flow rate for each of the five components are set to be 200 000 kg/h lower or higher than the initial solution, and this range is discretised to 30 intervals. The suction pressure can vary between 3 and 5 bar and the condenser pressure between 30 and 60 bar, both discretized to 30 intervals. This gives 30^7 or more than 20 billion possible points in the global search space. It should be noted that a large share of these possibilities will be infeasible. After 100 global iterations without improvement, the step size is multiplied by 3, which reduces the search space to about 10 million points. This will reduce the search time; however, it is possible that some good solutions will be omitted. If the optimization model finds a solution within 1.5% of the best known objective, then the step size will return to the initial fine coarseness.

A global iteration will take about two seconds, whereas a run of the local search may take up to two minutes. It is therefore important to reduce the number of local search runs. However, if a local search is performed at too few of the global

iterations, an improvement of the best known solution is less likely. One of the advantages with the optimization-simulation model is that the local searches will be performed from a starting simplex that consists of different points in a promising area. This increases the chance to find a good solution. This can be seen from Fig. 4.11, 4.14, and 4.16, where several hundred local searches are performed close to what is believed to be the optimal solution.

In case 1 and case 4 there is a penalty if the MITA is larger or smaller than 0.1°C. Since the penalty is introduced, a local search is required to find the best known solutions as there is a very small chance that the global search will find solutions that have a MITA close to 0.1°C. Also, since the search is performed close to an infeasible solution (MITA<0°C), several of the simulations done in HYSYS have been infeasible as changing one variable in the global or local search will cause a temperature crossover. The large heat exchanger resulting from a MITA of only 0.1°C will, of course, never be installed; the case is selected to show that the optimization-simulation approach also will work close to the feasible boundary. The chance of getting infeasible solutions for a MITA of 2°C will be much smaller; this does of course depend on the size and number of partitions for the variables. The cases with specifications for MITA or UA and an assigned penalty if these values are not achieved, are more difficult to optimize than assigning a cost to the UA. The reason for this is that small changes in the variables will give considerable deviations from specifications for MITA or UA, whereas the relative change in UA value and the corresponding cost is not so sensitive.

From Fig. 4.10, 4.13 and 4.15 it can be seen that the pinch point is in the cold end of the heat exchanger and that the CCs gradually open at higher temperatures. This is in accordance with the theoretical discussion in Section 4.3. It can also be seen that the gap in the hot end of the CCs is somewhat larger than wanted from a theoretical point of view. This could imply that the best solution is not yet found. However, this phenomena is known for all mixed refrigerant processes and is due to the fact that the refrigerant must be partly condensed in the cooling water HX. By decreasing the condenser temperature, even better matches between the CCs can be found. This is done in most large scale LNG plants, where either a propane precooling unit or a mixed propane precooling unit is used prior to the mixed refrigerant cycle.

The Prico process was selected for optimization as it is possible to verify the results by investigating the CCs. For all the six cases that are investigated, the CCs indicate that reasonable results have been obtained. It is also shown that the optimization-simulation tool has the ability to escape one local optimum to search for others. It can therefore be concluded that the optimization-simulation tool shows great potential for optimization of energy and petrochemical processes. It should be noted that the efficiency of the Prico process will increase significantly

by introducing another compressor with intermediate cooling. It should also be noted that the size of the plant used in these calculations, in terms of kg/h LNG produced, is in the upper end for an industrial Prico process. This will, however, not influence the variables that are optimized as the equipment costs are calculated as a linear function of size.

4.6 Conclusions

An optimization-simulation tool based on a global Tabu-Search and a local Nelder-Mead search for optimization of an LNG process modelled in the sequential modular process simulator HYSYS is developed. The tool has been successfully applied to optimize the Prico LNG process with 7 independent variables applying three different methods for selecting the heat exchanger area. The objective function value is improved from the initial feasible solution with 23% to 36% for the investigated cases. The first 100 iterations give the largest improvement. A theoretical analysis of the shape of the CCs and a comparison of the results from the tool indicate that the results obtained are optimal or very close to optimal. It is also shown that the optimization-simulation tool has the ability to escape one local optimum to search for others. It can therefore be concluded that the optimization-simulation tool shows great potential for optimization of energy and petrochemical processes. The main strength with the optimization-simulation model is that local searches are performed from several points in promising areas, whereas only a global search is performed in regions that are not promising. The optimization tool can be implemented to optimize other processes modelled in Aspen HYSYS.

Acknowledgements

The sponsors of the project are the Research Council of Norway (project 165818, Optimal Design and Operation of Gas Processing Plants), StatoilHydro and SINTEF Energy Research. Thanks to Per Eilif Wahl at SINTEF Energy Research for help with the HYSYS and VBA interface.

Bibliography

Barclay, M., Denton, N., 2005. Selecting offshore LNG processes. LNG Journal 10 (1), 34–36.

Cavin, L., Fischer, U., Glover, F., Hungerbüler, K., 2004. Multi-objective process design in multi-purpose batch plants using a Tabu Search optimization algorithm. Computers & Chemical Engineering 28 (4), 459–478.

Chelouah, R., Siarry, P., 2005. A hybrid method combining continuous tabu search and Nelder-Mead simplex algorithms for the global optimization of multiminima functions. European Journal of Operational Research 161 (3), 636–654.

Edgar, T. F., Himmelblau, D. M., Lasdon, L. S., 2001. Optimization of chemical processes, second edition. McGraw-Hill, New York.

Exler, O., Antelo, L. T., Egea, J. A., Alonso, A. A., Banga, J. R., 2008. A tabu search-based algorithm for mixed-integer nonlinear problems and its application to integrated process and control system design. Computers & Chemical Engineering 32 (8), 1877–1891.

Floudas, C. A., 1999. Deterministic global optimization. Kluwer Academic Publishers, Dordrecht.

Flynn, T. M., 2005. Cryogenic engineering. Marcel Dekker, New York.

Furman, K. C., Sahinidis, N. V., 2002. A critical review and annotated bibliography for heat exchanger network synthesis in the 20th century. Industrial & Engineering Chemistry Research 41 (10), 2335–2370.

Gendreau, M., 2002. Recent advances in tabu search. In: Ribeiro, C., Hansen, P. (Eds.), Essays and Surveys in Metaheuristics,. Kluwer, Boston, pp. 369–378.

Glover, F., August 1986. Future paths for integer programming and links to artificial intelligence. Computers and Operations Research 13 (5), 533–549.

Gundersen, T., Hertzberg, T., 1983. Partitioning and tearing of networks applied to process flowsheeting. Modeling, Identification and Control 4 (3), 139–165.

Gundersen, T., Naess, L., 1988. The synthesis of cost optimal heat exchanger networks. Computers & Chemical Engineering 12 (6), 503–530.

Hedar, A. R., Fukushima, M., 2006. Tabu search directed by direct search methods for nonlinear global optimization. European Journal of Operational Research 170 (2), 329–349.

Holland, J. H., 1975. Adaptation in Natural and Artificial Systems. University of Michigan Press, Ann Arbor.

Jezowski, J., 1994a. Heat exchanger network grassroot and retrofit design. the review of the state-of-the-art: Part i. heat exchanger network targeting and insight based methods of synthesis. Hungarian journal of industrial chemistry 22 (4), 279–294.

Jezowski, J., 1994b. Heat exchanger network grassroot and retrofit design. the review of the state-of-the-art: Part ii. heat exchanger network synthesis by mathematical methods and approaches for retrofit design. Hungarian journal of industrial chemistry 22 (4), 295–308.

Kirkpatrick, S. C. D., Gelatt, J., Vecchi, M. P., 1983. Optimization by simulated annealing. Science 220 (4598), 671–680.

Marti, K., 2003. Multi-start methods. In: Glover, F., Kochenberger, G. (Eds.), Handbook of metaheuristics. Springer-Verlag, Berlin, pp. 355–368.

Nelder, J. A., Mead, R., 1965. A simplex method for function minimization. The Computer Journal 7 (4), 308–313.

Paper IV

A. Aspelund, T. Gundersen, J. Myklebust, M.P. Nowak and A. Tomasgard:

Optimization-Simulation of a Combined LNG and LCO_2 Transport Chain

Submitted to an international journal

Optimization-Simulation of a Combined LNG and LCO_2 Transport Chain

Abstract:
A gradient free optimization-simulation model based on a Tabu Search (TS) and the Nelder-Mead Descent Search (NMDS) combined with the general purpose process simulator HYSYS is successfully applied to optimize the Liquefied Energy Chain (LEC). The LEC is a combined ship based transport chain for inbound transport of Liquefied Natural Gas (LNG) and outbound transport of Liquid Carbon Dioxide (LCO_2). The chain consists of two processes as well as two intermediate storages and a ship. The variables connecting the processes, such as transport pressures for the LNG and LCO_2, are optimized jointly with some of the individual process variables to find the minimum cost or maximum profit. The local optima from the TS are fine-tuned with NMDS to reduce the required number of simulation runs. The minimum cost and maximum profit are found for 13 cases, varying parameters such as distance, price of electricity, and amount of CO_2 to be transported as well as the prices of natural gas (NG) and CO_2. It has been shown that changes in these parameters will influence the transport pressures as well as the individual process variables. Hence, the best solution cannot be obtained without simultaneous optimization of the whole chain.

5.1 Introduction

The developed search procedure is general. It is applied to various cases of the Liquid Energy Chain (LEC). LEC is a combined ship based transport chain for inbound transport of Liquefied Natural Gas (LNG) and outbound transport of Liquid Carbon Dioxide (LCO_2). It consists of an integrated natural gas liquefaction and LCO_2 vaporization process, a combined gas carrier that transports LNG inbound and Liquid Inert Nitrogen (LIN) and LCO_2 outbound, and an integrated process for vaporization of LNG and liquefaction of CO_2 and N_2. The main advantage is that the cold exergy in LNG, LIN and LCO_2 is used in both processes to create an energy efficient transport chain. Furthermore, the gas carrier has a payload in both directions. The liquefied energy chain (LEC) is previously presented in detail in four papers. The first paper describes the concept and summarizes the results from the remaining three (Aspelund and Gundersen, 2009a). The second paper contains a detailed description of the offshore and onshore processes, including the process design methodology, design philosophy, costs and calculations of irreversibilities for all unit operations (Aspelund and

Ψ	Exergy (rational) efficiency
ASU	Air Separation Unit
CP	Critical point
EOR	Enhanced oil recovery
EUR	Euro
HHC	Heavy hydrocarbons
NG	Natural gas
LCO_2	Liquid carbon dioxide
LEC	Liquefied Energy Chain
LIN	Liquid inert nitrogen
LNG	Liquefied natural gas
MITA	Minimum internal temperature approach
MINLP	Mixed Integer Non-Linear Program
MH	Meta Heuristics
MTPA	Million tonnes per annum
NMDS	Nelder Mead Descent Search
TP	Triple point
TS	Tabu Search
UA	Heat transfer $\times$ heat exchanger area
VBA	Visual Basic for Applications
tph	metric tonne per hour

Table 5.1: Nomenclature

Gundersen, 2009b). The combined carrier is presented in the third paper (Aspelund, Tveit, and Gundersen, 2009c). Finally, the last paper contains sensitivity analysis of transport pressures and benchmarking with conventional technologies for gas transport, where it is shown that there is a trade-off between efficiency and ship utilization, depending on the selected transport pressures as well as the amount of LCO_2 and LIN to be transported (Aspelund and Gundersen, 2009c).

The initial design of the processes in the LEC is found by using a new methodology for Process Synthesis (PS) extending traditional Pinch Analysis (PA) with exergy calculations as well as pressure and phase considerations. The procedure, referred to as Extended Pinch Analysis and Design (ExPAnD), shows great potential for minimizing total shaft work in subambient processes. The methodology and a detailed description of the development of the offshore process can be found in the work by Aspelund, Berstad, and Gundersen (2007).

Furthermore, the intermediate pressures and temperatures in the nitrogen expander loop in the field-site process are optimized using mathematical programming and GAMS, with the global solver BARON to solve the resulting MINLP (Aspelund, Barton, and Gundersen, 2009a). The methodology which combines Pinch Analysis (PA), Exergy Analysis (EA) and mathematical programming (MP) found the minimal irreversibilities in a heat exchanger network that allowed for changes in the pressures of the process streams using compressors and expanders. Although this methodology was successfully used to optimize a part of the field site process, it became evident that it is not currently capable of optimizing the complete LEC. This is because the computational complexity must be compensated by some crude simplifications of the processes in order to optimize it in GAMS. Furthermore, since costs are to be evaluated, a large set of non-linear equations must be added which will increase the size and complexity of the problem significantly.

Since it is necessary to use rigorous thermodynamics, the selected approach is to use the commercial sequential process simulator HYSYS combined with an optimization method that does not require gradients.

Therefore, a gradient free optimization-simulation method for processes modelled with the simulator AspenTech HYSYS®(version 2004.2) is developed. The tool is based on a Tabu Search (TS) and the Nelder-Mead Descent Search (NMDS). The local optima that results from the TS are fine-tuned with NMDS to reduce the required number of simulation runs. In order to verify the tool, it has been applied to find the total refrigerant flow rate and composition as well as the refrigerant suction and condenser pressures that minimize the energy requirements of a Prico natural gas liquefaction process (Aspelund, Gundersen, Nowak, Myklebust, and Tomasgard, 2009b). The main strength with this method is that it has a high probability of obtaining a better solution with fewer simulation runs than trial and error methods. Also, by changing parameters such as the discretization

coarseness it is possible to influence the search pattern, thereby taking advantage of already gained process knowledge to speed up the search. In order to handle a larger set of variables, some modifications to the optimization-simulation tool has been done. The most important modification is that the variables that are dominated in the global search before the process settings are near a local optimum are only optimized locally by the NMDS.

Similar approaches are also presented by Chelouah and Siarry (2005) and Hedar and Fukushima (2006) that solved analytical test functions using global TS in combination with local NMDS. Exler, Antelo, Egea, Alonso, and Banga (2008) applied a TS based algorithm to a process and control model. They argue that mathematical programming using global optimization methods (GO) can only handle problems that are small, differentiable and continuous. Their model's restrictions are system of differential and algebraic equations. Their case is similar to this one in the sense that they make no assumptions about the topology of the objective, and treat it like a black box. Cavin, Fischer, Glover, and Hungerbüler (2004) apply a TS optimization algorithm to a batch plant. They discuss Genetic Algorithms (GA) versus TS and conclude that there are several factors that make GA unsuitable for such applications.

In this paper, the size of the field-site (offshore) and market-site (onshore) processes as well as the intermediate storages and the combined carrier are selected so that it can provide NG to a 400 MW net power plant with CO_2 capture that can be integrated with the LEC. The optimization-simulation tool is used to find the minimum annual costs (CAPEX and OPEX) and to maximize the total annual income for 13 cases, varying important parameters such as, location (distance), amount of CO_2 to be transported as well as the corresponding parameters e.g. prices of electricity, LNG and CO_2.

The main contribution of this paper is an optimization-simulation tool that can optimize the overall chain and individual process variables at the same time. The optimization-simulation tool has the ability to escape a local minimum and search for better solutions. Nine variables are optimized using a combined TS and NMDS. In addition, 9 process variables are optimized locally only using NMDS, giving a total of 18 variables that are optimized jointly. It is also shown that when changing or optimizing the strategic decision variables it is important to optimize the variables connecting the processes as well as the individual process variables at the same time, and that failing to do so will lead to sub-optimal solutions.

The optimization routine, the HYSYS model, the cost calculations, the exergy calculations and the ship utilization factor are presented in Section 5.2. Then a description of the LEC, showing the variables to be optimized with upper and lower bounds is given in Section 5.3, followed by Section 5.4 that describes the initial solution and the optimization settings. Then optimization-simulation

results are presented in Section 5.5, followed by a discussion and plans for further work in Section 5.6. Section 5.7 concludes the paper.

5.2 Methodology and framework

Optimization-simulation framework

The optimization method is based on the optimization-simulation tool described in Aspelund et al. (2009b). The main practical difference is that the number of variables is larger. Because of the curse of dimensionality, the larger number of variables has required a few modifications of the algorithm. Only a subset of the variables is tuned in both the TS and NMDS, while all decisions are tuned by the NMDS. Furthermore, the data are sent between the meta heuristic optimization model and the simulation model as a block rather than individually.

From the point of view of the search module, the objective function to be optimized is a black box. It contains a sequential modular based simulation model and an algorithm that aggregates the model output into a single number. Because the objective function is known to have multiple minima and cannot provide any gradient information, it requires global search methods. Among these, TS is expected to be the best suited for this problem because it gives the best control over how much the solution can change from one step of the search to the next. Otherwise more effort would be spent on error handling. The reason for combining the global TS with a local NMDS search, is that the local search usually converges faster to the best solution in the promising area that the TS has detected than the TS would on its own. Furthermore, the computational cost of the NMDS increases less than the cost TS would for the same increase in optimization variables.

The aggregation of process data to an objective value

The routine that returns the objective value consists of two parts; the simulation model and an algorithm that condenses the simulation output and possible warning messages into the objective value. The objective value is a measure of the quality of the evaluated solution. If the simulation model is able to find a feasible objective value then that will be the returned number, otherwise it will handle any error situation by returning a "very high number" that indicates that the solution is infeasible or that it is inconclusive whether it is feasible.

This objective value aggregation routine has several characteristics that are relevant for the choice of search method. It cannot provide any gradients, it has numerous local optima, and if the changes in the submitted solution from one step to the next are too large then it may not converge.

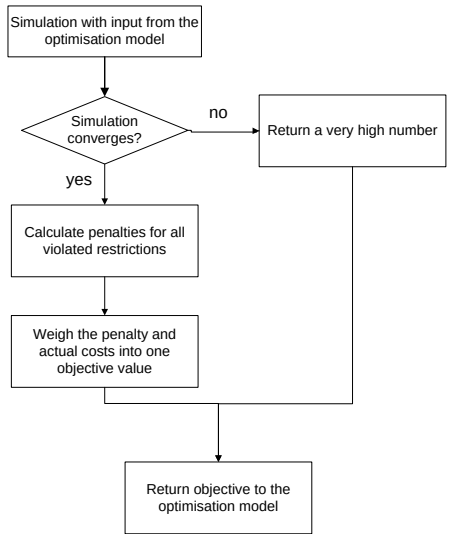

Figure 5.1: The objective value aggregation procedure

All the decision variables have finite domains (box constraints), which makes it possible to discretize them. Mass flows, pressures and absolute temperatures can neither be negative nor infinitely high. Specifications that cannot be formulated as lower and upper bounds and for numerical reasons cannot be fixed directly will be relaxed, i.e. their deviation from one or both sides of their target will be given a penalty in the objective value aggregation.

Because the HYSYS model is sensitive to large changes, diagonal *neighbours*, which would require more than one variable change in the same step, will not be considered. The objective value aggregation routine will evaluate all the current solution's *admissible* neighbour solutions sequentially. Solutions are admissible if all decision variables are within their domains, and not already on the list of recent *current* best solutions, called the *Tabu List* (TL). The global search module updates the TL in on a first in first out manner. After the last neighbour is processed the search module will rank them by their values and the best admissible solution becomes the new current best solution.

Each extra dimension corresponds to two extra neighbours in the TS, and will add two simulation runs per iteration. Some knowledge of the problem makes it possible to sort the decision variables into two groups with relatively high and low impact on the objective value before the process settings are close to a local optima. Computer capacity is likely to be wasted if too many simulations that are unlikely to result in a current best solution are run. The current best solution

will be the starting point for the next iteration. All the solutions that turned out to be worse have served their purpose as candidates and will stay on the TL for the rest of the search. The dominated variables are kept constant in the TS and will only change during the local NMDS.

Local search

The cost of having a large number of decision variables in the local search is limited to the generation of the initial simplex. In addition to the point of the global search where the local search was initiated, the same number of simulations as the number of variables is run. Once the initial simplex is generated, only one simulation is required per iteration regardless of the number of variables. When the potential to tune the dominating variables is exhausted, then tuning the less dominating variables will improve the solution.

The NMDS simplex method is suitable for continuous variables and does not require gradient information. It is also able to handle the "very high number" responses from the black box because it will move away from them in the search space, provided there are not too many of them in the simplex. The NMDS is initiated from a simplex that consists of $n + 1$ vertices (solutions), where n is the problem dimension. Each of these n extra vertices is generated by choosing randomly whether to increase or decrease a different variable for each vertex a small predetermined step from its value in the TS iteration where the NMDS was initiated. It is a descent method in the sense that the *worst* (highest objective value) vertex is rejected and replaced with a new vertex that is always better. Then the updated collection of vertices is sorted by their objective values and the procedure is repeated and the search converges towards the local optima. Finally, the local optimal solution is the *best* vertex when at least one of the stopping criteria is met. A detailed description of the NMDS procedure can be found in the original work by Nelder and Mead (1965).

Each of the geometric moves requires weights for calculation of linear combinations such as *midpoints*, degrees of *extensions*, *contractions* and *shrinkages*. In this application, the midpoints of two vertices are calculated with equal weights, extensions and reflections are extrapolations with length equal to the distance from the worst point to the point corresponding to the average of the best and the second best point, and contractions and shrinkages are half way between the relevant points.

Global search

The continuous problem is discretized by division of the domain of each variable into a finite number of steps. When no new local optima is discovered for given number of global iterations, then the discretization coarseness is increased by a

predetermined factor. At each of the iterations the candidate move is to take one of the decision variables a step of predetermined size up or down while all the other decision variables remain at the current values. Thus the maximum numbers of neighbour solutions is twice the number of decision variables minus the number of variables at their limits. This set of solutions is called neighbours of the current solution. If the current value of one of the decision variables is at either end of its domain, then the only feasible move is to remain unchanged or to take a step towards the interior of the domain. The NMDS is very time consuming, so in order to avoid initiating it at too many of the TS iterations, there is a criteria that no local search will be performed if the objective value of the current solution is more than a given percentage worse than the *best known* objective value. This percentage is higher when the global search is performed with coarse steps. Good solutions close to the end-points of the large steps are therefore less likely to be stepped over.

The new current solution is not necessarily better than the previous current solution. This makes the search able to escape local optima. When the new current solution is identified, it is compared to all its neighbour solutions. If it is sufficiently better than all of them, it is considered to be a local optimum and the region is explored with the NMDS method. If the new current objective is sufficiently worse than the best known objective, then it is considered unlikely that a better one will be detected, and the local search is skipped. The next step of the global search after a local search can either start from where the local search stopped, or from the best of the neighbours before the local search. The advantage of the first approach is that it saves searches when moving towards new local optima when all the local searches in a sequence pull in direction of the same solution. The advantage of the latter is that it is faster when moving away from a recently visited local optimum, where the local searches would pull the starting point of the next iteration towards the solution that the global search tries to escape.

In addition to the list of recently visited solutions, separate memory store the solutions that have been best known at preceding iterations and their corresponding objectives. The objective values of all current solutions are compared to the recent best known, and if a better one is found, then the best known solution is updated. Plots of design variables such as pressures, flow rates, and temperatures in these lists give a visual impression of how the search evolves from iteration to iteration. These lists are not required for the search procedure but provide valuable information for the calibration of search parameters such as step sizes and stopping criteria.

Since a heuristic cannot tell whether the optimal solution has been reached or not, the algorithm needs a stopping criterion, and there are many alternatives. The local search is assumed to have found an optimum when the differences

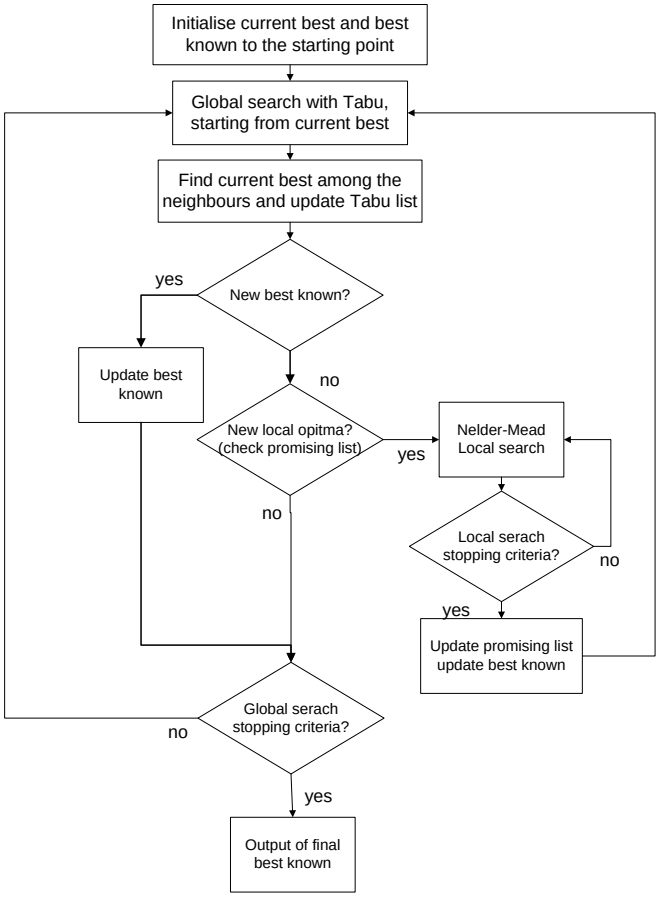

Figure 5.2: The search module

between the variables of two adjacent solutions of the search are less than a specified criterion. A second stopping criterion limits the number of iterations. The global search has several stopping criteria. It either stops after a given length of time, or if there is no improvement in the best known solution for a given number of global iterations, or after a maximum number of simulation runs.

Integration between HYSYS and the search procedure

HYSYS by AspenTech is an interactive simulation tool for steady state and dynamic processes. It also exposes a COM[7] interface that allows other programs to set and retrieve process data. Since HYSYS was designed as an interactive tool, some problems arose when integrating HYSYS into the optimization framework. Information about the simulation state appears on the screen but is not directly available to other programs; therefore so-called backdoors have been used to retrieve information about feasibility of the solution. In the cases where HYSYS displays warning messages, the candidate solution is declared infeasible, and the search continues from the best of the other neighbours.

The initial assumption, which turned out to be correct, is that a relatively large part of the computation time is spent on process simulation runs relative to the meta heuristic search; therefore Visual Basic for Applications (VBA) is an adequate surrounding layer. VBA provides the necessary means to get access to the COM functionality of HYSYS and is suitable for the development. In the beginning of the objective value aggregation sub-routine of the VBA implementation, the decision variables are written simultaneously to the HYSYS spread sheet. This avoids the hard-coding of each individual stream or unit, and makes the model more flexible. In the VBA implementation the HYSYS simulation is considered a part of the objective value aggregation sub-routine. At the beginning of each cycle, all relevant values are given to HYSYS, which is then started and runs until it either converges or warns that it is unable to. Then some of the calculated process values are retrieved, the feasibility status is checked, and the objective function procedure condenses this information into one value.

The HYSYS simulation model

The processes are simulated using the commercially available simulation tool HYSYS[8] using the Soave-Redlich-Kwong (SRK) equation of state. The two processes are simulated as one process, connected by the transport pressures and the flow rates of CO_2 and N_2. It is assumed that there is no heat leakage to the storages and ship tanks, alternatively that there is a re-liquefaction plant

[7] Component Object Module
[8] http://www.aspentech.com

Process unit	Property		
Compressors	Polytropic efficiency	82	%
Pumps	Isentropic efficiency	85	%
Expanders	Isentropic efficiency	85	%
Liquid expanders	Isentropic efficiency	85	%
Process HX	MITA (0°C and above)	5	°C
	MITA (-80°C to 0°C)	3	°C
	MITA (-80°C and below)	2	°C
	Pressure drop	0.2	bar
Ambient HX	MITA	5.0	°C
	Pressure drop	0.3	bar
Flash drums	Pressure drop	0	bar
	Efficiency	100	%
Mechanical to electrical	Efficiency	98	%

Table 5.2: Equipment data

onboard the gas carrier, so that the pressures and temperatures for the LNG, LIN and LCO_2 are the same in the onshore and offshore process. This is of course a simplification. The ship utilization, the costs and the exergy efficiency are calculated by spreadsheets in the HYSYS simulation. Equipment data for the processes are found in Table 5.2, ambient and feed gas data in Table 5.3. A more detailed description of the process assumptions can be found in Aspelund and Gundersen (2009b).

The cost model

The main equipment costs are found by using average vendor prices for similar equipment as a reference. The equipment cost data are from 2003. The difference between the vendor equipment cost estimates for compressors, ambient heat exchangers and pumps are within 20-30%. Since the design of the heat exchanger system is not complete, the costs for the process heat exchangers are uncertain. Hence, to be conservative, a relatively high specific cost, 750 EUR per kW/K (UA), is used in the cost calculations. The individual equipment costs are calculated by Eq. 5.1, where I_{eqr} is investment cost of reference equipment, S_p is the size of the equipment, S_r is the size of the reference equipment, S_f is the size factor for the specific type of equipment and I_f is a five year inflation factor. The total investment costs are then found by Eq. 5.2, where the sum of the main equipment (compressors, ambient heat exchangers, pumps and process heat exchangers) is multiplied with an equipment installation factor, EI_f. Financial

Stream	Property		
Ambient(seawater and air)	temperature	10	°C
	pressure	1	bar
Feed gas	flow rate	62.3	t LNG/h
	flow rate	0.545	MTPA LNG
	temperature	15	°C
	pressure	70	bar
	composition:		
	Nitrogen	1	mole %
	Methane	92	mole %
	Ethane	5	mole %
	Propane	1.8	mole %
	n-Butane	0.1	mole %
	i-Butane	0.1	mole %
	Carbon dioxide	0	ppm
	Water	0	ppm

Table 5.3: Ambient data, feed gas conditions and composition

data can be found in Table 5.4, equipment cost data in Table 5.5. The annual operational costs excluding cost of electricity are set to 1-3% of the investment cost. The annual capital and investment costs are found by using a project lifetime of 30 years, an annual interest rate of 7% and a yearly operation of 8760 hours.

$$Inv_{eq} = I_{eqr} \left(\frac{S_p}{S_r} \right)_f^S \cdot I_f \tag{5.1}$$

$$Inv_{tot} = EI_f \sum Inv_{eq} \tag{5.2}$$

The exergy model

Exergy is a measure of the quality of a process or energy stream, and it describes the maximum work that can be obtained in an ideal (reversible) engine. It is used to evaluate different energy and process streams on an equal basis. E.g. electricity is defined to be pure exergy, hence 1 kWh of electric energy contains 1 kWh of exergy. A hot stream above ambient temperature will always have a thermo-mechanical exergy content that is lower than its thermal energy content, heat has lower quality than electricity. The exergy content of a stream depends on

Factor	Type		
Operational costs	processes	3	%
	ship	3	%
	storage	1	%
	loading system	1	%
	unloading system (STL)	1	%
Installation factor, EI_f		4.0	
Inflation factor, I_f		1.47	(8%/ 5 years)
Interest rate		7	% /1 year
Lifetime in operation		30	years
Annual operation		8760	hours

Table 5.4: Financial data

Process unit	Reference size S_r	Reference cost I_{eqr}	Size factor S_f
Compressors and expanders	4000 kW	1 250 000 EUR	0.6
Pumps	200 kW	375 000 EUR	0.6
Ambient HX	5000 kW	220 000 EUR	0.7
Process HX	1000 UA	750 000 EUR	0.7

Table 5.5: Equipment cost data for the processes

	Ref. size S_r	Ref. cost I_r	Size factor S_f	C_f	I_f
Gas carrier	12000 m^3	40 MEUR	0.85	1.35	1
Storage	3000 m^3	2 MEUR	1.0	1	1.47

Table 5.6: Unit cost data for the gas carrier and storage

its duty and the difference between its own and the ambient temperature. A cold stream will have a lower thermo-mechanical exergy than energy content down to approximately -130°C, and higher exergy content for lower temperatures. The *exergy efficiency* describes the quality of the process. If the exergy efficiency is 100% there are no losses and the process, in thermodynamic terms, is reversible. If the exergy efficiency is 80% it means that there are 20% losses (irreversibilities) in the process. Neglecting the contributions from kinetic and potential energy and having no reactions or mixing of the fluids, the change of exergy in a stream j through a unit (Eq. 5.3) and the exergy (rational) efficiency (Eq. 5.4) can be written as (Kotas, 1995):

$$\Delta\epsilon_j^{tm} = (h_{out} - h_{in})_j - T_0(s_{out} - s_{in}) = (\epsilon_{out} - \epsilon_{in})_j \tag{5.3}$$

$$\Psi = \frac{\sum_{out} \dot{m}_{out}\epsilon_{out} + E_{out}}{\sum_{in} \dot{m}_{in}\epsilon_{in} + E_{in}} \tag{5.4}$$

Where ϵ is the specific exergy, h is the specific enthalpy, s is the specific entropy, and $\dot{m}$ is the mass flow of a stream. E is the exergy supplied to or removed from the system in the form of heat and/or work, and T_0 is the ambient temperature. The exergy conversion efficiency is defined as the exergy efficiency taking into account only the exergy components that change throughout the process (Aspelund et al., 2009a). The exergy efficiency is calculated for the field site process, the market site process and the overall transport chain, excluding the fuel for the gas carrier. Hence, for the field site process the exergy efficiency is the sum of the thermo-mechanical exergy in LNG at transport pressure and CO_2 at 150 bar divided by the sum of the thermo-mechanical exergy in NG at 70 bar, LCO_2 at transport pressure, LIN at transport pressure and work provided to the process. The exergy for the market site process is the sum of the thermo-mechanical exergy of NG at 25 bar, LIN at transport pressure and LCO_2 at transport pressure divided by the thermo-mechanical exergy of the LNG at transport pressure, and the work provided to the process. The exergy efficiency for the total chain is the sum of the thermo-mechanical exergy of NG at 25 bar, CO_2 at 150 bar divided by the thermo-mechanical exergy of NG at 70 bar and the work provided to the field site and the market site processes.

Definition of ship utilization

The ship utilization factor (SUF) is a concept used to quantify the efficiency of the cargo containment system. The SUF shows to what degree the cargo space is used to transport moneymaking cargo, in shipping known as the "payload". In the LEC concept the payload is LCO_2 and LNG. The LIN is transported only to make the production of LNG possible, thus not generating income by itself. The conventional way of defining ship utilization is to divide the volume

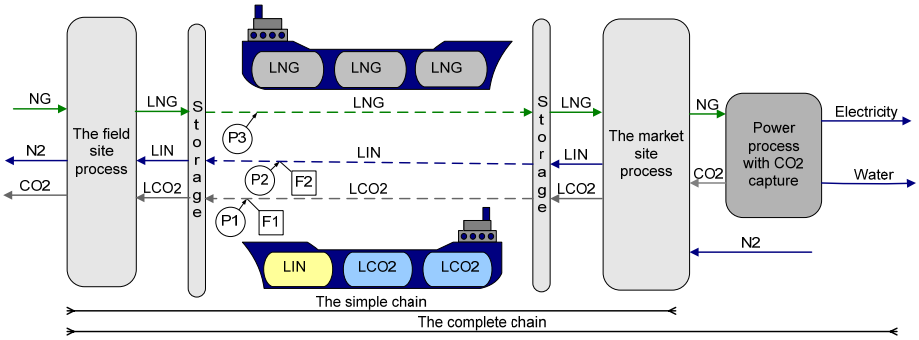

Figure 5.3: The Liquefied Energy Chain

of transported cargo per year on the maximum yearly transport capacity for a given ship assuming a one way payload only. Since the LEC ship carries load both ways, it is more effective than a typical liquefied gas ship, and could obtain a conventional SUF higher than 100%. Therefore, contrary to standard SUF calculations, the SUF in this paper is defined by adding the volume of outbound and inbound transported payload and dividing it by *two* times the available cargo volume. The intermediate storage tanks will have the same utilization factor as the gas carrier.

5.3 The Liquefied Energy chain

The Liquefied Energy Chain (LEC) is a novel energy and cost effective transport chain for stranded NG utilized for power production with CO_2 capture and storage. It includes a field site section, a combined gas carrier, and a market site section, see Fig. 5.3. In the field site section, NG is liquefied to LNG by the cold carriers Liquid Carbon Dioxide (LCO_2) and Liquid Inert Nitrogen (LIN). The nitrogen is emitted to the atmosphere at ambient conditions. The CO_2 at high pressure is transferred to an offshore oil field for Enhanced Oil Recovery (EOR). LNG, LIN and LCO_2 are contained in an intermediate storage at the field site. LNG is transported to the receiving terminal in the combined carrier.

At the receiving terminal, most of the cryogenic exergy in LNG is recovered by liquefaction of CO_2 and nitrogen. The onshore process is connected to a power plant with CO_2 capture where NG is converted to electricity, CO_2 and water. Initially water is removed from the CO_2 by condensation and adsorption, then the CO_2 is compressed to a pressure above the triple point (TP), and finally the

CO_2 is liquefied by vaporization of the remaining LNG. LNG, LIN and LCO_2 are contained in intermediate storages. The LCO_2 and LIN are transported offshore in a combined gas carrier. CO_2 can be provided by other sources as petrochemical industry, cement or steel production or hydrogen production, so more than 100% of the carbon of the LNG can potentially be returned. Nitrogen can be provided by an Air Separation Unit (ASU), however, in this paper only the basic transport chain is considered. As can be seen from Fig. 5.4, the chain consists of two processes that are connected with two intermediate storages and a combined carrier. For a fixed amount of NG to be transported, the variables that connect the processes are the transport pressures of LCO_2 (P1), LIN (P2) and LNG (P3) as well as the amounts of LCO_2 (F1) and LIN (F2). Changing these variables will affect the individual process variables, exergy efficiency and power requirements both in the field site and market site section, as well as the size of the intermediate storages and the size and ship utilization for the combined carrier.

The offshore LNG process

NG at 15 °C and 70 bar (NG-1) is compressed to a pressure between 80 and 100 bar (P4), a pressure that is higher than the cricondenbar pressure[9], and cooled by liquid CO_2 and gaseous nitrogen in HX-101 to a temperature between -70°C and -50°C (T1). The cooled NG in dense phase (NG-3) is expanded in a dense phase expander to 50 bar, which is close to the bubble point line. It is further subcooled before it is expanded to transport pressure between 1 and 3 bar (P3) and stored in an LNG tank. Stream (NG-6) is at the bubble point to avoid purge or recycling.

Liquid CO_2 (CO2-1) is pumped from bubble point (BP) temperature at a 5.5 to 10 bar (P1) transport pressure to 60 bar before it is heated in HX-101. The CO_2 pressure must be high enough to avoid vaporization. The CO_2 is then pumped to injection pressure and transferred to an oil reservoir for EOR. Liquid N_2, (N2-1) is pumped from a 4 to 10 bar (P2) transport pressure to 100 bar before it enters the cold-end of the main heat exchanger HX-102, where the dense phase nitrogen is heated to approximately -80 °C. The nitrogen is further heated to a temperature between -60°C and -40°C (T2) in HX-101 before it is expanded to a pressure between 4 and 10 bar (P5) in EXP-101. Then the cold nitrogen gas (N2-5) is sent to HX-102 and HX-101 where it is heated to approximately -80°C and a temperature between -60°C and 20°C (T3), respectively. The nitrogen gas (N2-7) is then compressed to a pressure between 15 and 35 bar (P6), and cooled by CO_2 to a temperature between -60°C and 20°C (T4) in HX-101. The gas (N2-9) is then expanded to 1.4 bar in EXP-102 and sent to HX-102 and HX-

[9]Maximum pressure at which two phases can coexist

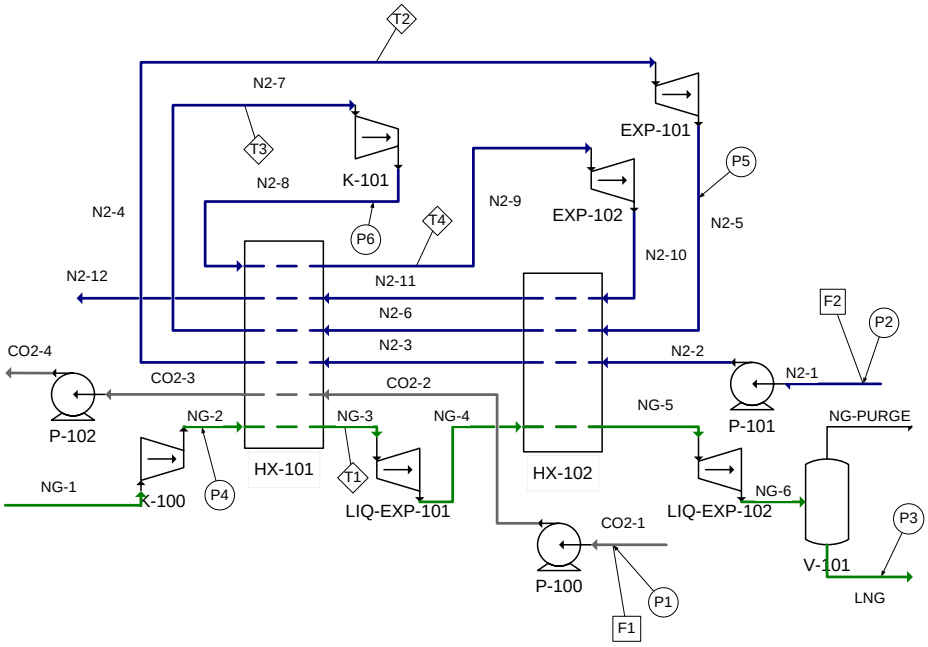

Figure 5.4: Process flow diagram with variables to be optimized for the offshore LNG process

Stream	Type I	Type II	Name	Unit	Initial value	Lower bound	Upper bound
CO2-1	Global	Pressure	P1	bar	6	5.5	10
CO2-1	Global	Flow rate	F1	kg/h	80000	60000	150000
N2-1	Global	Pressure	P2	bar	4	4	10
N2-1	Global	Flow rate	F2	kg/h	65000	55000	65000
LNG	Global	Pressure	P3	bar	1.1	1	3
NG-2	Global	Pressure	P4	bar	90	80	100
NG-3	Local	Temperature	T1	˚C	-61	-70	-50
N2-4	Local	Temperature	T2	˚C	-40	-60	0
N2-5	Global	Pressure	P5	bar	6	4	10
N2-7	Local	Temperature	T3	˚C	-40	-60	20
N2-8	Global	Pressure	P6	bar	28	15	35
N2-9	Local	Temperature	T4	˚C	-40	-60	20

Table 5.7: Variables in the field site process

101, where it is heated to -80°C and approximately 20 ˚C, respectively. Finally, nitrogen (N2-12) at atmospheric pressure and close to ambient temperature is emitted to the atmosphere.

As can be seen from Fig. 5.5, there are 12 variables to be optimized, 5 of which connects the field site and market site processes. The variables with their upper and lower bounds are given in Table 5.7.

The onshore process

The LNG is pumped to a pressure of 25 bar (NG-1) before it is heated by cooling of nitrogen in HX-102. To utilize the cryogenic exergy in the most efficient way, the LNG is then pumped to 74 bar (NG-3) and heated to 12°C, before it is expanded to 25 bar (NG-5) and re-heated to 12°C.

The nitrogen is compressed to 65 bar in four stages with intermediate cooling (N2-8) before it is pre-cooled to a temperature between -115°C and -80°C (T7), (N2-9), in HX-101. It is then liquefied and sub cooled in HX-102 and expanded through a valve to the 4 to 10 bar transport pressure, with a vapour fraction that can vary between 0.1 and 0.4 (VF1) (N2-11). The flash gas (N2-12) is heated to a temperature between -115°C and -80°C (T5) - and expanded in EXP-102 to 3.4 bar (N2-14), to provide additional cooling for the hot nitrogen stream. The nitrogen is then heated to a temperature between -132°C and -92°C (T6), (N2-15) before it is heated to atmospheric conditions and the nitrogen is recompressed.

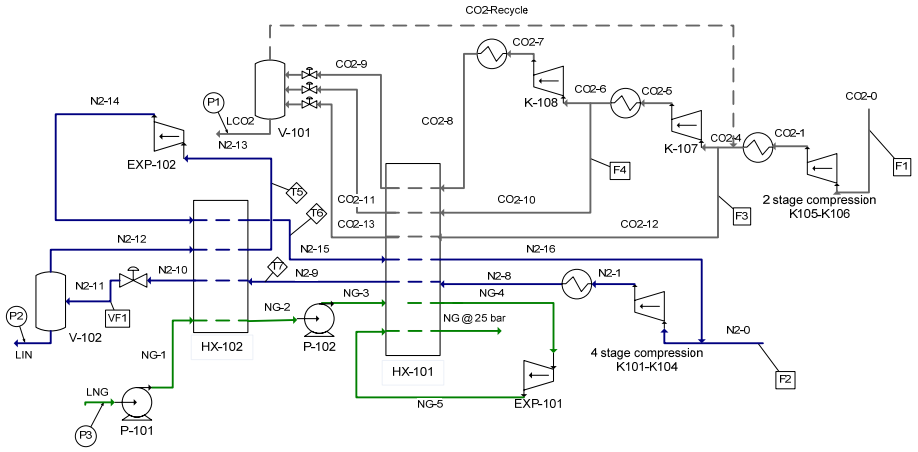

Figure 5.5: Process flow diagram for the onshore process

The CO_2 is compressed in two stages to 7.25 bar and cooled to ambient conditions before the stream is split into two parts. Approximately half of the CO_2, (F3), (CO2-12), is liquefied in HX-101. The other part (CO2-4) is compressed to 24 bar and cooled to ambient conditions. Stream CO2-4 is then split in two new streams, where one stream (F4), (CO2-10), is liquefied and subcooled to -55°C in HX-101. The other part (CO2-6) is compressed to 65 bar and liquefied by seawater. It is then subcooled to -55°C in HX-101. Due to the subcooling, there should not be any flash gas after expansion, however, a recycle stream is provided for start-up and increased flexibility.

As can be seen from Fig. 5.5, there are 12 variables to be optimized, 5 of which connects the field site and market site processes. The variables with their upper and lower bounds are given in Table 5.8.

5.4 Optimization-simulation settings

There are infinitely many combinations of settings for the search. The implemented parameter combination was chosen by trial and error. In order to make the 13 cases shown in the case studies section comparable the same combination of settings it was applied to all. The best known solution usually did not improve much after 100-150 global iterations, which was reached after 10 hours on a laptop with a 2.40 GHz Intel(R) Core(TM) 2 Duo CPU and 4.00 GB RAM. The stopping criteria were set to the first occurring of either 12 hours of simulation or 1000 global iterations. Memory usage seemed to accumulate for each run of the

Stream	Type I	Type II	Name	Unit	Initial value	Lower bound	Upper bound
LCO2	Global	Pressure	P1	bar	6	5.5	10
CO2-0	Global	Flow rate	F1	kg/h	80000	60000	150000
LIN	Global	Pressure	P2	bar	4	4	10
N2-0	Global	Flow rate	F2	kg/h	65000	55000	65000
LNG	Global	Pressure	P3	bar	1.1	1	3
CO2-12	Local	Flow rate	F3	kg/h	10500	9000	25000
CO2-6	Local	Flow rate	F4	kg/h	35000	30000	55000
N2-9	Local	Temperature	T7	°C	-96	-115	-80
N2-11	Global	Vapour fraction	VF1	-	0.4	0.1	0.5
N2-13	Local	Temperature	T5	°C	-101	-115	-80
N2-15	Local	Temperature	T6	°C	-115	-132	-92

Table 5.8: Variables in the market site process.

HYSYS model. Consequently, the practical limitation on iterations was the total number of simulation runs, independently of whether they were initiated by the TS or the NMDS. Settings such as step sizes in NMDS and TS and the tolerance for the check against the Tabu list in the TS were allowed to vary across the different decision variables. These are summarised in Table 5.9 where they are measured as fractions of the lower to upper bound range.

Case studies

In case A to case F, the LEC is optimized with respect to minimum transport costs, whereas in case G to case K revenue for the transport of LNG and LCO_2 is included in the objective function and makes it possible to maximize profit. Case A represents an initial feasible solution prior to optimization. In Case B, referred to as the base case, the chain is optimized using the base case conditions including the ship. In case C, the ship is excluded from the optimization and costs added later. Case D represents a longer journey with 5 days sailing. In case E and F, the amount of LCO_2 is set to 80% and 100% of the carbon from the NG respectively. In case G1, there are revenues of 150 and 10 EUR/tonne LNG and LCO_2 transport respectively. Whereas the revenue for transporting LCO_2 is increased to 50 EUR/tonne in case G2. In case H, a cost of 10 EUR/tonne nitrogen is included. Case H1 and H2 represent a 50% increase and a 50% decrease in the price of electricity. In case J, the cost of electricity is reduced with 50% offshore and increased with 50% onshore. Finally, in case K, the capacity is

Stream	Type I	Type II	Name	NMDS step size	TS step size	Tabu tolerance
CO2-1	Global	Pressure	P1	1/20	1/20	1/20
CO2-1	Global	Flow rate	F1	1/20	1/20	1/20
N2-1	Global	Pressure	P2	1/20	1/40	1/40
N2-1	Global	Flow rate	F2	1/20	1/10	1/10
LNG	Global	Pressure	P3	1/20	1/30	1/30
NG-2	Global	Pressure	P4	1/20	1/15	1/15
NG-3	Local	Temperature	T1	1/40	-	-
N2-4	Local	Temperature	T2	1/40	-	-
N2-5	Global	Pressure	P5	1/20	1/10	1/10
N2-7	Local	Temperature	T3	1/40	-	-
N2-8	Global	Pressure	P6	1/20	1/10	1/10
N2-9	Local	Temperature	T4	1/40	-	-
CO2-12	Local	Flow rate	F3	1/10	-	-
CO2-6	Local	Flow rate	F4	1/40	-	-
N2-9	Local	Temperature	T7	1/40	-	-
N2-11	Global	Vap. fract.	VF1	1/20	1/20	1/20
N2-13	Local	Temperature	T5	1/40	-	-
N2-15	Local	Temperature	T6	1/40	-	-

Table 5.9: Global and local search settings

Parameter	value	
Amount of LNG to be transported	62830	kg/h
Price of electricity offshore	150	EUR/MWh
Price of electricity onshore	100	EUR/MWh
Voyage time	24	h
Loading and unloading time	12	h

Table 5.10: Initial data for the base case

increased with 100% compared to case G1. Some initial data for the base case are given in Table 5.10, and the cases are summarized in Table 5.11.

5.5 Results

Optimization progress

Figure 5.6 shows the progress plot for case B, where the *current* and the *best known* objective values are plotted with the iteration number of the global search on the horizontal axis. The plot also shows where the local searches are performed; it has the value of one if a local search is initiated and zero otherwise. As can be seen there is a rapid decrease in the best known objective value during the first 25 global iterations and no local search are performed. At iteration 25 a local search is initiated which improves the objective value significantly. After approximately 40 global iterations a new local search is initiated, which again decreases the best known objective value. After about 60 iterations the current objective curve flattens out, and more local searches are performed. Then the current objective vary slightly during a number of iterations. However, the best known objective decreases slowly. Between iteration 150 and 200 the TS forces the solution out of a local minima. As can be seen the current objective value is so far worse than the best known objective value that the criteria for initiating local searches are not met. The final update of best known is in global iteration 317. The optimization-simulation continues until iteration 377, where it is ended after 12 hours. It is clear from the figure that there are several solutions that are close to the optimum value. This is often the case in process design, as there is a trade-off between investment and operational costs. Also, since the current objective is not far from the best known objective in the last iteration 377, it is likely that the model could find a better solution if allowed to run for a longer time.

To verify that the current best solution is at least a local minimum, case B is implemented from the best known solution with narrow bounds (about 2-4 times

Case	Description	Objective	Details
A	Initial	Cost	-
B	Base case	Cost	Ship and storage is included in the optimization, 1 day voyage
C	Excluding ship	Cost	Ship and storage is not included in the optimization
D	Long voyage	Cost	Ship and storage is included in the optimization, 5 days voyage
E	Fixed amount of CO_2	Cost	Base case, but 80% CO_2
F	Fixed amount of CO_2	Cost	Base case, but 100% CO_2
G1	Low price of LCO_2	Profit	Base case, but 10 EUR/ tonne CO_2, 150 EUR/tonne LNG
G2	High price of LCO_2	Profit	Base case, but 50 EUR/ tonne CO_2, 150 EUR/tonne LNG
H	Includes costs of Nitrogen	Profit	Base case, but 50 EUR/ tonne CO_2, 150 EUR/tonne LNG, -10 EUR/-tonne LIN
I1	Increased price of electricity	Profit	Base case, but 50 EUR/ tonne CO_2, 150 EUR/tonne LNG, -10 EUR/-tonne LIN, price of electricity + 50%
I2	Decreased price of electricity	Profit	Base case, but 50 EUR/ tonne CO_2, 150 EUR/tonne LNG, -10 EUR/-tonne LIN, price of electricity - 50%
J	Diverse price for electricity	Profit	Base case, but 50 EUR/ tonne CO_2, 150 EUR/tonne LNG, -10 EUR/-tonne LIN, price of electricity onshore + 50%, cost of electricity offshore - 50%
K	Increased capacity	Profit	Base case profit, 50 EUR/ tonne CO_2, 150 EUR/tonne LNG, -10 EUR/tonne LIN, capacity + 100%

Table 5.11: Case studies

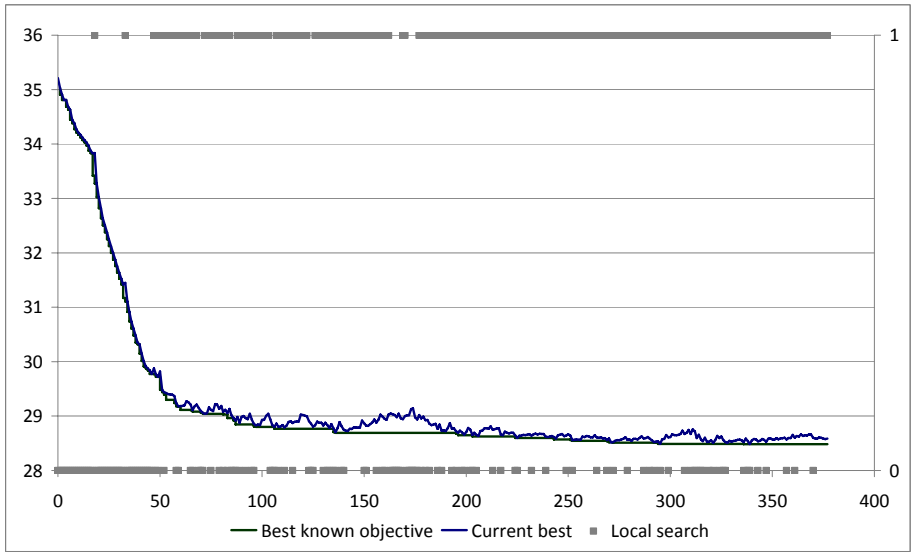

Figure 5.6: Progress plot for case B

the former step size apart) and restarted a few times with the same calculation time, 12 h. The optimization-simulation model is capable of finding solutions that are 0.05% better than the previous solution, however, some runs do not find better solutions. This indicates that a local optimum is found, and that there is practically no improvement from restarting the search from the best known solution.

The optimization-simulation tool also provides plots and tables showing the exact variations of the variables from iteration to iteration. It is seen from these plots (Fig. 5.6-5.8) that all variables change throughout the simulation, furthermore that some variables are first reduced in value and then increased, or opposite. These variable plots are valuable for understanding the behaviour of the processes and the total energy chain.

Overall results

The main results for the minimization of cost, case A to F are shown in Table 5.12. When optimizing the LEC from a reasonable initial solution it can be seen that the total and specific costs are reduced. The ship utilization factors and exergy efficiencies have all increased. The optimal transport pressures for LNG,

LCO_2 and LIN are 1.02, 5.53 and 7.47 bar, respectively, meaning that both LNG and LCO_2 are transported close to the minimum allowed transport pressures.

Case C, where the processes are optimized without considering the ship and storage (these costs are added subsequent of optimization), gives approximately the same result. However, the investment costs of the processes have been slightly reduced at the expense of higher costs for the ship and storage. Also, both LNG and LIN are transported at higher pressures, 1.20 and 9.69 bar respectively. Since the density decreases with higher pressures, this leads to a lower SUF. For a longer voyage time, 5 days instead of 1 day, it can be seen that the ship utilization has increased from 80.2% in the base case to 81.9% and that the transport pressure of LIN has decreased to 5.42 bar. The exergy efficiencies are slightly decreased resulting in increased power requirements. For all these cases, the amount of LCO_2 transported is as low as possible, 60 tph, whereas the amount of nitrogen varies between 61.5 and 64.9 tph.

In case E, a constraint is added for the amount of LCO_2 to be transported. This leads to a decrease in SUF and also a decrease in the required amount of LIN. The exergy efficiency for the offshore process has increased, however the exergy efficiency in the onshore process has decreased, so the overall exergy efficiency is still higher than the base case. Furthermore, the investment and electricity costs has increased leading to a higher specific cost of transported LNG, however, the specific cost of the total payload have decreased. Increasing the amount of LCO_2 to 100% (case F) gives similar results.

In case G1 to K, the objective function includes revenue from transporting LNG and LCO_2. In case G1 the LCO_2 revenue is low. Measured relative to the quantity of LNG it is only 10 EUR/tonne LNG. Thus the results are similar to the base case, where only 64.6 tph of LCO_2 is transported. It is worth noticing that there is a large annual profit of 59.4 MEUR per year or a specific income of 107.9 EUR/tonne LNG transported or 53.2 EUR per tonne payload (LNG and LCO_2). In case G2, the income for transporting LCO_2 is increased to 50 EUR per tonne. In this case as much LCO_2 as possible is transported. This result in a much lower SUF and higher investment and electricity costs, however, the exergy efficiency is actually increased. It is also worth noticing that less LIN is required and that LNG and LIN are transported at higher pressures, whereas the LCO_2 is still transported at the same pressure. The total yearly profit has increased to 70.6 MEUR and the specific profit LNG, LCO_2 and payload have also increased to 198.7, 83.2 and 58.7 EUR/tonne, respectively.

In case H, the cost of producing nitrogen is included in the objective function. This is the case if nitrogen is to be produced from an air separation unit (ASU). In this case, the transport pressures of LNG and LIN increases to 1.97 and 10.0 bar respectively, and the required amount of LIN is reduced to the minimum allowed 55.0 tph. This indicates that it could be beneficial to reduce the amount of LIN

CASE	Unit	A	B	C	D	E	F
Ship utilization	%	71.5	80.2	79.5	81.9	69.8	62.7
Ψ, offshore	%	81.3	83.4	83.0	82.8	85.7	87.0
Ψ, onshore	%	68.9	74.9	74.7	73.4	73.9	73.0
Ψ, total	%	44.1	50.1	49.8	48.6	52.0	53.1
Required power, offshore	MW	0.0	0.0	0.0	0.0	0.0	0.0
Required power onshore	MW	18.9	13.4	13.5	14.1	14.8	16.6
Required Power, total	MW	18.9	13.4	13.5	14.1	14.8	16.6
Yearly cost, offshore	MEUR	4.1	4.5	4.4	4.4	4.4	4.3
Yearly cost onshore	MEUR	7.0	5.9	5.8	6.0	6.4	6.7
Yearly cost, electricity	MEUR	16.6	11.7	11.8	12.4	13.0	14.5
Yearly cost, ship	MEUR	4.2	3.9	4.0	12.0	4.3	4.7
Yearly cost, storage	MEUR	2.8	2.5	2.6	8.9	2.8	3.1
Yearly cost, total	MEUR	34.7	28.5	28.6	43.6	30.9	33.4
Specific yearly cost LNG	EUR/t	63.0	51.8	52.0	79.2	56.1	60.6
Specific yearly cost CO_2	EUR/t	49.5	4.2	54.5	82.9	40.4	34.9
Specific yearly cost payload	EUR/t	27.7	26.5	26.6	40.5	23.5	22.1
Pressure LNG	bar	1.10	1.02	1.20	1.20	1.08	1.09
Pressure LCO_2	bar	6.00	5.53	5.51	5.51	5.50	5.50
Pressure LIN	bar	4.00	7.47	9.67	5.42	6.86	6.59
Flow rate LNG	tph	62.8	62.8	62.8	62.8	62.8	62.8
Flow rate LCO2	tph	80.0	60.0	60.0	60.0	87.3	109.1
Flow rate LIN	tph	65.0	63.9	64.9	61.5	60.3	58.7

Table 5.12: Results case A - F

CASE	Unit	G1	G2	H	I1	I2	J1	K
Ship Utilization	%	78.3	53.0	53.2	53.2	53.1	53.2	53.3
Ψ, offshore	%	83.9	88.4	88.1	88.2	88.1	88.0	87.7
Ψ, onshore	%	74.6	70.8	70.3	70.5	69.9	69.9	70.1
Ψ, total	%	50.6	53.8	53.5	54.8	52.8	52.9	53.1
Required power, offshore	MW	0.0	0.0	0.0	0.0	0.0	0.0	0.0
Required power onshore	MW	13.6	20.5	20.6	20.5	21.0	21.0	41.9
Required Power, total	MW	13.6	20.5	20.6	20.5	21.0	21.0	41.9
Yearly cost, offshore	MEUR	4.5	4.2	4.1	4.2	4.1 4	.0	6.3
Yearly cost onshore	MEUR	6.0	7.4	7.4	7.5	7.4	7.4	11.6
Yearly cost, electricity	MEUR	11.9	18.0	18.1	27.0	9.2	27.6	36.7
Yearly cost, ship	MEUR	3.9	5.6	5.5	5.5	5.4	5.4	10.2
Yearly cost, storage	MEUR	2.6	3.8	3.7	3.7	3.7	3.7	7.5
Yearly cost, N_2	MEUR	0.0	0.0	4.9	4.9	4.8	4.8	9.7
Yearly cost, total	MEUR	28.8	38.9	43.7	52.7	34.6	52.9	82.0
Yearly revenue, CO_2	MEUR	5.7	65.7	65.7	65.7	65.7	65.7	131.4
Yearly revenue LNG	MEUR	82.6	82.6	82.6	82.6	82.6	82.6	165.1
Yearly income total	MEUR	88.2	148.3	148.3	148.3	148.3	148.3	296.5
Total revenue	MEUR	59.4	109.4	104.5	95.6	113.7	95.3	214.5
Specific yearly cost LNG	EUR/t	52.4	70.6	79.4	95.8	62.8	96.2	74.5
Specific yearly cost CO_2	EUR/t	50.9	29.6	33.3	40.1	26.3	40.3	31.2
Specific yearly cost payload	EUR/t	25.8	20.9	23.4	28.3	18.5	28.4	22.0
Specific yearly revenue LNG	EUR/t	107.9	198.7	189.9	173.6	206.6	173.2	194.9
Specific yearly revenue CO_2	EUR/t	104.8	83.2	79.6	72.7	86.5	72.5	81.6
Specific yearly revenue payload	EUR/t	53.2	58.7	56.1	51.3	61.0	51.1	57.5
Pressure LNG	bar	1.09	1.43	1.97	1.90	1.77	1.90	2.03
Pressure LCO_2	bar	5.50	5.53	5.52	5.51	5.52	5.51	5.50
Pressure LIN	bar	7.75	9.70	10.0	10.0	7.45	8.35	9.30
Flowrate LNG	tph	62.8	62.8	62.8	62.8	62.8	62.8	125.7
Flowrate LCO_2	tph	64.7	150.0	150.	150.0	150.0	150.0	300.0
Flowrate LIN	tph	63.0	57.6	55.0	55.6	55.0	55.00	111.1

Table 5.13: Results Case G1 - K

even further. There are small differences in ship utilization, exergy efficiencies and costs for each chain element.

In case I1, the price of electricity is increased by 50% both offshore and onshore. This motivates a small increase in all exergy efficiencies that reduces total power requirements from 20.6 to 20.5 MW. This benefit comes at the expense of increased investment costs for the offshore and onshore plants. By investigating the processes it can be seen that the efficiency improvement could have been achieved by reducing the minimum internal temperature approach (MITA) in the heat exchangers. The consequential smaller driving force is compensated with larger (costlier) heat exchangers. In case I2, the price of electricity is decreased by 50%. This leads to a small decrease in exergy efficiency and an increase in required power from 20.6 to 21.0 MW. In case J, the cost of electricity is decreased by 50% in the offshore process and increased by 50% in the onshore process. Even if the price of electricity now is lower for the offshore process, the offshore power requirement is still zero, indicating that it is more cost efficient to provide the energy to the onshore process. Overall, apart from the change in costs for electricity, increasing or decreasing the electricity price lead to small changes for the processes and the results.

The capacity for the LEC is increased by 100% in case K. This leads to a reduction in the specific transport cost for LNG from 79.4 (case H) to 74.5 EUR/kWh. The exergy efficiency has decreased slightly, apart from this, there are only minor changes.

Changes in the process variables

The pressure variables for case A-K are shown in Fig. 5.7, the solution for the temperature variables are presented in Fig. 5.8, whereas the solution for the flow rate and vapour fraction variables are shown in Fig. 5.9. The dotted lines indicate the variables measured at the secondary axis. As can be seen from Fig. 5.7, the LCO_2 (P1) should always be transported at the lowest pressure 5.50 bar. The LNG (P3) should also be transported at low pressure, close to 1.0 bar for the cases that minimize cost. However, when there is a cost assigned to nitrogen, the optimal transport pressure of LNG increases to around 2.0 bar. The transport pressure of LIN (P2) changes more across the different cases. It varies from 5.5 bar in case D to 10.0 bar in case H, which is the chosen upper bound on transport pressure.

It can also be seen that the pressure at which natural gas (NG-2) is cooled, variable (P4) is close to maximum allowed pressure of 100 bar for all cases. However, the intermediate pressures in the offshore process (P5 and P6) vary significantly from case to case. This is especially true for the cases A-G1, where as little LCO_2 as possible is transported. From Fig. 5.8 it can be seen that all

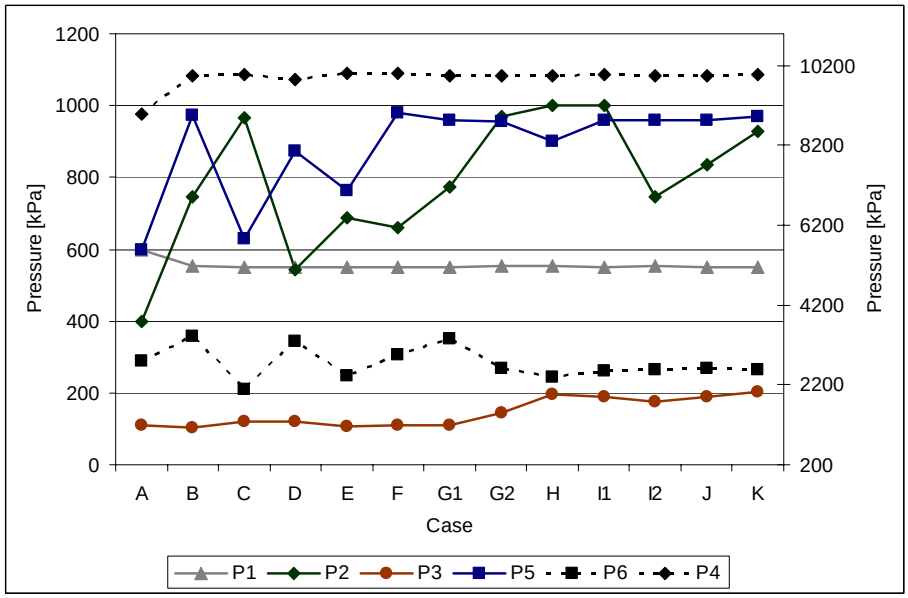

Figure 5.7: Pressure variables

the temperature variables change across the different cases. The intermediate temperatures in the offshore process (T1, T3 and T4) vary the most, especially for cases A-G1, where the quantity of LCO_2 transported is at the chosen lower bound.

As can be seen from Table 5.11, the flow rate for LCO_2 (F1) varies the most. It is at the lower bound for cases B, C, D and G1, when there is no revenue from the transport of LCO_2. However, when there is a 50 EUR/tonne revenue it is at the chosen upper bound. The flow rate of LIN (F2) is highest when the flow rate of LCO_2 is at its lowest value and at the lower bound when the flow rate of LCO_2 is at its highest value. F3 and F4 are the flow rates of CO_2 to be condensed at low and medium pressures respectively. As can be seen from the figure, these flow rates will vary from case to case and they follow a similar pattern as the flow rate of LCO_2. Of course, when the capacity is increased with 100% then the upper bound of the flow rate variables increases correspondingly. The vapour fraction of stream N2-11, entering the flash drum (VF1) changes quite a lot from case to case. This variable is very important for the energy balance in HX-101 in the onshore process and will also influence the temperature variables in the onshore process.

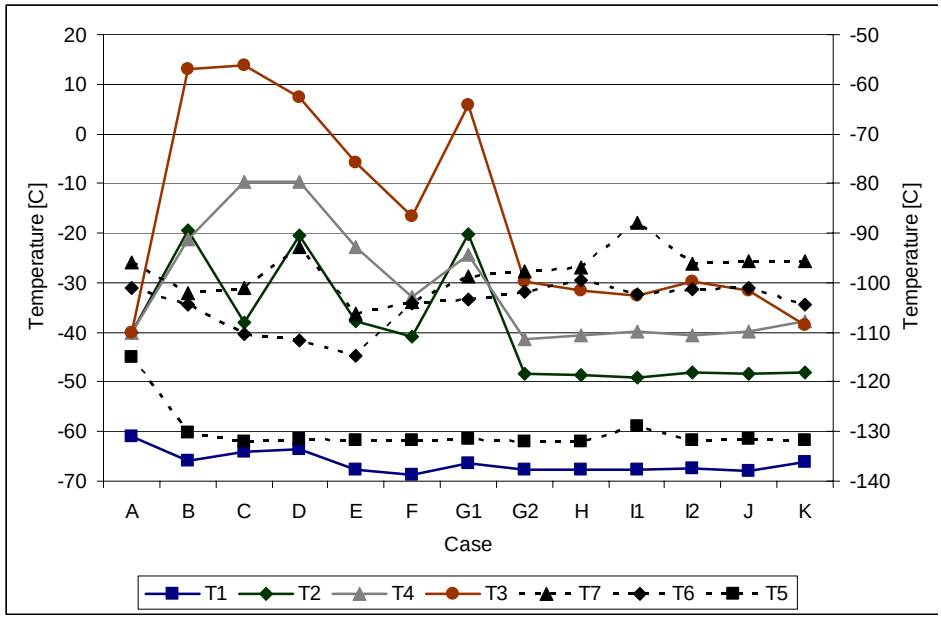

Figure 5.8: Temperature variables

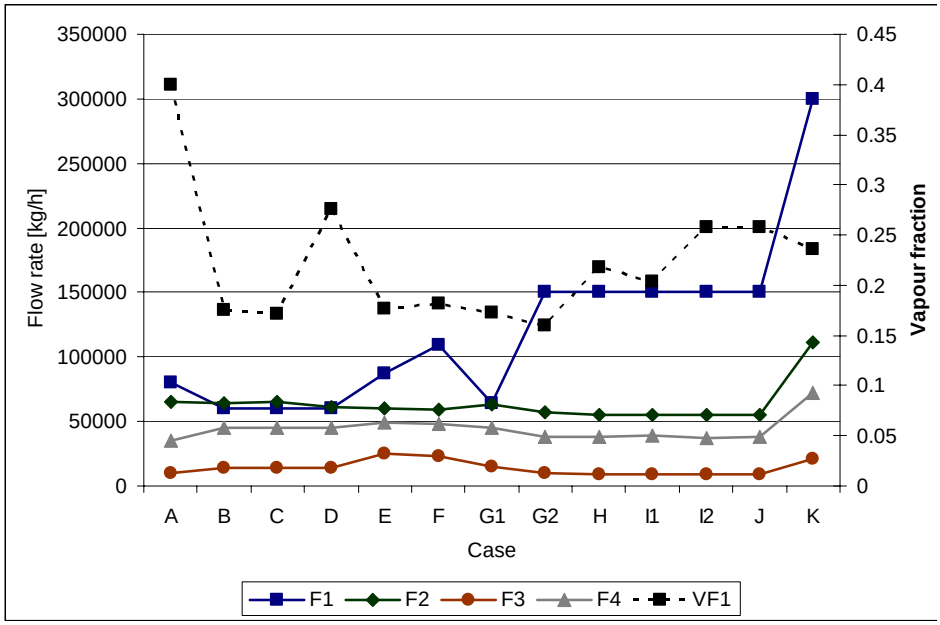

Figure 5.9: Flow rate variables

5.6 Discussion

Implementation and use of the model

The most difficult part of using the optimization-simulation tool is to select which variables to optimize, and to assign appropriate upper and lower bounds to them. The more variables that are included in the TS, the longer the computational time. Furthermore, with more variables it is less likely to end up in a good local minimum within the time constraint. It is possible to influence the search path of the meta heuristic to a certain degree by changing the global discretization coarseness for each variable that is a part of the TS. Too fine resolution will increase the calculation time, too coarse resolution may lead to infeasible solutions when changing the variable due to e.g. crossover in the heat exchangers. In the optimization-simulation cases there are 9 variables that are tuned both by the TS and by the local NMDS, and 9 variables that are tuned by the local NMDS only.

Since most of the computing time is used in the process calculations, it is extremely important to have a fast HYSYS model. Also, to avoid infeasible solutions that will return a very high number to the objective function, the model must be robust. Because we restrict the possible neighbours of a solution to be a change of no more than one of its variables either up or down, while all the other variables of the solution remain constant, a solution has twice as many neighbours as the number of variables that it consists of. Consequently, with 9 global variables it requires up to 18 HYSYS simulations per global search iteration (unless a local search is initiated). The current HYSYS model needs slightly more than half a second to run each simulation. Hence, each global search iteration requires about 10 seconds. Since there are 18 variables in the local search, the maximum number of local iterations is set to 150. This requires initially one HYSYS simulation per variable to generate the initial simplex for the local search, and then one for each iteration. Hence the total time for the local search is approximately 100 seconds. Assuming 400 global iterations 350 local iterations the total time required is roughly 10 hours.

In order to reduce the total computational time, or to increase the search space for the same available time, there are criteria for the initiation of local searches. A local search is only performed after an iteration of the global search if a promising region is detected, which requires the current objective value to be at least a certain percentage better than its neighbours. Furthermore, the current objective must be within a certain percentage from the best known objective. In order to escape regions that turn out not to be promising, the coarseness of the global search is increased after a predefined number of global iterations without any updates of the best known solution.

One particular challenge is that for some unknown reason the HYSYS application occupy more and more computer memory for each global or local iteration. Another problem experienced is that when the network is down, the HYSYS application cannot find the licence file and will terminate. For these reasons, as well as time constraints, the maximum simulation time is set to 12 hours.

By running the optimization-simulation tool for the 13 different cases it may seem like 9 variables are in the upper range of what the global search can handle, however it seems like even more variables can be optimized if adjusted in the local search only. Overall optimization of the transport chain including two processes connected by the intermediate storages and the gas carrier with 5 variables and adding 13 other individual process variables is a rather complex optimization problem. It is not possible to guarantee that the best solution is found, however, the tool did find good solutions for all 13 cases. Also it is seen that starting from the best known solutions with narrow domains and re-running the model does not improve the results with more than 0.05% which is not important for any practical reasons, and well within the uncertainties of the thermodynamic equations and investment costs, hence at least in this case, one run is sufficient.

Discussion of the optimization-simulation results

The first thing to notice is that the optimal transport pressure of LCO_2 (P1), is always close to its lower bound at 5.50 bar, hence this variable could be set to 5.50 bar and removed from the optimization. This will decrease the search space for the model. Furthermore, the pressure of NG-2 (P4) is always close to its upper bound of 100 bar and could also be removed. Both of these constraints are set due to process limitations (TP for CO_2 and maximum allowed pressure). The other variables do vary and should be kept as optimization variables.

It can also be seen that fixing the amount of CO_2 to be transported has a large impact on both the processes and the ship utilization. Furthermore, if the revenue for transporting LCO_2 is low, the total chain requires little CO_2. However, when the price is high, then it is optimal to ship more CO_2 offshore than the volume that corresponds to the carbon in the natural gas transported onshore. Surprisingly, the exergy efficiencies for the offshore process and the total chain also increase. This is due to the small difference in thermo-mechanical exergy in LCO_2 at 5.5 bar and high pressure CO_2 at 150 bar when temperature based exergy is transferred to pressure based exergy. Since more exergy is entering and exiting the offshore process, the exergy efficiency will increase, even if the process is not improved. It should also be noted that an increase in LCO_2 will decrease the need for LIN.

The required cold duty for producing LNG at 2 to 3 bar and upwards is lower than producing LNG at 1 bar, which is normally the case. Therefore one could be tempted to transport the LNG at higher pressures. However, the nitrogen cannot

be transported at too high pressures as the cargo tanks will be prohibitively expensive. If the temperature difference between the LIN and the LNG is too large, the efficiency of the offshore process will be reduced and more importantly the power requirements in the onshore process will be significantly increased leading to a decrease in the onshore process exergy efficiency. Therefore, if the transport pressure of LNG increases, then the transport pressure of nitrogen will also increase. This is probably also the reason why so many different solutions have objective values close to the best known objective value. The extra investment cost required to handle a higher pressures in the tanks is not included in the optimization; however this can be done by introducing binary variables in the optimization routine. It should also be mentioned that the density of LNG and LIN increases with lower pressures, enabling more LNG, LCO_2 and LIN to be transported for the same ship size.

By investigating the four process heat exchangers it can be seen that the MITA values will vary from case to case. Low driving forces in HX-102 in the onshore process is very important for the process efficiency, and the MITA varies between 0.6°C and 1.2°C, which is very low. The other heat exchangers have MITA values between 1.5°C and 3°C, which is normal for low temperature compact heat exchangers. It might therefore be necessary to introduce a penalty for HX-102 so that the lowest MITA is 1-2°C, alternatively a higher cost for this heat exchanger can be used. It is important to mention that the actual heat exchanger network is not designed. Even if all the streams in the heat exchangers are in liquid, gaseous or dens phase (there is no vaporization or condensation), the overall heat transfer value U may vary. The optimization-simulation tool can easily handle more advanced heat exchanger systems; however, this is not yet developed.

The change in price of electricity had a surprisingly small effect. The reason for this is twofold. First of all the compressors are expensive, hence it is important to reduce the power consumption also from an investment point of view. This will, of course lead to lower power requirements and higher exergy efficiencies. Second, the assumed price for electricity is high, 100 EUR/MWh and 150 EUR/MWh, so the efficiency will be very important even with a 50% reduction.

From the results it can be seen that the local variables (using the NMDS only) have been successfully optimized. The approach has been to set all the variables that connect the processes (P1, P2, P3, F1 and F2) to global variables. Also some important variables as the vapour fraction in N2-11 (VF1) and the intermediate pressures in the offshore process (P4, P5 and P6) are selected as global variables. However, the other individual process variables such as intermediate temperatures and pressures (T1-T7, F3 and F4) are successfully optimized using the local search only.

Further work

In this paper, several cases of the LEC were optimized and it is found that exogenous variables such as prices and transport distance will influence the variables connecting the processes as well as the individual process variables. It is therefore interesting to continue developing the methodology so that it can be used to simultaneously select the optimal sources of NG and CO_2 and design and optimize the processes, storages and gas carriers in the LEC.

5.7 Conclusions

A gradient free optimization-simulation model based on a Tabu Search (TS) and the Nelder-Mead Descent Search (NMDS) combined with the sequential modular process simulator HYSYS is successfully applied to optimize the Liquefied Energy Chain (LEC) consisting of two processes, two storages and a combined carrier. It has been shown that changes in the strategic decision variables will influence the transport pressures as well as the individual process variables and that the best solution cannot be obtained without simultaneous optimization-simulation.

Acknowledgements

The sponsors of the project are the Research Council of Norway , StatoilHydro and SINTEF Energy Research.

Bibliography

Aspelund, A., Barton, P., Gundersen, T., 2009a. Synthesis of heat exchanger networks with compression and expansion of the process streams. Manuscript in preparation.

Aspelund, A., Berstad, D. O., Gundersen, T., 2007. An extended pinch analysis and design procedure utilizing pressure based exergy for subambient cooling. Applied Thermal Engineering 27 (16), 2633–2649.

Aspelund, A., Gundersen, T., 2009a. A liquefied energy chain for transport and utilization of natural gas for power production with CO2 capture and storage - Part 1. Applied Energy 86 (6), 781–792.

Aspelund, A., Gundersen, T., 2009b. A liquefied energy chain for transport and utilization of natural gas for power production with CO2 capture and storage - Part 2: The offshore and the onshore processes. Applied Energy 86 (6), 793–804.

Aspelund, A., Gundersen, T., 2009c. A liquefied energy chain for transport and utilization of natural gas for power production with CO2 capture and storage - Part 4: sensitivity analysis of transport pressures and benchmarking with conventional technology for gas transport. Applied Energy 86 (6), 815–825.

Aspelund, A., Gundersen, T., Nowak, M., Myklebust, J., Tomasgard, A., 2009b. An optimization-simulation model of a for a simple LNG process. Article in Press, Computers & Chemical Engineering.

Aspelund, A., Tveit, S. P., Gundersen, T., 2009c. A liquefied energy chain for transport and utilization of natural gas for power production with CO2 capture and storage - Part 3: The combined carrier. Applied Energy 86 (6), 805–814.

Cavin, L., Fischer, U., Glover, F., Hungerbüler, K., 2004. Multi-objective process design in multi-purpose batch plants using a Tabu Search optimization algorithm. Computers & Chemical Engineering 28 (4), 459–478.

Chelouah, R., Siarry, P., 2005. A hybrid method combining continuous tabu search and Nelder-Mead simplex algorithms for the global optimization of multiminima functions. European Journal of Operational Research 161 (3), 636–654.

Exler, O., Antelo, L. T., Egea, J. A., Alonso, A. A., Banga, J. R., 2008. A tabu search-based algorithm for mixed-integer nonlinear problems and its application to integrated process and control system design. Computers & Chemical Engineering 32 (8), 1877–1891.

Hedar, A. R., Fukushima, M., 2006. Tabu search directed by direct search methods for nonlinear global optimization. European Journal of Operational Research 170 (2), 329–349.

Kotas, T., 1995. The Exergy Method of Thermal plant analysis. Krieger Publishing Company, Florida, USA.

Nelder, J. A., Mead, R., 1965. A simplex method for function minimization. The Computer Journal 7 (4), 308–313.

Paper V

J. Myklebust, A. Tomasgard and S. Westgaard:

Forecasting gas component prices with multivariate time series models

Submitted to an international journal

Forecasting gas component prices with multivariate time series models

Abstract:
Predicting gas component prices over different horizons is important for both energy producers and consumers. In this study we model and predict the joint dynamics of butanes, propane and naphtha traded in the north European market. Our approach is a multivariate time series with unobservable components. We apply monthly data over a 10 year period from 1995 to 2006 and test the predictive power of fitted models using various hold-out samples. The in-sample and out-of-sample results indicate that gas component prices follow stochastic processes with trend and autoregressive effects that continuously change over time, while the seasonal patterns seem to be stationary. The prediction results are compared to random walk for one-step and multi-step forecasts in each of the out-of-sample periods. The results are promising and indicate that our model can be used for short-/medium term forecasting of gas component prices.

6.1 Introduction and literature review

Energy producers and consumers regularly attempt to forecast the prices of oil, coal, gas, electricity and related products over various time horizons. Energy producers make these forecasts for risk management purposes (Value at Risk and Shortfall analysis) in the short term, production and transportation planning (what, where and when to produce) in the medium term as well as for investment analysis (type of technology/ships/plants etc. to invest/not to invest in) for the long term. Industrial consumers, such as petrochemical companies or electricity utilities, make these forecasts for the same reasons. Oil, coal and gas are important input factors so their prices affect production and investment decisions. Investors need price scenarios for different energy commodities as input for valuation of real assets (e.g. power plants) and financial assets (e.g. publicly listed and private energy companies). Further discussions of the role of forecasting in planning and strategy can be found in Makridakis (1996), Makridakis, Wheelwright, and Hyndman (1998), and Gooijer and Hyndman (2006). Discussion of the importance of modelling and forecasting the dynamics of energy prices for real investment analysis can be found in Dixit and Pindyck (1994), Pindyck (1999) and Pindyck (2001).

The academic literature covering time series modelling and the prediction of gas prices is very sparse in comparison to other energy markets such as oil and

electricity. Serletis and Gogas (1999) apply deterministic chaos models on a set of time series of natural gas liquids, crude oil and natural gas prices in the North American market. They find evidence of non-linear chaotic dynamics for all of the gas components.

Modjtahedi and Movassagh (2005) analyse US gas future prices. They find that spot and future prices are non-stationary and the observed trends are due to positive drifts in the random walk components of the prices rather than possible deterministic trends. Further, they find that market forecast errors are stationary and that there is some predictive power from the futures market with respect to future gas spot prices. Serletis and Shahmoradi (2005) analyse business cycles and natural gas prices in US. Their results indicate that natural gas prices are pro-cyclical and lag the cycle of industrial production. They also find that natural gas prices are positively contemporaneously correlated with consumer prices. However they focus less on forecasting. Ghouri (2006) forecasts international oil and gas prices using co-integration techniques. He finds oil and gas prices are non-stationary but have a long-run relationship (that might diverge in the short run). Forecasting from various co-integration equations indicate higher gas prices in the period 2005-2025. It is difficult to measure the quality of his forecast since this out-of-sample period is yet to come. Lee, List, and Strazicich (2006) analyse 11 non-renewable natural resource real prices from 1870 to 1990 (including gas prices). They find that natural resource prices vary around trends with structural breaks in both intercept and slope. Following their unit root tests, they examined forecasting models with breaks by employing both simulated and actual natural resource price data. Serletis (2007) discusses the dynamics of the gas market in a broader setting that also include other energy markets such as oil and electricity markets. He also analyses gas market volatility and the correlation with the electricity market.

Even though all the references mentioned above provide valuable insight, there is little knowledge of the full dynamics of gas component (wet gas, NGL) prices. It is also not clear whether gas component prices could be predicted or not. Several studies of dry gas prices exist. However, the end uses of gas components differ from the users of dry gas so their price processes are likely to be different. This research gap is the motivation for the modelling and predicting gas component prices in this paper. While dry gas is mainly used for heating, wet gas is also used for other purposes such as feedstock in the petrochemical industry. At the same time, supply and demand variables that affect dry gas also affect gas component prices in the area we analyse. Wet gas is a by-product from the processing of rich gas to dry gas. Most of the Norwegian dry gas production is exported in pipelines. Hence, disturbances in the pipeline capacity will affect the supply of the wet gas. Extreme cold weather conditions will affect their demand as they could be a marginal fuel for heating.

The time series literature offers a plethora of different models that can be applied for the prediction of gas prices, returns and volatility. Among these methods, state space models using the Kalman filter have had an impact (Harvey, 1989; Durbin and Koopman, 2001; Commandeur and Koopman, 2007). These methods have the flexibility to get stable estimates of non-stationary processes and have shown promising results in forecasting applications. However, the number of articles that include prediction with state space models is limited (Gooijer and Hyndman, 2006). Traditionally, energy prices have been modelled assuming fixed trends, seasonality, mean-reversion and possible cycles (when using long term data). We apply a framework of multivariate time series with unobservable components in place of the conventional deterministic trend model, thereby allowing for an unobservable underlying trend. The model has the flexibility to test whether the structures are deterministic or change over time. Initially all components are modelled as if they were stochastic, then the model results indicate which components are likely to be stationary. Similar studies modelling energy prices with stochastic components are Pindyck (1999), and Westgaard, Faria, and Fleten (2008). Pindyck (1999) analyses the long-run evolution of energy prices (oil, natural gas and coal) using structural models with a Kalman filter. In this study, the author finds mean reverting prices to a stochastic fluctuating trend analysing up to 127 years of yearly observations. Even though the results are mixed, the estimated model seems promising as a short- run forecasting tool for oil, gas and coal prices. Westgaard et al. (2008) have a narrower focus, analysing possible stochastic trends and seasonal patterns in three gas component prices from 1995-2006. The results from this study are that short term trends seem to fluctuate in a stochastic manner while the seasonality in the prices seems to be fixed. A random walk model with fixed seasonal variation is suggested. The forecasting results are as a consequence rather disappointing. Both these studies use univariate unobservable component models. Our extension from these articles is to estimate a set of energy prices as a system, accounting for cross-equation errors. We also add an autoregressive component to our analysis. We believe such models give a flexible structure that captures more of the joint dynamics in prices and improves the forecasting power of the models.

We ask the following questions in our analysis; what do our unique gas component data tell us about the stochastic dynamics of the joint price evolution, and how should it be modelled? What is the prediction power of the stochastic models in comparison to a naïve model (multivariate random walk)? What implications do the answers to these two questions have regarding production and investment decisions that are dependent on proper price forecasts? The paper is further organized as follows: In Section 6.2 we present the gas component value chain and the data we apply. In Section 6.3 we present the multivariate unobservable component model. Section 6.4 gives in-sample estimation results and

out-of-sample prediction tests. Finally, Section 6.5 discusses the implication of the results for natural gas producers and consumers and concludes the paper.

6.2 The gas component value chain and the data

In this article we analyse gas component prices of traded products from Kårstø in Norway. The gas components propane, (iso- and normal-) butanes and naphtha are by-products from oil refining as well as gas processing. Their chemical and physical properties are between dry gas and petrol. Gas components are heavier than dry gas, the main gas processing output, and lighter than petrol, the main refinery output. Depending on the composition of the crude oil, about 9% is dissolved gas. Gas components amount to a similar proportion of unprocessed ("rich") natural gas. Gas liquids must be separated from crude oil or unprocessed gas regardless of their value to ensure safe operation of the downstream infrastructure.

The unprocessed rich gas flows in pipelines from the offshore wells to process plants such as Kårstø and Kolsnes. At the processing plant, rich gas is separated into dry and wet gas. Dry gas is of growing importance as an energy resource. It is either compressed and sent in pipelines to market hubs in continental Europe and the UK, or refrigerated and shipped to the liquefied natural gas (LNG) market. The most important by-product of dry gas production is wet gas. Wet gas is liquefied to natural gas liquids (NGL), which can be fractioned into gas components. Gas components are exported by ship. Unlike dry gas, European gas components are not traded on an exchange but sold directly from gas processing plants to individual industrial users.

The main uses of gas components are octane enhancing additives for petrol, feedstock for petrochemical plants, enhancing oil recovery in oil wells, and less quality sensitive uses such as heating. There are many alternatives for heating; you can warm up your kettle with either with electricity or gas. However, the substitutes for gas components for use as petrochemical feed stocks must be synthesized, which is more costly than separation from crude oil or unprocessed gas. Petrochemical feedstock must be of higher purity than components intended for energy. Higher purity comes at the cost of more recycling in the separation tower. Because vapour pressure falls with temperature, lighter components can be added to the petrol in the cold season. Demand for the heaviest can be expected to increase during the summer because people drive more. Demand for the lightest gas component, propane, can be expected to follow a similar seasonal pattern as the heating demand. In rural areas where pipeline delivery of energy is uneconomical, propane can be the preferred alternative because it has high enough volumetric energy density to be distributed in bottles.

The production of NGL will inevitably increase as it is a by-product from natural gas production that gradually increases its share of world energy demand. In this paper we focus not on the NGL blend but NGL fractionated into propane, iso- and normal butanes and naphtha that are marketed individually. In 2007 the worldwide production of NGL was around 8050 thousand barrels per day (b/d), up from 6100 thousand b/d in 2002, which represents a growth of 32% in five years. The United States remained the largest producer of NGLs, followed by Saudi Arabia, Canada, Russia and Mexico in 2007. Nevertheless, from 2002 to 2007 the production of NGL in Saudi Arabia more than doubled, from 630 to 1430 thousand b/d, while in the same period the production in the United States decreased from 1900 to 1750 thousand b/d, and stayed almost constant in Canada and Mexico, at 690 and 410 thousand b/d, respectively. Another relevant increase in NGL production could be observed in Russian and Algeria, which changed their production from 240 to 420 and from 190 to 340 thousand b/d, respectively.

The first step of gas processing is phase separation where solids and liquids are removed. Then acids such as H_2S and CO_2 are removed in a process called sweetening. Finally dry gas is separated from wet gas in an extraction plant, a process called NGL recovery. Because the boiling temperatures of the NGL components are different, they can be separated by cryogenic distillation. The inlet rich gas is typically refrigerated to between minus 100°C and minus 90°C which ensures that there are both vapour and liquid phases. Then it is fed into a vertical separation tower called a demethanizer (Mokhatab, Poe, and Speight, 2006). The gaseous product that comes out at the top consists mainly of methane, called dry gas. The liquid product that comes out at the bottom is a mixture of different NGLs. The NGL mixture can either be sold as it is, or fed into a sequence of separation towers so it can be sold as individual commodities. Inside each tower a series of evaporation and condensation ensures that the *vapour* gets a higher and higher concentration of the *lightest* (driest) component as it rises to the top of the tower where it is collected as the top product. Consequently, the *liquid* gets a higher and higher concentration of *heavier* components as it flows to the bottom. The top product is then liquefied. The bottom product can be pumped to a successive column for further fractioning or sold as it is. If the bottom product is fed a successive column then the driest of the remaining components is separated from the blend in a similar process (Fig. 6.1). Whether fractionation is preferred or not depends on the difference between the cost of fractionation and the spread between the value of the NGL mixture and the sum of the values of the individual components. Like other by-products, the difficulty of attributing production costs results in inelastic supply, which could explain price spikes. The option not to fractionate NGL acts as a floor for individual component prices. Furthermore, because the marginal cost of production is hard

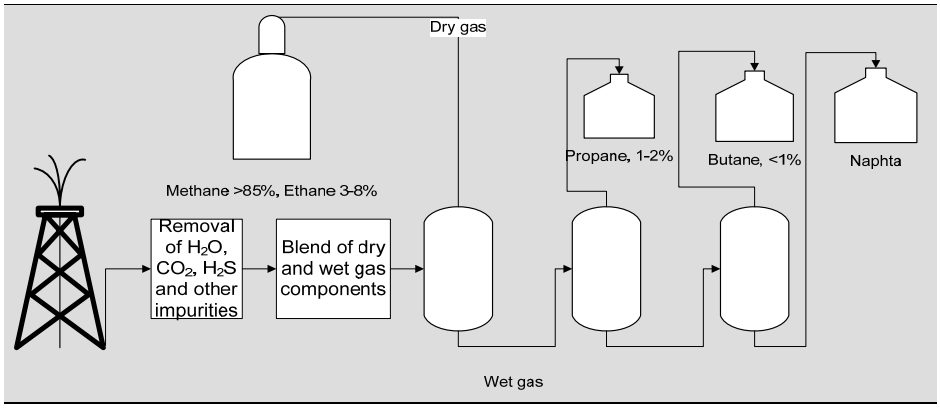

Figure 6.1: Illustration of the processing of gas components

to define, it is difficult to theoretically justify that prices should revert to a mean in the long run. Gas component prices are more likely to depend on their marginal revenue product in the industries where they are input, which vary with the available volume and technological progress.

The NGL and condensate (light oil) are exported by special carriers from Kårstø, where they receive 600-700 calls from such ships every year. The gas value chain is also shown in Fig. 6.2. For more information regarding processing, transportation, and markets/sales of these products in north-western Europe, (Gassco Homepage, 2009).

Our data consist of free on-board monthly average prices (USD per tonne) from January 1995 to December 2006, altogether 143 observations for each of the three price series. In Fig. 6.3 we show the development of indexed gas component prices and indexed NBP dry gas spot price (index = 1 1996(8)). We do not have prices before this date. In 1996 the dry gas markets in the UK and parts of Europe were exposed to competition combined with an over-supplied market, causing a downward trend in the prices 1997-1999. In 2000 the oil prices increased which led to a significant rise in dry gas prices that year. In the period 2001-2002 the global recession implied a falling trend in dry gas prices (though with sharp spikes and reversion from spikes). In the global economic boom 2003-2006, we again saw an increasing trend in prices following oil prices and general demand for energy commodities. An extreme price spike is seen around 2006, particular for dry gas. In late 2005, dry gas prices at the NBP rose to 160 p/therm as a result of colder than normal weather. In addition, imports of gas through the UK-Continent Interconnector were less than forecasted, producers had technical difficulties and LNG that was expected to be landed at Isle of Grain terminal

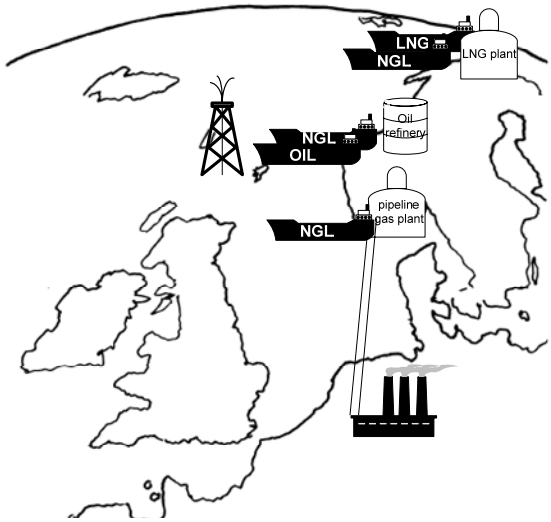

Figure 6.2: The gas component value chain

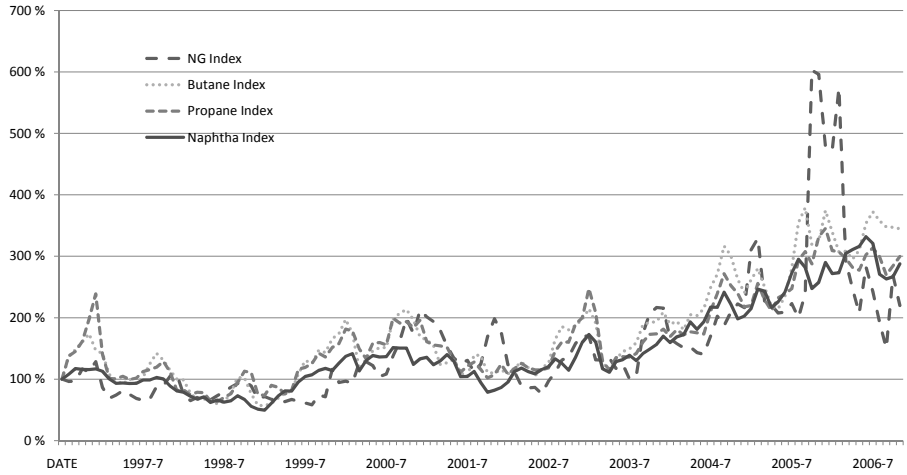

Figure 6.3: Indexed prices 1996(8)-2006(12) for butane, propane, naphtha and natural gas spot NBP

did not arrive (Wright, 2006). We also detect a seasonal pattern in all gas prices with generally higher prices in the winter season compared to the summer season. This is particular prevalent in natural gas prices, but also to some extent in the prices of butane and propane that can be used for heating. Naphtha prices have a less apparent seasonal pattern because its main use is as a fuel additive. We also detect that sharp price peaks follow a rather quick downward adjustment for all series due to the particular supply/demand conditions for gas markets. Whether prices are mean reverting in the long term or not is not easily seen from the graphs. The data simply cover periods which are too short to make such judgements.

Figure 6.3, Tables 6.1, 6.2 and 6.3 cover graphs and descriptive statistics of the three series for prices, logarithm of prices, absolute price changes and returns (changes in logarithm of price). According to ADF test, prices are still non-stationary after taking the log transform. However, both absolute and relative changes (returns) are stationary. When a larger part of the estimated parameters (such as trend, level or season) are non-stationary or random, forecasting will be more challenging. One of the nice features with unobservable component models is that it lets us model series (such as the logarithm of price levels) that consist of non-stationary parameters directly, and not transform the data (such as from levels to returns) like in applications of ARIMA-, VAR-, GARCH and similar types of time series models. Analysing returns, we find that monthly returns

	N.Obs	Mean	Median	Min.	Max.	Std.Dev.	Skew.	Kurt.	JB
Butane									
P_t	144	248.25	210.49	86.25	574.57	126.10	0.62	-0.54	10.97
ΔP_t	143	2.57	2.66	-97.00	113.32	31.89	-0.07	1.49	13.28
$\ln P_t$	144	5.40	5.35	4.46	6.35	0.48	0.24	-0.74	4.72
$\Delta \ln P_t$	143	0.01	0.01	-0.41	0.32	0.13	-0.36	0.82	7.17
Propane									
P_t	144	286.85	255.12	114.83	623.29	123.75	0.61	-0.63	11.20
ΔP_t	143	1.96	2.47 -	177.03	85.34	38.66	-0.92	3.83	107.51
$\ln P_t$	144	5.57	5.54	4.74	6.44	0.42	0.19	-0.75	4.25
$\Delta \ln P_t$	143	0.01	0.01	-0.53	0.35	0.14	-0.76	2.25	43.94
Naphtha									
P_t	144	270.89	225.18	95.70	641.98	133.10	0.75	-0.60	15.81
ΔP_t	143	2.76	5.17	-96.97	62.24	25.89	-0.09	1.30	10.30
$\ln P_t$	144	5.50	5.42	4.56	6.46	0.45	0.42	-0.55	6.05
$\Delta \ln P_t$	143	0.01	0.02	-0.32	0.20	0.09	-0.63	0.66	12.19

Table 6.1: Descriptive statistics of butane, propane and naphtha prices, price differences, logarithms of prices and price returns individually and static.

vary between -53% to +35% for butane. Similar figures indicate -41% to +32% for propane and -32% to 20% for naphtha respectively. This gives a picture of the price risk involved, which is much higher than figures seen for the financial market. The monthly (yearly) volatilities for butane, propane and naphtha are 14% (49%), 13% (35%) and 9% (31%) respectively. Normal distribution of returns is rejected for all components. Unlike most other energy prices, negative returns are less frequent but larger than positive, which results in negative skewness. There is significant autocorrelation present in all the series and gives an indication of autoregressive effects and seasonal serial-correlation in the return data. Note that both significant negative and positive correlations are observed. Independence of returns over time is clearly rejected. There is also a rather high correlation in returns for the series, in particular between butane and naphtha. The correlation figures for the logarithm of price changes are shown in the upper right panel of Table 6.1.

Price level (P_t), absolute returns (ΔP_t), logarithm of prices ($\ln P_t$), and returns of logarithms of prices ($\Delta \ln P_t$), which can be interpreted as percentage returns, are summarized in Table 6.1. For each of these time series for each gas component, the number of observations, Mean, Median, Min, Max, Standard-deviation, Skewness and Kurtosis for are shown. We also include autocorrelation coefficients

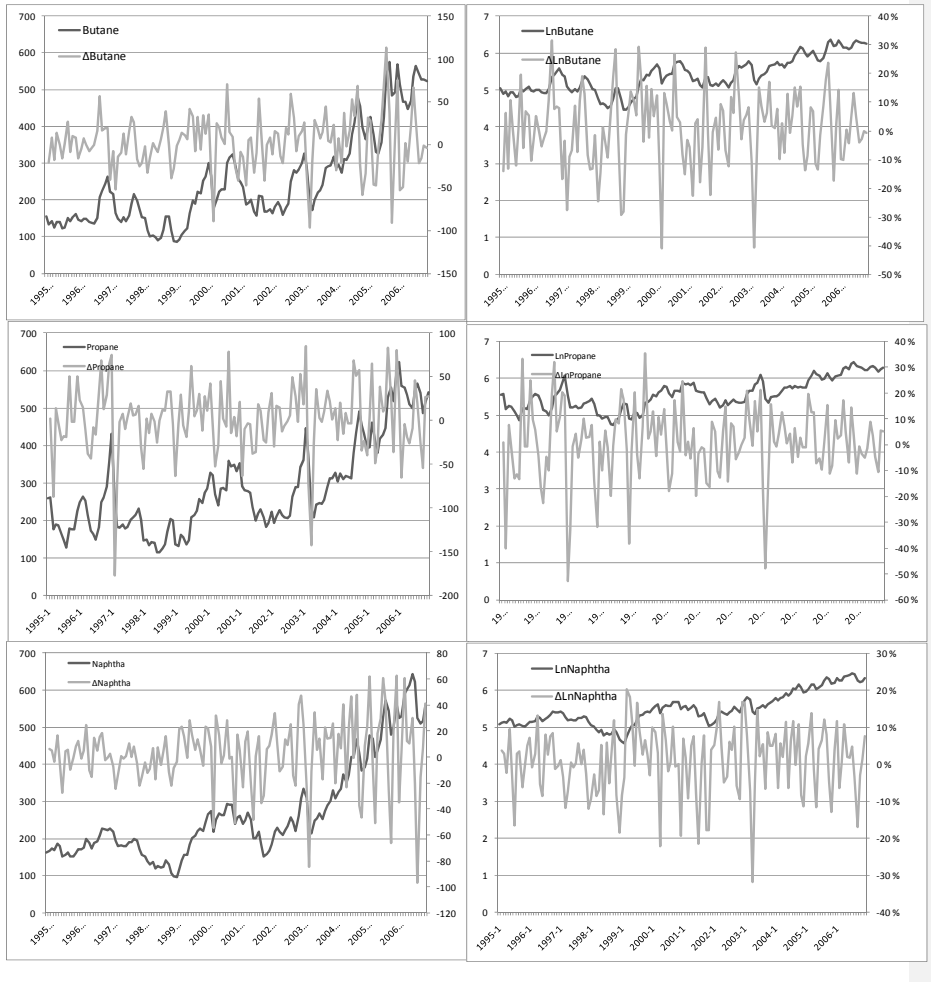

Figure 6.4: The three left panels show absolute prices and returns for butane, propane and naphtha respectively. Prices are USD/tonne free on board. The three right panels show the logarithm of prices and percentage returns of the same products

	$\Delta \ln P_{But}$	$\Delta \ln P_{Pro}$	$\Delta \ln P_{Nap}$	Period
$\Delta \ln P_{But}$		0,60	0,67	1995(2) - 2006(12)
$\Delta \ln P_{Pro}$			0,52	
$\Delta \ln P_{But}$		0,53	0,69	1995(2) - 2000(12)
$\Delta \ln P_{Pro}$			0,41	
$\Delta \ln P_{But}$		0,83	0,73	2001(12) - 2006(12)
$\Delta \ln P_{Pro}$			0,70	

Table 6.2: Butane, propane and naphtha percentage return cross correlations for total sample, first half and final half respectively.

ACF for lag 1, 2, 3,..., 12, 24, 36, 48. Significant autocorrelation at 5% level are found when the given figure is above |1.96/143| or |0.164|. The Q(12) is the Ljung Box statistics with 12 degrees of freedom. The critical value at 5% for rejecting zero autocorrelation from lag 1 up to 12 is 21.026. ADF is the augmented Dickey Fuller test with a constant and no trend including two augmented lags. Critical value for stationarity at 5% level is -2.86. Finally correlation matrices between the gas components are show for each variable in the upper right panel using logarithm of price changes.

6.3 Time series with unobservable components and the Kalman filter

Time series with unobservable components are formulated directly in terms of features such as trends, cycles, seasonality, and sensitivities to explanatory variables. Such regressors have a natural interpretation and represent the main features of the series under investigation. As in classical regression models the explanatory variables vary over time. However, in the state space model the coefficients are also allowed to vary over time. The Kalman filter method is applied for the estimation of the non-observed components involved in the stochastic process, which correspond to the state variables, or the state vector. In short, the Kalman filter is an efficient computational (recursive) algorithm used to update a *state vector*, in a way that minimizes the mean squared prediction error. The power of the Kalman filter algorithm is that it operates online. This implies that to compute the best estimate of the state and its uncertainty we can update the previous estimates by the new measurement, and this does not require all previous data to be kept in memory and reprocessed every time the new measurement is taken. This fact is of vital importance for the practicality of filter implementation. Time series with unobservable components are also suitable for forecasting future values

	Lag 1	Lag 2	Lag 3	Lag 4	Lag 5	Lag 6	Lag 7	Lag 8	Lag 9	Lag 10	Lag 11	Lag 12	ADF
Butane													
P_t	0.95	0.88	0.83	0.78	0.73	0.69	0.66	0.65	0.64	0.65	0.62	0.58	-0.30
ΔP_t	0.25	-0.21	-0.10	-0.05	-0.13	-0.11	-0.11	-0.26	-0.04	0.25	0.26	0.18	-3.15
$\ln P_t$	0.95	0.88	0.81	0.76	0.70	0.66	0.63	0.62	0.62	0.61	0.59	0.55	-1.07
$\Delta \ln P_t$	0.26	-0.12	-0.08	-0.06	-0.17	-0.16	-0.16	-0.17	0.03	0.19	0.18	0.22	-3.14
Propane													
P_t	0.94	0.86	0.81	0.76	0.70	0.66	0.64	0.62	0.61	0.60	0.57	0.51	-0.52
ΔP_t	0.14	-0.22	-0.03	0.00	-0.15	-0.17	-0.05	-0.10	0.02	0.14	0.20	0.05	-3.13
$\ln P_t$	0.93	0.85	0.78	0.72	0.66	0.61	0.60	0.59	0.59	0.58	0.56	0.50	-1.05
$\Delta \ln P_t$	0.18	-0.20	-0.03	0.00	-0.15	-0.28	-0.07	-0.04	0.03	0.14	0.26	0.10	-2.91
Naphtha													
P_t	0.96	0.92	0.90	0.88	0.84	0.80	0.76	0.72	0.69	0.67	0.63	0.59	-0.65
ΔP_t	0.14	-0.32	-0.15	-0.02	0.09	0.10	0.02	-0.18	-0.09	0.28	0.22	-0.05	-2.76
$\ln P_t$	0.97	0.93	0.89	0.87	0.83	0.79	0.75	0.71	0.68	0.65	0.61	0.56	-1.21
$\Delta \ln P_t$	0.17	-0.23	-0.08	0.00	0.06	0.06	-0.01	-0.10	-0.09	0.22	0.20	-0.02	-3.11

Table 6.3: Autocorrelations of absolute price levels, absolute returns, logarithms of prices and percentage returns for butane, propane and naphtha respectively.

using parameters from the end state estimation. The Kalman filter has been the subject of extensive research and applications, (Harvey, 1989; Durbin and Koopman, 2001). A nice starting reference and introduction is given by Commandeur and Koopman (2007). Reference books describing the various applications in economics and finance using time series with unobservable components / state space models can be found in Harvey, Koopman, and Shephard (2005), Harvey and Proietti (2005), and Shephard (2005). Implementation of unobservable component models in this study is performed using STAMP8.0™which is a module of Oxmetrics5.0™(Commandeur and Koopman, 2007).

A multivariate model with trend, seasonality, and first order autoregressive effects

The system of Equations (6.1)-(6.5) is recursively updated for each successive monthly observation t.

$$\ln \mathbf{P}_t = \boldsymbol{\mu}_t + \boldsymbol{\gamma}_t + \boldsymbol{\psi}_t + \boldsymbol{\epsilon}_t \qquad \boldsymbol{\epsilon}_t \sim NID(0, \Sigma_\epsilon) \tag{6.1}$$

$$\boldsymbol{\mu}_t = \boldsymbol{\mu}_{t-1} + \boldsymbol{\beta}_t + \boldsymbol{\eta}_t \qquad \boldsymbol{\eta}_t \sim NID(0, \Sigma_\eta) \tag{6.2}$$

$$\boldsymbol{\beta}_t = \boldsymbol{\beta}_{t-1} + \boldsymbol{\upsilon}_t \qquad \boldsymbol{\upsilon}_t \sim NID(0, \Sigma_\upsilon) \tag{6.3}$$

$$\boldsymbol{\psi}_t = \boldsymbol{\Phi}\boldsymbol{\psi}_{t-1} + \boldsymbol{\kappa}_t \qquad \boldsymbol{\kappa}_t \sim NID(0, \Sigma_\kappa) \tag{6.4}$$

$$\boldsymbol{\gamma}_{1,t+1} = -\boldsymbol{\gamma}_{1,t} - \cdots - \boldsymbol{\gamma}_{11,t} + \boldsymbol{\omega}_t \qquad \boldsymbol{\omega}_t \sim NID(0, \Sigma_\omega) \tag{6.5}$$

$$\boldsymbol{\gamma}_{2,t+1} = \boldsymbol{\gamma}_{1,t} \tag{6.6}$$

$$\boldsymbol{\gamma}_{3,t+1} = \boldsymbol{\gamma}_{2,t} \tag{6.7}$$

$$\boldsymbol{\gamma}_{4,t+1} = \boldsymbol{\gamma}_{3,t} \tag{6.8}$$

$$\boldsymbol{\gamma}_{5,t+1} = \boldsymbol{\gamma}_{4,t} \tag{6.9}$$

$$\boldsymbol{\gamma}_{6,t+1} = \boldsymbol{\gamma}_{5,t} \tag{6.10}$$

$$\boldsymbol{\gamma}_{7,t+1} = \boldsymbol{\gamma}_{6,t} \tag{6.11}$$

$$\boldsymbol{\gamma}_{8,t+1} = \boldsymbol{\gamma}_{7,t} \tag{6.12}$$

$$\boldsymbol{\gamma}_{9,t+1} = \boldsymbol{\gamma}_{8,t} \tag{6.13}$$

$$\boldsymbol{\gamma}_{10,t+1} = \boldsymbol{\gamma}_{9,t} \tag{6.14}$$

$$\boldsymbol{\gamma}_{11,t+1} = \boldsymbol{\gamma}_{10,t} \tag{6.15}$$

where $\ln \mathbf{P}_t$ refers to a vector of logarithms of prices for butane, propane, and naphtha observed in month t. All other factors and covariances are estimated. $NID(0, \Sigma)$ means normally independently distributed with 0 mean and Σ cross section covariance. In Eq. (6.1) the dependent variable $\ln \mathbf{P}_t$ is the sum of the

level factor $\boldsymbol{\mu}_t$, auto regression (cycle) factor $\boldsymbol{\psi}_t$, the seasonal factor $\boldsymbol{\gamma}_t$, which are called structural factors. $\boldsymbol{\epsilon}_t$ is a random disturbance. The structural factors are defined in Eq.(6.2), (6.4), and (6.5) respectively. If the variance of a factor disturbance is low relative to the overall variance, then the feature that this factor represents is likely to be stationary. The trend $\boldsymbol{\beta}_t$, (month on month change in the level $\boldsymbol{\mu}_t$), might be time-varying due to changing economic conditions such as technological changes, population growth, and greater supply of alternative energy sources. In such instances it is therefore important to allow for a stochastic trend, i.e. not restricting the disturbance $\boldsymbol{\upsilon}_t$ in Eq. (6.3) to be zero. However, if a factor is reasonable to assume is stationary then it can be restricted as such, which would save degrees of freedom corresponding to the number of parameters that otherwise would be estimated.

Sharp changes in gas price are observed during short periods for temporary events, such as weather conditions, technological interruptions or political tensions. These price rises tend to revert to "normal levels" over a longer period. This might be viewed as unsurprising; if demand is constant or slightly increasing over time and supply adjusts to this pattern, prices should stay roughly the same on average. The resulting properties of commodity prices are a consequence of the general behaviour of mean-reversion. The magnitude of mean reversion might change over time. We have therefore allowed for a time-varying mean reversion. We have specified the model to allow a first-order autoregressive effect ψ_t (a "short cycle"). In such a specification we also allow for negative autoregressive effects. STAMP will by default restrict the AR effect to be stationary, i.e. $|\psi_t| < 1$. We also specified the model to allow time varying seasonality. Seasonal fluctuations account for a major part of the variation in energy prices. In general it can be viewed as the systematic, although not necessarily regular. Intra-year movements can for example be caused by changes in the weather and other exogenous phenomena that follow an annual pattern. Whenever a time series consists of hourly, daily, monthly, or quarterly observations with respective periodicity of 24 (hours), 7 (days), 12 (months), or 4 (quarters), one should always be alert for possible seasonal effects in the series. In our case we have monthly data with a periodicity of 12. Since the NGLs, like dry gas, can be used for heating, we would expect their prices to be generally higher during the winter than during the summer. However, the NGLs have larger shares of non-heating uses than dry gas so their prices are likely to show a less pronounced seasonal price variation. Nevertheless, NGL supply is influenced by the seasonal variation of the natural gas extraction, and should show a similar pattern. We would expect naphtha to have less distinct seasonal demand variation than propane and butane since it is mainly used as a fuel alternative. As NGL also can be used for cooling, it might be worthwhile to allow for a stochastic specification of the seasonal component.

Air conditioning is more used in the summer on the European continent than before, and this could change the seasonal pattern of prices.

In a state space framework, the seasonal effect is modelled by adding a season contingent component $\gamma_{i,t}$ to the model (see Eq. 6.1 and 6.5). In contrast with the level and slope components, where each component requires one state equation, the s seasonal effects are linearly dependent and generally require $(s-1)$ state equations. However, only one of the seasonal equations is modelled with a disturbance. The disturbance ω_t (in Eq. 6.5) allows the seasonal pattern to change over time. If the variance of this disturbance is large relative to the overall variation, then it indicates that the seasonal pattern changes over time. Otherwise the seasonal pattern can be considered to be deterministic. The sequence of calendar months is obviously deterministic so no disturbances are added to those identities.

The identities that model the seasonal pattern can be interpreted as follows. The effect of the season in state t if the corresponding observation happens to be of calendar month i is denoted $\gamma_{i,t}$. The calendar month i of the next monthly observation (state $t+1$) equals the calendar month that succeeds the calendar month of the current observation (state t). The seasonal effects sum to zero so they are linearly dependent. Hence, the December effect is not directly modelled but is the negative of the sum of all other monthly effects. The first equation says that when the calendar month of observation t is December, then the calendar month of observation $t+1$ is January. The second equation says that when the calendar month of observation t is January, then the calendar month of observation $t+1$ is February, and so on.

Further we assume that the irregular ω_t, the level disturbance η_t, the slope disturbance ς_t, the autoregressive disturbance κ_t, and the seasonal disturbance ψ_t are all mutually uncorrelated.

The covariance-matrices Σ_ω, Σ_η, Σ_ς, Σ_κ, Σ_ψ are for the component-disturbances irregular, trend, level, slope, AR(1) and seasonal. The multivariate unobservable component model (1)-(5) allows for links across the different price series through correlations of their disturbances. At a cost of losing degrees of freedom we allow for a full rank of the disturbance matrices. For example, we observed positive correlation between the autoregressive disturbances of the logarithm of butane and propane prices of 0.62 and a similar correlation between butane and naphtha of 0.93.

To sum up, we have a multivariate system allowing for time-varying trend, seasonal, and autoregressive effects. Contemporaneous correlations can either be restricted, or degrees of freedom can be spent estimating them. The unrestricted alternative is analogous to the seemingly unrelated regression equation model (named after Harvey (1989)), or a system of seemingly unrelated time series equations (SUTSE) model. The link among the series through their off-diagonal

elements of the disturbance covariance matrix, will give (hopefully better) forecasts than modelling each of these series in a univariate fashion (as done in Westgaard et al. (2008)). Details of the estimation of such systems are given by Harvey (1989). Estimation is performed with STAMP8.0™(Doornik, Harvey, Koopman, and Shephard, 2007).

6.4 Results

Research strategy

The percentage growth rate of prices is usually more stable than absolute price changes, and the impact of the season and other exogenous events on the price level is more likely to be multiplicative rather than additive. The statistical software requires a linear relationship. A conversion from multiplicative to a linear relationship is achieved by a logarithmic transformation of the equations, called a log-linear model. Furthermore, the coefficients of a log-linear model can be interpreted as elasticities. Hence, we modelled the logarithm of prices. This turned out to fit better than the prices directly and resulted in more stable error variances. Despite that this transformation was not sufficient for stationarity, we still use the data directly. This is possible because we use an unobservable component model and estimate it by the Kalman filter (Harvey, 1989).

In order to test the predictive power of the model in various hold-out samples, we split the data for estimation and test as specified in Table 6.4.

We first estimate the multivariate unobservable model for our in-sample period. Parallel with this estimation, we estimate a random walk model for each price series. Then we perform both one-step predictions and multi-step predictions for both models.

In one-step prediction the model parameters are updated for each subsequent month. Consequently, the whole out-of-sample period from 1995(1) to 2006(12) can be done in the same operation. In the multi-step prediction we estimate the model to the end of the in-sample period (e.g. 1995(1)-2000(12)). Then we make the forecast for the all the 12 months of each out-of-sample period (e.g. 2001(1), 2001(2), ..., 2001(12)) without updating the parameters. That is, possible arrival of new information is not taken into account in a multi-step forecast.

In-sample results

For all in-sample periods, the selected models imply a smooth stochastic trend (that is the deterministic level and stochastic slope), deterministic seasonal pattern, and a stochastic autoregressive component.

In-sample	Observations	Out-of-sample	Observations
1995(1)-2000(12)	72	2001(1)-2001(12)	12
1995(1)-2001(12)	84	2002(1)-2002(12)	12
1995(1)-2002(12)	96	2003(1)-2003(12)	12
1995(1)-2003(12)	108	2004(1)-2004(12)	12
1995(1)-2004(12)	120	2005(1)-2005(12)	12
1995(1)-2005(12)	132	2006(1)-2006(12)	12

Table 6.4: Split of in-sample periods and out-of-sample periods (prediction test periods) for our models. The multivariate unobservable model is compare to random walks for each period. Both one-step and multi-step forecasts are performed

Table 6.5 reports the results of the specification test for the estimated models in the six in-sample periods. The table shows residuals tests of auto-correlation (r and Q, tests), hetero-scedastisity (H test) and the Jarque-Bera test of normality (JB). T is the number of observations in the in-sample period and p is the number of hyper-parameters (disturbances) in the model.

The individual autocorrelation at lag 1 ($r(1)$) and lag 24 ($r(24)$) are also shown in Table 6.5. If residuals are randomly distributed they should (at 95% confidence level) fall outside $\pm 2/\sqrt{n}$. In our case with n = 72, 84, 96, 108, 120, and 132, the ranges are ± 0.24, 0.22, 0.20, 0.19, 0.18, 0.17 respectively. There is some evidence of remaining positive first order autocorrelation for the series in the in-sample periods. Long run autocorrelations (lag 24) do not seem to be significant. The $Q(24, 19)$ is the Ljung Box statistics with 24 lags and 19 degrees of freedom. 19 degrees of freedom refers to the $T - p + 1$ where p is the number of parameters, in our case we have 24+5-1=19. The critical value at 5% for rejecting zero autocorrelation from lag 1 up to 24 with 19 degrees of freedom is 30.14. The figures above give indications that we have not been able to remove all the problems with serial-correlation. The H statistics tests whether the variances of two consecutive and equal parts of the residuals are equal to each other. In the present case, the test shows that the residual-variance of the first 20, 24, 27, 31, 35, 39 observations in our samples are unequal to the last 20, 24, 27, 31, 35, and 39 observations respectively. The critical values at 5% are

1995(1) - 2000(12)	$\ln P_{But}$	$\ln P_{Pro}$	$\ln P_{Nap}$	1995(1) - 2001(12)	$\ln P_{But}$	$\ln P_{Pro}$	$\ln P_{Nap}$
T	72	72	72	T	84	84	84
p	5	5	5	p	5	5	5
JB	2.77	8.17	8.69	JB	2.90	8.32	5.41
H(20)	2.95	0.76	1.35	H(24)	1.65	0.48	2.27
r(1)	0.15	0.26	0.15	r(1)	0.17	0.26	0.15
r(24)	0.04	-0.02	0.04	r(24)	-0.06	-0.06	-0.04
Q(24.19)	19.54	37.90	20.43	Q(24.19)	20.02	39.82	31.02
1995(1) - 2002(12)	$\ln P_{But}$	$\ln P_{Pro}$	$\ln P_{Nap}$	1995(1) - 2003(12)	$\ln P_{But}$	$\ln P_{Pro}$	$\ln P_{Nap}$
T	96	96	96	T	108	108	108
p	5	5	5	p	5	5	5
JB	2.51	11.29	2.97	JB	3.70	11.13	6.57
H(27)	1.25	0.33	2.51	H(31)	2.11	0.61	3.51
r(1)	0.22	0.22	0.18	r(1)	0.30	0.22	0.26
r(24)	-0.07	-0.07	-0.10	r(24)	-0.08	-0.11	-0.12
Q(24.19)	22.54	45.14	32.38	Q(24.19)	30.69	41.39	38.36
1995(1) - 2004(12)	$\ln P_{But}$	$\ln P_{Pro}$	$\ln P_{Nap}$	1995(1) - 2005(12)	$\ln P_{But}$	$\ln P_{Pro}$	$\ln P_{Nap}$
T	120	120	120	T	132	132	132
p	5	5	5	p	5	5	5
JB	4.88	14.45	7.43	JB	3.28	16.48	7.09
H(35)	1.37	0.51	2.33	H(39)	1.05	0.46	1.51
r(1)	0.26	0.21	0.26	r(1)	0.26	0.21	0.26
r(24)	-0.08	-0.11	-0.14	r(24)	-0.08	-0.09	-0.15
Q(24.19)	31.01	43.18	48.22	Q(24.19)	36.62	45.41	61.15

Table 6.5: Summary statistics In-Sample

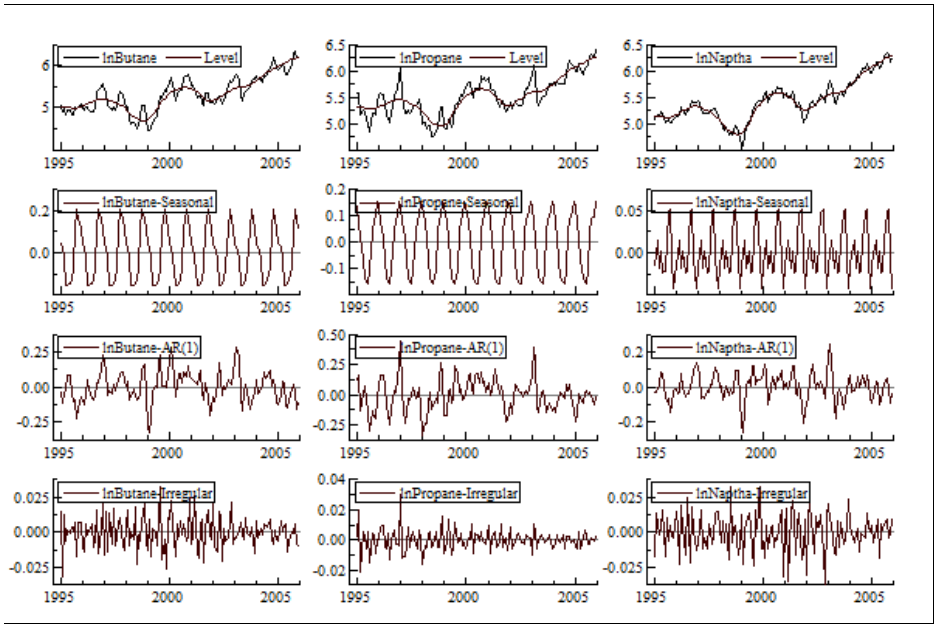

Figure 6.5: Shows the graphical results of the multivariate unobservable component model given in Section 3 for the natural logarithm of butane, propane and naphtha. The trend (level plus slope), seasonal, autoregression, and irregular are shown for the in-sample period 1995(1)-2005(12).

given by $F(20, 20, 0.025) = 2.46$, $F(24, 24, 0.025) = 2.27$, $F(27, 27, 0.025) = 2.16$, $F(31, 31, 0.025) = 2.05$, $F(35, 35, 0.025) = 1.96$, and $F(39, 39, 0.025) = 1.89$. Some remaining heteroscedasticity seems to be present, in particular for the shorter in-sample periods. Finally, we test for normality using the JB test. Normality is rejected at 5% level at a critical value of $Q(2, 0.05) = 5.99$. We cannot reject residuals being normal for butane prices, while normality is rejected for prices of propane and naphtha for most periods.

Figure 6.5 shows the time-varying values of the components (trend, seasonal, autoregressive effects, and the irregular) over the various in-sample periods for all price series. Keep in mind that these results are conditional upon the multivariate setting of the model; that is we take into account that the fact that the components disturbances are correlated across different price series.

From Fig. 6.5 we see the smooth stochastic trend of gas component prices. The seasonal pattern is deterministic and the magnitude is highest for butane. Propane has also a significant seasonal pattern, but it is less prominent for naphtha. This is in line with our earlier discussion. Naphtha is mainly used as a fuel additive, while butane and propane can be used as alternatives to heating. The auto-regressive effect is clearly stochastic and the coefficient is in the overall in range +0.25/-0.25. There is no clear short term mean reversion. As the in-sample period gets longer, the variance of the irregular component increases and the magnitude of the error (the difference between what is described by the component and the real data) gets smaller.

Out-of-sample results

We now turn to the fundamental concern - how to measure the predictive power of the models. In Fig. 6.6-6.11 we report the out-of-sample properties of the multivariate unobservable component models (MUCM) described in Section 3 as well as the results from the naïve model (random walk - RW). The upper panels show one-step forecasts, the lower panel shows multi-step ahead forecasts.

In order to measure the prediction power out-of-sample, we analyse the errors by calculating the mean error (ME), mean absolute error (MAE), mean square error (MSE), mean percentage error (MPE), and finally mean absolute percentage error (MAPE). For details regarding these measures and their use see Makridakis et al. (1998). For Fig. 6.6-6.11, the mean error (ME), mean absolute error (MAE), mean square error (MSE), mean percentage error (MPE) and mean absolute percentage error are reported under each graph.

In 2001, all gas component prices turned out to decline gradually in all months. In the one-step forecast for 2001, MUCM outperform RW for butane, while for propane and naphtha the out-of-sample performance is fairly similar (ME, MSE and MPE favour MUCM while MPE and MAPE are slightly better for RW). For multi-step forecasts, MUCM is clearly the better model for all measures. The MUCM capture to a large extend the falling price trend in 2001 for all series, while RW by construction uses the 2000(12) values for all observations out-of-sample, which are almost twice the values at the end of 2001 (Fig. 6.6).

At the second half of 2002, there was a sharp increase in butane and propane prices while there was a moderate increase in naphtha prices. The MUCM outperformed RW for all one-step ahead forecast measures for butane and propane apart from MPE propane. For naphtha MUCM outperformed RW for MSE and MAPE, while RW outperformed MUCM for ME, MAE, and MPE. The sharp trend-shift in prices from the summer was not captured by the MUCM for the multi-step forecast. On the contrary, the MUCM predicted that the recent nega-

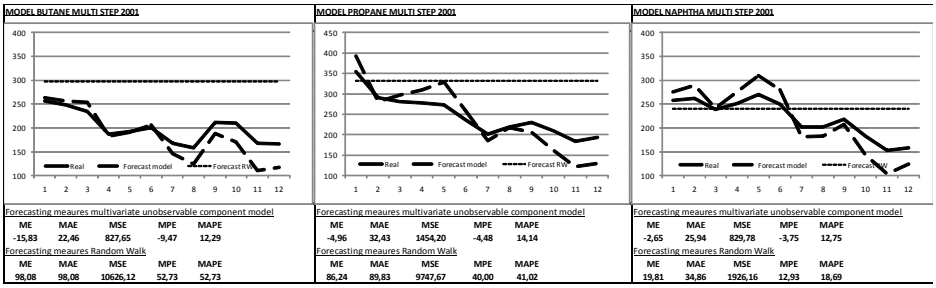

Figure 6.6: Shows graphically the out-of-sample multi-step ahead forecasts for 2001(1)-2001(12)

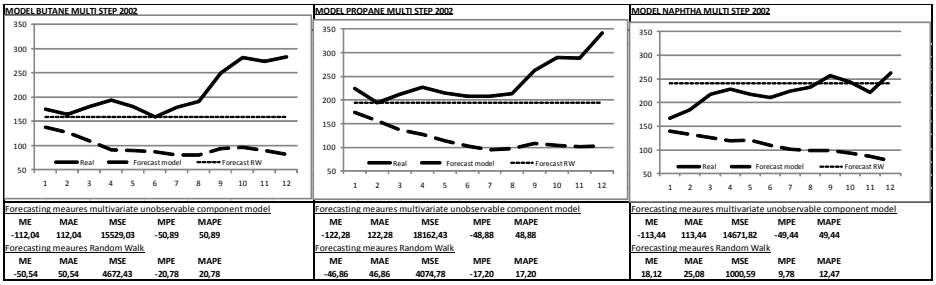

Figure 6.7: Shows the graphical multi-step ahead out-of-sample forecasts for 2002(1)-2002(12)

tive trend would continue. As a consequence, the RW outperformed the MUCM model for all series regarding the multi-step forecast (Fig. 6.7).

In 2003, butane and propane prices moved up during the winter and then fell down until the beginning of the summer before they went slowly upwards. Naphtha prices declined this year (Fig. 6.8). For one-step ahead forecast, the MUCM outperform RW for all measures when looking at propane. For butane, MUCM outperform RW when looking at MAE, MSE, and MAPE. For naphtha RW seems to outperform MUCM when looking at MAE and MPE. When looking at multi-step ahead forecast, the MUCM under-predict the true price paths and for butane RW outperform MUCM for all measures. For propane, MUCM outperform RW when looking at ME, MPE, and MAPE. For naphtha, MUCM outperform RW for all measures.

In 2004, butane and propane prices rose sharply until the end of the year when they fell. For naphtha prices first fell and then rose slowly. Apart from

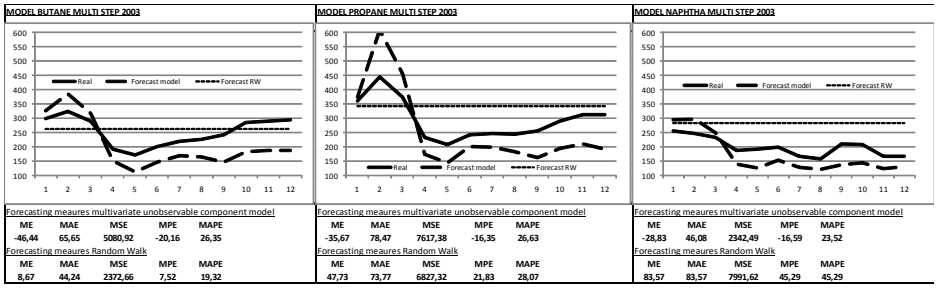

Figure 6.8: Shows the graphical out-of-sample multi-step forecasts for 2003(1)-2003(12)

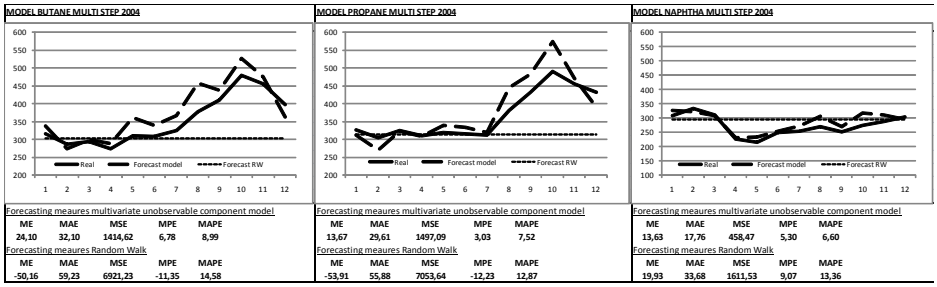

Figure 6.9: Shows the graphical out-of-sample multi-step forecasts for 2004(1)-2004(12)

MAE/MAPE propane, and ME naphtha, MUCM outperformed RW for both one-step and multi-step ahead forecasts (Fig. 6.9).

In 2005, prices went upwards following a wave pattern (Fig. 6.10). The RW outperforms MUCM for many of the one-step forecasts. For multi-step forecasts, MUCM outperform RW for all series (apart from MPE butane and MPE propane).

Finally in 2006 prices fell, then rose, then declined again for propane. For butane and naphtha prices though pick up at the end of the year. For naphtha MUCM outperform RW both for one-step and multi-step forecasts. For butane and propane, RW outperforms MUCM for one-step forecast (apart from ME butane). For propane multi-step, MUCM outperform RW for all measures, while RW outperforms MUCM for multi-step butane when looking at MAE, MSE, and MAPE (Fig. 6.11).

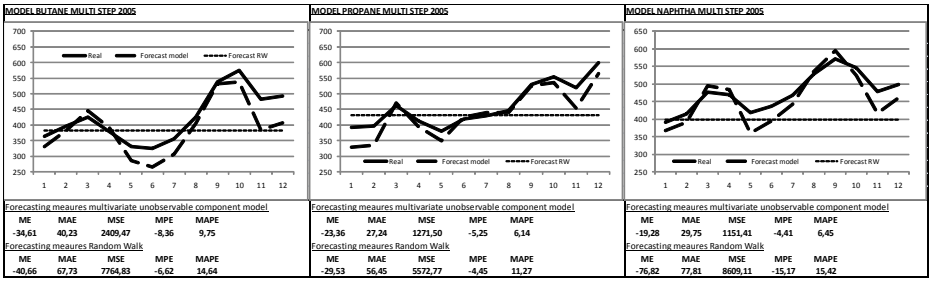

Figure 6.10: Shows the graphical out-of-sample multi-step forecasts for 2005(1)-2005(12)

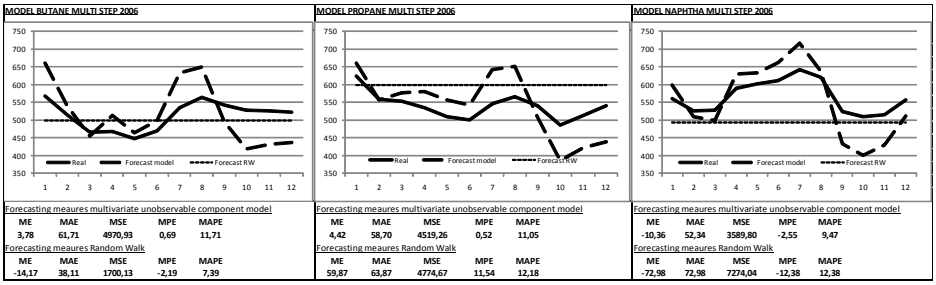

Figure 6.11: Shows the graphical out-of-sample multi-step ahead forecasts for 2006(1)-2006(12)

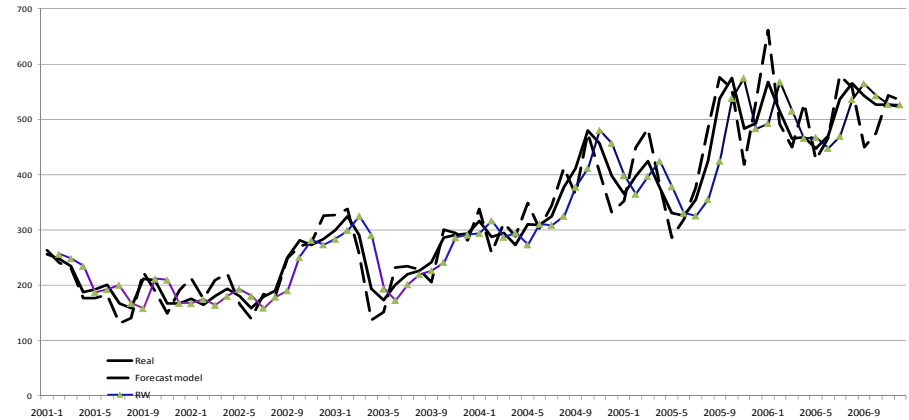

Figure 6.12: One step butane forecast. The one step forecast is updated for each month a can be done in a single operation

Figure 6.13: Propane one-step

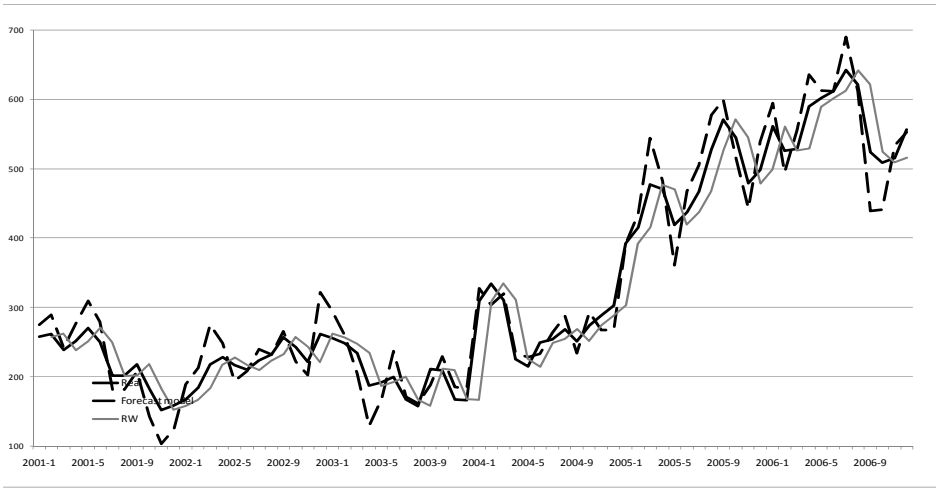

Figure 6.14: Naphtha one-step

Even though the MUCM do not fully capture the dynamics of the time series out-of-sample for the gas components prices, the results are promising. Looking at multi-step forecasts for the 6 out-of-sample periods with 5 forecasting error measures, MUCM "wins" 16 out of 30 for butane, 22 of 30 for propane, and 25 of 30 for naphtha. Similarly, for one-step forecasts, MUCM "wins" 22 out of 30 for butane, 18 of 30 for propane, and 15 of 30 for naphtha.

The time series seem to follow different stochastic processes for different subsamples. We have chosen to model it with MUCM, which let process parameters vary over time. A disadvantage of this method is that the accuracy of the forecast will vary. When the future turns out to be similar to the past, the realization of the process is near the middle of the confidence interval. However, when a regime shift has happened the prediction will be worse than a naïve model, and the realization is far outside the confidence interval. There are two ways of modelling such shifts. A deterministic specification with an intervention variable will improve fit, but the generated forecasts will not be meaningful unless the interventions can be predicted. A stochastic specification of regime shifts with a Markov chain allows estimation of the probabilities of shifts. These probabilities are useful when the application of the model is to find different scenarios and their probabilities rather than expectation and volatility alone. The implementation of such a model is left for future research.

6.5 Conclusions

In this study we have applied a multivariate unobservable component model for northern European prices of butane, propane, and naphtha. We tested several models and found that a model with stochastic trend and autoregressive effects and a fixed seasonal effect gave the best fit. We allow for correlated disturbances. We have split the data, validating the prediction power of different models in 6 independent out-of-sample periods. We test both one-step and multi-step prediction performance using 5 different measures for forecasting errors.

Most out-of-sample predictions show that our multivariate unobservable component models out-perform the naïve model (random walk). This is particular apparent for multi-step predictions. Looking at multi-step forecast performance for naphtha; our state space model outperforms random walk in all periods by all forecasting error measures. If forecasts are improved for the medium term (1 month to 1 year), it will have implications for energy-planning and strategy for producers and consumers of the gas components analysed in this paper (Midthun, 2007).

The findings in this article also have important implications for policy, risk management, and empirical research. It is generally believed by economists that energy commodity prices should be mean reverting, the "mean" being the marginal cost of extraction and Hotelling rent (Hotelling, 1931). Normally, the observed price should be the nominal marginal cost of extracting and producing gas. However, gas components are by-products so marginal cost might not be a meaningful concept. The by-product supply is given by the main product volume and the price is whatever balances supply and demand (Adland, Jia, and Lu, 2008).

As expected, we do not find any strong evidence of mean reversion for the gas component prices analysed here. This implies that a shock could have a permanent effect on the natural gas prices so that the observed prices are the accumulation of all the past shocks. Nevertheless, factors that cause price shocks could be temporary, and in that case a shock in one direction would sooner or later be followed by a shock in the opposite direction. However, only 10 years of data is not enough to draw a general conclusion whether component prices follow mean reversion or not. We believe that there are numerous factors on the demand side (rather than a possible marginal cost of production on the supply side) driving gas component prices in the short run. It is also generally believed that energy demand follow seasonal patterns. As many energy commodities are difficult to store and are used for heating in the winter, one would expect prices to be higher in the winter than in the summer. While this might be true for products like natural gas, it appears less likely for some of the gas components we analysed. In particular naphtha has alternative industrial use, and hence will

be influenced by other factors than seasonality. We could think of different extensions of our research. One will be to include exogenous variables that explain supply or demand shifts and study their effects. In this framework these regression sensitivities might also vary over time. One could also include other price series such as natural gas, oil and coal into the analysis to see how gas component prices vary with other energy commodities.

Acknowledgements

We would like to thank the research projects ELDEV, FINERGY, and OPTOP at Trondheim Business School and the Norwegian University of Science and Technology (NTNU). We are also indebted to Derek Bunn at the London Business School and Per Bjarte Sollibakke at Molde University College for their helpful comments at an internal seminar at NTNU in February 2009.

Bibliography

Adland, R., Jia, H., Lu, J., 2008. Price dynamics in the market for liquid petroleum gas transport. Energy Economics 30 (3), 818–828.

Commandeur, J., Koopman, S., 2007. An introduction to State Space Time Series Analysis. Oxford University Press, Oxford, UK.

Dixit, A. K., Pindyck, R. S., 1994. Investment under uncertainty. Princeton University Press, Princeton, NJ.

Doornik, J., Harvey, A., Koopman, S., Shephard, N., 2007. Time series with unobservable components Analyser, Modeller and Predictor: STAMP8.0™. Timberlake Consultants Press, London, UK.

Durbin, J., Koopman, S., 2001. Time Series Analysis by State Space Methods. Oxford University Press, Oxford, UK.

Gassco Homepage, 2009. Http://www.gassco.no/.

Ghouri, S., 2006. Forecasting natural gas prices using co-integration technique. OPEC Energy Review 30 (4), 249–269.

Gooijer, J., Hyndman, R., 2006. 25 years of time series forecasting. International Journal of Forecasting 22 (3), 443–473.

Harvey, A., Koopman, S., Shephard, N., 2005. State Space and Unobserved Component Models: Theory and Applications. Cambridge University Press, Cambridge, UK.

Harvey, A., Proietti, T., 2005. Readings in Unobservable Component Models. Oxford University Press, Oxford, UK.

Harvey, A. C., 1989. Forecasting, structural time series models and the Kalman filter. Cambridge University Press, Cambridge, UK.

Hotelling, H., 1931. The economics of exhaustible resources. Journal of Political Economy 39, 137–175.

Lee, J., List, J., Strazicich, M., 2006. Non-renewable resource prices: Deterministic or stochastic trends? Journal of Environmental Economics and Management 51 (3), 354–370.

Makridakis, S., 1996. Forecasting: its role and value for planning and strategy. International Journal of Forecasting 12 (4), 513–537.

Makridakis, S., Wheelwright, S., Hyndman, R., 1998. Forecasting: Methods and Applications. Wiley, New York, USA.

Midthun, K. T., 2007. Optimization models for liberalized natural gas markets. Ph.D. thesis, Norwegian University of Science and Technology, Trondheim, Norway.

Modjtahedi, B., Movassagh, N., 2005. Natural-gas futures: Bias, predictive performance and the theory of storage. Energy Economics 27 (4), 617–637.

Mokhatab, S., Poe, W. A., Speight, J. G., 2006. Handbook of natural gas transmission and processing. Gulf Professional Publishing, Burlington, MA, USA.

Pindyck, R., 1999. The long-run evolution of energy prices. The Energy Journal 20 (2), 1–27.

Pindyck, R., 2001. The dynamics of commodity spot and future markets: A primer. The Energy Journal 22 (3), 1–29.

Serletis, A., 2007. Quantitative and Empirical Analysis of Energy Markets. World Scientific, Singapore.

Serletis, A., Gogas, P., 1999. The north american natural gas liquids markets are chaotic. The Energy Journal 20 (1), 83–103.

Serletis, A., Shahmoradi, A., March 2005. Business cycles and natural gas prices. OPEC Review 29 (1), 75–84.

Shephard, N., 2005. Stochastic Volatility: Selected Readings. Oxford University Press, New York, USA.

Westgaard, S., Faria, E., Fleten, S.-E., 2008. Price dynamics of natural gas components: Empirical evidence. Journal of Energy Markets 1 (3), 37–68.

Wright, P., 2006. Gas prices in the UK - Markets and insecurity of supply. Oxford Institute for Energy Studies, Oxford, UK.